Springer-Verlag Berlin Heidelberg GmbH

Stefan Heinz

Statistical Mechanics of Turbulent Flows

With 42 Figures

Springer

Dr. Stefan Heinz
Technical University of Munich
Department of Fluid Mechanics
Boltzmannstraße 15
85747 Garching
Germany
E-mail: *heinz@flm.mw.tum.de*

ISBN 978-3-642-07261-1 ISBN 978-3-662-10022-6 (eBook)
DOI 10.1007/978-3-662-10022-6

Library of Congress Cataloging-in-Publication Data Applied For

A catalog record for this book is available from the Library of Congress.
Bibliographic information published by Die Deutsche Bibliothek
Die Deutsche Bibliothek lists this publication in die Deutsche Nationalbibliographie; detailed bibliographic data is available in the Internet at <http://dnb.ddb.de>.

Originally published by Springer-Verlag Berlin Heidelberg New York in 2004

Cover Design: Erich Kirchner, Heidelberg
Camera-ready by the author

Printed on acid free paper 32/3141 – 5 4 3 2 1 0

To my wife Petra,
and to our children Josephine and Jakob

Preface

The simulation of technological and environmental flows is very important for many industrial developments. A major challenge related to their modeling is to involve the characteristic turbulence that appears in most of these flows. The traditional way to tackle this question is to use deterministic equations where the effects of turbulence are directly parametrized, i.e., assumed as functions of the variables considered. However, this approach often becomes problematic, in particular if reacting flows have to be simulated. In many cases, it turns out that appropriate approximations for the closure of deterministic equations are simply unavailable. The alternative to the traditional way of modeling turbulence is to construct stochastic models which explain the random nature of turbulence. The application of such models is very attractive: one can overcome the closure problems that are inherent to deterministic methods on the basis of relatively simple and physically consistent models. Thus, from a general point of view, the use of stochastic methods for turbulence simulations seems to be the optimal way to solve most of the problems related to industrial flow simulations. However, it turns out that this is not as simple as it looks at first glance.

The first question concerns the numerical solution of stochastic equations for flows of environmental and technological interest. To calculate industrial flows, one often has to consider a number of grid cells that is of the order of 100^3. Unfortunately, a huge number of realizations (particles) are then required to compute such flows accurately. Without adopting statistical error reducing techniques, one needs, for instance, 10^4 or 10^6 particles in each cell to keep the statistical error below 1% or 0.1%, respectively. Thus, such flow calculations require the careful analysis of numerical solution strategies, error sources and the development of efficient error reducing techniques to limit the significant computational costs and computer memory requirements related to the use of stochastic methods. Fortunately, promising new solutions for this question have been presented recently (see the references given in section 5.6), which offer ways to solve this numerical problem. The second question concerns the stochastic modeling of the mechanism of turbulence. The simplest approach to tackle this problem is to use the equilibrium concept of classical statistical mechanics: fluctuations are generated randomly and relax linearly to zero (an essential underlying assumption is the definition of fluctuations as deviations from

ensemble means, see Appendix 1A). One can obtain good predictions for a variety of turbulent flows on this basis, but it is obvious now that such classical stochastic methods have their limitations – their use is no general way to obtain accurate predictions for any flow. Thus, one needs a better understanding of the conditions under which classical stochastic methods can be applied, and what can be done if the performance of these methods does not fulfil the needs.

The latter questions will be addressed here with regard to methods for the calculation of flows of environmental and technological relevance. An overview of the questions addressed and organization of the book is given in chapter 1. It is worth noting that there are significant differences with regard to both the flows considered and methods presented from the textbook "Turbulent Flows" published recently by Pope (2000). The most important advantage of stochastic turbulence models is given by their application to reacting flows, which, in general, are compressible. Therefore, the development of stochastic methods for the simulation of turbulent combustion problems is addressed here. The discussion of methods is not restricted to classical stochastic methods, but nonlinear stochastic methods and stochastic models for small-scale turbulence are also presented. The resulting question of the unification of modeling approaches is also addressed.

The book, which follows closely the theoretical part of lectures on fluid and thermodynamics given by the author at the Technical University of Munich, is written for students and researchers associated with environmental sciences, engineering sciences, applied mathematics and physics. The idea of presenting the material is to explain the physics (the advantages and disadvantages) of different methods. No attempt is made to present a complete review of stochastic methods for turbulence. Instead, the hierarchical structure of velocity and scalar models is discussed in order to explain which processes can be simulated by which type of model. Further, no attempt is made to describe applications of stochastic methods for the solution of specific technological and environmental problems in detail: a huge number of references related to that may be found in the literature. Instead, it is explained how solutions for characteristic problems can be developed, which appear in conjunction with the application of stochastic methods to simulations of specific turbulent flows.

Several restrictions were required to realize this concept. First, only one-point methods are considered (i.e., the construction of closed models for the properties of turbulence at one point in space). There are several interesting new developments regarding the construction of (formally more general) two-point methods (see for instance Piquet (1999)). However, as far as I know, these methods are not developed at present such that flows of environmental and technological relevance could be calculated. Second, the developments described here apply to single-phase flows. New developments have been made recently

regarding the construction of stochastic models for two-phase flows (see for instance the review of Minier & Peirano (2001)). These methods are based on the same physical principles as single-phase flow models, such that many of the features pointed out here apply similarly to two-phase flow models.

I would like to thank many people for significant support and discussions which were very helpful for this work. In particular, I am profoundly grateful to R. Friedrich, F. T. M. Nieuwstadt, S. B. Pope, D. Roekaerts and H. van Dop for their continuous support over many years. I would also like to thank D. Anfossi, H. Fortak, P. Givi, M. Gonzales, J.-P. Minier, B. L. Sawford, D. J. Thomson and P. Zannetti for exiting discussions of questions related to stochastic particle methods. I am thankful to J. J. Riley for helpful comments on parts of this book. In addition, thanks are due to many colleagues with whom I have worked: A. Dörnbrack, R. Dubois, I. Hadžić, R. Knoche, L. Martini and all my colleagues at the TU Munich. Many thanks also to W. Engel, K. Fancett, S. Pohl and L. Tonarelli of Springer-Verlag for the good collaboration regarding the production of this book. But first of all, I want to thank my wife Petra.

Unterschleißheim, June 2003 Stefan Heinz

Contents

Nomenclature

Upper-case Roman

A_i	velocity derivative ($A_i = DU_i / Dt$)
A_i^*	component of the particle acceleration vector $\mathbf{A}^* = (A_1^*, A_2^*, A_3^*)$
A_α	scalar derivative ($A_\alpha = D\Phi_\alpha / Dt$)
A_0	universal constant in Kolmogorov's theory
B	buoyancy production ($B = \overline{F_k'' u_k}$)
$B()$	beta function
C_K	Kolmogorov constant of the energy spectrum (see (4.86))
$C_{\varepsilon 1}$	parameter in dissipation equation (5.83)
$C_{\varepsilon 2}$	parameter in dissipation equation (5.83)
$C_{\varepsilon 3}$	parameter in dissipation equation (5.83)
$C_{\varepsilon 4}$	parameter in dissipation equation (5.83)
$C_{\varepsilon 5}$	parameter in dissipation equation (5.83) (added in section 5.6.4)
C_μ	parameter in turbulent viscosity $\nu_T = C_\mu k \tau$
C_ξ	characteristic function of the variable ξ
C_φ	mechanical-to-scalar time scale ratio ($C_\varphi = 2\tau / \tau_\varphi$)
$C_{\varphi 0}$	coefficient of the RIEM model
C_0	parameter in stochastic velocity models
$C_0(\infty)$	Kolmogorov constant (limit of C_0 for $Re_\lambda \to \infty$)
$D^{(n)}$	Kramers-Moyal coefficients
D_i	drift coefficient in Fokker-Planck equation
D_{ij}	diffusion coefficient in Fokker-Planck equation
$E()$	energy spectrum function
$E_\varphi()$	scalar energy spectrum function
F	turbulent velocity-scalar PDF or FDF
$F^{(m)}$	molecular velocity PDF
F_i	component of an external force in the velocity equation
$F_i^{(m)}$	component of an external force in the molecular velocity equation
F_u	turbulent velocity PDF or FDF
F_ξ	PDF of the variable ξ
$F_{\boldsymbol{\xi}}$	PDF of the vector $\boldsymbol{\xi}$

$F_{\xi\xi}$	joint PDF
$F_{\xi\vert\xi}$	conditional PDF
F_{φ}	turbulent scalar PDF or FDF
G	coefficient tensor in stochastic and Fokker-Planck equations
$G(\mathbf{r})$	filter function
K_n	cumulant of n^{th} order
K_{ij}	diffusion coefficient
Kn	Knudsen number ($Kn = Ma / Re$)
Kn_r	residual Knudsen number ($Kn_r = (2 / 3)^{1/2} \ell / L_0$)
Ku	Kurtosis (see (2.11))
L	length scale of large-scale eddies ($L = k^{1/2} \tau = k^{3/2} / \varepsilon$)
M	total mass within the domain considered
M_g	gradient Mach number (see (5.69))
M_t	turbulence Mach number ($M_t^2 = 2\,k / \overline{aa}$)
M_α	mass of substance α
Ma	Mach number ($Ma = U_0 / a_0$)
P	shear production ($P = -\overline{u_i u_k}\,\overline{S}_{ki}$)
P_r	shear production related to the SGS stress tensor ($P_r = -\overline{\overline{u_i u_k}}\,\overline{S}_{ki}$)
P_ξ	distribution function of the variable ξ
$P_{\boldsymbol{\xi}}$	distribution function of the vector $\boldsymbol{\xi}$
$P_{\xi\xi}$	joint distribution function
Pr	Prandtl number
Pr_k	Prandtl number in turbulent kinetic energy equation (5.82)
Pr_ε	Prandtl number in dissipation equation (5.83)
Q_B	external force-velocity correlation in the energy equation (4.14c)
R	gas constant ($R = c_p - c_v$)
R()	velocity autocorrelation function
R_u	universal gas constant
Re	Reynolds number ($Re = U_0 L_0 / \nu$)
Re	channel flow Reynolds number ($Re = U_b h / \nu$)
Re_L	turbulence Reynolds number ($Re_L = k^2 / (\varepsilon\,\nu)$)
Re_λ	Taylor-scale Reynolds number ($Re_\lambda^2 = 20\,Re_L / 3$)
Re_τ	friction Reynolds number ($Re_\tau = u_\tau h / (2\,\nu)$)
Re_0	channel flow Reynolds number ($Re = U_0 h / (2\,\nu)$)
Ri	gradient Richardson number ($Ri = \beta\,g\,\vert\overline{S}\vert^{-2} \partial\overline{T} / \partial x_3$)
S	entropy
S^*	entropy functional
S	shear rate in a homogeneous shear flow ($S = \partial\overline{U}_1 / \partial x_2$)
$\vert\overline{S}\vert$	characteristic strain rate ($\vert\overline{S}\vert = (2\overline{S}_{kl}\overline{S}_{lk})^{1/2}$)
$\vert\overline{S}\vert_r$	characteristic strain rate within the FDF approach ($\vert\overline{S}\vert_r = (2\overline{S}_{kl}\overline{S}_{lk})^{1/2}$)

S_T source term in temperature equation (see (4.72))
S_{ij} rate-of-strain tensor ($S_{ij} = \frac{1}{2} [\partial U_i / \partial x_j + \partial U_j / \partial x_i]$)
S_{ij}^d deviatoric part of S_{ij}($S_{ij} = \frac{1}{2} [\partial U_i / \partial x_j + \partial U_j / \partial x_i] - \partial U_n / \partial x_n \delta_{ij} / 3$)
S_{kk} dilatation
S_α chemical source rate of substance α
Sc Schmidt number
Sc_t turbulence Schmidt number
Sk skewness (see (2.11))
T temperature
T dimensionless time ($T = 2 \int_0^t ds\, \tau_\varphi^{-1}$)
U_b bulk velocity (see (5.41))
U_0 centerline velocity (see (5.41))
U_i component of the fluid velocity $\mathbf{U} = (U_1, U_2, U_3)$
U_i^* component of the particle velocity vector $\mathbf{U}^* = (U_1^*, U_2^*, U_3^*)$
V_i component of the molecular velocity vector $\mathbf{V} = (V_1, V_2, V_3)$
V_i^* component of the molecular particle velocity vector $\mathbf{V}^* = (V_1^*, V_2^*, V_3^*)$
W mass of one mole
W_α mass of one mole of substance α
W_i component of a Wiener process in particle equations
ΔW_i increment of a Wiener process (see 3.45)
X_i^* force in (1.1b)

Lower-case Roman

a speed of sound ($a^2 = \gamma\, p / \rho$)
a_i systematic term in stochastic differential equations
a_i acceleration fluctuation around $\overline{A}_i$ ($a_i = A_i - \overline{A}_i$)
a_{ij} standardized anisotropy tensor (see (5.22))
a_α scalar derivative fluctuation around $\overline{A}_\alpha$ ($a_\alpha = A_\alpha - \overline{A}_\alpha$)
b_{ij} coefficient of the noise term in stochastic differential equations
c_p specific heat at constant pressure
c_v specific heat at constant volume
$c_{v,\alpha}$ specific heat of substance α at constant volume
c_S Smagorinsky coefficient (see (6.27))
det() determinant
e molecular kinetic energy ($e = \overline{v_i v_i} / 2$)
e specific internal energy
e_α specific internal energy of substance α
erf() error function
f_i stochastic force
$f_i^{(m)}$ fluctuation around F_i ($f_i^{(m)} = F_i^{(m)} - F_i$)

f_φ PDF of scalar fluctuations
g gravity acceleration
h channel height
h_α specific enthalpy of substance α ($h_\alpha = e_\alpha + p_\alpha / \rho_\alpha$)
i_r residual turbulence intensity ($i_r = (2 k_r / 3)^{1/2} / U_0$)
k turbulent kinetic energy ($k = \overline{u_i u_i} / 2$)
k_r residual turbulent kinetic energy ($k_r = \overline{u_i u_i} / 2$)
ℓ length scale within the FDF approach
ℓ^* standardized length scale within the FDF approach
ℓ_φ^* standardized length scale within the scalar FDF approach
m_α mass fraction of substance α
p pressure ($p = p_{ii} / 3$)
p_α partial pressure of substance α
p_{ik} molecular stress tensor ($p_{ik} = \rho \overline{v_i v_k}$)
q_k component of the heat flux vector ($q_k = \rho \overline{v_k v_n v_n} / 2$)
t time
u_i velocity fluctuation around $\overline{U}_i$ ($u_i = U_i - \overline{U}_i$)
u_η Kolmogorov velocity scale ($u_\eta = (\varepsilon \nu)^{1/4}$)
u_τ friction velocity
v_i fluctuation around $\overline{V}_i$ ($v_i = V_i - \overline{V}_i$)
w_i component of the sample space velocity $\mathbf{w} = (w_1, w_2, w_3)$
x_i component of the position vector $\mathbf{x} = (x_1, x_2, x_3)$
x_i^* component of the particle position vector $\mathbf{x}^* = (x_1^*, x_2^*, x_3^*)$
x_α mole fraction of substance α

Upper-case Greek

Γ diffusion coefficient ($\Gamma = 8 k \tau / (9 C_0)$)
$\Gamma()$ gamma function
Δ filter width
Π_d pressure-dilatation correlation (see (5.65))
Σ_{ij} rate-of-rotation tensor ($\Sigma_{ij} = \frac{1}{2} [\partial U_i / \partial x_j - \partial U_j / \partial x_i]$)
Φ_α component of the scalar vector $\boldsymbol{\Phi} = (\Phi_1, \ldots, \Phi_{N+1})$
Φ_α^* component of the particle scalar vector $\boldsymbol{\Phi}^* = (\Phi_1^*, \ldots, \Phi_{N+1}^*)$

Lower-case Greek

β thermal expansion coefficient (see (4.83))
γ ratio of the constant-pressure to constant-volume specific heats ($\gamma = c_p / c_v$)
γ_{ij} abbreviation ($\gamma_{ij} = \delta_{ij} + \tau_L \partial \overline{U}_i / \partial x_j$)
$\delta()$ delta function

δ_{ij}	Kronecker delta ($\delta_{ij}= 1$ if $i = j$ and $\delta_{ij}= 0$ if $i \neq j$)
ε	dissipation rate of turbulent kinetic energy ($\varepsilon = \varepsilon_s + \varepsilon_d$)
ε_d	dilatational dissipation rate
ε_r	dissipation rate within the FDF approach
ε_s	solenoidal dissipation rate
η	Kolmogorov length scale ($\eta = u_\eta \tau_\eta$)
$\theta()$	theta (or Heaviside step) function
κ	heat conduction coefficient ($\kappa = \rho\, \nu$ / Pr)
κ	wavenumber ($\kappa = 2\, \pi$ / λ)
κ_B	Batchelor-scale wavenumber ($\kappa_B = Sc^{1/2} \kappa_k$)
κ_K	Kolmogorov-scale wavenumber ($\kappa_K = Re_L^{3/4} \kappa_0$)
κ_0	integral-scale wavenumber
λ	wave length
λ_n	Lagrangian multiplier
μ	viscosity ($\mu = \rho\, \nu$)
ν	kinematic viscosity ($\nu = \tau_m e$ / 3)
ν_r	residual viscosity ($\nu_r = \tau_L k_r$ / 3)
ν_T	turbulent viscosity ($\nu_T = C_\mu k\, \tau$)
ν_u	turbulent viscosity that unifies ν_r and ν_T
$\nu_{(\alpha)}$	molecular diffusivity for $\alpha = 1, N$ ($\nu_{(\alpha)} = \nu$ / Sc)
$\nu_{(\alpha)}$	thermal diffusivity for $\alpha = N + 1$ ($\nu_{(N+1)} \nu$ / Pr)
ξ	stochastic variable
ξ_i	component of the stochastic vector $\boldsymbol{\xi} = (\xi_1, \xi_2, \cdots)$
π_{ij}	deviatoric part of the molecular stress tensor ($\pi_{ij} = p_{ij} - p\, \delta_{ij}$ / 3)
ρ	fluid mass density
$\rho^{(m)}$	instantaneous molecular mass density
ρ_α	mass density of substance α
σ^2	variance
σ_{ij}	variance matrix
τ	dissipation time scale ($\tau = k$ / ε)
τ_f	correlation time scale of stochastic forces
τ_L	characteristic velocity time scale in (6.5b)
τ_m	characteristic time scale of molecular motion
τ_r	dissipation time scale ($\tau_r = k_r$ / ε_r)
τ_u	characteristic velocity time scale in (5.1)
τ_{ik}	deviatoric part of the SGS stress tensor ($\tau_{ik} = \overline{u_i u_k} - 2\, k_r \delta_{ik}$ / 3)
τ_η	Kolmogorov time scale ($\tau_\eta = (\nu$ / $\varepsilon)^{1/2}$)
τ_φ	characteristic scalar time scale
ϕ	standardized scalar fluctuation in (5.48a)
ϕ	scalar fluctuation around $\overline{\Phi}$ ($\phi = \Phi - \overline{\Phi}$)

ϕ_α	scalar fluctuation around $\overline{\Phi}_\alpha$ ($\phi_\alpha = \Phi_\alpha - \overline{\Phi}_\alpha$)
ϕ_+	upper scalar bound in the RIEM model
ϕ_-	lower scalar bound in the RIEM model
ψ	scalar derivative (see (5.48b))
ω_{ij}	abbreviation ($\omega_{ij} = \partial \overline{U}_i / \partial x_j - G_{ij}$)

Symbols

$\langle Q \rangle$	ensemble mean or (in chapters 6 and 7) filtered value
$\overline{Q}$	mass density-weighted mean ($\overline{Q} = \langle\rho\rangle^{-1}\langle\rho\, Q\rangle$)
$\overline{Q \mid \mathbf{y}}$	average conditioned on $\mathbf{y}$
Q'	fluctuation around $\langle Q \rangle$ ($Q' = Q - \langle Q \rangle$)
Q''	fluctuation around $\overline{Q}$ ($Q'' = Q - \overline{Q}$)
$\mathbf{Q}$	vector
Q_i	component of a vector $\mathbf{Q}$ of fluid dynamic variables
Q_α	component of a vector $\mathbf{Q}$ of scalars (mass fractions or temperature)
$Q_{(\alpha)}$	no summation over α
Q	matrix
Q_{ij}	matrix element of fluid dynamic variables
$Q_{\alpha\beta}$	matrix element of scalars (mass fractions or temperature)
Q_{kk}	sum over all elements with the same subscripts ($Q_{kk} = Q_{11} + Q_{22} + Q_{33}$)
$\{Q\}$	trace of a matrix ($\{Q\} = Q_{kk}$)
Q^{-1}	inverse matrix Q
Q^+	standardized variable (normalized to $U_0, L_0, \cdots$)
$\int dx$	operator acting on the following term (integral over all possible x)
$\partial / \partial x$	operator acting on the following term (partial derivative)
DQ / Dt	substantial derivative of Q ($DQ / Dt = \partial Q / \partial t + U_k \partial Q / \partial x_k$)

Abbreviations

CBL	convective boundary-layer
DM	diffusion model
DNS	direct numerical simulation
ELM	extended Langevin model
ETBL	equilibrium turbulent boundary layer
FDF	filter density function
GLM	generalized Langevin model
HIST	homogeneous, isotropic, stationary turbulence
IEM	interaction by exchange with the mean
LES	large-eddy simulation
LM	Langevin model

PDF	probability density function
RANS	Reynolds-averaged Navier-Stokes
RIEM	Refined interaction by exchange with the mean
RSM	Reynolds stress model
SGS	subgrid scale
SIEM	stochastic interaction by exchange with the mean
SLM	simplified Langevin model
SML	statistically most-likely

1. Introduction

The understanding of turbulence is highly relevant to the protection of our natural living conditions and many technological developments. To develop environmental protection control strategies, we need knowledge about the mechanisms of the global warming up of our earth's atmosphere, the development and path of hurricanes and the transport of (radioactive) substances in the turbulent atmosphere. With regard to technological developments, we are interested to see how the efficiency of the mixing of species in chemical reactors or propulsion systems of high-speed aircraft can be enhanced. Studies of turbulent phenomena by means of measurements are usually very expensive. In addition to this, one obtains in this way only limited (and often quite inaccurate) information about some of the quantities of interest. To understand turbulent phenomena in their complexity, we need models that enable the simulation of turbulent flows. Basic ways to construct such models, and characteristic advantages and disadvantages of different approaches, will be described in this book, as illustrated in Fig. 1.1.

An overview of essential features of computational methods for turbulent flows will be given first in order to explain the motivation for the discussions performed in the following chapters. In section 1.1, this is done with regard to the construction of the basic equations of fluid and thermodynamics. These equations become inapplicable to flows with a well-developed turbulence as usually occurs in nature or technological problems. The question how suitable equations for such flows can be constructed will be addressed in section 1.2. In agreement with the course of their development, this discussion will be split into the consideration of stochastic models for large-scale turbulence and stochastic models for small-scale turbulence (which are currently under development). This leads then to the important question of the unification of turbulence models.

1.1. The basic equations

There are different ways to derive the basic equations for turbulent flows. One way is the use of empirical assumptions in combination with symmetry constraints. Another way is to develop a model for the underlying molecular motion and to derive then the basic equations of fluid and thermodynamics as a consequence of

S. Heinz, *Statistical Mechanics of Turbulent Flows*

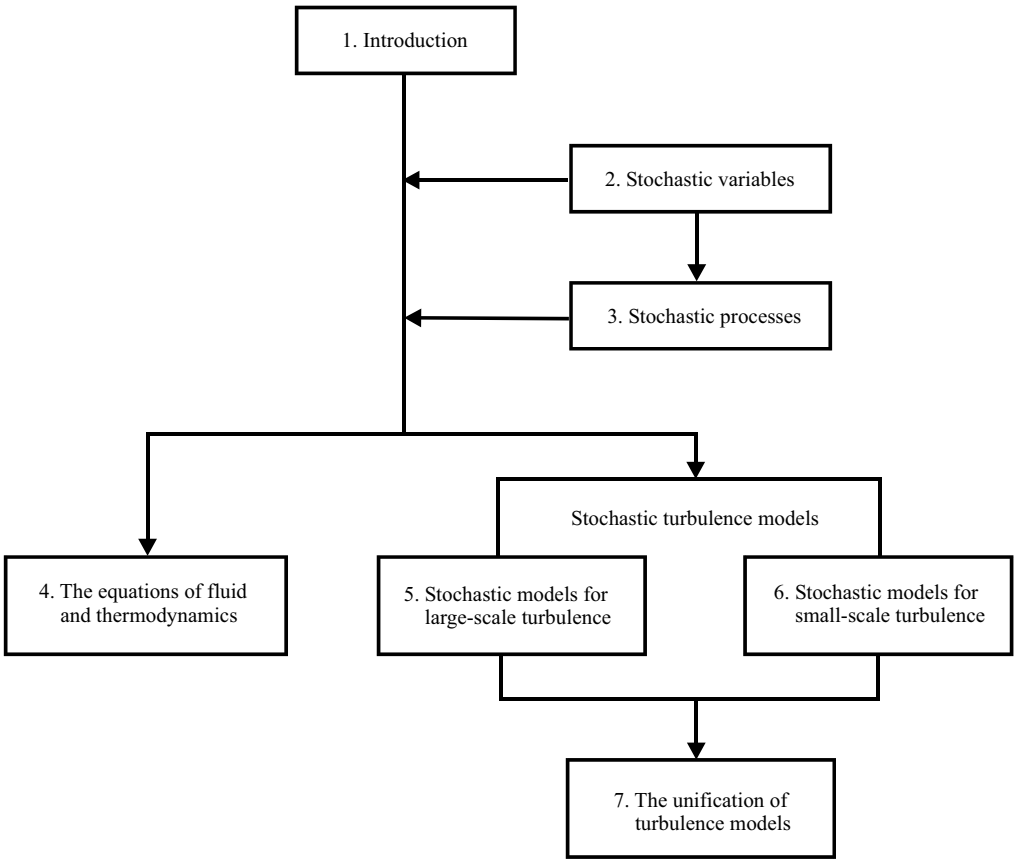

Fig. 1.1. An illustration of the organization of the book. Chapter 1 provides an overview on the questions addressed. Chapters 2 and 3 deal with fundamentals regarding the use of stochastic variables and processes. The basic equations of fluid and thermodynamics are then introduced in chapter 4. Environmental and technological flows are usually characterized by a well-developed turbulence. The problem related to the basic equations is that they are practically inapplicable to calculate such turbulent flows. Therefore, one has to develop models for turbulent motions on the fluid dynamic scale. The question how such stochastic turbulence models can be constructed is the main object of this book. This question will be differentiated into the consideration of models for large- and small-scale turbulence, which are treated in chapters 5 and 6. The unification of these approaches is the concern of chapter 7.

this molecular model. This approach will be applied here in order to demonstrate the analogy to the construction of stochastic turbulence models and to explain the limitations of the applicability of the basic equations.

1.1.1. The molecular dynamics

We consider a macroscopic volume (1 cm^3) of a gas that consists of a very large number (10^{20}) of molecules. The molecules may be seen as particles (mass points) that move in an irregular way. We assume that the changes of the i^{th} components of the position $\mathbf{x}^* = (x_1^*, x_2^*, x_3^*)$ and velocity $\mathbf{V}^* = (V_1^*, V_2^*, V_3^*)$ of a molecule in time t are given by the equations

$$\frac{dx_i^*}{dt} = V_i^*, \tag{1.1a}$$

$$\frac{dV_i^*}{dt} = X_i^*\left(\mathbf{V}^*, \mathbf{x}^*, t\right). \tag{1.1b}$$

This presentation of evolution equations is called the Lagrangian approach. One considers the variables of interest as properties of particles. The mathematical expression of this idea is equation (1.1a), which defines the position of a particle that moves with the velocity V_i^*. X_i^* is a force that will be specified in chapter 4.

By providing initial and boundary conditions for all the particles considered, the dynamics of the fluid would be completely described by (1.1a-b). However, because of the huge number of particles, the equations (1.1a-b) for the molecular motion are not very helpful to solve problems of practical relevance. On the other hand, one is in general not so much interested in having information on the state of each molecule, but in characteristic properties of a large number of molecules, that is, in averages (or means, both terms will be applied throughout this book as having the same meaning). The value of (1.1a-b) arises then from the fact that these equations can be used to construct equations for means.

1.1.2. The basic equations

The simplest way to construct equations for means is the use of ensemble means, which are defined in Appendix 1A. The fluid and thermodynamic equations can be obtained then on the basis of a stochastic model for the molecular motion, as shown in chapter 4. This can be done by rewriting stochastic equations that have the structure of (1.1a-b) into a corresponding Fokker-Planck equation for the probability density function (PDF). This corresponds to the transition into the Eulerian approach where fluid properties are considered at fixed positions. The reduction of this Fokker-Planck equation to equations for the fluid mass density ρ and velocity U_i results (without involving external forces) in

$$\frac{\partial \rho}{\partial t} + \frac{\partial \rho U_k}{\partial x_k} = 0, \tag{1.2a}$$

$$\frac{\partial \rho U_i}{\partial t} + \frac{\partial \rho U_k U_i}{\partial x_k} + \frac{\partial p_{ik}}{\partial x_k} = 0. \tag{1.2b}$$

The molecular stress tensor p_{ik} is defined in terms of molecular quantities. Suitable approximations for it can be found by means of (1.1a-b).

The application of (1.2a-b) combined with the Navier-Stokes model for p_{ik} to the simulation of turbulent flows is called direct numerical simulation (DNS). This technique is a unique tool to investigate basic mechanisms of turbulence – but its use is restricted to weakly turbulent flows because the computational costs grow rapidly with the Reynolds number, which represents a measure for the intensity of turbulence. Unfortunately, it is obvious today that DNS cannot be used (at least for the foreseeable future) for the calculation of flows of technological or environmental relevance.

1.2. Turbulence models

To overcome this problem of the inapplicability of the basic equations of fluid and thermodynamics to most of the industrial problems one used these equations to construct equations for coarser quantities, this means for variables that represent fluid properties on a coarser scale.

The first way that was applied to obtain such equations is to average the basic equations by adopting ensemble means. The Reynolds-averaged Navier-Stokes (RANS) equations obtained in this way read

$$\frac{\partial \langle \rho \rangle}{\partial t} + \frac{\partial \langle \rho \rangle \overline{U}_i}{\partial x_i} = 0, \tag{1.3a}$$

$$\frac{\partial \overline{U}_i}{\partial t} + \overline{U}_k \frac{\partial \overline{U}_i}{\partial x_k} + \langle \rho \rangle^{-1} \frac{\partial \langle \rho \rangle \overline{u_k u_i}}{\partial x_k} + \langle \rho \rangle^{-1} \frac{\partial \langle p_{ik} \rangle}{\partial x_k} = 0. \tag{1.3b}$$

Here, <···> refers to the ensemble average, and the overbar describes a mass density-weighted mean $\overline{Q} = \langle \rho \rangle^{-1} \langle \rho\, Q \rangle$, where Q is any function. $\overline{u_k u_i}$ is called the Reynolds stress tensor, which appears as unknown in (1.3b).

The problem related to use of (1.3a-b) for turbulent flow simulations is the closure of equation (1.3b) in terms of $\langle \rho \rangle$ and $\overline{U}_i$, which are calculated. Suitable approximations for the Reynolds stress tensor can often be found by adopting approximations in a transport equation for it, which can be obtained in analogy to (1.3b). Nevertheless, such a closure strategy becomes unfeasible with regard to the simulation of reacting flows. To model them, one needs closed transport equations for thermochemical variables as mass fractions or temperature. In these equations

one finds mean reaction rates that represent averages over highly nonlinear terms. Apart from some cases where one can successfully assess the deviations from limiting cases of very fast or slow chemistry, suitable closure of such equations for mean quantities can hardly be obtained on the basis of direct parametrizations of unclosed terms in general.

1.2.1. Stochastic models for large-scale turbulence

The extension of the equations (1.3a-b) to a model that involves both the dynamics of means and fluctuations represents a relatively simple way to handle the closure problems described above. Such PDF methods can be constructed by postulating a stochastic model for instantaneous velocities in analogy to the equations (1.1a-b). The significant advantage of this approach is that the closure problems related to the use of RANS equations can be overcome on the basis of a physically consistent model, see the detailed discussion in chapter 5.

However, a problem that concerns the application of both RANS and PDF methods is related to the reference to ensemble-averaged fluid dynamic variables. According to the ergodic hypothesis, see the explanations given in Appendix 1A, such means have to be seen as relatively coarse quantities that represent mean values of fluid dynamic variables within volumes that are not always small compared to the flow domain considered. This fact implies several problems. The first one concerns the modeling of the dynamics of fluctuations, this means the determination of a suitable model structure. The fact that fluctuations are taken with reference to ensemble averages implies the possibility that significant deviations from means occur. This may cause nonlinear fluctuation dynamics and non-trivial interactions between various fluctuations. The second problem is that such models cannot be universal. Usually, model parameters are related to standardized flow statistics, as specific components of the normalized Reynolds stress tensor. Apparently, such parameters must depend on the flow considered, but they also may vary significantly in different regions of one flow. This poses the problem of finding optimal values for model parameters. Even if the modeling task is performed in an optimal way, the third problem is the impossibility to resolve several details of the physics of flows. It is for instance impossible to resolve the structure of the turbulent mixing of scalars in mixing layers in a way that is comparable to the information obtained by DNS results.

1.2.2. Stochastic models for small-scale turbulence

A way to overcome these problems related to the reference to ensemble averages is to apply a spatial filter operation with a filter width that is small compared to the length scale of large-scale fluid motions. This may be performed

in two ways: RANS equations can be replaced by large-eddy simulation (LES) equations (which agree with the equations (1.3a-b) if the ensemble averages are replaced by the corresponding filtered values), or PDF equations can be replaced by so-called filter density function (FDF) equations (which look as PDF equations, one just has to reinterpret the averages involved). A discussion of essential features of FDF methods as extension of LES methods will be presented in chapter 6.

Accordingly, FDF methods are characterized by the combination of two essential advantages: large-scale fluid motions are treated without adopting modeling assumptions, and small-scale fluid motions are partly treated exactly and partly modeled on the basis of a physically consistent model. However, these advantages have their price. Such FDF calculations are found to require a computational effort that is less than that required for DNS, but this effort is still very expensive.

1.2.3. The unification of turbulence models

An optimal solution to the problems related to the application of models for small- and large-scale turbulence is the construction of unified (or bridging) models, this means models that can be used to perform for instance DNS, LES or RANS simulations. The development of such models would allow calibration of relatively coarse models by high-resolving simulations. The resulting optimally calibrated models could be used then to perform relatively inexpensive routine investigations.

It is essential to emphasize that the construction of models that apply a variable filter width does not solve the problem of constructing bridging models. With regard to this, the limit of a vanishing filter width does not pose any problem, but the limit of an extremely large filter width requires a careful consideration. Such questions related to the construction of unified turbulence models will be addressed in chapter 7 in conjunction with a discussion of further developments that may be expected in this field.

Appendix 1A: Filter operations

1A.1. Spatial averages

Let us assume that we are interested in (equations for the evolution of) averaged quantities that characterize any flow considered. From a practical point of view, the most convenient way to formulate a filter operation is the use of time-, space- or space-time averaging: such averages can be obtained at best by measurements. By restricting the attention to space-averages for simplicity, such an average of any function $Q(\mathbf{x}, t)$ could be defined by

$$\langle Q(\mathbf{x},t)\rangle = \int d\mathbf{r}\; Q(\mathbf{x}+\mathbf{r},t)\, G(\mathbf{r}). \qquad (1A.1)$$

$G(\mathbf{r})$ is a filter function with properties as described in chapter 6. The disadvantage of defining averages by means of the relation (1A.1) is that transport equations for filtered variables must depend on the specification of the properties of $G(\mathbf{r})$. Thus, equations derived in this way are faced again with a closure problem since there is no general methodology to determine $G(\mathbf{r})$.

1A.2. Ensemble averages

A simple way to avoid this problem is the use of ensemble averages as they are defined in the theory of probability. In contrast to the need to specify $G(\mathbf{r})$ in equation (1A.1), the application of ensemble means does not require further information that has to be provided. To define them, one considers an infinite number of equivalent systems which are called an ensemble. From a physical point of view, equivalent systems means that one considers systems with initial and boundary conditions that are the same according to our observation (which is insufficient to distinguish all the details of these states, as for instance the concrete values of all the molecule velocities). The ensemble mean of a property $Q(\mathbf{x}, t)$ at a position $\mathbf{x}$ and time t is then defined as the arithmetic mean of corresponding values in each system,

$$\langle Q(\mathbf{x},t)\rangle_e = \frac{1}{N}\sum_{n=1}^{N} Q^{(n)}(\mathbf{x},t). \qquad (1A.2)$$

$Q^{(n)}$ is the value of Q obtained for the n^{th} flow, and N is the total number of flows. The subscript e is used here to distinguish between spatial filter operations defined by (1A.1) and ensemble means. This subscript will be neglected in the chapters 2 – 5 (where only ensemble means are used) to simplify the notation.

To compare theoretical predictions for $<Q>_e$ with measurements, one would have to perform a large number of measurements carried out in a long series of repeated similar experiments. Obviously, such a series of measurements is unavailable in general: one often has to use data derived from just one experiment. Usually, such data are given as spatially filtered values. This leads to the essential question about the consistency of ensemble means predicted by theory and quantities that can be obtained by measurements.

1A.3. The ergodic theorem

This question is the concern of the ergodic theorem. To illustrate the content of this important theorem we consider a spatial filtering of any function Q of the form

$$\widetilde{Q}(\mathbf{x}) = \frac{1}{ABC} \int_{-A/2}^{A/2} dy_1 \int_{-B/2}^{B/2} dy_2 \int_{-C/2}^{C/2} dy_3 \; Q(\mathbf{x}+\mathbf{y}), \tag{1A.3}$$

and ask for the conditions for the convergence between $\widetilde{Q}$ and the ensemble mean $<Q>_e$. This question can be treated analytically for the case of homogeneous turbulence (a homogeneous shear flow). The latter assumption can be considered as a reasonable approximation for small flow regions. As pointed out by Monin and Yaglom (1971, §§4.7), one finds for sufficiently large A, B, C the following asymptotic expression for the mean squared difference between $\widetilde{Q}$ and $<Q>_e$,

$$\left\langle \left(\widetilde{Q}(\mathbf{x}) - \langle Q \rangle \right)^2 \right\rangle \rightarrow \frac{\upsilon_c}{\upsilon} = \frac{1}{ABC} \int_{-A/2}^{A/2} dy_1 \int_{-B/2}^{B/2} dy_2 \int_{-C/2}^{C/2} dy_3 \; C_Q(\mathbf{y}). \tag{1A.4}$$

The last expression represents the box-filtered correlation function

$$C_Q(\mathbf{y}) = \left\langle \left(Q(\mathbf{y}) - \langle Q \rangle \right) \left(Q(0) - \langle Q \rangle \right) \right\rangle. \tag{1A.5}$$

υ = A B C is the volume of the box considered. υ_c may be seen as a "correlation volume" or "integral volume scale", this means a measure for the volume occupied by a typical eddy of the flow considered. Therefore, the conclusion that can be drawn from (1A.4) is that $\widetilde{Q}$ converges to $<Q>_e$ provided the box volume υ used for the spatial filtering is much larger than the characteristic eddy volume υ_c. In other words, ensemble means may be seen as box-averages where the boxes are large compared to the characteristic eddy volume υ_c.

2. Stochastic variables

To develop equations for turbulent flows one needs knowledge about the characterization of stochastic variables (at any time) and properties of stochastic processes (the structure of equations for the evolution of stochastic variables in time). The properties of stochastic variables will be pointed out in this chapter, and the most important features of stochastic processes will be discussed in chapter 3.

The characterization of a single stochastic variable will be considered in sections 2.1 and 2.2. The extensions of these definitions to the case of many variables is the concern of section 2.3. It will be shown that stochastic variables are defined via their PDFs. An important problem is then the question of how it is possible to estimate the shape of a PDF. This will be addressed in section 2.4, where a systematic procedure for the construction of PDF parametrizations is presented. Examples for PDFs obtained in this way are then given in section 2.5. Unfortunately, such PDFs are not always easy to use. Thus, section 2.6 deals with the explanation of ways to construct simpler PDFs.

2.1. PDFs of one variable

2.1.1. The need for the usage of probabilistic concepts

The states of turbulent systems are often extremely complex. They depend on many different factors which are unknown or not assessable for us. Usually, we are only able to recognize a small part of the complete state of turbulent systems, which is called the observable state. This inability to get knowledge about the complete state of turbulent systems may have serious consequences. This is illustrated in Fig. 2.1. Ξ refers to the complete state of a system, and ξ denotes the observable state (which could be a hurricane position). Fig. 2.1b demonstrates that the lack of knowledge about the complete system state Ξ results in the fact that the exact value of ξ is unpredictable at later times. Impressive examples for the unpredictability of the path of hurricanes may be found in the storm archive of the US National hurricane center, see http://www.nhc.noaa.gov.

What we have to do in this case is to consider the observable state ξ as a stochastic variable, this means a variable that takes (due to unknown factors) values that we cannot predict accurately. Nevertheless, our experience shows that

S. Heinz, *Statistical Mechanics of Turbulent Flows*

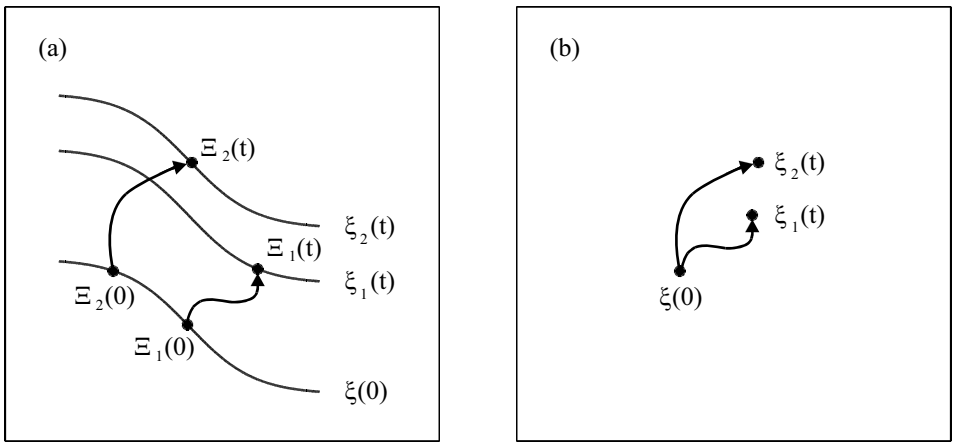

Fig. 2.1. The evolution of two complete system states Ξ_1 and Ξ_2 in time t is shown in (a). At the initial time t = 0, both states lie on a hyper-surface that is defined by the same value of an observable quantity $\xi(0)$. At the time t, Ξ_1 and Ξ_2 have different ξ values. The corresponding evolution of the variable ξ is shown in (b).

the probability for the appearance of certain values (events) can be very different (e.g., the probability that Europe and Northern America are hit by hurricanes). Therefore, we may define stochastic variables by considering the range of all possible values and specifying the probability for the realization of certain values.

2.1.2. The definition of PDFs

To calculate the probability for the appearance of certain values of a stochastic variable ξ (for which N data are assumed to be given), we apply the following procedure in practice:

(i) We define a so-called sample space $L_- \le x \le L_+$ that is limited by suitably chosen lower and upper bounds L_- and L_+. This sample space is used to determine the probability for the appearance of certain values of ξ. For this, we divide the sample space into N_x intervals $\Delta x = (L_+ - L_-) / N_x$.

(ii) We count the number N_k ($k = 1, N_x$) of ξ values that fall within each of the intervals considered.

(iii) We calculate N_k / N for each interval. These values N_k / N shown as a function of $x = (k - 0.5)\,\Delta x$ represent the probability $p_\xi(x, t)$ to find a value of ξ near x.

(iv) The integral over the curve N_k / N does not integrate to unity. It is equal to the difference $L_+ - L_-$, this means curves of various variables may look (depending on the value of $L_+ - L_-$) very different. It is therefore convenient to introduce the corresponding PDF F_ξ of ξ, which is given by $N_k / (N\,\Delta x)$. This quantity F_ξ is standardized: its integral over the sample space $L_- \le x \le L_+$ is equal to unity.

An example for the application of this procedure will be given in chapter 5, where vertical velocity PDFs are calculated in exactly this way for convective boundary layer turbulence.

The procedure described above is equivalent to the following expression for the probability $p_\xi(x, t)$ to find values of $\xi(t)$ within the interval $(x, x + \Delta x)$,

$$p_\xi(x,t) = P_\xi(x+\Delta x,t) - P_\xi(x,t), \tag{2.1}$$

where the distribution function $P_\xi(x, t)$ is defined by

$$P_\xi(x,t) = \frac{1}{N}\sum_{n=1}^{N}\theta\left(x-\xi^{(n)}(t)\right) = \left\langle\theta\left(x-\xi(t)\right)\right\rangle. \tag{2.2}$$

The ensemble average referred to by the brackets in (2.2) is defined by (1A.2), and the properties of the theta function θ are described in Appendix 2A. $\xi^{(n)}$ refers to the value of ξ in the realization (or the sample) n.

As pointed out above, it is usually more convenient to consider the PDF F_ξ for the appearance of ξ values instead of $p_\xi(x, t)$. This PDF is given by dividing the probability $p_\xi(x, t)$ by Δx,

$$F_\xi(x,t) = \frac{1}{N}\sum_{n=1}^{N}\frac{\theta\left(x+\Delta x-\xi^{(n)}(t)\right)-\theta\left(x-\xi^{(n)}(t)\right)}{\Delta x}. \tag{2.3}$$

The expression inside the sum is a discrete representation of the derivative of the theta function, which is given by the delta function (see the explanations given in Appendix 2A). In the limit $\Delta x \to 0$, we obtain therefore the following formula for the calculation of F_ξ,

$$F_\xi(x,t) = \left\langle\delta\left(x-\xi(t)\right)\right\rangle. \tag{2.4}$$

Sometimes, the reference to ξ leads to the question on which variables F_ξ depends. For given x and t, F_ξ represents the ensemble mean of a function of ξ (of the delta function). In other words, F_ξ is a deterministic and continuous function of x and t. Further, it is worth noting that the PDF F_ξ and distribution function P_ξ are related according to their definitions in the following way,

$$F_\xi(x,t) = \frac{d}{dx}\left\langle\theta\left(x-\xi(t)\right)\right\rangle = \frac{dP_\xi(x,t)}{dx}. \tag{2.5}$$

The middle expression of the relation (2.5) results from the relation between theta and delta functions (see Appendix 2A), and the fact that the derivative can be drawn in front of the ensemble average. This expression is consistent with (2.3) in the limit $\Delta x \to 0$. The last expression follows from (2.2).

2.1.3. General properties of PDFs

To prepare the following developments we consider some fundamental properties of the distribution function P_ξ. These are given by

$$P_\xi(-\infty) = 0, \tag{2.6a}$$

$$P_\xi(\infty) = 1, \tag{2.6b}$$

$$0 \le P_\xi(x) \le P_\xi(x + dx) \le 1. \tag{2.6c}$$

The relations (2.6a-b) follow by considering (2.2) for the limit cases $|x| \to \infty$. Relation (2.6c) follows from the relations (2.6a-b) in conjunction with the fact that the probability $p_\xi(x) = P_\xi(x + dx) - P_\xi(x)$ (which is given by N_k / N, see the procedure pointed out above) must be non-negative. Hence, the distribution function P_ξ is a non-decreasing function of x that increases from 0 to 1 as x varies from $-\infty$ to ∞.

The fundamental properties of the PDF F_ξ are the following ones,

$$\int dx\ F_\xi(x) = P_\xi(\infty) - P_\xi(-\infty) = 1, \tag{2.7a}$$

$$F_\xi(-\infty) = F_\xi(\infty) = 0, \tag{2.7b}$$

$$F_\xi(x) \ge 0. \tag{2.7c}$$

Relation (2.7a) follows by integration of (2.5) and use of (2.6a-b). For $|x| \to \infty$, the distribution function P_ξ monotonically tends to a constant, see (2.6a-c). Therefore, its derivative F_ξ has to tend to zero, which implies (2.7b). The validity of (2.7c) becomes obvious by adopting (2.6c): the derivative of a non-decreasing function has to be non-negative. It is worth noting that the properties (2.6a-c) and (2.7a-c) also apply to vectorial stochastic processes considered in section 2.3.

2.2. The characterization of PDFs by moments

2.2.1. The calculation of moments by PDFs

PDFs may have a variety of different forms. Very often, one is not so much interested in all this detailed information but first of all in a few global parameters that characterize essential characteristics of PDFs. Such parameters are given by the moments of a PDF. They are defined by ($n = 0, 1, \cdots$)

$$\left\langle \xi^n \right\rangle = \int dx\ x^n F_\xi(x). \tag{2.8}$$

The dependence of ξ on t is not indicated to simplify the following explanations. The consistency of (2.8) may be proved by replacing F_ξ by the expression (2.4) and adopting the properties of delta functions. The power n determines the order of a moment. Thus, $<\xi^n>$ is called the moment of n^{th}-order.

The moment of first-order $<\xi>$ is nothing but the mean of ξ. It provides essential information: this is the value which we have to expect for ξ. However, most of the values of ξ will have some deviations

$$\xi' = \xi - \langle\xi\rangle \tag{2.9}$$

from the mean $<\xi>$, which are called fluctuations. To characterize such deviations, one applies (the root of) the variance σ^2 of ξ, which is defined by

$$\sigma^2 = \langle\xi'^2\rangle = \int dx \left(x - \langle\xi\rangle\right)^2 F_\xi(x). \tag{2.10}$$

Examples for the effect of σ will be given in section 2.2.3.

Further characteristic measures for the properties of PDFs are the skewness Sk and kurtosis Ku. They are defined by

$$Sk = \frac{\langle\xi'^3\rangle}{\sigma^3}, \qquad Ku = \frac{\langle\xi'^4\rangle}{\sigma^4}. \tag{2.11}$$

These parameters are standardized in terms of σ such that they are dimensionless. The skewness is used to assess the asymmetry of PDFs. For symmetric PDFs, the kurtosis indicates the deviation from a Gaussian PDF that describes usually the equilibrium distribution of stochastic variables. Examples for the influence of Sk and Ku on PDF shapes will be given below.

2.2.2. The calculation of PDFs by moments

The moments of a PDF are therefore fully determined by the knowledge of this PDF. Vice versa, the knowledge of all the moments of a PDF F_ξ also enables the construction of F_ξ. To see this, we consider the characteristic function C_ξ that is defined by ($i^2 = -1$)

$$C_\xi(u) = \langle e^{iu\xi}\rangle = \int dx\, e^{iux} F_\xi(x). \tag{2.12}$$

The n^{th}-moment of F_ξ can be obtained from C_ξ by differentiation,

$$\langle\xi^n\rangle = \frac{1}{i^n}\left[\frac{d^n C_\xi(u)}{du^n}\right](u = 0). \tag{2.13}$$

Therefore, the Taylor expansion of C_ξ may be written as

$$C_\xi(u) = 1 + \sum_{n=1}^{\infty} \frac{(iu)^n}{n!} \langle \xi^n \rangle. \tag{2.14}$$

The function C_ξ is nothing but the Fourier transform of the PDF F_ξ (if we assume that x runs from minus to plus infinity). Thus, the PDF F_ξ may be written as the inverse Fourier transform of C_ξ,

$$F_\xi(x) = \frac{1}{2\pi} \int du\ e^{-iux} C_\xi(u) = \frac{1}{2\pi} \int du\ e^{-iux} \left\{ 1 + \sum_{n=1}^{\infty} \frac{(iu)^n}{n!} \langle \xi^n \rangle \right\}, \tag{2.15}$$

where relation (2.14) is used. The expression (2.15) reveals that the PDF F_ξ is uniquely determined by its moments. Unfortunately, there is no way to construct specific PDFs by truncating the series in (2.15) at any order: moments of high-order involve information that has the same relevance as that of low-order moments. The latter may be seen by means of the relation $<\xi^n> \le <\xi^{2n}>^{1/2}$, which follows from Schwarz's inequality (2.30) by setting $\varphi = \xi^n$ and $\psi = 1$. This relation states that the root of the high-order moment $<\xi^{2n}>$ is at least of the same order as the low-order moment $<\xi^n>$.

A way to construct at least some specific PDFs is to rewrite (2.15) by the introduction of cumulants K_n. These are defined by the relation

$$C_\xi(u) = 1 + \sum_{n=1}^{\infty} \frac{(iu)^n}{n!} \langle \xi^n \rangle = \exp\left\{ \sum_{n=1}^{\infty} \frac{(iu)^n}{n!} K_n \right\}. \tag{2.16}$$

The development of the exponential and comparison of coefficients of terms in growing order in iu shows that the first n cumulants can be expressed by the first n moments and vice versa. The relations up to the order n = 4 may be written

$$K_1 = \langle \xi \rangle, \qquad K_2 = \langle \xi'^2 \rangle, \qquad K_3 = \langle \xi'^3 \rangle, \qquad K_4 = \langle \xi'^4 \rangle - 3 \langle \xi'^2 \rangle^2. \tag{2.17}$$

In contrast to the properties of moments, cumulants of high order may be seen to be less relevant than cumulants of low order. This is caused by the fact that cumulants of higher than second order describe deviations from Gaussian PDFs (see section 2.2.3) that are often found to provide reasonable approximations for PDFs of stochastic variables. However, it is impossible to truncate (2.16) at any K_n. The theorem of Marcienkiewicz (1939) shows that one has two possibilities: (i) one considers zero (K_2 cannot be taken as equal to zero but has to be considered as a vanishing parameter, see the relation (2.21)) or nonzero K_1 and K_2 but neglects all K_n with $n \ge 3$, or (ii) one considers all K_n to be nonzero. In all the other cases the PDF cannot be positive everywhere. The implications of the relevant first case will be shown in the next subsection.

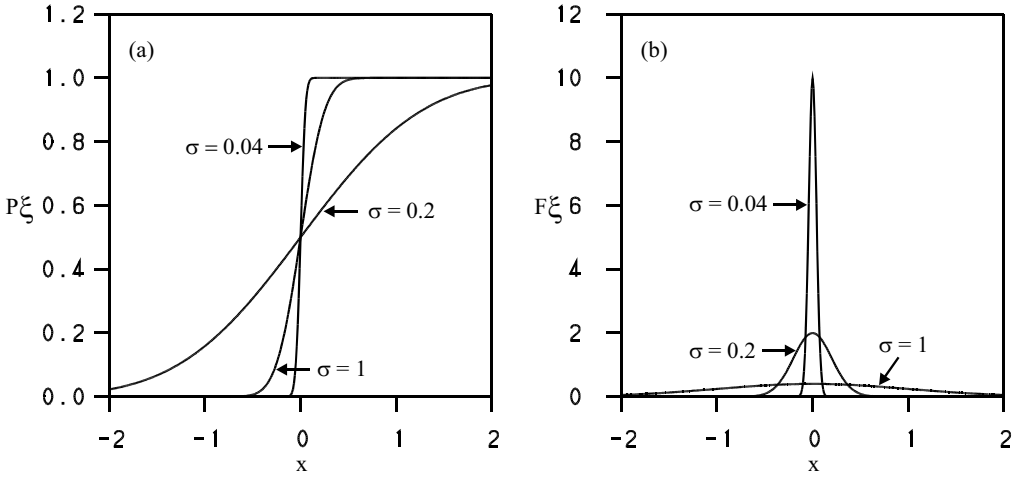

Fig. 2.2. Various Gaussian distribution functions and PDFs according to (2.19) and (2.18) in dependence on $\sigma = K_2^{1/2}$ for $K_1 = 0$.

2.2.3. An example: the Gaussian PDF and its moments

By neglecting all K_n with $n \geq 3$, the general expression (2.15) for a PDF reduces in combination with (2.17) to

$$F_\xi(x) = \frac{1}{\sqrt{2\pi K_2}} \exp\left\{ -\frac{(x - K_1)^2}{2K_2} \right\}. \tag{2.18}$$

This PDF is called a Gaussian PDF. Examples are given in Fig. 2.2 together with the corresponding distribution functions, which are given by the expression

$$P_\xi(x) = \frac{1}{2} + \frac{1}{2} \operatorname{erf}\left(\frac{x - K_1}{\sqrt{2K_2}} \right). \tag{2.19}$$

Here, erf(y) refers to the error function that is defined by

$$\operatorname{erf}(y) = \frac{2}{\sqrt{\pi}} \int_0^y dt\, e^{-t^2}. \tag{2.20}$$

Characteristic properties of a Gaussian PDF are given by a skewness Sk = 0 and a kurtosis Ku = 3 (which implies $K_3 = K_4 = 0$). Another relevant feature of a Gaussian PDF is that F_ξ approaches to a delta function for a vanishing variance,

$$\lim_{K_2 \to 0} \frac{1}{\sqrt{2\pi K_2}} \exp\left\{ -\frac{(x - K_1)^2}{2K_2} \right\} = \delta(x - K_1). \tag{2.21}$$

2.3. PDFs of several variables

2.3.1. PDFs

The definitions (2.2) and (2.4) for distribution functions and PDFs can be easily rewritten to cover the case of several variables. For doing this, we consider a vector $\boldsymbol{\xi}(t) = \{\xi_1(t), \xi_2(t), \cdots, \xi_N(t)\}$ of N stochastic variables. For simplicity, we restrict the attention to the consideration of the probability for the combined event to find the vector $\boldsymbol{\xi}$ at the time t' at $\mathbf{x}'$, and at the (later) time t at $\mathbf{x}$ (the following definitions can be straightforwardly extended to other cases). The joint distribution function $P_{\xi\xi}$ reads for this case

$$P_{\xi\xi}(\mathbf{x},t;\mathbf{x}',t) = \left\langle \theta\left(\mathbf{x}-\boldsymbol{\xi}(t)\right)\theta\left(\mathbf{x}'-\boldsymbol{\xi}(t')\right)\right\rangle, \tag{2.22}$$

and the corresponding joint PDF $F_{\xi\xi}$ follows in extension of equation (2.4) as

$$F_{\xi\xi}(\mathbf{x},t;\mathbf{x}',t') = \left\langle \delta\left(\mathbf{x}-\boldsymbol{\xi}(t)\right)\delta\left(\mathbf{x}'-\boldsymbol{\xi}(t')\right)\right\rangle. \tag{2.23}$$

The vectorial theta and delta functions $\theta(\mathbf{x} - \boldsymbol{\xi}(t))$ and $\delta(\mathbf{x} - \boldsymbol{\xi}(t))$ involved here are defined in Appendix 2A.

The knowledge of $F_{\xi\xi}$ enables the calculation of averages of functions Q by means of the relation

$$\left\langle Q(\boldsymbol{\xi}(t),t;\boldsymbol{\xi}(t'),t')\right\rangle = \int d\mathbf{x}\, d\mathbf{x}'\, Q(\mathbf{x},t;\mathbf{x}',t')\, F_{\xi\xi}(\mathbf{x},t;\mathbf{x}',t). \tag{2.24}$$

The consistency of this relation with the definition of $F_{\xi\xi}$ may be seen by adopting relation (2.23) for $F_{\xi\xi}$ on the right-hand side in combination with the properties of delta functions. Another way is to set $Q = \delta(\mathbf{x} - \boldsymbol{\xi}(t))\, \delta(\mathbf{x}' - \boldsymbol{\xi}(t'))$ in (2.24), which recovers the definition (2.23) of $F_{\xi\xi}$. The specification Q = 1 reveals the normalization constraint for $F_{\xi\xi}$ to integrate to unity.

For a function Q that is only a function of $\boldsymbol{\xi}(t)$, we may rewrite relation (2.24) into the corresponding relation for the one-point case,

$$\left\langle Q(\boldsymbol{\xi}(t),t)\right\rangle = \int d\mathbf{x}\, Q(\mathbf{x},t) F_{\xi}(\mathbf{x},t). \tag{2.25}$$

To obtain this relation, we applied the following relation between the one-point PDF F_ξ and two-point PDF $F_{\xi\xi}$,

$$F_{\xi}(\mathbf{x},t) = \int d\mathbf{x}'\, F_{\xi\xi}(\mathbf{x},t;\mathbf{x}',t), \tag{2.26}$$

which results from the integration of relation (2.23) and the use of the properties of delta functions. Hence, the knowledge of the two-point PDF $F_{\xi\xi}$ implies the knowledge of the one-point statistics.

2.3.2. Correlations

The consideration of the joint statistics of several stochastic variables leads to a new question: how is it possible to assess the intensity of the coupling of different stochastic variables? This question is very relevant in particular to theoretical analyses because the consideration of the limiting case of statistically independent stochastic variables is often a requirement for the applicability of approximations and the derivation of basic conclusions.

This question of the intensity of the coupling of different stochastic variables is addressed in terms of correlation coefficients, as pointed out now. Let us consider any stochastic variables φ and ψ which are defined on the same sample space. In terms of the notation applied above, we could set $\xi_i'(t) = \varphi$ and $\xi_k'(t') = \psi$. Further, it is convenient to look at these variables in their standardized form, this means we take $\varphi^* = \varphi / \langle\varphi^2\rangle^{1/2}$ and $\psi^* = \psi / \langle\psi^2\rangle^{1/2}$. The ensemble-averaged product of these variables defines then their correlation coefficient

$$r_{\varphi\psi} = \left\langle \varphi^* \psi^* \right\rangle. \tag{2.27}$$

To assess the bounds of $r_{\varphi\psi}$ we define a non-negative functional H as a function of any parameter p by

$$H = \left\langle \left(\varphi^* + p\psi^*\right)^2 \right\rangle = 1 + p^2 + 2pr_{\varphi\psi} \geq 0. \tag{2.28}$$

This relation implies $-1 \leq h\, r_{\varphi\psi}$, where the abbreviation $h = 2p / (1 + p^2)$ is introduced. The differentiation between the cases that h is positive or negative leads then to the constraint

$$-\frac{1}{|h|} \leq r_{\varphi\psi} \leq \frac{1}{|h|}. \tag{2.29}$$

A simple analysis of h as a function of p reveals that $|h| \leq 1$. Therefore, $r_{\varphi\psi}$ satisfies the condition (2.29) provided

$$|r_{\varphi\psi}| \leq 1. \tag{2.30}$$

This is the unequality of Schwarz, which leads to many relevant implications.

Accordingly, $|r_{\varphi\psi}|$ has 0 as lower and 1 as upper bound. The lower limit $|r_{\varphi\psi}| = 0$ applies to the case that φ^* and ψ^* are uncorrelated. The upper limit $|r_{\varphi\psi}| = 1$ appears if φ^* and ψ^* are related to each other by a deterministic relation. We may assume that there exists any linear relationship between them, $\varphi^* + p\,\psi^* = 0$. In this case, the calculation of $r_{\varphi\psi}$ according to (2.27) leads to $r_{\varphi\psi} = -p$, and relation (2.28) provides $1 + p^2 + 2\,p\,r_{\varphi\psi} = 0$. These two constraints imply then $|r_{\varphi\psi}| = 1$. The consideration of these limit cases reveals that correlations appear if the evolution

of stochastic variables is governed (at least partly) by the same cause. This is for instance the case if two scalars are transported by the same turbulent eddy.

2.3.3. Conditional PDFs

It is very advantageous for some analyses to present joint PDFs of several variables such that one takes reference to the important special case that there is no correlation between different stochastic variables. This can be achieved by introducing conditional PDFs. Regarding the joint PDF (2.23), such a conditional PDF $F_{\xi|\xi}$ is defined by the relation

$$F_{\xi\xi}\left(\mathbf{x},t;\mathbf{x}',t'\right)=F_{\xi|\xi}\left(\mathbf{x},t\,\middle|\,\mathbf{x}',t'\right)F_{\xi}\left(\mathbf{x}',t'\right), \tag{2.31}$$

this means $F_{\xi|\xi}$ is given by dividing the left-hand side by $F_{\xi}(\mathbf{x}', t)$. The conditional PDF $F_{\xi|\xi}$ represents the PDF of $\boldsymbol{\xi}(t)$ under the condition that $\boldsymbol{\xi}(t') = \mathbf{x}'$ (see below equation (2.36)). $F_{\xi|\xi}$ becomes equal to the unconditional PDF $F_{\xi}(\mathbf{x}, t)$ if $\boldsymbol{\xi}(t)$ is independent of $\boldsymbol{\xi}(t')$. Only in this case, the two-point PDF $F_{\xi\xi}$ is given by the product of the single-variable PDFs.

By adopting (2.26), the integration of (2.31) over $\mathbf{x}'$ leads to

$$F_{\xi}\left(\mathbf{x},t\right)=\int d\mathbf{x}'\,F_{\xi|\xi}\left(\mathbf{x},t\,\middle|\,\mathbf{x}',t'\right)F_{\xi}\left(\mathbf{x}',t'\right). \tag{2.32}$$

This relation explains the relevance of conditional PDFs for the modeling of the evolution of PDFs. The PDF $F_{\xi}(\mathbf{x}, t)$ may be seen as the result of the dynamics of the system considered (its evolution equation which is independent of the specification of initial conditions), and concrete initial conditions for a case considered. Information on these initial conditions is provided via $F_{\xi}(\mathbf{x}', t')$, which may be considered as an initial PDF. Information on the system dynamics is provided by the conditional PDF $F_{\xi|\xi}$. Therefore, general solutions (independent of initial conditions) for stochastic systems can be presented in terms of $F_{\xi|\xi}$ (see the example in chapter 3), and (2.32) is used then in conjunction with the specification of the initial PDF $F_{\xi}(\mathbf{x}', t')$ to calculate a specific PDF $F_{\xi}(\mathbf{x}, t)$.

Conditional means can be defined in correspondence to (2.31),

$$\left\langle Q(\boldsymbol{\xi}(t),t;\boldsymbol{\xi}(t'),t')\right\rangle=\int d\mathbf{x}'\left\langle Q(\boldsymbol{\xi}(t),t;\boldsymbol{\xi}(t'),t')\,\middle|\,\mathbf{x}',t'\right\rangle F_{\xi}\left(\mathbf{x}',t'\right), \tag{2.33}$$

where the conditional mean is given by the expression,

$$\left\langle Q(\boldsymbol{\xi}(t),t;\boldsymbol{\xi}(t'),t')\,\middle|\,\mathbf{x}',t'\right\rangle=\int d\mathbf{x}\;Q\left(\mathbf{x},t;\mathbf{x}',t'\right)F_{\xi|\xi}\left(\mathbf{x},t\,\middle|\,\mathbf{x}',t'\right). \tag{2.34}$$

Hence, conditional means are calculated as means of the conditional PDF. The consistency of (2.33) with (2.24) can be seen by inserting (2.34) into (2.33) and adopting (2.31).

An important specification of (2.33) is given by

$$\left\langle Q(\xi(t),t;\xi(t'),t')\,\delta\left(\mathbf{x}'-\xi(t')\right)\right\rangle = \int d\mathbf{x}\; Q(\mathbf{x},t;\mathbf{x}',t')\left\langle \delta\left(\mathbf{x}-\xi(t)\right)\delta\left(\mathbf{x}'-\xi(t')\right)\right\rangle$$

$$= \left\langle Q(\xi(t),t;\xi(t'),t')\middle|\, \mathbf{x}',t'\right\rangle F_{\xi}(\mathbf{x}',t'). \qquad (2.35)$$

The first rewriting of the left-hand side results from the properties of delta functions. The second line makes use of the definitions of $F_{\xi\xi}$, $F_{\xi|\xi}$ and (2.34). Such expressions as (2.35) will be used frequently regarding the construction of PDF transport equations. The choice $Q = \delta(\mathbf{x} - \xi(t))$ in (2.35) implies the relation

$$F_{\xi|\xi}(\mathbf{x},t;\mathbf{x}',t') = \left\langle \delta(\mathbf{x}-\xi(t))\middle|\, \mathbf{x}',t'\right\rangle, \qquad (2.36)$$

which makes again use of the definitions of $F_{\xi\xi}$ and $F_{\xi|\xi}$. This relation explains conditional PDFs as means of corresponding conditional delta functions. For $t = t'$, we know that $\xi(t) = \mathbf{x}'$. Relation (2.36) then implies

$$F_{\xi|\xi}\left(\mathbf{x},t'\middle|\, \mathbf{x}',t'\right) = \delta\left(\mathbf{x}-\mathbf{x}'\right), \qquad (2.37)$$

which has to be used as initial condition for the calculation of $F_{\xi|\xi}$, see chapter 3.

2.4. Statistically most-likely PDFs

After considering essential properties of PDFs, let us address now the question how specific PDFs can be constructed for a given case. It was shown in section 2.2.2 that a general solution of this question cannot be found by a formal approach (the truncation of cumulant series at any order of approximation). Thus, a physical concept has to be involved. This can be done by taking reference to the predictability of the state of a stochastic variables considered, which is illustrated in Fig. 2.3. This figure shows that the predictability of the state of a stochastic variable is determined by L. For $L \to 0$, the PDF becomes a delta function. The predictability is maximal in this case (the uncertainty is minimal): we know that $\xi(t)$ will realize the value zero. For $L \to \infty$, the predictability of the state of $\xi(t)$ is minimal (the uncertainty is maximal): the probability of their realization is equal for all states.

The concept of the predictability of states of stochastic variables can be used in the following way for the construction of PDFs. Very often we do not know anything about a PDF with the exception of a few low-order moments (means and variances). This knowledge is insufficient to determine the PDF, for which one would have to provide all its moments. What one can do in this case is to apply information about known moments combined with the constraint that the predictability related to the PDF to be constructed has to be minimal. This approach makes only use of available information. Its details will be described now.

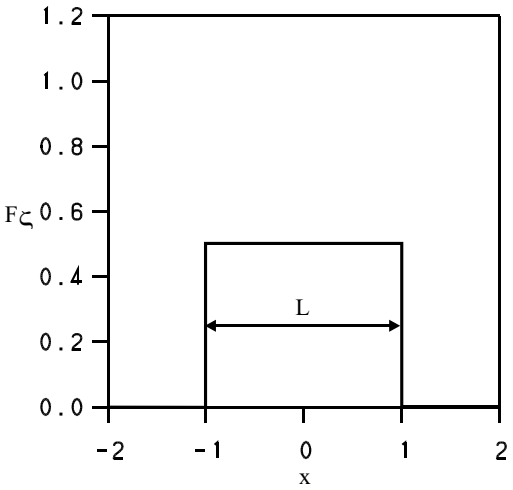

Fig. 2.3. The PDF of a uniformly distributed stochastic variable $\xi(t)$. L refers to the interval in which the PDF is nonzero.

2.4.1. The measurement of uncertainty

The first step to realize this concept is to define a unique measure S of the predictability of the state of stochastic variables. This measure S, which is called entropy, has to be a functional of the joint PDF F_ξ of the variables involved, this means $S = S[F_\xi]$. Without restriction of generality, we may expect S to be the average of any function $H(F_\xi)$ that has to be determined,

$$S\left[F_\xi\right] = \int d\mathbf{x}\; F_\xi(\mathbf{x},t) H(F_\xi(\mathbf{x},t)). \tag{2.38}$$

To derive a constraint that enables the specification of the concrete structure of S one considers at best the special case of two independent variables $\xi_1(t)$ and $\xi_2(t)$. Their joint PDF is given by the product of the PDF for $\xi_1(t)$ and PDF for $\xi_2(t)$. In this case, S should satisfy the equation (Shannon 1948, Jaynes 1957)

$$S\left[F_{\xi_1} F_{\xi_2}\right] = S\left[F_{\xi_1}\right] + S\left[F_{\xi_2}\right]. \tag{2.39}$$

Relation (2.39) states that the uncertainty related to a joint PDF of independently distributed variables has to arise from independent contributions, this means the uncertainty related to the PDF of $\xi_2(t)$ should not affect the uncertainty related to the PDF of $\xi_1(t)$.

By inserting (2.38) into (2.39) we obtain the relation

$$0 = \int dx_1 \int dx_2\, F_{\xi_1} F_{\xi_2} \left\{ H(F_{\xi_1} F_{\xi_2}) - H(F_{\xi_1}) - H(F_{\xi_2}) \right\}, \tag{2.40}$$

where the normalization conditions for the PDFs of $\xi_1(t)$ and $\xi_2(t)$ are applied. To satisfy equation (2.40), it is required that the bracket term vanishes. In order to solve the resulting equation for H, we rewrite it by means of the parametrization $H(F_\xi) = -K(F_\xi) \ln(F_\xi)$, where $K(F_\xi)$ is any unknown function. This results in the

following constraint for K,

$$0 = \ln\left(F_{\xi_1}\right)\left\{K(F_{\xi_1}F_{\xi_2}) - K(F_{\xi_1})\right\} + \ln\left(F_{\xi_2}\right)\left\{K(F_{\xi_1}F_{\xi_2}) - K(F_{\xi_2})\right\}. \tag{2.41}$$

The independence of the PDFs of $\xi_1(t)$ and $\xi_2(t)$ implies the need to consider $K(F_\xi)$ as a constant, $K(F_\xi) = K$. This constant K is called the Boltzmann constant in the classical statistical mechanics, where it is introduced to give the entropy a suitable dimension. Regarding the use of S here, it is convenient to set K = 1. Thus, we derive for S the expression

$$S = -\int d\mathbf{x}\; F_\xi(\mathbf{x},t)\ln\left(F_\xi(\mathbf{x},t)\right). \tag{2.42}$$

The appearance of the minus sign may be justified by inserting the Gaussian PDF (2.18) into relation (2.42), which results in a positive entropy $S = \ln(2\,\pi\,e\,\sigma^2)^{1/2}$. Obviously, σ determines the uncertainty related to a Gaussian function in analogy to L in Fig. 2.3. For $\sigma \to 0$ (F_ξ approaches to a delta function), S goes to minus infinity so that the uncertainty is minimal. For $\sigma \to \infty$ (F_ξ approaches to zero), S goes to plus infinity so that the uncertainty is maximal. It is worth noting that the absolute value of S depends on the units of sample space variables. This may be seen by rewriting (2.42) in terms of dimensionless sample space variables $\mathbf{y} = \mathbf{x} / a$, where a refers to the normalization of **x**. This results in the relation (N being the dimension of the sample space)

$$S = N\ln(a) - \int d\mathbf{y}\; F_\xi(\mathbf{y},t)\ln\left(F_\xi(\mathbf{y},t)\right). \tag{2.43}$$

Nevertheless, entropy changes are unaffected by such transformations such that they can be used to study differences of the uncertainty related to various PDFs.

2.4.2. Statistically most-likely PDFs

Next, we construct a PDF according to the concept described above. This will be done for a PDF of only one variable. The extension to the case of several variables can easily be performed. We assume that we know $n = 1, \cdots, s$ moments

$$\left\langle \xi^n \right\rangle = \int dx\; x^n F_\xi(x). \tag{2.44}$$

The time dependence of F_ξ is not indicated for simplicity. The goal is to construct a PDF which has s moments that agree with the given ones but maximizes the entropy S (and therefore the uncertainty). According to the calculus of variations, we extend the entropy S to a functional S^* by involving the conditions (2.44),

$$S^* = -\int dx\left\{F_\xi(x)\ln\left(F_\xi(x)\right) + \sum_{n=0}^{s}\mu_n x^n F_\xi(x) - F_\xi(x)\right\}. \tag{2.45}$$

The μ_n are Lagrange multipliers which have to be chosen such that the conditions (2.44) are satisfied. The last term on the right-hand side of (2.45) modifies the multiplier μ_0, which simplifies the following explanations. To find the maximum of S^*, we have to set the functional variation of S^* regarding to F_ξ equal to zero,

$$\frac{\delta S^*}{\delta F_\xi} = 0 = -\int dx \left\{ \ln\left(F_\xi(x)\right) + \sum_{n=0}^{s} \mu_n x^n \right\}. \tag{2.46}$$

The resulting expression for the PDF F_ξ reads

$$F_\xi(x) = \exp\left\{ -\sum_{n=0}^{s} \mu_n x^n \right\}. \tag{2.47}$$

The calculation of the second functional variation of S^* reveals that expression (2.47) maximizes the functional (2.45). The PDF (2.47) is called a statistically most-likely (SML) PDF. By introducing modified Lagrange multipliers λ_n, relation (2.47) may be rewritten into

$$F_\xi(x) = \exp\left\{ -\sum_{n=0}^{s} \frac{\lambda_n}{n} \left(x - \langle \xi \rangle\right)^n \right\}. \tag{2.48}$$

The s + 1 factors λ_n are uniquely determined by the s conditions (2.44) and the normalization of F_ξ. By reformulating the λ_n, one may see that (2.48) corresponds to the Taylor series of $\ln(F_\xi)$ at $x = \langle\xi\rangle$, which is truncated at the order s.

2.5. Examples for statistically most-likely PDFs

2.5.1. Second-order SML PDF: unbounded variables

As a first example we consider a second-order SML PDF for the case of a N-dimensional vector process of unbounded variables (e.g., the components of the velocity vector). We assume that the first two moments are known,

$$1 = \int d\mathbf{x}\, F_\xi(\mathbf{x}), \tag{2.49a}$$

$$\langle \xi_i \rangle = \int d\mathbf{x}\, x_i F_\xi(\mathbf{x}), \tag{2.49b}$$

$$\langle \xi_i \xi_j \rangle = \int d\mathbf{x}\, x_i x_j F_\xi(\mathbf{x}). \tag{2.49c}$$

One may prove that the corresponding SML PDF has the following structure,

$$F_\xi(\mathbf{x}) = \frac{1}{N_F} \exp\left\{ -\lambda_m \left(x_m - \langle \xi_m \rangle\right) - \frac{1}{2} \lambda_{mn} \left(x_m - \langle \xi_m \rangle\right)\left(x_n - \langle \xi_n \rangle\right) \right\}. \tag{2.50}$$

The Lagrangian multipliers N_F, λ_m and λ_{mn} are uniquely determined by (2.49a-c). A simple way to adopt these relations for the calculation of λ_m and λ_{mn} is the use of partial integration. This results in

$$0 = \int d\mathbf{x}\, \frac{\partial F_\xi(\mathbf{x})}{\partial x_k} = -\lambda_k, \qquad 0 = \int d\mathbf{x}\, \frac{\partial\left[\left(x_l - \langle \xi_l \rangle\right) F_\xi(\mathbf{x})\right]}{\partial x_k} = \delta_{kl} - \lambda_{kn}\sigma_{nl}, \qquad (2.51)$$

where the variance matrix $\sigma_{nl} = \langle \xi'_n\, \xi'_l \rangle$ is introduced. Hence, one obtains $\lambda_m = 0$ and $\lambda_{mn} = \sigma^{-1}{}_{mn}$, where σ^{-1} is the inverse matrix of σ. The remaining multiplier N_F has to be calculated by adopting the constraint (2.49a). This provides

$$N_f = \int d\mathbf{x}\, \exp\left\{-\frac{1}{2}\sigma^{-1}{}_{mn}\left(x_m - \langle \xi_m \rangle\right)\left(x_n - \langle \xi_n \rangle\right)\right\} = \left|\det\left(\sigma^{1/2}\right)\right| \int d\mathbf{z}\, \exp\left\{-\frac{z_n z_n}{2}\right\}$$

$$= \left|\det\left(\sigma^{1/2}\right)\right| \left[\int dz_1 \exp\left\{-\frac{z_1^2}{2}\right\}\right]^N = (2\pi)^{N/2}\sqrt{\det(\sigma)}. \qquad (2.52)$$

The integral over $\mathbf{x}$ is rewritten by means of the transformation $x_k - \langle \xi_k \rangle = \sigma^{1/2}{}_{kn}\, z_n$. The integration over $\mathbf{z}$ can be reduced then to the calculation of an one-dimensional integral. The last expression is obtained by calculating it and applying the relation $\det(\sigma) = \det(\sigma^{1/2}\, \sigma^{1/2}) = \det(\sigma^{1/2})\, \det(\sigma^{1/2})$. Accordingly, the SML PDF is found to be

$$F_\xi(\mathbf{x}) = \frac{1}{(2\pi)^{N/2}\sqrt{\det(\sigma)}} \exp\left\{-\frac{1}{2}\sigma^{-1}{}_{mn}\left(x_m - \langle \xi_m \rangle\right)\left(x_n - \xi_n\right)\right\}. \qquad (2.53)$$

This expression is nothing but the extension of the Gaussian PDF (2.18) to the case of several variables.

Essential properties of this PDF may be found again by partial integration. By replacing the linear term $x_l - \langle \xi_l \rangle$ in the integral of relation (2.51) by the quadratic $(x_l - \langle \xi_l \rangle)\,(x_m - \langle \xi_m \rangle)$ and cubic expression $(x_l - \langle \xi_l \rangle)\,(x_m - \langle \xi_m \rangle)\,(x_n - \langle \xi_n \rangle)$, one derives (after multiplication of these relations with σ_{jk})

$$\left\langle \xi'_j\, \xi'_l\, \xi'_m \right\rangle = 0, \qquad (2.54a)$$

$$\left\langle \xi'_j\, \xi'_l\, \xi'_m\, \xi'_n \right\rangle = \sigma_{jl}\sigma_{mn} + \sigma_{jm}\sigma_{ln} + \sigma_{jn}\sigma_{lm}. \qquad (2.54b)$$

Hence, the triple correlations of Gaussian processes vanish, and the fourth-order moments are found to be parametrized by a symmetric combination of variances. Corresponding relations may be found for higher-order moments: all the odd moments are equal to zero and even moments are determined by symmetric combinations of variances.

2.5.2. Fourth-order SML PDF: unbounded variables

As a second example, we assume that the first four PDF moments are known. The inclusion of third- and fourth-order moments permits the consideration of turbulence structure effects. The incorporation of third-order moments enables the simulation of bimodal turbulent motions (transports in updrafts and downdrafts in convective boundary layer turbulence, see chapter 5). The incorporation of fourth-order moments enables the simulation of an enhancement of the turbulent transport efficiency due to the appearance of large-scale structures (Heinz & Schaller 1996).

We consider again the case of one variable that is assumed to be unbounded. The corresponding SML PDF reads

$$F_\xi(x) = \frac{1}{N_F}\exp\left\{-\lambda_1\left(x-\langle\xi\rangle\right)-\frac{\lambda_2}{2}\left(x-\langle\xi\rangle\right)^2-\frac{\lambda_3}{3}\left(x-\langle\xi\rangle\right)^3-\frac{\lambda_4}{4}\left(x-\langle\xi\rangle\right)^4\right\}. \tag{2.55}$$

A third-order SML PDF would be obtained by neglecting the last term in the exponential, but such a PDF diverges at high positive or negative values of x. This gives a mathematical reason for involving fourth-order moments.

The coefficient N_F has to be obtained by the normalization condition of F_ξ, and the multipliers λ_k (k = 1, 4) have to the calculated by the first four moments of (2.55). Such relations for λ_k can be derived by partial integration in accordance with (2.51). This results in

$$\lambda_1 + \lambda_3\langle\xi'^2\rangle + \lambda_4\langle\xi'^3\rangle = 0, \tag{2.56a}$$

$$\lambda_2\langle\xi'^2\rangle + \lambda_3\langle\xi'^3\rangle + \lambda_4\langle\xi'^4\rangle = 1, \tag{2.56b}$$

$$\lambda_2\langle\xi'^3\rangle + \lambda_3\left(\langle\xi'^4\rangle - \langle\xi'^2\rangle^2\right) + \lambda_4\left(\langle\xi'^5\rangle - \langle\xi'^3\rangle\langle\xi'^2\rangle\right) = 0, \tag{2.56c}$$

$$\lambda_2\langle\xi'^4\rangle + \lambda_3\left(\langle\xi'^5\rangle - \langle\xi'^3\rangle\langle\xi'^2\rangle\right) + \lambda_4\left(\langle\xi'^6\rangle - \langle\xi'^3\rangle^2\right) = 3\langle\xi'^2\rangle. \tag{2.56d}$$

Unfortunately, analytical expressions for λ_k (as functions of the first four moments of F_ξ) cannot be obtained due to the appearance of the fifth- and sixth-order moments. However, the latter may be found by successive approximation: (i) appropriate initial values are chosen for them, (ii) λ_1, λ_2, λ_3, λ_4 are calculated by the equations (2.56a-d), and (iii) the third- up to the sixth-order moments of F_ξ are computed by means of (2.55). By choosing the calculated fifth- and sixth-order moments as new initial values, this procedure has to be repeated until the third- and fourth-order moments provided by (2.55) agree with their known values. A unique solution of that variation problem always exists.

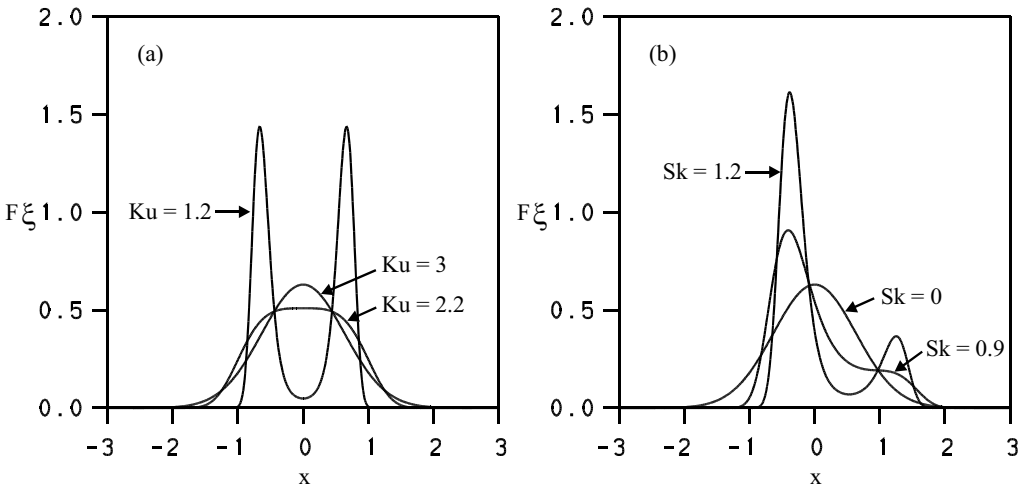

Fig. 2.4. Fourth-order SML PDFs for a unbounded variable in dependence on (a) Ku where Sk = 0, and (b) Sk where Ku = 3. $\sigma^2 = \langle \xi'^2 \rangle = 0.4$ was kept constant.

Examples for such fourth-order SML PDFs are given in Fig. 2.4, which shows the effects of the kurtosis Ku and skewness Sk. The possibility of such variations is restricted. The unequality of Schwarz (2.30) provides the constraint $Sk^2 + 1 \leq Ku$, which leads to a lower limit $1 \leq Ku$ regarding the Ku variations in Fig. 2.4a and to a upper limit $Sk \leq 2^{1/2}$ for the Sk variations in Fig. 2.4b. In addition to this, one has the constraint $Ku \leq 3$ regarding the Ku-variations in Fig. 2.4a. This follows as a consequence of the fact that λ_4 has to be non-negative to assure that F_ξ vanishes at high x. The lower bound $\lambda_4 = 0$ of λ_4 corresponds to a Gaussian PDF in Fig. 2.4a, which implies the upper limit Ku = 3. These figures reveal that Ku and Sk variations enable the simulation of a variety of processes that may be seen as a superposition of two modes. Applications of (2.55) will be presented in chapter 5.

2.5.3. Second-order SML PDF: bounded variables

As a third example for a SML PDF we consider the case of one variable which is bounded. This is relevant to simulations of scalar fluctuations that are usually bounded (for instance mass fractions of substances are bounded by zero and unity due to their definition). As in section 2.5.1, we assume that the first two moments are known. The corresponding SML PDF of second-order is given by

$$F_\xi(x) = \frac{1}{N_F} \exp\left\{ -\lambda_1 \left(x - \langle \xi \rangle \right) - \frac{\lambda_2}{2} \left(x - \langle \xi \rangle \right)^2 \right\}, \tag{2.57}$$

where N_F, λ_1 and λ_2 are Lagrangian multipliers. Their calculation is now more complicated than for the case of unbounded variables. Instead of the relations (2.51) we obtain for λ_1 and λ_2 the relations

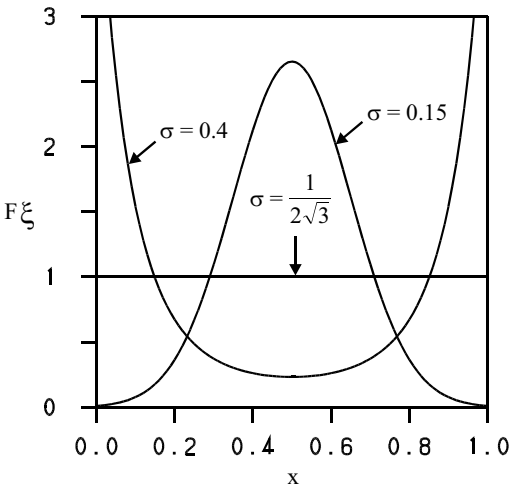

Fig. 2.5. A second-order SML PDF for a bounded variable (<ξ> = 0.5).

$$F_\xi(1) - F_\xi(0) = -\lambda_1, \qquad F_\xi(1) - \langle\xi\rangle\big(F_\xi(1) - F_\xi(0)\big) = 1 - \lambda_2\langle\xi'^2\rangle. \tag{2.58}$$

The constraint that the PDF has to integrate to unity implies for N_F the expression

$$N_F = \sqrt{\frac{\pi}{2\lambda_2}}\exp\left\{\frac{\lambda_1^2}{2\lambda_2}\right\}\left[\operatorname{erf}\left(\sqrt{\frac{\lambda_2}{2}}\big(1-\langle\xi\rangle\big)+\frac{\lambda_1}{\sqrt{2\lambda_2}}\right)+\operatorname{erf}\left(\sqrt{\frac{\lambda_2}{2}}\langle\xi\rangle-\frac{\lambda_1}{\sqrt{2\lambda_2}}\right)\right], \tag{2.59}$$

where the error function defined by (2.20) is used. The simplest way to calculate this PDF is to vary λ_1 and λ_2 until the relations (2.58) are satisfied. For a symmetric PDF, this problem is reduced to find λ_2 since $\lambda_1 = 0$.

An example for such a PDF is given in Fig. 2.5, where $0 \le \xi \le 1$ is assumed. Such PDFs are relevant to the simulation of scalar mixing processes: the PDF with $\sigma = 0.4$ describes the existence of two (unmixed) states near zero and unity, whereas the PDF with $\sigma = 0.15$ describes a PDF of one (mixed) state.

2.6. Examples for other PDFs

The non-algebraic relations between the parameters of non-Gaussian SML PDFs and PDF moments may significantly hamper applications. Thus, one often applies other PDFs, which enable the simulation of similar PDF features but such that simple algebraic relations between PDF parameters and moments exist. With regard to unbounded variables, a simple way to construct such PDFs is to apply a superposition of (two) Gaussian modes, see for instance Luhar et al. (1996). Ways to simulate such non-Gaussian PDFs for bounded variables will be pointed out next.

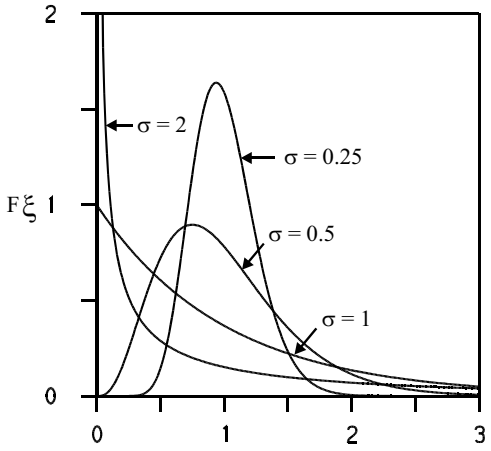

Fig. 2.6. Gamma PDFs for $\langle\xi\rangle = 1$.

2.6.1. Gamma and exponential PDFs

A PDF, which is often applied to simulate scalar distributions (for instance the distribution of the frequency of turbulence, see Pope (2000)), is the gamma PDF. This PDF is defined by

$$F_\xi(x) = \frac{1}{\Gamma(\mu)} \frac{\mu^\mu}{\langle\xi\rangle^\mu} x^{\mu-1} \exp\left\{-\mu \frac{x}{\langle\xi\rangle}\right\}, \tag{2.60}$$

where $\mu = (\langle\xi\rangle / \sigma)^2$. $\sigma^2 = \langle\xi'^2\rangle$ refers as before to the variance. $\Gamma(\mu)$ is called the gamma function,

$$\Gamma(\mu) = \int_0^\infty ds\, s^{\mu-1} e^{-s}, \tag{2.61}$$

which can be calculated in terms of polynomial approximations (Abramowitz & Stegun 1984). As a special case of the gamma PDF, we find for $\mu = 1$ the exponential PDF,

$$F_\xi(x) = \frac{1}{\langle\xi\rangle} \exp\left\{-\frac{x}{\langle\xi\rangle}\right\}. \tag{2.62}$$

Fig. 2.6 illustrates the broad range of PDF shapes, which may be found by variations of the model parameters of a gamma PDF. The PDFs for $\sigma = 0.25$ or $\sigma = 0.5$ are similar to fourth-order SML PDFs, which were presented in section 2.5.2. These PDFs are clearly non-Gaussian: we have for instance Ku = 3.4 and Sk = 0.5 for the case that $\sigma = 0.25$. Obviously, the behaviour of the gamma PDF strongly changes for $\sigma > 1$: the highest probability is not given then for values near the mean $\langle\xi\rangle = 1$ but for values near zero.

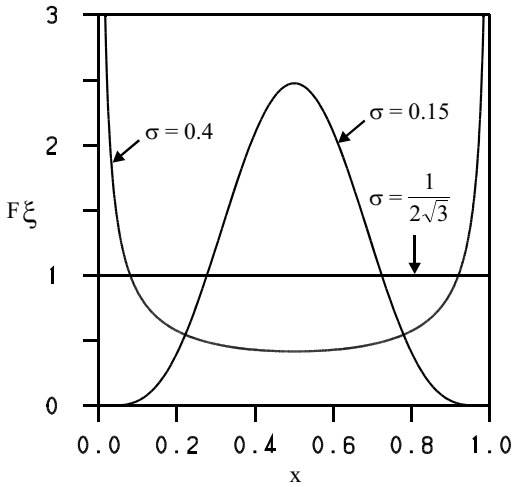

Fig. 2.7. Beta PDFs for <ξ> = 0.5.

2.6.2. The beta PDF

Another PDF, which is often applied to simulate the turbulent mixing of passive scalars, is given by the beta PDF. This PDF is defined by

$$F_\xi(x) = \frac{1}{B(\alpha,\beta)} x^{\alpha-1}(1-x)^{\beta-1}. \tag{2.63}$$

$B(\alpha, \beta)$ is called the beta function,

$$B(\alpha,\beta) = \int_0^1 ds\, s^{\alpha-1}(1-s)^{\beta-1} = \frac{\Gamma(\alpha)\Gamma(\beta)}{\Gamma(\alpha+\beta)}. \tag{2.64}$$

This function can be calculated via its relation to the gamma function, see for instance Abramowitz & Stegun (1984). The parameters α and β of the beta function are related to the first two moments of F_ξ by

$$\alpha = \langle\xi\rangle\left[\frac{\langle\xi\rangle(1-\langle\xi\rangle)}{\sigma^2} - 1\right], \qquad \beta = (1-\langle\xi\rangle)\left[\frac{\langle\xi\rangle(1-\langle\xi\rangle)}{\sigma^2} - 1\right]. \tag{2.65}$$

Several characteristic shapes of the beta PDF are shown in Fig. 2.7 in dependence of σ. It is worth noting that the PDF for $\sigma = 0.15$ is non-Gaussian: we have Ku = 2.5 in this case. These PDF shapes are very similar to those found for a second-order SML PDF of bounded variables, see Fig. 2.5. The advantage of using the beta function is that its parameters are related to PDF moments in a much simpler way. This enables more efficient flow calculations. The application of such beta functions for reacting flow simulations is described for instance by Wall et al. (2000).

Appendix 2A: Theta and delta functions

2A.1. A theta function for one variable

The theta (and delta) function will be introduced first with regard to the case of one variable: the extension of these expressions to the many-variable case is very simple, see the explanations given in section 2A.4.

There are many different ways to define a theta function $\theta(y)$ of one variable. One possibility is given by

$$\theta(y) = \lim_{N\to\infty} \theta_N(y) = \lim_{N\to\infty} \frac{1}{2}\left(1 + \tanh(Ny)\right). \tag{2A.1}$$

Examples for $\theta_N(y)$ are given in Fig. 2.9. This figure reveals that $\theta_N(y)$ tends for large N to

$$\theta(y) = \left\{ \begin{array}{ll} 0 & y < 0 \\ 1/2 \quad \text{for} & y = 0 \\ 1 & y > 0 \end{array} \right\}. \tag{2A.2}$$

This function (2A.2) is also called a Heaviside or step function.

2A.2. A delta function for one variable

The delta function $\delta(y)$ is defined as the derivative of the theta function,

$$\delta(y) = \frac{d\theta(y)}{dy}. \tag{2A.3}$$

Regarding the definition of $\theta(y)$ by means of the relation (2A.1), the delta function $\delta(y)$ is given by

$$\delta(y) = \lim_{N\to\infty} \delta_N(y) = \lim_{N\to\infty} \frac{N}{2\cosh^2(Ny)}. \tag{2A.4}$$

Examples for $\delta_N(y)$ are also given in Fig. 2.8. This figure shows that δ vanishes for all $y \neq 0$, and it diverges for $y \to 0$. For that reason, the delta function is referred to as a generalized function or a distribution. These are functions which do not have to exist for all arguments, but integrals over such functions (multiplied with other functions) have to exist. An inspection of the properties of delta functions reveals that they have all the properties of PDFs. The normalization condition (2.7a) is satisfied because

$$\int dy\ \delta(y) = \int dy\ \frac{d\theta}{dy}(y) = \theta(\infty) - \theta(-\infty) = 1. \tag{2A.5}$$

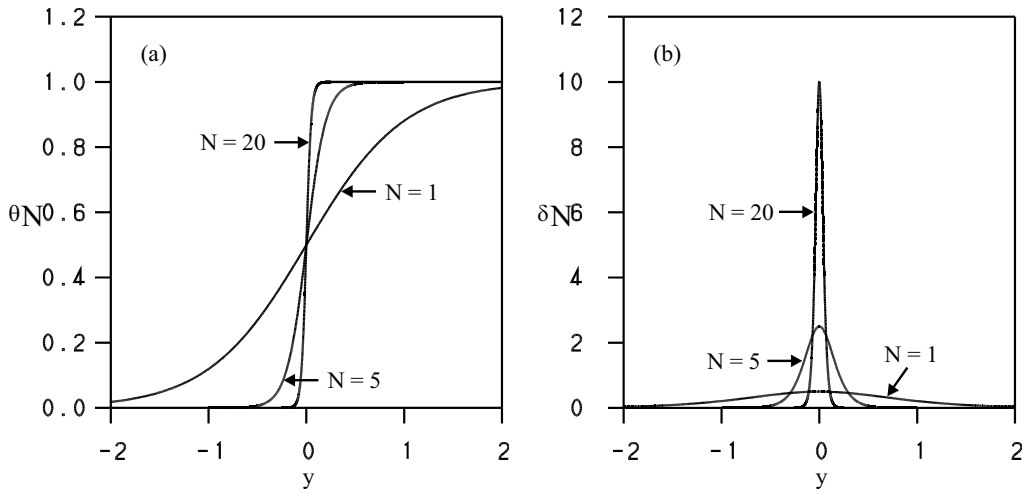

Fig. 2.8. θ_N and δ_N according to (2A.1) and (2A.4) for various values of N.

Obviously, the other two constraints (2.7b-c) are also satisfied: the delta function is positive everywhere and vanishes at infinity.

2A.3. The properties of delta functions

The delta function is characterized by the following essential integral properties (g(y) and h(y) are any test function and a is any number),

$$\int dy\, g(y)\, \delta(y-a) = \int dy\, g(a)\, \delta(y-a), \tag{2A.6a}$$

$$\int dy\, g(y) \frac{d\delta}{dy}(y-a) = -\int dy\, \frac{dg}{dy}(a)\, \delta(y-a), \tag{2A.6b}$$

$$\int dy\, h(y) \delta[g(y)] = \sum_i \int dy\, h(y) \frac{1}{|g_i|} \delta(y-y_i). \tag{2A.6c}$$

Relation (2A.6a) results from the fact that $\delta(y-a)$ vanishes with the exception at $y = a$. Obviously, the right-hand side of this relation reduces to g(a), as may be seen by means of (2A.5). Relation (2A.6b) can be proved by replacing the derivative dg/dy(a) by dg/dy(y) according to (2A.6a), and combining the left- and right-hand sides to the derivative of $g(y)\,\delta(y-a)$. Due to the properties of the delta function at infinity, the integral over this derivative must vanish. In relation (2A.6c), y_i are the monomial roots of the equation $g(y) = 0$ (such that $g(y_i) = 0$). Further, the abbreviation $g_i = [dg / dy](y = y_i)$ is used. These derivatives are assumed to exist. To prove (2A.6c), we consider the integral (L being any parameter that goes to infinity)

$$\int_{-\infty}^{\infty} dy\ h(y)\delta[g(y)] = \sum_i \int_{-L}^{L} dy\ h(y)\delta[g(y)]_{y \to y_i} = \sum_i h(y_i) \int_{-L}^{L} dy\ \delta[g_i(y - y_i)]$$

$$= \sum_i \frac{h(y_i)}{g_i} \int_{-g_i(L+y_i)}^{g_i(L-y_i)} dz_i \delta[z_i] = \sum_i \frac{h(y_i)}{|g_i|} \int_{-L|g_i|}^{L|g_i|} dz_i \delta[z_i]. \qquad (2A.7)$$

The first rewriting of the left-hand side makes use of the fact that $\delta[g(y)]$ contributes only near the roots of $g(y) = 0$. The second rewriting applies (in the first-order of approximation) the Taylor series of g at the corresponding root y_i (the zeroth-order terms vanish). $h(y)$ can be replaced by $h(y_i)$ according to (2A.6a). The third rewriting applies the transformation $z_i = g_i\ (y - y_i)$. The neglect of y_i compared to the infinite L and the consideration of the cases that g_i may be positive or negative results in the fourth rewriting. The right-hand side of (2A.6c) is then obtained by writing $h(y_i)$ into the integral and replacing z_i by $y - y_i$.

It is worth noting that the properties (2A6.a-c) of the delta function imply further properties that are used frequently,

$$\int dy\ h(y)\ \delta(y - b)\,\delta(y - a) = \int dy\ h(y)\ \delta(a - b)\,\delta(y - a), \qquad (2A.8a)$$

$$\int dy\ h(y)\ \delta(-y) = \int dy\ h(y)\ \delta(y), \qquad (2A.8b)$$

$$\int dy\ h(y)\ \delta(ay) = |a|^{-1} \int dy\ h(y)\ \delta(y). \qquad (2A.8c)$$

Relation (2A.8a) is implied by (2A.6a) if we set $g(y) = h(y)\ \delta(y - b)$. The relations (2A.8b-c) are specifications of (2A.6c).

2A.4. The extension to the case of several variables

The theta and delta functions of a vector $\boldsymbol{\xi}(t) = \{\xi_1(t), \xi_2(t), \cdots, \xi_N(t)\}$ of stochastic variables are defined by,

$$\theta(\mathbf{x} - \boldsymbol{\xi}(t)) = \theta(x_1 - \xi_1(t))\,\theta(x_2 - \xi_2(t)) \cdots \theta(x_N - \xi_N(t)), \qquad (2A.9a)$$

$$\delta(\mathbf{x} - \boldsymbol{\xi}(t)) = \delta(x_1 - \xi_1(t))\,\delta(x_2 - \xi_2(t)) \cdots \delta(x_N - \xi_N(t)), \qquad (2A.9b)$$

this means one has simply to multiply all the functions of one variable.

3. Stochastic processes

Next, we turn to the modeling of the evolution of stochastic variables. There are two ways to address this question. The first way is to describe the evolution of the PDF that characterizes a stochastic process. This approach will be described in the first three sections. A general transport equation for the PDF of a stochastic process will be derived in section 3.1. This equation will be simplified in section 3.2 to a Fokker-Planck equation. Section 3.3 deals with an example: it presents an exact solution to this Fokker-Planck equation. The second way to describe the evolution of stochastic processes is to postulate stochastic equations for them. Basics of this approach will be presented in section 3.4, and a more general (and more demanding) approach to solve this question is given in Appendix 3A. An essential element of this introduction of stochastic equations is the explanation of the relationships between processes that are described by stochastic differential equations and Fokker-Planck equations. Section 3.5 provides a link to the following chapters: it specifies the requirements for the construction of closed stochastic equations for any specific case considered.

3.1. PDF transport equations

3.1.1. The Kramers-Moyal equation

To prepare for the consideration of Fokker-Planck equations in section 3.2, we introduce first a general frame for PDF transport equations. For simplicity, we consider only one stochastic variable ξ. According to (2.4), its PDF is given by

$$F_\xi(x, t+\Delta t) = \left\langle \delta\big(x - \xi(t+\Delta t)\big) \right\rangle, \tag{3.1}$$

where Δt is a positive, infinitesimal time interval. To relate the right-hand side to the PDF at the previous time step $F_\xi(x, t)$, we expand the delta function into a Taylor series at $x - \xi(t)$,

$$\delta\big(x - \xi(t) + \xi(t) - \xi(t+\Delta t)\big) = \sum_{n=0}^{\infty} \frac{1}{n!} \frac{d^n \delta\big(x - \xi(t)\big)}{dx^n} \big[\xi(t) - \xi(t+\Delta t)\big]^n. \tag{3.2}$$

S. Heinz, *Statistical Mechanics of Turbulent Flows*

By inserting (3.2) into (3.1) we obtain

$$F_\xi(x,t+\Delta t)-F_\xi(x,t)=\sum_{n=1}^{\infty}\frac{1}{n!}\left(-\frac{d}{dx}\right)^n\left\langle\left[\xi(t+\Delta t)-\xi(t)\right]^n\delta(x-\xi(t))\right\rangle, \tag{3.3}$$

where the term of zeroth-order is written onto the left-hand side. We may now adopt (2.35) for conditional means to rewrite the right-hand side of (3.3) into

$$F_\xi(x,t+\Delta t)-F_\xi(x,t)=\sum_{n=1}^{\infty}\frac{1}{n!}\left(-\frac{d}{dx}\right)^n\left\langle\left[\xi(t+\Delta t)-\xi(t)\right]^n\middle|\, x,t\right\rangle F_\xi(x,t). \tag{3.4}$$

The division of (3.4) by Δt and consideration of the limit $\Delta t \to 0$ then results in

$$\frac{\partial}{\partial t}F_\xi(x,t)=\sum_{n=1}^{\infty}\left(-\frac{\partial}{\partial x}\right)^n D^{(n)}(x,t)\,F_\xi(x,t), \tag{3.5}$$

where the coefficients $D^{(n)}(x, t)$ are given by ($n \geq 1$)

$$D^{(n)}(x,t)=\lim_{\Delta t\to 0}\frac{1}{\Delta t\, n!}\left\langle\left[\xi(t+\Delta t)-\xi(t)\right]^n\middle|\, x,t\right\rangle. \tag{3.6}$$

Equation (3.5) is called the Kramers-Moyal equation (Kramers 1940, Moyal 1949). It may be seen as the most general form of a PDF transport equation (if it is written for the case of a vector of several variables).

3.1.2. Markov processes

The difference $\Delta\xi = \xi(t + \Delta t) - \xi(t)$ in the coefficients (3.6) may depend on all the values of the stochastic variable ξ at earlier times, this means on $\xi(t - k\,\Delta t)$ with $k = 0, 1, \cdots$. However, very often one finds that the influence of such memory effects becomes negligible after a characteristic relaxation time. Thus, if we choose Δt such that it is large compared to this relaxation time of memory effects, we find that $\Delta\xi$ is fully determined by the state $\xi(t)$ (which is correlated to $\xi(t)$ in the difference $\Delta\xi$) and independent of states at earlier times. This assumption is found to be a good approximation under many circumstances provided a suitable set of stochastic variables is chosen; see for instance the detailed discussion of this question regarding the construction of stochastic velocity models in chapter 5.

Stochastic processes for which $\Delta\xi$ only depends on the state $\xi(t)$ are referred to as Markov processes (Gardiner 1983; Risken 1984). They will be considered now, which makes the general PDF transport equation (3.5) to an applicable tool for the investigation of the evolution of stochastic processes. In this case, the coefficients $D^{(n)}(x, t)$ depend only on x and t. Equation (3.5) represents then with respect to time t a differential equation of first-order. Combined with appropriate boundary

conditions and the specification of an initial PDF $F_\xi(x, t_0)$, equation (3.5) uniquely determines the PDF $F_\xi(x, t)$.

3.1.3. Implications for PDF transport equations

To solve equation (3.5), one needs knowledge about the number of terms on the right-hand side that have to be considered. Regarding this, an important constraint arises from the theorem of Pawula (1967). This theorem may be shown by considering the implications of Schwarz's unequality (2.30), which also applies to conditional means (all the arguments given in section 2.3.2 may be repeated for the sample space considered). By choosing $\varphi = (\Delta\xi)^k$ and $\psi = (\Delta\xi)^{k+m}$, where $k \geq 1$ and $m \geq 1$, Schwarz's unequality implies for the coefficients (3.6) that

$$\left[(2k+m)!\, D^{(2k+m)}\right]^2 \leq (2k)!(2k+2m)!\, D^{(2k)}\, D^{(2k+2m)}. \tag{3.7}$$

First, we assume that $D^{(2k)} = 0$. This implies according to relation (3.7) that $D^{(2k+m)} = 0$; this means all the higher-order coefficients have to vanish. Second, we assume that $D^{(2k+2m)} = 0$. Relation (3.7) then implies that $D^{(2k+2m-m)} = 0$; this means all the lower-order coefficients have to vanish then (with the exception of $D^{(1)}$ and $D^{(2)}$ because $2k + m$ is bounded from below by 3). These two cases can be combined to produce the following result

$$D^{(2n)} = 0 \quad \rightarrow \quad D^{(3)} = D^{(4)} = \cdots = D^{(\infty)} = 0 \quad (n \geq 1). \tag{3.8}$$

Hence, $D^{(1)}$ may be zero or nonzero, this does not imply any restrictions. If we take $D^{(2)} = 0$, we have to restrict the series in (3.5) to the first term. If we take $D^{(2)} \neq 0$, we have two possibilities: we may consider only the first two terms in equation (3.5), or we have to involve an infinite number of nonzero coefficients of even order. We see therefore that the theorem of Pawula (1967) is very similar to the theorem of Marcienkiewicz (1939), see section 2.2.2. Both theorems make use of the definition of PDFs as positive definite quantities, i.e., PDFs may have negative values if the requirements of these theorems are not satisfied.

The consideration of an infinite number of coefficients of even order leads to the notable problems of providing all these coefficients as functions of the sample space variable x, and of solving such an equation numerically. Thus, the neglect of these coefficients $D^{(m)}$ ($m = 3, 4, \cdots$) seems to be the better way in general. However, this leads to the question under which conditions this is justified. The answer is closely related to the consideration of the continuity of the sample path of stochastic processes. By considering an infinitesimal time increment Δt, one can often expect that the change $\Delta\xi = \xi(t + \Delta t) - \xi(t)$ of a stochastic variable is bounded (i.e., small). Such stochastic processes have a continuous sample path,

and one can show that the assumption of such a process implies the neglect of $D^{(m)}$ ($m = 3, 4, \cdots$), see Gardiner (1983). In other words, one takes jump processes into account (instantaneous changes $\Delta\xi$ that may be very large) which imply discontinuous sample paths if coefficients $D^{(m)}$ ($m = 3, 4, \cdots$) are involved. To exclude this case, we will neglect coefficients of higher than second order from now.

3.2. The Fokker-Planck equation

3.2.1. The Fokker-Planck equation

We consider a vectorial stochastic process $\boldsymbol{\xi} = \{\xi_1(t), \xi_2(t), \cdots, \xi_N(t)\}$ which is assumed to be Markovian and to have continuous sample paths. The corresponding extension of equation (3.5) reads

$$\frac{\partial}{\partial t} F_\xi(\mathbf{x},t) = -\frac{\partial}{\partial x_i} D_i(\mathbf{x},t)\, F_\xi(\mathbf{x},t) + \frac{\partial^2}{\partial x_i \partial x_j} D_{ij}(\mathbf{x},t)\, F_\xi(\mathbf{x},t). \tag{3.9}$$

This equation is called a Fokker-Planck equation (Fokker 1914, Planck 1917). Its coefficients D_i and D_{ij} are given by the vectorial generalizations of $D^{(1)}$ and $D^{(2)}$,

$$D_i(\mathbf{x},t) = \lim_{\Delta t \to 0} \frac{1}{\Delta t} \left\langle \xi_i(t+\Delta t) - \xi_i(t) \,\middle|\, \mathbf{x}, t \right\rangle, \tag{3.10a}$$

$$D_{ij}(\mathbf{x},t) = \lim_{\Delta t \to 0} \frac{1}{2\Delta t} \left\langle \left[\xi_i(t+\Delta t) - \xi_i(t)\right]\left[\xi_j(t+\Delta t) - \xi_j(t)\right] \,\middle|\, \mathbf{x}, t \right\rangle. \tag{3.10b}$$

The conditional means refer to the condition $\boldsymbol{\xi}(t) = \mathbf{x}$. D_i may be seen as a generalized velocity if $\mathbf{x}$ is interpreted as generalized coordinate in sample space. Equation (3.9) corresponds then to a diffusion equation with D_{ij} as diffusion coefficient. Important properties of D_{ij} are that D_{ij} is symmetric and semidefinite. The latter may be seen by multiplying (3.10b) with any vectors c_i and c_j,

$$D_{ij} c_i c_j = \lim_{\Delta t \to 0} \frac{1}{2\Delta t} \left\langle \left\{ \left[\xi_i(t+\Delta t) - \xi_i(t)\right] c_i \right\}^2 \,\middle|\, \mathbf{x}, t \right\rangle \geq 0. \tag{3.11}$$

Usually, we will assume that D_{ij} is positive definite, $D_{ij}\, c_i\, c_j > 0$ for $c_i\, c_i > 0$. The inverse matrix of D_{ij} exists in this case.

To prove the consistency of (3.9), we integrate it over the sample space $\mathbf{x}$,

$$\frac{\partial}{\partial t} \int d\mathbf{x}\, F_\xi(\mathbf{x},t) = -\int d\mathbf{x}\, \frac{\partial}{\partial x_i} D_i(\mathbf{x},t) F_\xi(\mathbf{x},t) + \int d\mathbf{x}\, \frac{\partial^2}{\partial x_i \partial x_j} D_{ij}(\mathbf{x},t) F_\xi(\mathbf{x},t). \tag{3.12}$$

The left-hand side of (3.12) vanishes (F_ξ is assumed to be normalized to unity). By setting $D_i\, F_\xi$ and $\partial(D_{ij}\, F_\xi) / \partial x_j$ equal to L, respectively, the integrals on the right-hand side may be written as volume integrals over derivatives of L. The latter can be rewritten as surface integrals,

$$\int d\mathbf{x}\, \frac{\partial L}{\partial x_i} = \int_s ds\; L\, \mathbf{n}\, \boldsymbol{\eta}_i. \tag{3.13}$$

Here, s is the surface that surrounds the domain considered, and ds is a differential element of s. The unit vector of the x_i-axis is referred to by $\boldsymbol{\eta}_i$, and $\mathbf{n}$ is the normal vector of s. By considering an infinite domain, the integrals on the right-hand side of (3.13) will vanish if L is zero at the surface. Therefore, the consistency of the formulation of equation (3.9) requires the assumption that the PDF F_ξ and its derivatives vanish at $|\mathbf{x}| \to \infty$.

3.2.2. Transport equations for moments

The implications of equation (3.9) for the transport of moments of the PDF F_ξ will be considered next. By multiplying this equation with x_k and integration over the sample space we obtain

$$\frac{\partial}{\partial t}\langle \xi_k \rangle = -\int d\mathbf{x}\; x_k\, \frac{\partial}{\partial x_i} D_i(\mathbf{x},t) F_\xi(\mathbf{x},t) + \int d\mathbf{x}\; x_k\, \frac{\partial^2}{\partial x_i \partial x_j} D_{ij}(\mathbf{x},t)\, F_\xi(\mathbf{x},t). \tag{3.14}$$

As done before, we set $D_i\, F_\xi$ and $\partial(D_{ij}\, F_\xi) / \partial x_j$ equal to L, respectively. The integrals of (3.14) may be rewritten then by adopting partial integration,

$$\int d\mathbf{x}\, \frac{\partial x_k L}{\partial x_i} = \delta_{ki} \int d\mathbf{x}\; L + \int d\mathbf{x}\; x_k\, \frac{\partial L}{\partial x_i}. \tag{3.15}$$

According to (3.13), combined with the assumption L = 0 at $|\mathbf{x}| \to \infty$, the left-hand side of (3.15) vanishes. By adopting the resulting relation in (3.14) we then obtain

$$\frac{\partial}{\partial t}\langle \xi_k \rangle = \langle D_k \rangle = \int d\mathbf{x}\; D_k(\mathbf{x},t) F_\xi(\mathbf{x},t) \tag{3.16}$$

since the last integral in (3.14) does not contribute. Hence, $<D_k>$ determines the transport of the means $<\xi_k>$. For that reason, D_k is called a drift coefficient.

In analogy to the derivation of (3.16), one may obtain the following relation for second-order moments by multiplication of (3.9) with $x_k\, x_n$ and integrating it over the sample space,

$$\frac{\partial}{\partial t}\langle \xi_k \xi_n \rangle = \langle D_k\, \xi_n \rangle + \langle D_n\, \xi_k \rangle + 2\langle D_{kn} \rangle. \tag{3.17}$$

To obtain this relation, partial integration has to be applied twice in accordance with (3.15). The combination of (3.16) and (3.17) can be used then to derive a transport equation for the variance

$$\langle \xi'_k \, \xi'_n \rangle = \Big\langle \big(\xi_k - \langle \xi_k \rangle\big)\big(\xi_n - \langle \xi_n \rangle\big) \Big\rangle = \langle \xi_k \xi_n \rangle - \langle \xi_k \rangle \langle \xi_n \rangle . \tag{3.18}$$

This variance transport equation reads

$$\frac{\partial}{\partial t} \langle \xi'_k \, \xi'_n \rangle = \langle D'_k \, \xi'_n \rangle + \langle D'_n \, \xi'_k \rangle + 2 \langle D_{kn} \rangle , \tag{3.19}$$

where $D'_k = D_k - \langle D_k \rangle$ is written for fluctuations of D_k. Hence, variances are produced by $\langle D_{kn} \rangle$ provided that D_{kn} is positive definite. The appearance of D_{kn} causes a diffusion process (the width of the PDF increases), which is the reason for the consideration of D_{kn} as a diffusion coefficient. An equilibrium state may be reached asymptotically if the first two terms on the right-hand side of (3.19) appear with a negative sign, i.e., if they are able to balance the variance production. These two terms then describe the dissipation (or destruction) of variance.

3.2.3. The limiting PDF

An important question concerns the conditions for the existence of a unique asymptotic state. To clarify this, we have to consider the asymptotic features of the PDF F_ξ that obeys the Fokker-Planck equation (3.9). As done by Lebowitz & Bergmann (1957) and Risken (1984), we consider an infinite domain and define the entropy difference related to two solutions $F_1(\mathbf{x}, t)$ and $F_2(\mathbf{x}, t)$ of the Fokker-Planck equation (3.9) (which may result from different initial PDFs) according to the entropy definition (2.42) by

$$h(t) = S_2(t) - S_1(t) = \left\langle \ln\left(\frac{F_1}{F_2}\right) \right\rangle = \int d\mathbf{x} \, F_1(\mathbf{x},t) \ln\left(\frac{F_1(\mathbf{x},t)}{F_2(\mathbf{x},t)}\right). \tag{3.20}$$

The purpose of the following explanations is to show that $h(t) \geq 0$ and $dh / dt \leq 0$, this means h evolves towards $h = 0$. This limit $h = 0$ corresponds then to the asymptotic agreement of both solutions.

To show $h(t) \geq 0$, we rewrite relation (3.20) by adopting the normalization constraints for F_1 and F_2,

$$h(t) = \int d\mathbf{x} \left[F_1 \ln(R) - F_1 + F_2 \right] = \int d\mathbf{x} \, F_2 \, g(R), \tag{3.21}$$

where the abbreviations $R = F_1 / F_2$ and $g(R) = R \ln(R) - R + 1$ are introduced. The analysis of the function g(R) reveals that it takes its minimum zero at $R = 1$. Consequently, we find that h(t) always has to be non-negative.

To show $dh / dt \leq 0$, we calculate the derivative of h(t),

$$\frac{dh}{dt}(t) = \int d\mathbf{x} \left[\frac{\partial F_1}{\partial t} \ln(R) + \frac{\partial F_1}{\partial t} - R \frac{\partial F_2}{\partial t} \right] = \int d\mathbf{x} \left[\frac{\partial F_1}{\partial t} \ln(R) - R \frac{\partial F_2}{\partial t} \right]. \qquad (3.22)$$

The last expression arises from the fact that the integral over $\partial F_1 / \partial t$ has to vanish due to the normalization constraint. By adopting (3.9) to replace in equation (3.22) the derivatives of F_1 and F_2, we obtain

$$\frac{dh}{dt}(t) = - \int d\mathbf{x} \left\{ \ln(R) \frac{\partial}{\partial x_i} \left[D_i F_1 - \frac{\partial D_{ij} F_1}{\partial x_j} \right] - R \frac{\partial}{\partial x_i} \left[D_i F_2 - \frac{\partial D_{ij} F_2}{\partial x_j} \right] \right\}. \qquad (3.23)$$

This expression may be rewritten by means of partial integration. We consider integrals over derivatives $\partial / \partial x_i$ in correspondence to relation (3.15), rewrite them according to (3.13), and assume that the integrands vanish at $|\mathbf{x}| \to \infty$. This leads to

$$\frac{dh}{dt}(t) = - \int d\mathbf{x} \left\{ \frac{\partial \ln(R)}{\partial x_i} \left[- D_i F_1 + \frac{\partial D_{ij} F_1}{\partial x_j} \right] - \frac{\partial R}{\partial x_i} \left[- D_i F_2 + \frac{\partial D_{ij} F_2}{\partial x_j} \right] \right\}. \qquad (3.24)$$

This relation reduces to

$$\frac{dh}{dt}(t) = - \int d\mathbf{x} \left\{ \frac{\partial \ln(R)}{\partial x_i} \frac{\partial D_{ij} F_1}{\partial x_j} - \frac{\partial R}{\partial x_i} \frac{\partial D_{ij} F_2}{\partial x_j} \right\} \qquad (3.25)$$

because the terms that involve D_i cancel each other. The latter may be seen by rewriting the derivative of ln(R) into a derivative of R. We replace F_2 by F_1 / R and apply partial integration to obtain

$$\frac{dh}{dt}(t) = - \int d\mathbf{x} \; D_{ij} F_1 \left\{ \frac{1}{R} \frac{\partial^2 R}{\partial x_j \partial x_i} - \frac{\partial^2 \ln(R)}{\partial x_i \partial x_j} \right\}. \qquad (3.26)$$

The first term within the bracket on the right-hand side may be rewritten by means of the relation $\partial R / \partial x_i = R \, \partial \ln(R) / \partial x_i$. This leads then to

$$\frac{dh}{dt}(t) = - \int d\mathbf{x} \; D_{ij} F_1 \frac{\partial \ln(R)}{\partial x_j} \frac{\partial \ln(R)}{\partial x_i}. \qquad (3.27)$$

Hence, $dh / dt \leq 0$ if D_{ij} is positive definite. This means, h will evolve towards its minimum h = 0 provided D_i and D_{ij} have no singularities and do not permit that infinite values of solutions of (3.9) appear at $|\mathbf{x}| \to \infty$. For h = 0, different solutions of the Fokker-Planck equation have to coincide such that $F_1 = F_2$. This unique

asymptotic solution is the stationary solution of (3.9) for the case that D_i and D_{ij} are independent of time.

To show the relation of these conclusions to the consideration of the entropy in chapter 2, we consider a special case. We assume that the limiting PDF was chosen to be the initial PDF of F_2, so that F_2 will not change in time. h(t) is then the positive difference of the entropies related to the limiting PDF F_2 and F_1, respectively. The fact that h evolves towards its minimum h = 0 describes the increase of entropy of a system for which a limiting state exists. The entropy will become maximal if this limiting state is reached. Due to the disappearance of the left-hand side, the Fokker-Planck equation (3.9) implies in the equilibrium case

$$\frac{\partial \ln\left(F_\xi\right)}{\partial x_j} = D^{-1}{}_{jk}\left(D_k - \frac{\partial D_{kj}}{\partial x_j}\right). \tag{3.28}$$

This expression is consistent with the structure of SML PDFs considered in chapter 2: the choice of D_k as a polynomial of n^{th}-order corresponds to the specification of a SML PDF of n^{th}-order.

3.3. An exact solution to the Fokker-Planck equation

3.3.1. The equation considered

To illustrate the application of Fokker-Planck equations and characteristics of their solutions, let us consider an example that enables the derivation of analytical results. In conjunction with the assumption of natural boundary conditions (this means $F_\xi(\mathbf{x}, t) \to 0$ for $|\mathbf{x}| \to \infty$), we specify the Fokker-Planck equation (3.9) in the following way,

$$\frac{\partial}{\partial t} F_\xi(\mathbf{x}, t) = -\frac{\partial}{\partial x_i}\left[G_i(t) + G_{ik}(t)\left\{x_k - \langle \xi_k \rangle\right\}\right] F_\xi(\mathbf{x}, t) + \frac{\partial^2}{\partial x_i \partial x_j} D_{ij}(t) F_\xi(\mathbf{x}, t). \tag{3.29}$$

The drift coefficient D_i is written as a linear function of the variables $\mathbf{x}$, which may be seen as the Taylor series of D_i in the first order of approximation. The inclusion of $\langle \xi_k \rangle$ in (3.29) defines G_{ik} as the coefficient that controls the intensity of fluctuations around the mean $\langle \xi_k \rangle$. It will be shown in the following chapters that such linear models for D_i are well suited to characterize near-equilibrium processes. The diffusion coefficient D_{ij} is assumed to be only a function of time. This choice is convenient with regard to many applications, see the explanations given in the following chapters. In addition to this, one can guarantee in this way the important property of D_{ij} to be semidefinite.

3.3.2. The solution to the Fokker-Planck equation

The solution to the Fokker-Planck equation (3.29) depends on the initial PDF $F_\xi(\mathbf{x}', t')$ according to relation (2.32),

$$F_\xi(\mathbf{x}, t) = \int d\mathbf{x}' \, F_{\xi|\xi}(\mathbf{x}, t \,|\, \mathbf{x}', t') F_\xi(\mathbf{x}', t'). \tag{3.30}$$

Therefore, to obtain a general solution to equation (3.29) one has to calculate the conditional PDF $F_{\xi|\xi}$. Specific solutions $F_\xi(\mathbf{x}, t)$ can be obtained then in dependence on specified initial PDFs $F_\xi(\mathbf{x}', t')$ by integration according to (3.30). By inserting relation (3.30) into equation (3.29) one may prove that the conditional PDF $F_{\xi|\xi}$ also satisfies the Fokker-Planck equation (3.29). According to (2.37), the required initial condition for $F_{\xi|\xi}$ is given by

$$F_{\xi|\xi}(\mathbf{x}', t' \,|\, \mathbf{x}', t') = \delta(\mathbf{x} - \mathbf{x}'). \tag{3.31}$$

The coefficients in (3.29) are specified as linear functions of the sample space variables $\mathbf{x}$. Thus, one may assume that the PDF evolves towards a Gaussian shape. To prove this idea, we consider the conditional PDF $F_{\xi|\xi}$ as a N-dimensional Gaussian PDF,

$$F_{\xi|\xi}(\mathbf{x}, t \,|\, \mathbf{x}', t') = \frac{1}{(2\pi)^{N/2}\sqrt{\det(\alpha)}} \exp\left\{-\frac{1}{2}\alpha^{-1}{}_{kl}(x_k - \alpha_k)(x_l - \alpha_l)\right\}. \tag{3.32}$$

The means of this PDF are given by α_k, the variances by α_{kl}, and $\det(\alpha)$ is the determinant of the matrix α with the elements α_{kl}. What one has to do now is to explain the relationship between α_k and α_{kl} with the coefficients G_i, G_{ik}, and D_{ij} of the Fokker-Planck equation (3.29). To do this, we calculate the corresponding derivatives of (3.32) and insert them into (3.29). This leads to three conditions for the coefficients of terms of zeroth-, first- and second-order in the variables considered. One condition is satisfied identically, and the other two constraints lead to the following equations for the means α_k and variances α_{kl} of (3.32),

$$\frac{\partial \alpha_k}{\partial t} = G_k + G_{kn}(\alpha_n - \langle \xi_n \rangle), \tag{3.33a}$$

$$\frac{\partial \alpha_{kl}}{\partial t} = G_{kn}\alpha_{nl} + G_{ln}\alpha_{nk} + 2D_{kl}. \tag{3.33b}$$

To derive (3.33a-b) we applied the following relations for the variances α_{kl},

$$\frac{1}{\det(\alpha)}\frac{\partial \det(\alpha)}{\partial t} = -\frac{\partial \alpha^{-1}{}_{mn}}{\partial t}\alpha_{nm}, \qquad \frac{\partial \alpha^{-1}{}_{mn}}{\partial t} = -\alpha^{-1}{}_{mk}\frac{\partial \alpha_{kl}}{\partial t}\alpha^{-1}{}_{ln}. \tag{3.34}$$

The first relation of (3.34) may be obtained by the differentiation of (3.32) by time and integration over the sample space. The second relation can be derived by the differentiation of the identity $\alpha_{in}\,\alpha^{-1}{}_{nj} = \delta_{ij}$. Hence, we find that (3.32) provides the solution to (3.29) provided the means α_k and variances α_{kl} satisfy (3.33a-b). The initial conditions for these equations (3.33a-b) are given by

$$\alpha_k(t') = x'_k\,, \tag{3.35a}$$

$$\alpha_{kl}(t') = 0. \tag{3.35b}$$

By adopting the properties of delta functions, one may prove that (3.32) combined with (3.35a-b) recovers the initial condition (3.31) for the conditional PDF $F_{\xi|\xi}$.

3.3.3. Means, variances and correlations

Next, let us have a look at the means and variances of $F_\xi(\mathbf{x}, t)$, which are implied by the Fokker-Planck equation (3.29). One way to obtain these quantities is to derive them from expression (3.30) for the PDF $F_\xi(\mathbf{x}, t)$ in combination with (3.32) for the conditional PDF $F_{\xi|\xi}$. However, this approach requires the specification of the initial PDF $F_\xi(\mathbf{x}', t')$ and integration of the transport equations (3.33a-b) for α_k and α_{kl}. A simpler way is to derive directly transport equations for the means and variances of $F_\xi(\mathbf{x}, t)$, as pointed out in section 3.2.2. In this way, we find the equations

$$\frac{\partial\langle\xi_k\rangle}{\partial t} = G_k\,, \tag{3.36a}$$

$$\frac{\partial\langle\xi'_k\,\xi'_l\rangle}{\partial t} = G_{kn}\langle\xi'_n\,\xi'_l\rangle + G_{ln}\langle\xi'_n\,\xi'_k\rangle + 2D_{kl}, \tag{3.36b}$$

which have to be solved in conjunction with the corresponding initial conditions provided by the initial PDF.

The equations (3.36a-b) can be used to rewrite the equations (3.33a-b) for α_k and α_{kl}. The combination of these equations leads to

$$\frac{\partial}{\partial t}\left(\alpha_k - \langle\xi_k\rangle\right) = G_{kn}\left(\alpha_n - \langle\xi_n\rangle\right), \tag{3.37a}$$

$$\frac{\partial}{\partial t}\left(\alpha_{kl} - \langle\xi'_k\,\xi'_l\rangle\right) = G_{kn}\left(\alpha_{nl} - \langle\xi'_n\,\xi'_l\rangle\right) + G_{ln}\left(\alpha_{nk} - \langle\xi'_n\,\xi'_k\rangle\right). \tag{3.37b}$$

These equations show that α_k and α_{kl} relax to the means and variances of $F_\xi(\mathbf{x}, t)$. Asymptotically, the left hand sides of (3.37a-b) vanish, and α_k and α_{kl} become equal to the means and variances of $F_\xi(x, t)$,

$$\alpha_k = \langle \xi_k \rangle, \tag{3.38a}$$

$$\alpha_{kl} = \langle \xi'_k \, \xi'_l \rangle. \tag{3.38b}$$

In this case, the conditional PDF is independent of **x'**, as may be seen by adopting (3.38a-b) in the parametrization (3.32) for $F_{\xi|\xi}$. Equation (3.30) reveals then that the PDF F_ξ is equal to the conditional PDF $F_{\xi|\xi}$. Accordingly, the unconditional PDF F_ξ and conditional PDF $F_{\xi|\xi}$ relax asymptotically (independent of the initial conditions) to a Gaussian function.

Another relevant characteristics of the Fokker-Planck equation (3.29) is the two-point correlation function, which is defined by ($s \geq 0$)

$$\langle \xi'_k(t) \, \xi'_l(t+s) \rangle = \int d\mathbf{x} \, d\mathbf{x}' \left(x_k - \langle \xi_k(t) \rangle \right) \left(x'_l - \langle \xi_l(t+s) \rangle \right) F_{\xi\xi}(\mathbf{x}, t; \mathbf{x}', t+s). \tag{3.39}$$

The two-point PDF $F_{\xi\xi}$ has also to satisfy equation (3.29), as may be seen by means of the definition (2.31) of the two-point PDF. The integration of (3.29) multiplied with the corresponding variables results then in the following equation for the correlation function,

$$\frac{\partial}{\partial s} \langle \xi'_k(t) \, \xi'_l(t+s) \rangle = G_{km} \langle \xi'_m(t) \, \xi'_l(t+s) \rangle. \tag{3.40}$$

The initial condition is given by the variance of $F_\xi(\mathbf{x}, t)$ at t. Accordingly, the correlation decays exponentially for the dynamics considered: the memory lost is controlled by $- G_{km}$, which represents a frequency (inverse time scale) matrix. In contrast to the evolution of variances, which is determined by equation (3.36b), there is no production mechanism for correlations (provided that $- G_{km}$ is non-negative as usually assumed): memory can only be lost.

3.4. Stochastic equations for realizations

One way to model the evolution of stochastic variables was considered in the previous three sections, where equations for the PDF of stochastic variables were introduced. It was argued that the reduction of the Kramers-Moyal equation (3.5) (written for the case of several variables) to the Fokker-Planck equation (3.9) has to be seen as the most suitable way of constructing a PDF transport equation. An alternative approach is to postulate differential equations for the calculation of the evolution of stochastic variables. The stochastic processes determined in this way can then be applied to calculate all the coefficients of the Kramers-Moyal equation, this means this approach results, too, in a specific PDF transport equation. The relations between these two approaches will be considered next.

3.4.1. Stochastic differential equations

A general evolution equation for a vector $\boldsymbol{\xi}(t) = \{\xi_1(t), \xi_2(t), \cdots, \xi_N(t)\}$ of N stochastic variables may be written in the following way ($0 \le s \le t$),

$$\frac{d\xi_i}{dt} = a_i\left[\boldsymbol{\xi}(s), s\right] + f_i. \tag{3.41}$$

f_i represents any stochastic force which produces fluctuations of $\boldsymbol{\xi}$. We assume that f_i vanishes in the ensemble average, and that it has a characteristic correlation time τ_f (fluctuations of f_i are relaxed, basically, after the time τ_f). Usually, a_i represents the dynamics of mean values of $\boldsymbol{\xi}$ and the relaxation of fluctuations of $\boldsymbol{\xi}$. This term is a deterministic functional that may depend on all states $\boldsymbol{\xi}(s)$ at earlier times (which makes $\boldsymbol{\xi}$ to a non-Markovian process, see section 3.1.2).

Obviously, the consideration of memory effects in a_i and a finite correlation time τ_f of stochastic forces may hamper analyses and applications of (3.41) significantly. A very important experience is that a suitable choice of variables often enables the consideration the characteristic relaxation time τ_f of f_i as infinitely small compared to the typical time scales of the problem considered (this may require, for instance, the extension of the set of variables considered by constructing models that include equations for derivatives of $\boldsymbol{\xi}$, see the explanations given in Appendix 3A and chapter 5). In this case, the stochastic forces in (3.41) can be seen to be uncorrelated and the influence of memory effects on a_i can be neglected (the close relation between stochastic force correlations and memory effects is pointed out in detail in Appendix 3A). This assumption of vanishing memory effects and correlation times τ_f will be made now, this means we restrict the attention to the consideration of the equation

$$\frac{d\xi_i}{dt} = a_i\left(\boldsymbol{\xi}, t\right) + b_{ik}\left(\boldsymbol{\xi}, t\right)\frac{dW_k}{dt}. \tag{3.42}$$

In this equation, a_i and b_{ik} are any deterministic functions of $\boldsymbol{\xi}(t)$ and t. The stochastic process dW_k / dt represents the derivative of the k^{th} component of a vectorial Gaussian process $\mathbf{W} = (W_1, \cdots, W_N)$, which is called a Wiener process (Gardiner 1983, Risken 1984). Hence, dW_k / dt is fully determined by its first two moments that are given by

$$\left\langle \frac{dW_k}{dt} \right\rangle = 0, \tag{3.43a}$$

$$\left\langle \frac{dW_k}{dt}(t)\frac{dW_l}{dt}(t') \right\rangle = \delta_{kl}\delta(t - t'). \tag{3.43b}$$

In accord with the assumed properties of the stochastic force f_i, the relations (3.43a-b) mean that f_i vanishes in the ensemble average, and that its correlation time is zero (it is uncorrelated for different times). In addition to this, it is assumed that there are no correlations between different stochastic force components. Hence, the change of ξ_i modeled by (3.42) is completely determined by the state of $\boldsymbol{\xi}$ at t, such that $\boldsymbol{\xi}(t)$ represents a Markov process.

It is essential to note that (in contrast to the integration of ordinary differential equations) the value of integrals that involve stochastic variables may depend on the definition of the integration. Throughout this book we will use the Itô-definition for this (Gardiner 1983, Risken 1984). The latter assumes that the formal solution of the equation (3.42) is given by

$$\begin{aligned}\xi_i(t+\Delta t)-\xi_i(t) &= \int_t^{t+\Delta t} ds\; a_i(\boldsymbol{\xi}(s),s) + \int_t^{t+\Delta t} ds\; b_{ik}(\boldsymbol{\xi}(s),s)\frac{dW_k}{ds}(s) \\ &= a_i(\boldsymbol{\xi}(t),t)\,\Delta t + b_{ik}(\boldsymbol{\xi}(t),t)\,\Delta W_k(t), \end{aligned} \tag{3.44}$$

where Δt is an infinitesimal time increment. The assumption related to the second line of equation (3.44) is that the coefficients a_i and b_{ik} in the integrals are taken at the previous time step t. Further, we introduced the variable

$$\Delta W_k(t) = \int_t^{t+\Delta t} ds\; \frac{dW_k}{ds}(s) = W_k(t+\Delta t) - W_k(t). \tag{3.45}$$

By adopting the properties (3.43a-b) of dW_k / dt, the properties of the Gaussian process ΔW_k are found to be

$$\langle \Delta W_k(t) \rangle = 0, \tag{3.46a}$$

$$\begin{aligned}\langle \Delta W_k(t)\,\Delta W_l(t') \rangle &= \int_t^{t+\Delta t} ds \int_{t'}^{t'+\Delta t} ds' \left\langle \frac{dW_k}{ds}(s)\frac{dW_l}{ds'}(s') \right\rangle = \delta_{kl} \int_t^{t+\Delta t} ds \int_{t'}^{t'+\Delta t} ds'\,\delta(s'-s) \\ &= \delta_{kl} \int_t^{t+\Delta t} ds\,[\theta(t'+\Delta t - s) - \theta(t'-s)] = (1-k)\,\Delta t\,\delta_{kl}, \end{aligned} \tag{3.46b}$$

where $t' = t - k\,\Delta t$ ($k = 0, 1$) is applied as an abbreviation. Therefore, the values of ΔW_k at the same time step ($k = 0$) are correlated, whereas values at different times ($k = 1$) are uncorrelated (obviously, $\Delta W_k(t)$ is also uncorrelated to $\Delta W_k(t')$ with $k = 2, 3, \cdots$). Two examples for realizations of ΔW_k normalized to $(\Delta t)^{1/2}$ are shown in Fig. 3.1. This figure reveals that there is no correlation between adjacent values and various realizations. According to the relations (3.46a-b), these standardized numbers have a zero mean and a variance equal to unity.

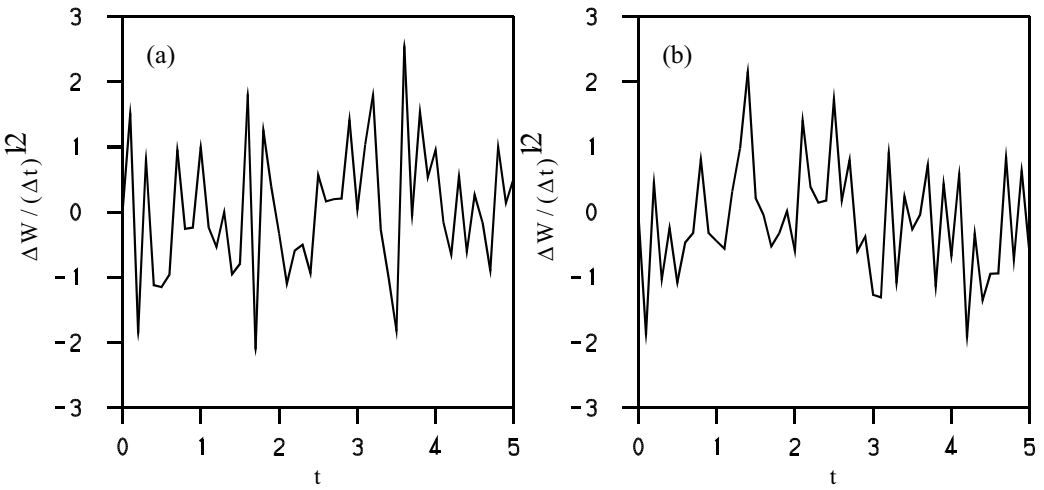

Fig. 3.1. Two examples for realizations of one component of $\Delta W / (\Delta t)^{1/2}$.

According to its definition (3.45), $\Delta W_k / \Delta t$ represents the derivative of W_k. By dividing (3.46b) by $(\Delta t)^2$, we see that the variance of $\Delta W_k / \Delta t$ does not exist: it diverges proportional to $(\Delta t)^{-1/2}$, this means it goes to infinity for $\Delta t \to 0$. Consequently, W_k is not differentiable because the probability for the appearance of $\Delta W_k / \Delta t$ values that are larger than any limit is equal to unity (Gardiner 1983). For that reason, stochastic equations are often written according to the formulation (3.44) where ΔW_k behaves properly. Nevertheless, the equation (3.42) will be used here in general to represent stochastic equations, having in mind that it states nothing else than the formulation (3.44).

3.4.2. The relationship to Fokker-Planck equations

Equation (3.42) determines the evolution of the stochastic process ξ. Consequently, it has to imply a PDF transport equation. This fact leads then to the question about the relation of the PDF transport equation implied by (3.42) to the Fokker-Planck equation (3.9). To address this, we calculate the first two coefficients of the Kramers-Moyal equation (written for the case of several variables), which are equal to the coefficient D_i and D_{ij} of the Fokker-Planck equation (3.9). By inserting (3.44) into (3.10a-b) we find

$$D_i(\mathbf{x},t) = a_i(\mathbf{x},t), \tag{3.47a}$$

$$D_{ij}(\mathbf{x},t) = \frac{1}{2} b_{ik}(\mathbf{x},t)\, b_{jk}(\mathbf{x},t). \tag{3.47b}$$

where the properties (3.46a-b) of ΔW_k are used. The corresponding calculation of higher-order coefficients of the Kramers-Moyal equation reveals that all these

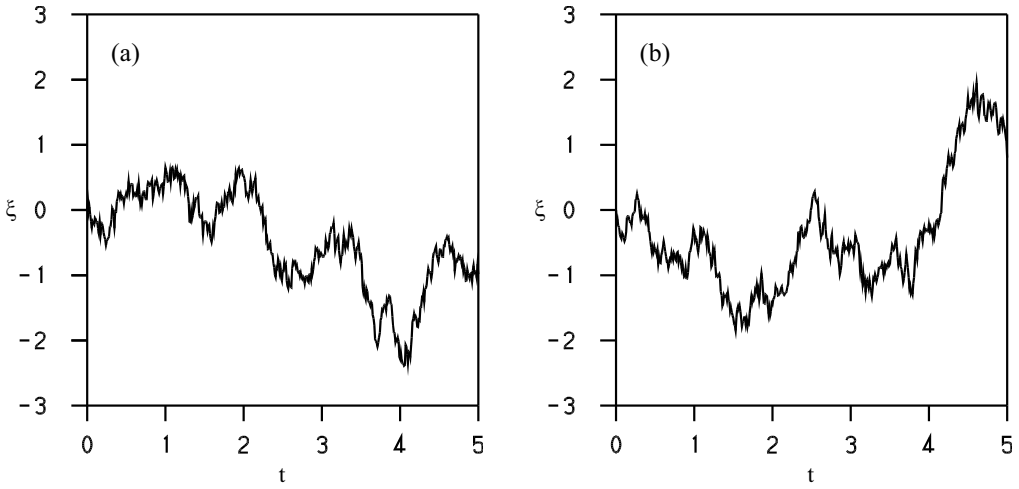

Fig. 3.2. Two examples for realizations of the stochastic equation (3.48).

coefficients vanish because they are of higher order in Δt. Hence, the stochastic equation (3.42) uniquely determines a Fokker-Planck equation that describes the PDF evolution. However, the opposite is not the case in general. For N variables, equation (3.47b) represents $N (N + 1) / 2$ equations for N^2 elements of b_{ij}. Thus, the coefficients of the equation (3.42) are uniquely determined by the coefficients D_i and D_{ij} of the Fokker-Planck equation only if b_{ij} is assumed to be symmetric.

3.4.3. Monte Carlo simulation

Applications of Fokker-Planck equations to turbulent reacting flows often require the consideration of a large number of variables, which makes the direct solution of Fokker-Planck equations extremely complicated or even impossible. This problem can be avoided if stochastic differential equations are used which correspond to a given Fokker-Planck equation. This means one solves equation (3.42) with a_i and (a symmetric) b_{ij}, which are derived according to the relations (3.47a-b) from the coefficients D_i and D_{ij} of a Fokker-Planck equation.

The advantage of such Monte Carlo simulations is given by the fact that stochastic equations can be solved easily. The statistics of ΔW_k, which are required to solve (3.44), are available in standard routines, and all the means and the PDF of a stochastic process considered can be obtained by summation. Suitable techniques to solve such equations are described, e.g., by Kloeden and Platen (1992). As an example, two realizations of a specification of (3.42)

$$\frac{d\xi}{dt} = -\xi + \frac{dW}{dt}, \tag{3.48}$$

are shown in Fig. 3.2. These solutions were obtained for $\xi(0) = 0$ and $\Delta t = 0.01$.

The drawback of Monte Carlo methods for the solution of Fokker-Planck equations is that they are often time-consuming, and generally have high memory requirements. The statistical accuracy decreases only with $N^{1/2}$, where N is the number of realizations (Risken 1984). Hence, one needs, for example, 100 times more particles to improve the accuracy by an order of magnitude. Correspondingly, the deviations from the exact mean and variance of $\Delta W_k / (\Delta t)^{1/2}$ are about 1% if 10^4 realizations are considered, and 0.1% for 10^6 realizations.

3.5. Stochastic modeling

The reduction of the general stochastic model (3.41) to the Markov model (3.42) is a very important step regarding the construction of a stochastic model for any specific case considered. However, to obtain closed stochastic differential equations one still has to solve two important problems: one has to choose an appropriate set of stochastic variables, and the coefficients in the stochastic equations have to be determined as functions of the variables considered.

3.5.1. The set of variables considered

The first problem to find a suitable set of stochastic variables can be solved by estimating the correlation time scale of the forces that drive the dynamics of the quantities of interest. Usually, one will find that this time scale is nonzero, such that the structure of equation (3.42) cannot be used directly. However, as pointed out in detail in Appendix 3A, it is then possible to extend the set of variables considered such that (3.42) can be used. A detailed application of this concept will be given in chapter 5 regarding the construction of models for turbulent velocities.

3.5.2. The coefficients of stochastic equations

The second problem to provide the coefficients a_i and b_{ik} in the stochastic equation (3.42) as explicit functions of the stochastic variables can be addressed in the following way. In many cases one can find simple and well-justified parametrizations for the diffusion coefficient b_{ik}. This is not surprising because b_{ik} just simulates the intensity of the unordered, chaotic production of fluctuations. The determination of a_i is much more complicated. Simple solutions (isotropic linear relaxation models) are available for systems in equilibrium states, and the extension of such equations (anisotropic linear relaxation models with mixing frequencies that vary in space and time) for the simulation of systems in near-equilibrium states does often work successfully. However, the simulation of nonequilibrium processes requires the consideration of nonlinear stochastic models. Various ways to construct them will be discussed in chapter 5.

Appendix 3A: The dynamics of relevant variables

A systematic procedure for the construction of stochastic equations for any variables considered (which will be referred to as relevant variables) will be presented here. This methodology is called the projection operator technique. Its basic idea is to extract the dynamics of relevant variables from any complete, deterministic dynamics. This results in contributions to the dynamics of relevant variables that are explicit deterministic functions of the relevant variables (which may involve memory effects), and remaining contributions that involve the influence of all the other quantities. The latter terms have the properties of stochastic forces.

The projection operator technique may be applied in various variants, see for instance Grabert (1982), Lindenberg & West (1990) and Zubarev et al. (1996, 1997). One way is to derive a PDF transport equation for relevant variables, which has (by adopting the Markov assumption) a structure that corresponds to that of the Fokker-Planck equation. Another way is to separate the instantaneous dynamics of relevant variables from the complete dynamics, see Heinz (1997). This approach will be presented here to contrast the derivation of PDF transport equations in the sections 3.1 and 3.2 with a corresponding construction of stochastic models.

3A.1. The problem considered

We assume that the dynamics of a system considered are completely described by a set of variables $\boldsymbol{\Xi}(t) = \{\boldsymbol{\xi}(t), \boldsymbol{\eta}(t)\}$, see Fig. 2.1 in chapter 2 for an illustration. The vector $\boldsymbol{\xi}(t)$ refers to variables that we consider to be relevant, and $\boldsymbol{\eta}(t)$ denotes the vector of the remaining (irrelevant) variables. Instead of $\boldsymbol{\Xi}(t)$, we may consider the corresponding instantaneous PDF $\Psi^*(\mathbf{x}, \mathbf{y}, t) = \delta(\boldsymbol{\xi}(t) - \mathbf{x})\, \delta(\boldsymbol{\eta}(t) - \mathbf{y})$. An equation for the evolution of this PDF may be obtained by differentiating it by time. This results in

$$\frac{\partial \Psi^*(\mathbf{x},\mathbf{y},t)}{\partial t} = -\left[\frac{\partial}{\partial x_k} \frac{d\xi_k}{dt}(\boldsymbol{\xi}(t),\boldsymbol{\eta}(t),t) + \frac{\partial}{\partial y_n} \frac{d\eta_n}{dt}(\boldsymbol{\xi}(t),\boldsymbol{\eta}(t),t) \right] \Psi^*(\mathbf{x},\mathbf{y},t). \quad (3A.1)$$

The derivatives by the arguments of the delta functions are rewritten into the corresponding sample space derivatives ($\partial\Psi^* / \partial(\xi_1(t) - x_1) = -\partial\Psi^* / \partial x_1$). The sample space derivatives may be drawn in front of $d\xi_k / dt$ and $d\eta_n / dt$ since the latter are independent of $\mathbf{x}$ and $\mathbf{y}$. Equation (3A.1) corresponds to the Liouville equation of classical statistical mechanics. It is unclosed due to the appearance of the unknown derivatives $d\xi_k / dt$ and $d\eta_n / dt$. The explicit time dependence in these derivatives may be caused for instance by the appearance of external forces.

In general, there is neither a way to assess the detailed dynamics of the complete set of variables $\boldsymbol{\Xi}(t)$ nor an interest to have all this information. Therefore, we restrict the attention to the dynamics of relevant variables $\boldsymbol{\xi}(t)$, which may by obtained from (3A.1) by integration over the **y**-space. This leads to

$$\frac{\partial \Psi(\mathbf{x},t)}{\partial t} = -\frac{\partial}{\partial x_k}\frac{d\xi_k}{dt}(\boldsymbol{\xi}(t),\boldsymbol{\eta}(t),t)\Psi(\mathbf{x},t) = \left[L^{rel}(\mathbf{x},t) + L^{ext}(\mathbf{x},t) + L(\mathbf{x},\boldsymbol{\eta},t)\right]\Psi(\mathbf{x},t), \tag{3A.2}$$

where the instantaneous PDF of the process $\boldsymbol{\xi}(t)$ is referred to

$$\Psi(\mathbf{x},t) = \delta(\boldsymbol{\xi}(t) - \mathbf{x}). \tag{3A.3}$$

The sum of the operators L^{rel}, L^{ext} and L is defined by the middle expression of (3A.2). This differentiation of different contributions to the evolution of relevant variables is applied to refer to the possibility of the appearance of contributions that are explicit functionals of the relevant variables, this means contributions that do not require assumptions to take them into account. Terms related to L^{rel} are found, e.g., if x_n denotes coordinates in physical space and $d\xi_n / dt$ corresponding velocities. L^{ext} refers to a possible contribution due to external forces, which is also assumed to be known. Due to the fact that the consideration of L^{rel} and L^{ext} does not pose any difficulties, we will neglect them for simplicity. Consequently, we consider the following basic equation

$$\frac{\partial}{\partial t}\Psi(\mathbf{x},t) = L(\mathbf{x},\boldsymbol{\eta},t)\,\Psi(\mathbf{x},t). \tag{3A.4}$$

Regarding the dynamics of $\boldsymbol{\xi}(t)$, equation (3A.4) is unclosed due to the appearance of irrelevant variables $\boldsymbol{\eta}(t)$. The rewriting of (3A.4) by means of the projection operator technique will be considered next.

3A.2. The projection operator

To rewrite the dynamics (3A.4) we need a projection operator P that projects any functions $A = A(\boldsymbol{\xi}(t), \boldsymbol{\eta}(t), t)$ of relevant and irrelevant variables onto the subspace of relevant variables. Such an operator will be defined by

$$PA(\boldsymbol{\xi}(t),\boldsymbol{\eta}(t),t) = \int d\mathbf{x}\, \left\langle A(\boldsymbol{\xi}(t),\boldsymbol{\eta}(t),t) \,\middle|\, \boldsymbol{\xi}(0) = \mathbf{x} \right\rangle \Psi(\mathbf{x},0), \tag{3A.5}$$

where the initial time is assumed to be zero. The conditional mean on the right-hand side is defined by (2.35). P is characterized by the properties (A and B are any functions of relevant and irrelevant variables)

$$\langle (PA)\,B\rangle = \langle A\,(PB)\rangle, \qquad P\,\Psi(\mathbf{x},0) = \Psi(\mathbf{x},0), \qquad P^2 = P. \tag{3A.6}$$

The validity of the relations (3A.6) may be proved by means of (3A.5) combined with the definition (2.35) of conditional means,

$$\langle (PA)B\rangle = \int d\mathbf{x}\, \langle A\,|\,\xi(0)=\mathbf{x}\rangle \langle \Psi(\mathbf{x},0)B\rangle = \int d\mathbf{x}\, \langle B\,|\,\xi(0)=\mathbf{x}\rangle \langle A\,\Psi(\mathbf{x},0)\rangle = \langle A\,(PB)\rangle,$$

$$P\Psi(\hat{\mathbf{x}},0) = \int d\mathbf{x}\, \langle \Psi(\hat{\mathbf{x}},0)\,|\,\xi(0)=\mathbf{x}\rangle\, \Psi(\mathbf{x},0) = \int d\mathbf{x}\, \delta(\mathbf{x}-\hat{\mathbf{x}})\,\Psi(\mathbf{x},0) = \Psi(\hat{\mathbf{x}},0),$$

$$P^2A = \int d\hat{\mathbf{x}} \left\langle \int d\mathbf{x}\, \langle A\,|\,\xi(0)=\mathbf{x}\rangle \Psi(\mathbf{x},0)\,\middle|\,\xi(0)=\hat{\mathbf{x}}\right\rangle \Psi(\hat{\mathbf{x}},0)$$

$$= \int d\hat{\mathbf{x}}\, \langle A\,|\,\xi(0)=\hat{\mathbf{x}}\rangle \Psi(\hat{\mathbf{x}},0) \left\langle \int d\mathbf{x}\, \Psi(\mathbf{x},0)\,\middle|\,\xi(0)=\hat{\mathbf{x}}\right\rangle = PA. \qquad (3A.7)$$

Alternatively, the relations (3A.6) may be formulated by adopting the complement operator $Q = 1 - P$,

$$\langle (QA)\,B\rangle = \langle A\,(QB)\rangle, \qquad Q\Psi(\mathbf{x},0) = 0, \qquad Q^2 = Q. \qquad (3A.8)$$

The latter relations will be used frequently below.

3A.3. An operator identity

To transform (3A.4) in the way described above we consider its formal solution

$$\Psi(\mathbf{x},t) = e^{Lt}\Psi(\mathbf{x},0) = \left\{1 + \sum_{n=1}^{\infty} \frac{t^n}{n!} L^n\right\} \Psi(\mathbf{x},0). \qquad (3A.9)$$

The operator exp(Lt) can be considered as the sum of two contributions,

$$e^{Lt} = U_1(t) + U_2(t), \qquad (3A.10)$$

where U_1 describes the part of the dynamics which is explicit in the relevant variables (it may depend on all the history of the relevant variables), and U_2 is the remainder, i.e., U_2 a function of the irrelevant variables. To determine U_2, we will assume that it is determined by the following equation and initial condition,

$$\frac{dU_2}{dt} = QLU_2, \qquad U_2(0) = 1. \qquad (3A.11)$$

Due to $PQ = P\,(1 - P) = 0$, which follows from the last part of (3A.6), the assumed evolution equation for U_2 assures that the projection of dU_2 / dt vanishes in the ensemble average. This enables the interpretation of dU_2 / dt as a stochastic force, see the explanations given below. The condition $U_2(0) = 1$ implies $U_1(0) = 0$. This corresponds with the assumption that $U_1(t)$ is independent of its initial condition. As a consequence of (3A.11), U_1 is determined by the following equation and

initial condition,

$$\frac{dU_1}{dt} = \frac{de^{Lt}}{dt} - \frac{dU_2}{dt} = LU_1 + PLU_2, \qquad U_1(0) = 0. \tag{3A.12}$$

By adopting the formal solutions of (3A.11) and (3A.12), the evolution operator exp(Lt) can be rewritten into

$$e^{Lt} = e^{QLt} + \int_0^t dt'\, e^{L(t-t')} PLe^{QLt'}. \tag{3A.13}$$

We transform the integrand by setting t' = t – s. This results in the operator identity

$$e^{Lt} = e^{QLt} + \int_0^t ds\, e^{Ls} PLe^{QL(t-s)}. \tag{3A.14}$$

Its consistency may be seen by comparing the initial values and derivatives by t of both sides.

3A.4. The dynamics of relevant variables

The use of the operator identity (3A.14) in (3A.9) allows now the rewriting of the evolution equation (3A.4). By adopting the definition (3A.5) of the projection operator P we obtain

$$\Psi(\hat{\mathbf{x}},t) = \int_0^t ds \int d\mathbf{x} \left\langle Le^{QL(t-s)} \Psi(\hat{\mathbf{x}},0) \middle| \boldsymbol{\xi}(0) = \mathbf{x} \right\rangle \Psi(\mathbf{x},s) + e^{QLt}\, \Psi(\hat{\mathbf{x}},0). \tag{3A.15}$$

We differentiate (3A.15) by time, multiply it by x_i and integrate it over the space of relevant variables. This leads to the following equation for relevant variables ξ_i,

$$\frac{d\xi_i}{dt} = -\int d\mathbf{x}\; M_i(\mathbf{x},0)\, \Psi(\mathbf{x},t) - \int_0^t ds \int d\mathbf{x}\; \frac{dM_i}{dt}(\mathbf{x},t-s)\, \Psi(\mathbf{x},s) + f_i(t), \tag{3A.16}$$

where we applied the abbreviations

$$M_i(\mathbf{x},t) = -\int d\hat{\mathbf{x}}\; \hat{x}_i \left\langle Le^{QLt} \Psi(\hat{\mathbf{x}},0) \middle| \boldsymbol{\xi}(0) = \mathbf{x} \right\rangle, \tag{3A.17a}$$

$$f_i(t) = \int d\hat{\mathbf{x}}\; \hat{x}_i QLe^{QLt} \Psi(\hat{\mathbf{x}},0) = QLe^{QLt} \xi_i(0). \tag{3A.17b}$$

The last term f_i in equation (3A.16) is a function of the irrelevant variables. By adopting the relations (3A.8), we find

$$\left\langle f_i(t)\, \Psi(\mathbf{x},0) \right\rangle = \left\langle Qf_i(t)\, \Psi(\mathbf{x},0) \right\rangle = \left\langle f_i(t)\, Q\Psi(\mathbf{x},0) \right\rangle = 0. \tag{3A.18}$$

The integration of this relation over **x** leads then to the result

$$\left\langle f_i(t)\right\rangle = 0. \tag{3A.19}$$

This important property of f_i to vanish in the ensemble mean enables its interpretation as a stochastic force.

The first two terms on the right-hand side of equation (3A.16) are functions of relevant variables. They are characterized by the memory function $M_i(\mathbf{x}, t)$, which represents the averaged influence of irrelevant variables on the dynamics of relevant variables. By means of (3.17a), we find for $M_i(\mathbf{x}, 0)$, which appears in the first term,

$$M_i(\mathbf{x},0) = -\left\langle \frac{d\xi_i}{dt}(0) \,\middle|\, \boldsymbol{\xi}(0) = \mathbf{x} \right\rangle. \tag{3A.20}$$

This expression may be rewritten into an equation that relates $M_i(\mathbf{x}, 0)$ to the PDF $\langle\delta(\boldsymbol{\xi}(t) - \mathbf{x})\rangle$,

$$\frac{\partial}{\partial x_i} M_i(\mathbf{x},0)\left\langle \Psi(\mathbf{x},0)\right\rangle = -\frac{\partial}{\partial x_i}\left\langle \Psi(\mathbf{x},0)\frac{d\xi_i}{dt}(0)\right\rangle = \left[\frac{\partial}{\partial t}\left\langle \Psi(\mathbf{x},t)\right\rangle\right](t=0). \tag{3A.21}$$

This result shows that $M_i(\mathbf{x}, 0)$ vanishes under stationary conditions. With regard to $dM_i(\mathbf{x}, t) / dt$ in the second term on the right-hand side of (3A.16) we obtain by the differentiation of the expression (3A.17a)

$$\frac{dM_i}{dt}(\mathbf{x},t) = -\left\langle Lf_i(t) \,\middle|\, \boldsymbol{\xi}(0) = \mathbf{x}\right\rangle. \tag{3A.22}$$

This relation is an essential result of the approach presented here. It provides a link between the stochastic force f_i, which generates fluctuations of relevant variables, and $dM_i(\mathbf{x}, t) / dt$, which controls the relaxation (the dissipation) of fluctuations of relevant variables. Such relations are called fluctuation-dissipation theorems. The value of (3A.22) arises from the possibility of calculating the function $dM_i(\mathbf{x}, t) / dt$ on the basis of assumption about the statistics of stochastic forces. This will be pointed out in the next three subsections.

3A.5. The equilibrium dynamics of relevant variables

The use of the fluctuation-dissipation theorem (3A.22) for the calculation of $dM_i(\mathbf{x}, t) / dt$ requires assumptions on L to relate the right-hand side to measurable quantities. For statistically stationary processes, L is characterized by the property

$$\frac{\partial\langle AB\rangle}{\partial t} = 0 = \langle (LA)B\rangle + \langle A(LB)\rangle. \tag{3A.23}$$

This relation may be used to rewrite the expression (3A.22). We obtain

$$\frac{dM_i}{dt}(\mathbf{x},t)\langle\Psi(\mathbf{x},0)\rangle = -\langle Lf_i(t)\Psi(\mathbf{x},0)\rangle = \langle f_i(t)L\Psi(\mathbf{x},0)\rangle = \langle f_i(t)QL\Psi(\mathbf{x},0)\rangle$$

$$= -\frac{\partial}{\partial x_k}\langle f_i(t)\Psi(\mathbf{x},0)QL\xi_k(0)\rangle = -\frac{\partial}{\partial x_k}\langle f_i(t)f_k(0)\Psi(\mathbf{x},0)\rangle$$

$$= -\frac{\partial}{\partial x_k}\langle f_i(t)f_k(0)|\xi(0)=\mathbf{x}\rangle\langle\Psi(\mathbf{x},0)\rangle. \qquad (3A.24)$$

The first rewriting of the left-hand side results from the definition (2.35) of conditional means. The second rewriting makes use of (3A.23). Then, we replace f_i by $Q\,f_i$, and apply the first part of relation (3A.8) to obtain the third rewriting. The expressions on the second line may be obtained by applying L to $\Psi(\mathbf{x}, 0)$ and adopting the definition (3A.17b) of stochastic forces. The definition of conditional means is then applied again to obtain the last line of (3A.24).

The application of the relation (3A.24) in equation (3A.16) implies then the following equilibrium dynamics of relevant variables,

$$\frac{d\xi_i}{dt} = \int_0^t ds \int d\mathbf{x}\,\langle\Psi(\mathbf{x},0)\rangle^{-1}\frac{\partial\langle f_i(t-s)f_k(0)|\xi(0)=\mathbf{x}\rangle\langle\Psi(\mathbf{x},0)\rangle}{\partial x_k}\Psi(\mathbf{x},s) + f_i(t), \qquad (3A.25)$$

where $M_i(\mathbf{x}, 0) = 0$ is applied for the stationary case considered. Thus, the specification of the equilibrium PDF $<\Psi(\mathbf{x}, 0)>$ and statistics of the stochastic force f_i completely determines the dynamics of relevant variables. Examples for such assumptions will be considered next.

3A.6. Colored Gaussian noise

The consideration of the vector of relevant variables $\xi(t)$ as a continuous process requires the assumption that the stochastic force f_i is a Gaussian process (Gardiner 1983, Thomson 1987). Therefore, f_i is completely specified by its zero mean and correlation. First, we will assume that f_i is a colored noise process, this means its correlation function is characterized by an exponential function,

$$\langle f_i(t)f_k(s)\rangle = \langle f_i(t-s)f_k(0)\rangle = \frac{1}{2\tau_f}b_{in}b_{kn}\exp\left\{-\frac{|t-s|}{\tau_f}\right\}. \qquad (3A.26)$$

b_{in} denotes a constant coefficient and τ_f represents the constant correlation time of f_i. The first rewriting of the left-hand side results from the fact that the correlation

function only depends on the difference of the time argument under statistically stationary conditions. The use of (3A.26) in equation (3A.25) leads then to the equilibrium dynamics

$$\frac{d\xi_i}{dt} = -\frac{1}{2\tau_f} b_{in} b_{kn} \sigma^{-1}{}_{km} \int_0^t ds \, \exp\left\{-\frac{t-s}{\tau_f}\right\} \left(\xi_m(s) - \langle \xi_m \rangle\right) + f_i(t) \qquad (3A.27)$$

if the equilibrium PDF is specified as a Gaussian PDF with constant variance matrix σ. The inverse variance matrix is denoted by σ^{-1}.

The inclusion of correlated noise and memory effects in (3A.27) hampers analyses and the application of standard methods for the solution of stochastic differential equations (Kloeden & Platen 1992). In order to rewrite equation (3A.27), we represent f_i as solution of the equation

$$\frac{df_i}{dt} = -\frac{1}{\tau_f} f_i + \frac{1}{\tau_f} b_{in} \frac{dW_n}{dt}. \qquad (3A.28)$$

By adopting the relations between stochastic equations and Fokker-Planck equations pointed out in section 3.4 in combination with the findings presented in section 3.3, one can prove that this equation determines f_i as a Gaussian process. Its means vanish for the assumed stationarity, and the correlation function of f_i satisfies for $s \geq 0$ according to (3.40) the equation

$$\frac{\partial}{\partial s} \langle f_i(t) f_k(t+s) \rangle = -\frac{1}{\tau_f} \langle f_i(t) f_k(t+s) \rangle. \qquad (3A.29)$$

This equation provides the same evolution of the correlation function of f_i as given by (3A.26). Therefore, the definition of f_i by (3A.28) is equivalent to (3A.26) provided the variance of f_i (which represents the initial condition to equation (3A.29)) is also consistent with the corresponding implication of (3A.26),

$$\langle f_i(t) \, f_k(t) \rangle = \frac{1}{2\tau_f} b_{in} b_{kn}. \qquad (3A.30)$$

This is the case, see equation (3.36b) for the stationary case considered.

By adopting (3.A28) we can transform (3A.27) into the frame of the stochastic equations (3.42). This may be seen by differentiation of (3A.27),

$$\begin{aligned} \frac{d}{dt}\frac{d\xi_i}{dt} &= -\frac{1}{2\tau_f} b_{in} b_{kn} \sigma^{-1}{}_{km} \left(\xi_m(t) - \langle \xi_m \rangle\right) - \frac{1}{\tau_f}\left(\frac{d\xi_i}{dt} - f_i(t)\right) + \frac{df_i}{dt} \\ &= -\frac{1}{2\tau_f} b_{in} b_{kn} \sigma^{-1}{}_{km} \left(\xi_m(t) - \langle \xi_m \rangle\right) - \frac{1}{\tau_f}\frac{d\xi_i}{dt} + \frac{1}{\tau_f} b_{in} \frac{dW_n}{dt}. \end{aligned} \qquad (3A.31)$$

Hence, the enlarged set of variables (ξ, $d\xi$ / dt) represents a Markov process that satisfies the structure of the equations (3.42). Such a rewriting of the equations (3A.27) is usually very helpful because many results related to Fokker-Planck equations and their solutions can be applied then.

3A.7. White Gaussian noise

A further specification of the dynamics of relevant variables is given by the assumption that f_i becomes delta-correlated ($\tau_f \to 0$). In this case, the correlation function (3A.26) reduces to

$$\left\langle f_i(t)\, f_k(s)\right\rangle = \lim_{\tau_f \to 0} \frac{1}{2\tau_f} b_{in} b_{kn} \exp\left\{-\frac{|t-s|}{\tau_f}\right\} \delta_{ik} = b_{in} b_{kn} \delta(t-s). \qquad (3A.32)$$

The comparison of the properties of f_i with those of dW_i / dt, see the relations (3.43a-b), shows that f_i has to be proportional to dW_i / dt in this case. This relation can be derived from the stochastic model (3A.28) for f_i, which reduces for $\tau_f \to 0$ to the expression

$$f_i(t) = b_{ik} \frac{dW_k}{dt}. \qquad (3A.33)$$

The use of (3A.32) and (3A.33) in (3A.27) leads then to the equation

$$\frac{d\xi_i}{dt} = -\frac{1}{2} b_{in} b_{nk} \sigma^{-1}{}_{km} \left(\xi_m - \left\langle \xi_m \right\rangle\right) + b_{in} \frac{dW_n}{dt}. \qquad (3A.34)$$

Thus, for the case of white-noise forces f_i one obtains equations for the set $\xi(t)$ of relevant variables which agree with the structure of the stochastic equations (3.42).

4. The equations of fluid and thermodynamics

The fundamentals for the calculation of turbulent flows are given by the basic equations of fluid and thermodynamics. There are several ways to introduce these equations. After introducing the fluid dynamic variables in section 4.1, these equations will be derived here in sections 4.2 and 4.3 on the basis of a model for the underlying molecular motion. This approach explains all the quantities involved as means over molecular quantities, and it reveals the range of applicability of the basic equations. In addition to this, the approach applied here illustrates the use of an analysis technique that will also be applied in chapter 5 to construct turbulence models. Section 4.4 deals with the generalization of these equations for the case of multi-component flows. The essential problem related to applications of the basic equations of fluid and thermodynamics is then pointed out in section 4.5. The simplest approach to overcome this problem is the use of the basic equations for the construction of transport equations for averaged variables. However, this approach is also related to significant problems, which will be described in section 4.6. The conclusion that can be drawn from these explanations is the requirement to develop stochastic methods for the simulation of turbulent reacting flows. Several ways to realize this task will be addressed in chapters 5, 6 and 7.

4.1. The fluid dynamic variables

4.1.1. Means conditioned on the position

In fluid dynamics one is usually interested in the prediction of variables at any positions: they can be measured at best. Such Eulerian fluid dynamic variables can be defined by adopting the relation (2.35) for conditional means. Correspondingly, the mean of any function Q of molecular properties (e.g., velocities and positions) conditioned on the position $\mathbf{x}$ in physical space is defined by the expression

$$\overline{Q}(\mathbf{x},t) = \frac{1}{\rho(\mathbf{x},t)} \left\langle \rho^{(m)}(\mathbf{x},t) Q \right\rangle . \tag{4.1}$$

S. Heinz, *Statistical Mechanics of Turbulent Flows*

Such means (4.1) will be referred to below as mass-weighted means. The symbol <⋯> denotes an ensemble mean, see chapter 1, $\rho^{(m)}$ refers to the instantaneous molecular mass density

$$\rho^{(m)}(\mathbf{x},t) = M\,\delta\left(\mathbf{x}^*(t) - \mathbf{x}\right), \tag{4.2}$$

and the mean mass density $\rho(\mathbf{x}, t)$ is defined as the ensemble mean of $\rho^{(m)}$,

$$\rho(\mathbf{x},t) = \left\langle \rho^{(m)}\left(\mathbf{x},t\right)\right\rangle. \tag{4.3}$$

In (4.2), $\mathbf{x}^*(t)$ denotes the position of a molecule at time t (Lagrangian particle properties are always referred to by an asterisk throughout the book). It is worth noting that $\rho^{(m)}$ (and therefore ρ) is not normalized to unity. The integration of (4.2) shows that

$$M = \int d\mathbf{x}\,\rho^{(m)}(\mathbf{x},t). \tag{4.4}$$

Hence, M is the total mass of molecules within the domain considered.

By invoking the ergodic theorem, see chapter 1, the ensemble averaging considered here represents a spatial filter procedure where the filter width is much smaller than the domain considered but such that a very large number of molecules is involved into the calculation of means at **x**. Therefore, such ensemble-averaged variables describe the properties of a continuum, they represent fluid dynamic variables as for instance the fluid mass density or velocity, see section 4.1.3.

4.1.2. The conditioned velocity PDF

As pointed out in section 2.3.3, the conditional mean (4.1) may also be represented as a mean of a PDF. This relation reads

$$\overline{Q}(\mathbf{x},t) = \int d\mathbf{w}\; Q\left(\mathbf{w},\mathbf{x},t\right)F^{(m)}\left(\mathbf{w},\mathbf{x},t\right), \tag{4.5}$$

where the conditional PDF of molecular velocities is given by

$$F^{(m)}\left(\mathbf{w},\mathbf{x},t\right) = \frac{1}{\rho(\mathbf{x},t)}\left\langle \rho^{(m)}(\mathbf{x},t)\,\delta\left(\mathbf{V}^*\left(\mathbf{x}^*(t),t\right) - \mathbf{w}\right)\right\rangle. \tag{4.6}$$

Here, $\mathbf{V}^*(\mathbf{x}^*(t), t) = (V_1^*, V_2^*, V_3^*)$ is the velocity of a molecule. The consistency of the definitions (4.1) and (4.5) for $\overline{Q}$ may be seen by inserting (4.6) into (4.5). The use of the shifting property of delta functions and integration over the velocity sample space recovers the relation (4.1).

The definition (4.6) represents a relation between Eulerian and Lagrangian variables: the Eulerian PDF $F^{(m)}$, which is considered at a position **x**, is defined in

terms of the Lagrangian particle properties $\mathbf{x}^*(t)$ and $\mathbf{V}^*(t)$. This relation is very helpful regarding the modeling of fluid dynamic processes. One may apply models for the molecular motion and calculates $F^{(m)}$ (and related fluid dynamic variables, see section 4.1.3) by means of (4.6). However, to compare such model predictions with measurements one likes to have a definition of $F^{(m)}$ in terms of measurable Eulerian quantities. Such a definition is given by rewriting the relation (4.6) into

$$F^{(m)}(\mathbf{w},\mathbf{x},t) = \overline{\delta(\mathbf{V}(\mathbf{x},t)-\mathbf{w})}. \tag{4.7}$$

Here, the Lagrangian particle velocity is written $\mathbf{V}^*(\mathbf{x}^*(t), t) = \mathbf{V}^*(\mathbf{x}, t) = \mathbf{V}(\mathbf{x}, t)$. The replacement of $\mathbf{x}^*(t)$ by $\mathbf{x}$ in $\mathbf{V}^*$ is a consequence of the properties of delta functions. $\mathbf{V}$ is used then to denote the corresponding Eulerian velocity. The latter is nothing but the velocity of the molecule which has the property $\mathbf{x}^*(t) = \mathbf{x}$ (we consider a continuum where one finds a molecule at each point).

4.1.3. The fluid dynamic variables

The knowledge of $F^{(m)}$ enables the calculation of fluid dynamic variables in addition to the mass density ρ that is defined by (4.3). The most important fluid dynamic variable is the fluid velocity U_i (i = 1, 3), which is given by the mean velocity of molecules in an infinitesimal vicinity of $\mathbf{x}$,

$$U_i(\mathbf{x},t) = \overline{V_i(\mathbf{x},t)} = \int d\mathbf{w}\; w_i F^{(m)}(\mathbf{w},\mathbf{x},t). \tag{4.8}$$

In general, molecular velocities $V_i(\mathbf{x}, t)$ differ from the mean velocities $U_i(\mathbf{x}, t)$. Such differences are measured by fluctuations, which are denoted by small letters,

$$v_i(\mathbf{x},t) = V_i(\mathbf{x},t) - \overline{V_i(\mathbf{x},t)}. \tag{4.9}$$

The fluctuations v_i vanish in the mass-weighted mean,

$$\overline{v_i(\mathbf{x},t)} = 0, \tag{4.10}$$

but they do not vanish in the ensemble mean in general, $\langle v_i \rangle \neq 0$. The properties of fluctuations v_i are characterized essentially by the specific (this term will be used for quantities that are normalized by mass) kinetic energy e, which is defined by

$$e(\mathbf{x},t) = \frac{1}{2}\overline{v_i v_i} = \frac{1}{2}\int d\mathbf{w}\,(w_i - U_i)(w_i - U_i)F^{(m)}(\mathbf{w},\mathbf{x},t). \tag{4.11}$$

Further fluid dynamic variables will be considered below in conjunction with the consideration of transport equations for the calculation of ρ, U_i, and e.

4.2. From the molecular to fluid dynamics

Next, we address the calculation of $F^{(m)}$ and related fluid dynamic variables on the basis of a model for the motion of molecules. Usually for this one applies the Boltzmann equation, see for instance Cercignani (1988) or Bird (1994). However, this approach is faced with several questions. The first problem arises from the fact that such equations are related to the consideration of rarefied gases, whereas one is interested in dense fluids (gases and liquids) in fluid mechanics in general. The second problem arises from the fact that the derivation of the fluid dynamic equations in this way poses a non-trivial problem. By adopting this approach one may find equations as they are postulated in empirical approaches, but other equations may be found, too. The physical relevance of such extensions of the equations of fluid dynamics cannot be seen to be fully clarified until now (Cercignani 1988, Alexeev 1994, Levermore et al. 1998, Esposito et al. 1999).

4.2.1. A model for the molecular motion

An alternative way to the derivation of the fluid dynamic equations on the basis of the Boltzmann equation is to apply the equations for the dynamics of relevant variables derived in Appendix 3A. First, we will restrict the attention in the sections 4.2 and 4.3 to the case of monatomic fluids which do not have internal degrees of freedom (rotational or vibrational energy). The more general case of polyatomic fluids will be addressed in section 4.4.

The state of each molecule is then completely described by its position and velocity. We consider the velocity V_i^* of a molecule to be the relevant variable ξ_i. According to the explanations given in section 3A.1, we extend equation (3A.34) by the consideration of external forces $F_i^{(m)}$, which could be caused by gravity, and particle positions x_i^*. This results in

$$\frac{dx_i^*}{dt} = V_i^*, \tag{4.12a}$$

$$\frac{dV_i^*}{dt} = -\frac{1}{\tau_m}\left(V_i^* - U_i\right) + F_i^{(m)} + \sqrt{\frac{4e}{3\tau_m}}\frac{dW_i}{dt}. \tag{4.12b}$$

The fluid velocity U_i is defined by (4.8). To obtain the equations (4.12a-b), we assumed in addition to (3A.34) isotropic coefficient matrices, $b_{in} = b_{mm} / 3\ \delta_{in}$ and $\sigma_{in} = 2\ e / 3\ \delta_{in}$, and we introduced the characteristic time scale $\tau_m = 12\ e / b_{mm}^2$. In contrast to (3A.34), e and τ_m do not have to be constant here, they may depend on position and time. This corresponds to the consideration of a local equilibrium in extension of the equilibrium assumption related to the derivation of (3A.34).

The properties of dW_i / dt in (4.12b) were explained in detail in section 3.4.1: this is a Gaussian process with means and correlations according to the relations (3.43a-b). Compared to the application of the Boltzmann equation for the simulation of molecular dynamics, the appearance of the stochastic force in (4.12b) may be seen as the effect of the interaction of long-range forces between the molecules which produce a continuous sequence of small and almost stochastic velocity changes. It is worth noting that the particles are assumed to move independently in this way. This corresponds to the consideration of a perfect gas.

4.2.2. The unclosed fluid dynamic equations

As shown in chapter 3, the stochastic model (4.12a-b) can be rewritten into an equivalent Fokker-Planck equation. The definition (4.6) of $F^{(m)}$ reveals that the joint PDF of particle positions and velocities is equal to $F^{(m)}\,\rho / M$. We multiply the transport equation implied by (4.12a-b) for this PDF with M to obtain

$$\frac{\partial \rho F^{(m)}}{\partial t} = -\frac{\partial \rho w_i F^{(m)}}{\partial x_i} - \frac{\partial}{\partial w_i}\left[-\frac{1}{\tau_m}\left(w_i - U_i\right) + F_i^{(m)} \right] \rho F^{(m)} + \frac{2e}{3\tau_m}\frac{\partial^2 \rho F^{(m)}}{\partial w_j \partial w_j}. \tag{4.13}$$

The multiplication of equation (4.13) with the corresponding variables and integration over the velocity space (see the explanations given in section 3.2.2) results in transport equations for the fluid dynamic variables. For the mass density $\rho(\mathbf{x}, t)$, fluid velocity $U_i(\mathbf{x}, t)$ and specific kinetic energy $e(\mathbf{x}, t)$, we obtain in this way the equations

$$\frac{\partial \rho}{\partial t} + \frac{\partial \rho U_i}{\partial x_i} = 0, \tag{4.14a}$$

$$\frac{\partial \rho U_j}{\partial t} + \frac{\partial \rho U_i U_j}{\partial x_i} + \frac{\partial p_{ij}}{\partial x_i} = \rho F_j, \tag{4.14b}$$

$$\frac{\partial \rho e}{\partial t} + \frac{\partial \rho U_k e}{\partial x_k} + \frac{\partial q_k}{\partial x_k} + p_{jk}\frac{\partial U_j}{\partial x_k} = \rho Q_B. \tag{4.14c}$$

On the right-hand sides, we applied the following abbreviations for source terms due to external forces,

$$F_j = \overline{F_j^{(m)}}, \qquad Q_B = \overline{f_k^{(m)} v_k}, \tag{4.15}$$

where $f_k^{(m)} = F_k^{(m)} - F_k$ represents fluctuations of molecular forces. On the left-hand sides of (4.14b-c), we defined the stress tensor p_{ij} and heat flux vector q_k via the

relations

$$p_{ij} = \rho\overline{v_i v_j}, \tag{4.16a}$$

$$q_k = \frac{1}{2}\rho\overline{v_k v_n v_n}. \tag{4.16b}$$

The equations (4.14a-c) were derived here as a consequence of the stochastic model (4.12a-b), but it is worth emphasizing that they are independent of all the model details (with the exception of the appearance of the known external force $F_i^{(m)}$). The same equations (4.14a-c) can be obtained by adopting the Boltzmann equation for the molecular motion, see for instance Cercignani (1988). Therefore, all the physics is contained in the unknown quantities of (4.14b-c): Q_B, p_{ij} and q_k. The source term Q_B is usually assumed to be known (it is neglected in general). The problem to calculate p_{ij} can be reduced by splitting it into an isotropic and deviatoric part,

$$p_{ij} = p\delta_{ij} + \pi_{ij}. \tag{4.17}$$

The isotropic part, which is referred to as pressure, is related to ρ and e via

$$p = \frac{p_{ii}}{3} = \rho\frac{2e}{3}, \tag{4.18}$$

this means p is a known function in (4.14b-c). Thus, the remaining question is to provide closures of π_{ij} and q_k.

This problem is often addressed in an empirical way. As a consequence of symmetry constraints, one parametrizes π_{ij} in terms of the rate-of-strain tensor

$$S_{ij} = \frac{1}{2}\left(\frac{\partial U_i}{\partial x_j} + \frac{\partial U_j}{\partial x_i}\right). \tag{4.19}$$

In particular, one considers π_{ij} to be proportional to the deviatoric part of S_{ij} (Kuo 1986), which is given by

$$S_{ij}^{\ d} = \frac{1}{2}\left(\frac{\partial U_i}{\partial x_j} + \frac{\partial U_j}{\partial x_i} - \frac{2}{3}\frac{\partial U_n}{\partial x_n}\delta_{ij}\right). \tag{4.20}$$

However, this empirical approach leads to questions, for instance on the range of applicability of such parametrizations. In contrast to this, the consideration of the stochastic model (4.12a-b) enables the systematic calculation of π_{ij} and q_k on the basis of their transport equations, which are implied by the Fokker-Planck equation (4.13). This will be demonstrated in section 4.3.

4.3. The closure of the fluid dynamic equations

4.3.1. The calculation of the deviatoric stress tensor

To derive a closure model for the deviatoric part π_{ij} of the stress tensor p_{ij}, we have to consider the transport equation for p_{ij}. This equation can be obtained from (4.13), as pointed out in section 3.2.2. It reads

$$\frac{\partial p_{ij}}{\partial t}+\frac{\partial U_k p_{ij}}{\partial x_k}+\frac{\partial \rho\overline{v_k v_i v_j}}{\partial x_k}+p_{jk}\frac{\partial U_i}{\partial x_k}+p_{ik}\frac{\partial U_j}{\partial x_k}=-\frac{2}{\tau_m}\pi_{ij}+\rho\overline{f_i^{(m)}v_j}+\rho\overline{f_j^{(m)}v_i}. \tag{4.21}$$

This equation can be reduced to an equation for p,

$$\frac{\partial p}{\partial t}+\frac{\partial U_k p}{\partial x_k}+\frac{2}{3}\frac{\partial q_k}{\partial x_k}+\frac{2}{3}p_{nk}\frac{\partial U_n}{\partial x_k}=\frac{2}{3}\rho Q_B, \tag{4.22}$$

and the π_{ij} equation is obtained by combining the equations (4.21) and (4.22),

$$\frac{\partial \pi_{ij}}{\partial t}+\frac{\partial U_k \pi_{ij}}{\partial x_k}+\frac{\partial \rho\overline{v_k(v_i v_j-v_n v_n\delta_{ij}/3)}}{\partial x_k}-\rho\left(\overline{f_i^{(m)}v_j}+\overline{f_j^{(m)}v_i}-\frac{2}{3}\overline{f_n^{(m)}v_n}\,\delta_{ij}\right)=$$

$$=-\frac{2}{\tau_m}\pi_{ij}-2pS_{ij}^{\ d}-\pi_{jk}\frac{\partial U_i}{\partial x_k}-\pi_{ik}\frac{\partial U_j}{\partial x_k}+\frac{2}{3}\pi_{nk}\frac{\partial U_n}{\partial x_k}\delta_{ij}. \tag{4.23}$$

To derive an algebraic expression for π_{ij} one has to neglect the first two gradient terms on the left-hand side. By adopting the continuity equation (4.14a), these two terms may also be written

$$\frac{\partial \pi_{ij}}{\partial t}+\frac{\partial U_k \pi_{ij}}{\partial x_k}=\rho\frac{D}{Dt}\left(\overline{v_i v_j}-\frac{2e}{3}\delta_{ij}\right), \tag{4.24}$$

where the substantial (or sometimes also called total) derivative is abbreviated by

$$\frac{D}{Dt}=\frac{\partial}{\partial t}+U_k\frac{\partial}{\partial x_k}. \tag{4.25}$$

Thus, the neglect of the first two gradient terms on the left-hand side of (4.23) corresponds to the assumption that the anisotropic component of the velocity variance matrix reached an equilibrium stage where the memory of any initial conditions is lost. This assumption is consistent with those which underlie the derivation of the stochastic model (4.12a-b), see the explanations given in chapter

3. The third term on the left-hand of relation (4.23) represents an anisotropic contribution due to molecular diffusion, see, for instance, equation (4.33) below. In accord with the assumptions made to derive (4.12a-b), we may neglect such contributions to the budget of π_{ij}. With a corresponding argument, we may neglect the last three terms on the left-hand side of (4.23), which involve the anisotropic part of the production by external forces. The resulting algebraic relation for π_{ij} then reads

$$\frac{2}{\tau_m}\pi_{ij} = -\frac{4e}{3}\rho S_{ij}^{\ d} - \pi_{jk}\frac{\partial U_i}{\partial x_k} - \pi_{ik}\frac{\partial U_j}{\partial x_k} + \frac{2}{3}\pi_{nk}\frac{\partial U_n}{\partial x_k}\delta_{ij}. \tag{4.26}$$

This equation for π_{ij} can be solved by adopting a technique that is described in more detail in chapter 6. The resulting general expression for π_{ij} can be written in terms of contributions of growing order in velocity gradients. A simple method to obtain the terms of low order of the general expression for π_{ij} is given by the following successive approximation.

In the first order of approximation we assume that π_{ij} is a linear function of velocity gradients. This is equivalent to the neglect of all the terms that involve π_{ij} multiplied by velocity gradients in equation (4.26). In this case, we find for π_{ij} the expression

$$\pi_{ij}^{(1)} = -2\mu S_{ij}^{\ d}, \tag{4.27}$$

where we introduced the viscosity

$$\mu = \rho\nu. \tag{4.28}$$

The kinematic viscosity ν is an abbreviation for the expression

$$\nu = \frac{\tau_m e}{3}. \tag{4.29}$$

This quantity appears as a diffusion coefficient (which is also called diffusivity) in relation (4.27).

In the second order of approximation, we apply the first-order approximation (4.27) in the terms that involve π_{ij} on the right-hand side of (4.26). This leads to an expression for π_{ij}, which involves velocity gradients of second order,

$$\pi_{ij}^{(2)} = \pi_{ij}^{(1)} - \pi_{jk}^{(1)}\frac{\tau_m}{2}\frac{\partial U_i}{\partial x_k} - \pi_{ik}^{(1)}\frac{\tau_m}{2}\frac{\partial U_j}{\partial x_k} + \pi_{nk}^{(1)}\frac{\tau_m}{3}\frac{\partial U_n}{\partial x_k}\delta_{ij}. \tag{4.30}$$

Higher-order approximations can be constructed correspondingly by repeating this successive approximation procedure.

4.3.2. The heat flux calculation

A transport equation for q_i may be obtained on the basis of the PDF transport equation (4.13) in the same way as the transport equation for π_{ij}. However, this equation involves triple correlations which appear as unknowns in the q_i equation. Therefore, the most convenient way to address the determination of q_i is to consider its calculation as a special case of the calculation of triple correlations. Their transport equation is given according to (4.13) by

$$\frac{\partial\rho\overline{v_i v_j v_k}}{\partial t}+\frac{\partial\rho U_m\overline{v_i v_j v_k}}{\partial x_m}-\rho\overline{f_i^{(m)}u_j u_k}-\rho\overline{f_j^{(m)}u_i u_k}-\rho\overline{f_k^{(m)}u_i u_j}=$$

$$=-\frac{\partial\rho\overline{v_m v_i v_j v_k}}{\partial x_m}-\rho\frac{\partial U_i}{\partial x_m}\overline{v_m v_j v_k}-\rho\frac{\partial U_j}{\partial x_m}\overline{v_m v_i v_k}-\rho\frac{\partial U_k}{\partial x_m}\overline{v_m v_i v_j}$$

$$+\frac{\partial\rho\overline{v_i v_m}}{\partial x_m}\overline{v_j v_k}+\frac{\partial\rho\overline{v_j v_m}}{\partial x_m}\overline{v_i v_k}+\frac{\partial\rho\overline{v_k v_m}}{\partial x_m}\overline{v_i v_j}-\frac{3\rho}{\tau_m}\overline{v_i v_j v_k}. \quad (4.31)$$

With the same arguments as applied above, we neglect all the terms on the left-hand side. Further, we approximate (in consistency with the assumptions leading to (4.12a-b)) the velocity correlations of fourth order by their Gaussian expressions, see relation (2.54b). This leads in combination with the assumption of isotropic velocity variances to the relation

$$\frac{3}{\tau_m}\overline{v_i v_j v_k}=-\frac{4e}{9}\frac{\partial e}{\partial x_m}\left(\delta_{im}\delta_{jk}+\delta_{jm}\delta_{ik}+\delta_{km}\delta_{ij}\right)$$

$$-\frac{\partial U_i}{\partial x_m}\overline{v_m v_j v_k}-\frac{\partial U_j}{\partial x_m}\overline{v_m v_i v_k}-\frac{\partial U_k}{\partial x_m}\overline{v_m v_i v_j}. \quad (4.32)$$

In analogy to the derivation of the expression (4.27), the first approximation for triple correlations is obtained by neglecting the last three terms related to the production by velocity gradients,

$$\overline{v_i v_j v_k}^{(1)}=-\frac{4\nu}{9}\frac{\partial e}{\partial x_m}\left(\delta_{im}\delta_{jk}+\delta_{jm}\delta_{ik}+\delta_{km}\delta_{ij}\right). \quad (4.33)$$

The second order of approximation is found by inserting (4.33) into the last three terms of (4.32),

$$\overline{v_i v_j v_k}^{(2)}=\overline{v_i v_j v_k}^{(1)}-\frac{\tau_m}{3}\left(\frac{\partial U_i}{\partial x_m}\overline{v_m v_j v_k}^{(1)}+\frac{\partial U_j}{\partial x_m}\overline{v_m v_i v_k}^{(1)}+\frac{\partial U_k}{\partial x_m}\overline{v_m v_i v_j}^{(1)}\right).$$

(4.34)

According to its definition (4.16b), the heat flux q_i is then given in the first order of approximation by a reduction of (4.33),

$$q_i^{(1)} = -\kappa \frac{\partial e}{\partial x_i}. \tag{4.35}$$

Here, we introduced the heat conduction coefficient κ that is determined by

$$\kappa = \frac{10}{9}\rho\nu. \tag{4.36}$$

The ratio of the diffusion coefficients $\mu = \rho\,\nu$ in (4.27) and κ in (4.35) determines the Prandtl number

$$Pr = \frac{\mu}{\kappa}. \tag{4.37}$$

The use of expression (4.36) in the definition (4.37) of the Prandtl number implies then the value

$$Pr = \frac{9}{10} \tag{4.38}$$

as a consequence of the stochastic model (4.12a-b). This result is found in between the standard values $0.7 \le Pr \le 1$ that are usually applied for gas flow simulations.

The calculation of q_i in the second order of approximation leads by means of (4.34) to the expression

$$q_i^{(2)} = q_i^{(1)} - \frac{\tau_m}{3}\left(\frac{\partial U_i}{\partial x_n} q_n^{(1)} + \frac{\partial U_k}{\partial x_n} \rho \overline{v_n v_i v_k}^{(1)} \right). \tag{4.39}$$

The last term can rewritten by replacing the gradient of the kinetic energy e in (4.33) by means of expression (4.35),

$$\overline{v_n v_i v_k}^{(1)} = \frac{2}{5\rho} q_m^{(1)} \left(\delta_{nm}\delta_{ik} + \delta_{im}\delta_{nk} + \delta_{km}\delta_{ni} \right). \tag{4.40}$$

This results then in the following expression for the heat flux q_i in the second order of approximation,

$$q_i^{(2)} = q_i^{(1)} - \frac{\tau_m}{3}\frac{\partial U_i}{\partial x_n} q_n^{(1)} - \frac{2\tau_m}{15}\frac{\partial U_k}{\partial x_n} q_m^{(1)} \left(\delta_{nm}\delta_{ik} + \delta_{im}\delta_{nk} + \delta_{km}\delta_{ni} \right). \tag{4.41}$$

Higher-order approximations may be found correspondingly.

4.3.3. Scaling parameters

A way to assess the conditions for the applicability of (simple) models for π_{ij} and q_i is to rescale the equations of fluid dynamics that result from the use for instance of the second-order approximations (4.30) and (4.41) for π_{ij} and q_i in (4.14b-c). For this we use a reference length L_0, density ρ_0, velocity U_0 and kinetic energy e_0. The consideration of these four quantities allows the rewriting of the equations (4.14a-c) into equations for non-dimensional variables. In particular, the time is scaled in terms of the reference time scale L_0 / U_0.

The only parameter that enters the equations (4.14a-c) is the kinematic viscosity ν, which is related by (4.29) to the only parameter τ_m in the stochastic model (4.12a-b). The non-dimensional parameter related to ν is the Reynolds number

$$\mathrm{Re} = \frac{U_0 L_0}{\nu}. \tag{4.42}$$

This characteristic number Re describes the relative weight of the smoothing influence of the viscosity ν. A low relative value of ν (Re is high) corresponds to the consideration of a flow that is turbulent. Large-scale structures (turbulent eddies) may appear in such flows, which could be produced for instance by velocity gradients (shear). A high relative value of ν (Re is low) corresponds to the consideration of a quiet (laminar) flow. In this case, developing turbulent eddies will be destroyed by friction. Therefore, Re represents a measure for the intensity of (large-scale) turbulence.

With regard to e_0, it is convenient to apply the following parametrization,

$$e_0 = \frac{3p_0}{2\rho_0} = \frac{3}{2\gamma} a_0^{\,2}. \tag{4.43}$$

The middle expression determines a reference pressure p_0 according to (4.18). The last expression defines the squared speed of sound by $a_0^2 = \gamma\, p_0 / \rho_0$. The parameter $\gamma = c_p / c_v$ refers to the ratio of the constant-pressure to constant-volume specific heats. For monatomic fluids, γ has the value $\gamma = 5 / 3$. By applying a_0 instead of e_0, the ratio between the characteristic velocity scale U_0 to the velocity scale a_0 related to the energy equation can be determined by the Mach number

$$\mathrm{Ma} = \frac{U_0}{a_0}. \tag{4.44}$$

By adopting the relation between a_0 and e_0 given by (4.43), one may see that Ma^{-1} represents a measure for the molecular turbulence intensity (the intensity of molecular velocity fluctuations). The use of Ma as a coupling parameter of the velocity and energy equations will be pointed out in section 4.4.

4.3.4. The closure of the velocity and energy equations

By scaling the basic equations (4.14a-c) in terms of the scaling parameters introduced before, one obtains the following expressions for the scaled deviatoric part of the stress tensor π_{ij} and heat flux q_i in the first order of approximation (the plus refers to scaled quantities),

$$\frac{\pi_{ij}^{(1)}}{\rho_0 U_0^{\,2}} = -\frac{2}{\mathrm{Re}}\rho^+ S_{ij}^{\,d\,+}, \tag{4.45a}$$

$$\frac{q_i^{(1)}}{\rho_0 U_0 e_0} = -\frac{10}{9\,\mathrm{Re}}\rho^+ \frac{\partial e^+}{\partial x_i^{\,+}}. \tag{4.45b}$$

The Reynolds number Re is often found to be extremely high. For the atmospheric boundary layer, we may assume $\nu = 1.5\ 10^{-5}$ m^2 / s, $L_0 = 100$ m and $U_0 = 15$ m / s. These values imply $\mathrm{Re} = 10^8$. Thus, π_{ij} and q_i are small in general compared to the other terms in (4.14b-c). However, this does not mean that they can be neglected. The latter would result in the reduction of (4.14b-c) to partial differential equations of first order, such that the solutions to these equations could not satisfy the boundary conditions related to (4.14b-c) in general.

The expressions (4.30) and (4.41), which were obtained for the deviatoric part of the stress tensor π_{ij} and heat flux q_i in the second order of approximation, reveal that the dimensionless quantity $\tau_m\ \partial U_i / \partial x_j$ controls the appearance of additional contributions to the corresponding first-order approximations. By adopting (4.29) for τ_m, this quantity $\tau_m\ \partial U_i / \partial x_j$ can be written

$$\tau_m \frac{\partial U_i}{\partial x_j} = \frac{3\nu}{e}\frac{\partial U_i}{\partial x_j} = \frac{2\gamma}{e^+}\frac{\mathrm{Ma}^2}{\mathrm{Re}}\frac{\partial U_i^{\,+}}{\partial x_j^{\,+}} = \frac{2\gamma}{e^+}\mathrm{Re}\,\mathrm{Kn}^2\frac{\partial U_i^{\,+}}{\partial x_j^{\,+}}. \tag{4.46}$$

This expression makes use of the definition of the Knudsen number

$$\mathrm{Kn} = \frac{\mathrm{Ma}}{\mathrm{Re}} = \frac{e^+}{\sqrt{6\gamma}}\frac{\tau_m\sqrt{e_0}}{L_0}. \tag{4.47}$$

The last expression results from the application of the definitions of Ma and Re combined with (4.29) for ν and (4.43) for e_0. Hence, the Knudsen number is a measure for the ratio of the characteristic length scale $\tau_m\ e_0^{\,1/2}$ of the molecular motion to the macroscopic length scale L_0. The second-order approximations (4.30) and (4.41) for π_{ij} and q_i appear as sums of products of $\tau_m\ \partial U_i / \partial x_j$ with $\pi_{ij}^{(1)}$ and $q_i^{(1)}$, respectively. The combination of (4.45a-b) and (4.46) then reveals that the terms in addition to $\pi_{ij}^{(1)}$ and $q_i^{(1)}$ scale with the squared Knudsen number.

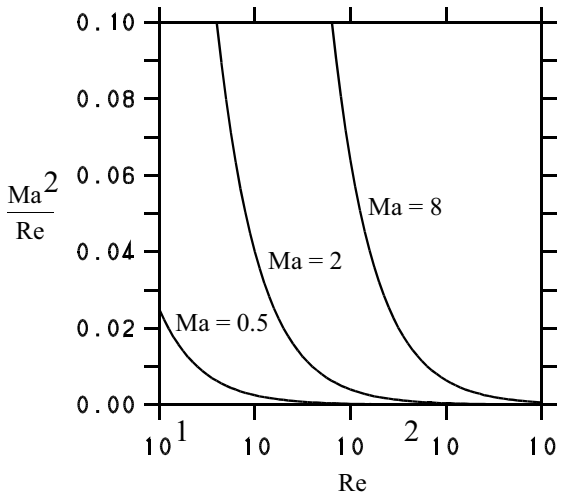

Fig. 4.1. The parameter Ma^2 / Re in the relation (4.46) against the Reynolds number Re for different values of the Mach number Ma.

Expression (4.46) can be used to assess the requirement to involve terms in addition to the first-order approximations for π_{ij} and q_i. Compared to first-order contributions, second-order contributions scale with $Re\ Kn^2 = Ma^2 / Re$. The latter quantity is shown in Fig. 4.1 for different values of Ma. The Mach number Ma is often found to be small because molecules move with very high velocities (air molecules have a mean velocity of about 500 m / s at a temperature of 273 K). Therefore, Mach numbers of order unity are only found for fluids with very high (macroscopic) velocities. By adopting for instance a characteristic velocity U_0 = 1,000 m / s and speed of sound a_0 = 500 m / s for a combustion chamber, one finds Ma = 2. Fig. 4.1 shows that even for this case Ma = 2 the parameter Ma^2 / Re is negligibly small provided the Reynolds number exceeds Re = 1,000, which is usually the case.

However, in flow regions with a relatively high Mach number and a relatively low level of turbulence intensity there may arise the need to consider corrections to the first-order approximations for π_{ij} and q_i. In particular, additional contributions to $\pi_{ij}^{(1)}$ and $q_i^{(1)}$ can become relevant in the vicinity of shocks, which may appear for instance by obstacles in supersonic flows, see the explanations given in section 5.6. It is commonly accepted that first-order approximations for π_{ij} and q_i are capable of modeling most of the aspects of flows involving weak shocks accurately. For strong shocks, the presence of large gradients and the highly nonequilibrium state of the fluid suggest that the applicability of first-order approximations may become questionable. This issue was addressed by Levermore et al. (1998) by investigating stationary planar shock profiles with different methods. According to their results, the applicability of first-order approximations for π_{ij} and q_i is well justified for Ma ≤ 2. For Ma = 3, they observed deviations of 10%, and they found an unacceptable performance of first-order approximations for the case Ma = 4.

4.3.5. The resulting basic equations

From now, the attention will be restricted to the consideration of the deviatoric part of the stress tensor π_{ij} and heat flux q_i in the first order of approximation. The combination of the equations (4.14a-c) with (4.17), (4.27) and (4.35) leads then to the following basic equations of fluid and thermodynamics,

$$\frac{D\rho}{Dt} = -\rho S_{kk}, \tag{4.48a}$$

$$\frac{DU_i}{Dt} = \frac{2}{\rho}\frac{\partial}{\partial x_k}\rho\nu S_{ik}{}^{d} - \frac{1}{\rho}\frac{\partial p}{\partial x_i} + F_i, \tag{4.48b}$$

$$\frac{De}{Dt} = \frac{1}{\rho}\frac{\partial}{\partial x_k}\frac{\rho\nu}{Pr}\frac{\partial e}{\partial x_k} - \frac{p}{\rho}S_{kk} + 2\nu S_{jk}{}^{d} S_{kj}{}^{d} + Q_B. \tag{4.48c}$$

The differential operator D / Dt is given by (4.25). To obtain (4.48b-c) one has to apply (4.48a) and the relations

$$S_{jk}{}^{d}\frac{\partial U_j}{\partial x_k} = S_{jk}{}^{d} S_{kj}{}^{d}, \qquad S_{kk} = \frac{\partial U_k}{\partial x_k}. \tag{4.49}$$

According to (4.18), the equations (4.48b) and (4.48c) are coupled via the relation $p = 2\,\rho\,e / 3$. A discussion of the equations (4.48a-c) will be postponed to section 4.4, where the more general case of multicomponent reacting systems will be considered.

4.4. The equations for multicomponent reacting systems

The equations (4.48a-c) can be applied for simulations of any laminar or turbulent flow, provided its Mach number is not too high. However, the solution of these equations does not provide specific information about combustion processes, as for instance the varying composition of a fluid considered. Therefore, we have to extend the equation system (4.48a-c) in order to involve such knowledge.

4.4.1. The mass fraction equations

For doing this, we specify the fluid mass density ρ as the sum of partial densities of N_S species,

$$\rho = \sum_{\alpha=1}^{N_S} \rho_\alpha. \tag{4.50}$$

The partial densities

$$\rho_\alpha = \rho m_\alpha \tag{4.51}$$

are defined in terms of mass fractions m_α. These quantities are given by

$$m_\alpha = \frac{M_\alpha}{M}. \tag{4.52}$$

M_α is the mass of substance α, and M the total mass of the mixture,

$$M = \sum_{\alpha=1}^{N_S} M_\alpha. \tag{4.53}$$

In the definition (4.50), the fluid mass density ρ is defined by equation (4.48a), but the mass fractions m_α are unknown. Equations for these quantities could be derived by extending the stochastic model (4.12a-b) for the molecular motion to the case that the fluid involves various components. However, to keep the developments simple this will be not done here but the equations for the mass fractions m_α are introduced in correspondence to the energy equation (4.48c),

$$\frac{Dm_\alpha}{Dt} = \frac{1}{\rho}\frac{\partial}{\partial x_k}\frac{\rho\nu}{Sc}\frac{\partial m_\alpha}{\partial x_k} + S_\alpha. \tag{4.54}$$

In these equations, we have a source rate S_α due to chemical reactions instead of the source terms in (4.48c). The structure of the diffusion term in the equations (4.54) corresponds to that in (4.48c), with the exception that the Schmidt number Sc appears here instead of the Prandtl number Pr in the energy equation. By postulating (4.54) it is assumed that all the species have the same molecular diffusivity ν / Sc. The consideration of one (effective) Schmidt number Sc for the mixture appears to be an appropriate approximation under many conditions. Nevertheless, specific Schmidt numbers for each scalar may be needed for specific applications. This case is not considered here to simplify the following explanations. Obviously, one has to make sure that the calculation of mass fractions is consistent with their important property to sum to unity. This is guaranteed provided that

$$\sum_{\alpha=1}^{N_S} S_\alpha = 0, \tag{4.55}$$

as may be seen by taking the sum over all the components in (4.54). This relation states that the destruction of species has always to be in balance with the formation of other species.

4.4.2. The caloric equation of state

The source rate S_α that involves chemical reactions in the mass fraction equations (4.54) is in general a nonlinear function of temperature T. However, the latter is not defined by the equation system (4.48a-c) and (4.54).

The temperature is a measure for all the energy related to the motion of molecules, which is called internal energy. In monatomic fluids, where the particles do not have internal degrees of freedom, the internal energy is equal to the kinetic (or translational) energy of molecules. However, in polyatomic fluids, where the molecules may have internal degrees of freedom, there may appear additional contributions to the internal energy due to rotational or vibrational energy. Thus, the kinetic and internal energy are different, but one applies the same equation (4.48c) to calculate the changes of these variables (which is only extended by an additional external heat source Q_R related, for instance, to radiation processes in the case of the internal energy, see Kuo (1986)). Accordingly, we will use e from now to denote the internal energy. This implies the need to reformulate the pressure parametrization in (4.48b), which will be done in section 4.4.3.

The relation of the temperature T to the internal energy is defined in terms of the partial internal energies e_α for each substance, which sum (multiplied with the mass fractions m_α) to the specific internal energy e of the mixture,

$$e = \sum_{\alpha=1}^{N_S} m_\alpha e_\alpha . \tag{4.56}$$

T is then introduced via the relation

$$\frac{de_\alpha}{dT} = c_{v,\alpha} . \tag{4.57}$$

To close (4.57), one has to provide $c_{v,\alpha} = c_{v,\alpha}(T)$, which is the specific heat of substance α at a constant volume. According to (4.57), $c_{v,\alpha}$ determines the increase of specific internal energy of substance α due to a small increase of temperature. Such heat dT supplied to a system does not always have to result in an increase of kinetic energy, it is also possible that this additional energy is stored as rotational or vibrational energy. Instead of (4.57) one usually considers its integral form

$$e_\alpha = e_\alpha(T_0) + \int_{T_0}^{T} dT'\, c_{v,\alpha}(T'), \tag{4.58}$$

where T_0 describes a reference temperature. Equation (4.58) between e_α and temperature T is called caloric equation of state. Another way of introducing the relation between T and e is to postulate in correspondence with (4.58) an equation for the specific enthalpy $h_\alpha = e_\alpha + p_\alpha / \rho_\alpha$, where p_α is given below by (4.67).

In order to obtain an equation for the temperature, we insert (4.58) into (4.56) and differentiate e by time. This leads to

$$c_v \frac{DT}{Dt} = \frac{De}{Dt} - \sum_{\alpha=1}^{N_S} e_\alpha \frac{Dm_\alpha}{Dt}, \tag{4.59}$$

where we applied

$$c_v = \sum_{\alpha=1}^{N_S} m_\alpha c_{v,\alpha}. \tag{4.60}$$

The use the internal energy equation (4.48c) (combined with an additional external heat source Q_R) and the mass fraction equations (4.54) in (4.59) results then in a transport equation for T,

$$\frac{DT}{Dt} = \frac{1}{\rho}\frac{\partial q_{Tk}}{\partial x_k} - \frac{p}{\rho c_v} S_{kk} + \frac{2}{c_v} \nu S_{jk}{}^{d} S_{kj}{}^{d} - \frac{1}{c_v} \sum_{\alpha=1}^{N_S} e_\alpha \frac{Dm_\alpha}{Dt} + \frac{Q_B + Q_R}{c_v} + \frac{q_{Tk}}{\rho c_v}\frac{\partial c_v}{\partial x_k}, \tag{4.61}$$

where the heat flux q_{Tk} in the temperature equation is given by

$$q_{Tk} = \frac{\rho\nu}{Pr}\left(\frac{\partial T}{\partial x_k} + \frac{1}{c_v} \sum_{\alpha=1}^{N_S} e_\alpha \frac{\partial m_\alpha}{\partial x_k} \right). \tag{4.62}$$

Usually, the last terms in (4.61) and (4.62) are neglected, and the substantial derivative of m_α is replaced by S_α.

4.4.3. The thermal equation of state

The calculation of temperature instead of the kinetic energy implies the need to reformulate the relation (4.18) between p and the kinetic energy into a relation between p and T. To do this, we use the essential property of the internal energy to be equally distributed over all available degrees of freedom and to be proportional to the temperature T if the system is in an equilibrium state. This theorem is called the equipartition law of classical statistical mechanics. An important consequence of this theorem is the thermal equation of state, which provides a link between p and the temperature T,

$$\frac{p}{\rho} = RT. \tag{4.63}$$

By multiplying (4.63) with 1 / 2 we see that p / (2ρ), which is according to (4.18) nothing but the mean kinetic energy of particles per degree of freedom, is considered to be proportional to T / 2.

The proportionality constant R in (4.63), which is called gas constant, is the Boltzmann constant $k = 1.38\ 10^{-23}$ J / K divided by the mass m_p of one particle. The latter is given by $m_p = W / N_L$, where W is the mass of one mole (which is also called molar mass) and $N_L = 6.023\ 10^{23}$ / mol is the Loschmidt number that defines the number of particles of one mole. Hence, R is determined by

$$R = \frac{R_u}{W}, \tag{4.64}$$

where we introduced the universal gas constant $R_u = k\ N_L = 8.31$ J / (K mol). The mass W of one mole is given by the average over the molar masses W_α (the masses of one mole of the substance α),

$$W = \sum_{\alpha=1}^{N_S} x_\alpha W_\alpha = \left[\sum_{\beta=1}^{N_S} \frac{m_\beta}{W_\beta} \right]^{-1}. \tag{4.65}$$

The last expression follows from the definition of the mole fraction x_α,

$$x_\alpha = \left[\sum_{\beta=1}^{N_S} \frac{M_\beta}{W_\beta} \right]^{-1} \frac{M_\alpha}{W_\alpha} = \left[\sum_{\beta=1}^{N_S} \frac{m_\beta}{W_\beta} \right]^{-1} \frac{m_\alpha}{W_\alpha}. \tag{4.66}$$

The ratio M_α / W_α is equal to the number of moles of one substance. Hence, x_α gives the relative contribution of moles of the substance α to the mixture. The last expression in (4.66) indicates the relationship of mass and mole fractions: the knowledge of mass fractions determines the mole fractions and vice versa. As with the mass fractions, the mole fractions sum to unity. Further, we note that the use of (4.64) and (4.65) in (4.63) implies Dalton's law

$$p = \sum_{\alpha=1}^{N_S} p_\alpha = \sum_{\alpha=1}^{N_S} \rho_\alpha \frac{R_u}{W_\alpha} T \tag{4.67}$$

for the partial pressures p_α, which are defined by the last expression.

The connection between the relation (4.63) for twice the internal energy per degree of freedom and (4.56) for the total internal energy becomes clear by writing (4.56) for a system in a local equilibrium state

$$e = c_v T. \tag{4.68}$$

This relation may be obtained by considering $c_{v,\alpha}$ as constant in (4.58) (which is often justified for perfect gases), setting $T_0 = e_\alpha(T_0) = 0$ and adopting (4.60). Obviously, the right-hand sides of (4.63) and (4.68) have to be equal if (4.63) is multiplied with f / 2, where f refers to the effective number of degrees of freedom

(which does not have to be equal to all available degrees of freedom). This implies

$$c_v = \frac{f}{2} R. \tag{4.69}$$

By adopting $R = c_p - c_p$, where c_p is the constant pressure specific heat, and dividing (4.69) by c_v, we find for $\gamma = c_p / c_v$ the relation

$$\gamma = \frac{2}{f} + 1. \tag{4.70}$$

Therefore, the value of γ depends on the mixture considered. Monatomic gases (He, Ar) have f = 3 degrees of freedom, which implies $\gamma = 5 / 3$. Gases with two atoms (H_2, N_2, O_2) have f = 5 effective degrees of freedom, such that $\gamma = 7 / 5$. For more complex molecules with a higher number of effective degrees of freedom, the value of γ then approaches unity.

4.4.4. The equations for multicomponent reacting systems

According to the equations (4.48a-b), (4.54) and (4.61), the fluid dynamic and thermochemical equations read

$$\frac{D\rho}{Dt} = -\rho S_{kk}, \tag{4.71a}$$

$$\frac{DU_i}{Dt} = \frac{2}{\rho}\frac{\partial}{\partial x_k}\rho\nu {S_{ik}}^d - \frac{1}{\rho}\frac{\partial p}{\partial x_i} + F_i, \tag{4.71b}$$

$$\frac{Dm_\alpha}{Dt} = \frac{1}{\rho}\frac{\partial}{\partial x_k}\frac{\rho\nu}{Sc}\frac{\partial m_\alpha}{\partial x_k} + S_\alpha, \tag{4.71c}$$

$$\frac{DT}{Dt} = \frac{1}{\rho}\frac{\partial}{\partial x_k}\frac{\rho\nu}{Pr}\frac{\partial T}{\partial x_k} + S_T. \tag{4.71d}$$

The source term in the temperature equation (4.71d) is given by

$$S_T = -(\gamma - 1) S_{kk} T + \frac{2}{R}(\gamma - 1)\nu {S_{jk}}^d {S_{kj}}^d - \frac{1}{c_v}\sum_{\alpha=1}^{N_S} e_\alpha S_\alpha + \frac{Q_B + Q_R}{c_v}. \tag{4.72}$$

To obtain expression (4.72), one has to use the thermal equation of state $p = \rho R T$ and definitions of R and γ. To simplify the explanations in the following chapters, the diffusive (last) terms in (4.61) and (4.62) are neglected, and, correspondingly, Dm_α / Dt is replaced by S_α in the chemical reaction term of (4.61).

The equations (4.71a-b) are called Navier-Stokes equations. Equation (4.71a) shows that density variations are controlled by the dilatation S_{kk}. Alternatively, one could rewrite (4.71a) into an equation for the specific volume ρ^{-1},

$$\frac{1}{\rho^{-1}}\frac{D\rho^{-1}}{Dt} = S_{kk}. \tag{4.73}$$

The body force F_i and the molecular transport term (the first term on the right-hand side) often play a minor role in (4.71b), this means the pressure gradient is mainly responsible for velocity changes. It acts such that the velocity is decelerated (accelerated) if the pressure increases (decreases) in the i^{th} direction. Regarding the specification of the equations (4.71a-d) to the case of incompressible flow considered below, it is relevant to note that equation (4.71b) can be reduced by differentiation by x_i to an equation for the dilatation S_{kk},

$$\frac{D}{Dt}S_{kk} = \frac{\partial}{\partial x_i}\frac{2}{\rho}\frac{\partial \rho \nu S_{ik}^{\ d}}{\partial x_k} + \frac{\partial F_i}{\partial x_i} - \frac{\partial}{\partial x_i}\frac{1}{\rho}\frac{\partial p}{\partial x_i} - \frac{\partial U_k}{\partial x_i}\frac{\partial U_i}{\partial x_k}. \tag{4.74}$$

The first two terms on the right-hand side are often of minor relevance. The term involving the viscosity ν scales with the inverse Reynolds number, and the specification of F_i as gravitational force (see section 4.4.6) implies $\partial F_i / \partial x_i = 0$.

According to the thermal equation of state $p = \rho R T$, the equations (4.71a-b) are coupled to the equations (4.71c-d). The first terms on the right-hand sides of (4.71c-d) represent molecular transport. In (4.71c), S_α is a chemical reaction rate that has to be provided. Equation (4.71d) represents one possible formulation of the first principle of thermodynamics (which is usually formulated in terms of the internal energy). The first term of the source S_T arises from density variations. A negative dilatation S_{kk} is related to a compression (an increase of the mass density) of a system. Such an increase of potential energy of a system cannot be converted into work but has to be stored as internal energy. Therefore, the temperature grows. The second term on the right-hand side of (4.72) is always non-negative. This term describes the increase of temperature by friction. The third term is related to temperature changes due to combustion processes. The last two terms in (4.72) represent source terms related to body forces and radiation.

4.4.5. Incompressible flows

The fluid dynamic equations (4.71a-b) and thermochemical equations (4.71c-d) are coupled via the pressure calculation: one has to provide the mass fractions and temperature in order to know p in (4.71b) in terms of the thermal equation of state $p = \rho R T$. This need to solve all the equations (4.71a-d) makes turbulent reacting

flow simulations very complicated in general. It is therefore essential to see the conditions for a reduction of this task. This question will be addressed now.

To do this, we may consider the non-dimensional version of (4.73),

$$\frac{1}{\rho^{-1}}\frac{D\rho^{-1}}{Ds} = S_{kk}\tau_m = \frac{2\gamma}{e^+}\frac{Ma^2}{Re}S_{kk}{}^+, \tag{4.75}$$

where the dimensionless time scale $s = \int_0^t dt'\, \tau_m{}^{-1}$ is introduced. The last expression results from the use of (4.46). Hence, in the limit case of a vanishing Mach number Ma the density ρ of a particle that moves with the flow remains constant,

$$\frac{D\rho}{Dt} = 0. \tag{4.76}$$

Such flows are called incompressible. The comparison of (4.71a) with (4.76) shows that S_{kk} vanishes for an incompressible flow. In this case, equation (4.74) implies an equation for the pressure p which is given by equating its right-hand side to zero. Usually, one neglects the first two terms on the right-hand side to obtain the pressure via the Poisson equation

$$\frac{\partial}{\partial x_i}\frac{1}{\rho}\frac{\partial p}{\partial x_i} = -\frac{\partial U_k}{\partial x_i}\frac{\partial U_i}{\partial x_k}. \tag{4.77}$$

Therefore, in the limit case of an incompressible flow the coupling of the fluid dynamic to the thermochemical equations is significantly reduced. Density and pressure obey the equations (4.76) and (4.77), respectively, and one just has to consider a possible coupling via the viscosity ν (which may depend on the temperature).

4.4.6. The Boussinesq approximation

In some cases, and in particular with regard to atmospheric boundary layer simulations, it is very helpful to incorporate some effects of compressibility within a frame that corresponds to the consideration of an incompressible flow. For that, we consider equation (4.71b) for the case $F_i = -\, g\, \delta_{i3}$, where g is the gravitational acceleration,

$$\frac{DU_i}{Dt} = \frac{2}{\rho}\frac{\partial}{\partial x_k}\rho\nu S_{ik}{}^d - \frac{1}{\rho}\frac{\partial p}{\partial x_i} - g\delta_{i3}. \tag{4.78}$$

Next, we assume that there exists a static reference state (referred to by a subscript s) such that the deviations of pressure, mass density and temperature

$$\Delta p = p - p_s, \qquad \Delta\rho = \rho - \rho_s, \qquad \Delta T = T - T_s, \tag{4.79}$$

from these reference values are small. The gas constant R is considered to be constant. The static reference state is defined by the assumption of a zero velocity $\mathbf{U}_s = 0$. A consequence of this assumption is that the static pressure p_s and density ρ_s are related according to (4.78) by

$$\frac{\partial p_s}{\partial x_i} = -\rho_s g \delta_{i3}. \tag{4.80}$$

Due to the consideration of an incompressible reference state, the reference density has to satisfy $D\rho_s / Dt = 0$. The thermal equation of state $p_s = \rho_s R T_s$ then provides a constraint to calculate the static temperature T_s in terms of the static pressure p_s, density ρ_s and gas constant R.

By adopting the definitions (4.79) and relation (4.80), equation (4.78) can be rewritten into

$$\frac{DU_i}{Dt} = \frac{2}{\rho}\frac{\partial}{\partial x_k}\rho\nu S_{ik}^{\ d} - \frac{1}{\rho}\frac{\partial \Delta p}{\partial x_i} - \frac{\Delta\rho}{\rho} g \delta_{i3}. \tag{4.81}$$

Next, we replace ρ by ρ_s in (4.81) and calculate the difference $\Delta\rho$ in the last term by the corresponding Taylor series in the first order of approximation,

$$\frac{\Delta\rho}{\rho} = \frac{\rho - \rho_s}{\rho_s} = \frac{1}{\rho_s}\left[\left(\frac{\partial\rho}{\partial T}\right)_s \Delta T + \left(\frac{\partial\rho}{\partial p}\right)_s \Delta p\right] = -\frac{\Delta T}{T_s} + \frac{\Delta p}{p_s}. \tag{4.82}$$

Usually, one neglects the last term in the calculation of atmospheric flows, which corresponds to the so-called Boussinesq approximation. By inserting (4.82) into (4.81) one obtains

$$\frac{DU_i}{Dt} = \frac{2}{\rho_s}\frac{\partial}{\partial x_k}\rho_s\nu S_{ik}^{\ d} - \frac{1}{\rho_s}\frac{\partial \Delta p}{\partial x_i} + \beta \Delta T\, g\, \delta_{i3}, \tag{4.83}$$

where the abbreviation $\beta = 1 / T_s$ is introduced. This parameter is called the thermal expansion coefficient. The static temperature T_s, which is required in the last term, is usually assumed as a mean temperature. Δp obeys a Poisson equation that follows by taking the divergence of equation (4.83). Thus, the Boussinesq approximation corresponds to the consideration of an incompressible flow with a body force that involves the effect of buoyancy.

4.5. Direct numerical simulation

The numerical solution of the fluid dynamic and thermochemical equations (4.71a-d) is called direct numerical simulation (DNS). Some basic questions related to its application will be addressed now. To do this we consider equation (4.71b) (for simplicity without external force) in terms of the scaled variables introduced in section 4.3.3,

$$\frac{DU_i^+}{Dt^+} = \frac{2}{\rho^+}\frac{\partial}{\partial x_k^+}\frac{\rho^+}{Re}S_{ik}{}^{d+} - \frac{1}{\rho^+}\frac{\partial p^-}{\partial x_i^+}. \qquad (4.84)$$

Here, $p^- = p / (\rho_0 U_0^2)$ refers to a normalized pressure. The Poisson equation (4.77) reveals that p^- is of order unity as are all the quantities denoted by a plus (the minus is used to distinguish the standardization to U_0^2 applied here from the use of e_0 for the normalization of p in section 4.3.3). The only parameter that enters (4.84) is the Reynolds number Re. For relatively small Re one finds regular (non-chaotic) solutions to (4.84). However, Re is often very high (about 10^8) for flows of engineering or environmental interest. To calculate such flows, the solution of (4.84) requires a balance between terms of order unity and extremely small terms (of order 10^{-8}). Such solutions to (4.84) become chaotic: one obtains completely different results if the initial or boundary conditions are somewhat modified, but there is in general no way to determine the "correct" initial and boundary conditions. Thus, the fluid dynamic and thermochemical equations have stochastic solutions ($U_i(\mathbf{x}, t)$ becomes a stochastic variable) if they are used to calculate high-Re flows. The need to involve such fluctuations into numerical solutions of the basic equations leads to a significant increase of computational costs.

4.5.1. The energy cascade

To understand the requirements related to DNS in more detail it is helpful to consider the fluid dynamics as motions of fluid particles (eddies). In this way one considers the variables (velocities) as properties of particles. It is worth noting that such particles do not exist in reality: the use of this idea is just a way to illustrate the mechanism of turbulent flows. The Reynolds number gives us a relative measure for the extent L_0 and velocity U_0 of eddies that are injected into a flow. For low Reynolds numbers, these eddies are relatively small and have relatively small velocities: U_0 is of the same order as the characteristic velocity scale $e^{1/2}$ of molecular motion, and L_0 is of the same order as the characteristic length scale $\tau_m e^{1/2}$ of molecular motion. Such small-scale eddies are significantly affected by viscous friction, this means they are destroyed (their kinetic energy is converted into heat). For high Reynolds numbers, the flow is fed with large eddies ($L_0 >>$

$\tau_m\, e^{1/2}$) that have large velocities ($U_0 >> e^{1/2}$). The existence of such large eddies is equivalent to the existence of stochastic solutions of the Navier-Stokes equations (the unordered motion of eddies causes the appearance of fluctuations). The dynamics of large eddies are very different from those of small eddies in low-Re flows since the smoothing influence of viscosity is irrelevant to the first stage of their life where they interact with other eddies of comparable size. They become smaller and smaller by such friction processes until their velocity and length scales become comparable with the corresponding molecular scales $e^{1/2}$ and $\tau_m\, e^{1/2}$, respectively. Then, dissipation takes place, this means their energy is converted into heat. This cascade concept of the energy transfer was introduced by Richardson (1922). He explained his ideas such:

Big whorls have little whorls,
Which feed on their velocity;
And little whorls have lesser whorls,
And so on to viscosity
(in the molecular sense).

Fig. 4.2 schematically illustrates the energy cascade for both velocities and scalars. This is done in spectral space. $\kappa = 2\,\pi\,/\,\lambda$ is the wavenumber and λ the wavelength, which may be considered as a measure for the size of an eddy. The energy spectrum function $E(\kappa, t)$ satisfies the following integral equation,

$$\int d\kappa\, E(\kappa, t) = k. \tag{4.85}$$

k refers to the turbulent kinetic energy of fluctuations of U_i, see chapter 5. $E(\kappa, t)\, d\kappa$ represents the spectral contribution to the turbulent kinetic energy: it is the contribution provided by eddies with wavenumbers inside the interval $(\kappa, \kappa + d\kappa)$. As may be seen by means of Fig. 4.2, $E(\kappa, t)$ has a relatively simple shape only in the inertial subrange, where, according to Kolmogorov (1941)

$$E(\kappa) = C_K \varepsilon^{2/3} \kappa^{-5/3}. \tag{4.86}$$

The Kolmogorov constant $C_K = 1.62 \pm 0.17$ (Sreenivasan 1995), and ε is the dissipation rate of k. The scalar spectrum density function $E_\varphi(\kappa, t)$ obeys

$$\int d\kappa\, E_\varphi(\kappa, t) = \frac{1}{2}\overline{\phi^2}, \tag{4.87}$$

where $\overline{\phi^2}$ refers to the variance of a scalar considered. More detailed explanations to spectral representations of turbulence may be found for instance in the text books of Baldyga & Bourne (1999) and Pope (2000).

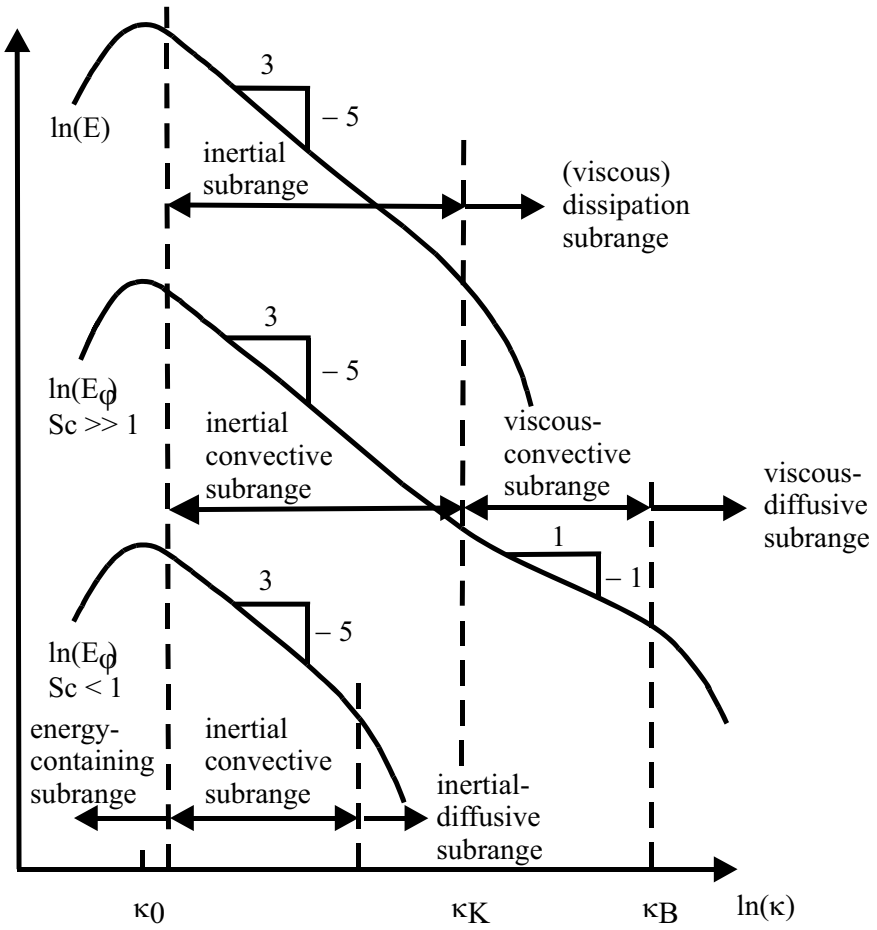

Fig. 4.2. Idealized energy spectrum functions E and E_φ of velocities and scalars, respectively, in fully developed homogeneous, isotropic turbulence according to Tennekes & Lumley (1972). Energy is introduced on the integral-scale $\kappa_0 = 2\ \pi\ /\ L_0$, where L_0 is a characteristic length scale of the domain considered. Eddies on this scale have the highest energy. Within the inertial subrange, they decay due to turbulent mixing (friction) processes. According to Kolmogorov (1941), one finds a universal scaling behaviour for the inertial subrange, which is given by (4.86). The decay process proceeds until the eddy wavenumber becomes comparable to the Kolmogorov-scale wavenumber $\kappa_K = Re_L^{3/4}\ \kappa_0$. Re_L denotes the turbulence Reynolds number which is given by (4.90). Finally, the eddies dissipate in the (viscous) dissipation subrange. In contrast to fluids with Sc < 1 (gases), the scalar spectrum has for Schmidt numbers Sc >> 1 (liquids) a viscous-convective subrange in addition to the inertial-convective subrange. The Kolmogorov-scale wavenumber is related to the Batchelor-scale wavenumber κ_B by the relation $\kappa_B = Sc^{1/2}\ \kappa_K$. The slopes − 5 / 3 and − 1 refer to the universal scaling laws $E_\varphi(\kappa) \sim \kappa^{-5/3}$ and $E_\varphi(\kappa) \sim \kappa^{-1}$ in these subranges.

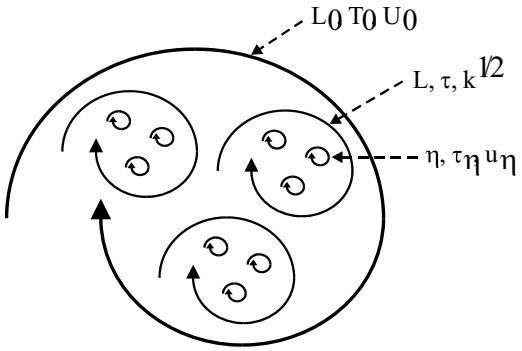

Fig. 4.3. A sketch of eddy types involved in the energy cascade. The variables give the corresponding length, time and velocity scales.

4.5.2. The simulation of the energy cascade

The calculation of the energy cascade by DNS requires knowledge about the characteristic scaling parameters of the processes on the largest and smallest (dissipative) scales of the cascade. With regard to large-scale processes, these parameters are given by the characteristic velocity scale $k^{1/2}$ and dissipation time scale $\tau = k / \varepsilon$, where ε is the dissipation rate of turbulent kinetic energy k, see chapter 5. These two scales can be combined to the length scale $L = k^{1/2} \tau = k^{3/2} / \varepsilon$ of large-scale eddies. To determine the characteristic scales of the smallest, dissipative eddies one has to make sure that one covers the processes at the end of the energy cascade. This can be done by choosing the dissipation rate ε as the first characteristic variable of small-scale processes. As shown in chapter 5, this quantity determines the coupling between turbulent and molecular scales: it appears as a sink term in the transport equation for k, and as a source term in the temperature equation. To determine a second characteristic variable z, we parametrize z by means of the variables that determine the molecular dynamics (4.12b). We set $z = e^{\alpha} \tau_m^{\beta}$, where α and β are any powers that have to be determined. The combination of ε and z has to be proportional to powers of a velocity scale u_η and time scale τ_η (the exchange of u_η and τ_η in (4.88) leads to the same conclusion regarding the second characteristic variable),

$$\frac{k}{\tau} e^{\alpha} \tau_m^{\beta} \sim u_\eta^{\lambda_1}, \qquad \frac{k}{\tau} \frac{1}{e^{\alpha} \tau_m^{\beta}} \sim \tau_\eta^{\lambda_2}. \tag{4.88}$$

λ_1, and λ_2 are any unknown powers. Obviously, the relations (4.88) are satisfied if $\alpha = \beta = 1$. The comparison of $z = e^{\alpha} \tau_m^{\beta}$ with (4.29) results then in the conclusion that one has to choose the viscosity ν as the second characteristic variable. This important finding that ν and ε determine (at sufficiently high Reynolds numbers) the statistics of small-scale motions was obtained first by Kolmogorov (1941) and is referred to as his first similarity hypothesis. The combination of ν and ε allows us to construct unique velocity, time and length scales. The Kolmogorov velocity

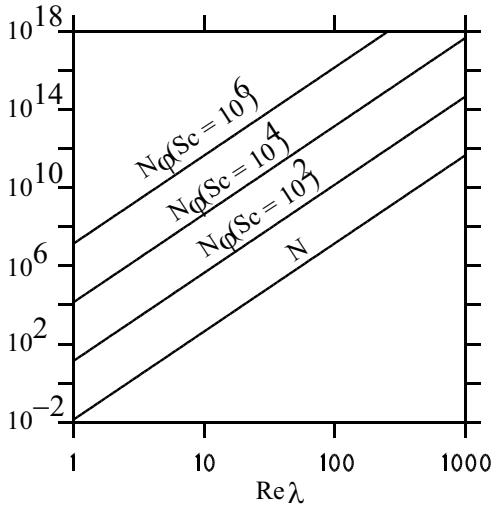

Fig. 4.4. The numbers N and N_φ of grid nodes which are required according to (4.89) and (4.92) to perform DNS. Re_λ is the Taylor-scale Reynolds number.

scale is given by $u_\eta = (\varepsilon\,\nu)^{1/4}$, and the time scale by $\tau_\eta = (\nu / \varepsilon)^{1/2}$. The characteristic Kolmogorov length scale is then given by $\eta = u_\eta\,\tau_\eta$. An illustration of eddies involved in the energy cascade and their characteristic scales is shown in Fig. 4.3. L_0, T_0 and U_0 represent the injection scales, see section 4.5.1.

To simulate the energy cascade numerically, one has to apply a grid length that is at least of the order of the Kolmogorov length scale η. The three-dimensional simulation of large eddies having a length L then requires

$$N = \left(\frac{L}{\eta}\right)^3 = Re_L^{\,9/4} \tag{4.89}$$

grid nodes. Here, the turbulence Reynolds number Re_L is given by

$$Re_L = \frac{k^{1/2} L}{\nu} = \frac{\tau^2}{\tau_\eta^{\,2}} = \frac{k^2}{\varepsilon\nu}. \tag{4.90}$$

The first expression for Re_L reveals that Re_L is the Reynolds number of large-scale eddies. Instead of Re_L, one also applies (in particular for homogeneous flows) the Taylor-scale Reynolds number Re_λ,

$$Re_\lambda = \sqrt{\frac{20}{3} Re_L}\,. \tag{4.91}$$

The comparison of (4.89) with the ratio of the integral-scale to Kolmogorov-scale wavenumbers (see Fig. 4.2) shows that the number of grid nodes $N = \kappa_K^{\,3} / \kappa_0^{\,3}$. By replacing κ_K by the Batchelor-scale wavenumber $\kappa_B = Sc^{1/2}\,\kappa_K$, this relation can be used to assess the number of grid nodes N_φ that is required for the DNS of scalar transport in high-Sc flows (liquids). We obtain in this way

$$N_\varphi = \left(\frac{\kappa_B}{\kappa_0} \right)^3 = Sc^{3/2} Re_L^{9/4}. \qquad (4.92)$$

Therefore, the computational effort grows in this case proportional to $Sc^{3/2}$.

Fig. 4.4 reveals the huge computational costs related to the DNS of turbulent flows. At present, one is able to involve about $N \approx 10^8 - 10^9$ grid nodes for such calculations. This permits the simulation of moderately turbulent gas flows with $Re_\lambda < 200$, or higher-Sc flows at lower Reynolds numbers. To calculate for example atmospheric boundary layer processes where $Re_\lambda \approx 10^3$ (Sawford & Yeung 2001), one needs a computational effort which is 1,400 times higher than for $Re_\lambda = 200$. Obviously, the use of DNS for reacting flow computations is faced with particular problems. One has to restrict such calculations to the consideration of extremely simple reaction schemes (with a slow chemistry, see Baldyga & Bourne (1999)). As demonstrated in Fig. 4.4, the calculation of reacting liquid phase flows is unfeasible in general. Because of these reasons, DNS represents a unique tool to investigate basic mechanisms, to get a better insight into the physics of turbulence and to validate the applicability of simplifying assumption (Moin & Mahesh 1998). Nevertheless, DNS cannot be applied (at least for the foreseeable future) to calculate most of the flows of engineering or environmental interest. This results in the need to simplify the equations of fluid and thermodynamics to equations which can be solved with lower computational costs.

4.6. Reynolds-averaged Navier-Stokes equations

As pointed out in section 4.5, the appearance of fluctuations of velocities and scalars (mass fractions and temperature) in high-Reynolds number turbulent flows implies significant problems due to the related computational effort. However, one is often not interested in having all the detailed information on fluctuations but the knowledge of some basic quantities as mean velocities and scalars is sufficient with regard to many questions. In particular, one is interested in ensemble-averaged variables which do not fluctuate (in contrast to filtered variables that will be considered in chapter 6).

4.6.1. Ensemble-averaged equations

Such ensemble-averaged fluid dynamic and thermochemical variables will be defined by adopting the same symbols as used for the averaging of molecular quantities: the brackets $\langle \cdots \rangle$ refer to the ensemble average and the overbar is used to denote mass density-weighted functions Q of velocities and scalars,

$$\overline{Q} = \langle\rho\rangle^{-1}\langle\rho Q\rangle. \tag{4.93}$$

The fluctuating mass density ρ appears here as weighting function instead of the mass density $\rho^{(m)}$ in the corresponding definition (4.1), which fluctuates on a molecular scale. Fluctuations of mass density-weighted variables will be denoted in general by

$$Q'' = Q - \overline{Q}. \tag{4.94}$$

An exception is made with regard to frequently used velocity fluctuations that are written as small quantities, $u_i = U_i - \overline{U}_i$.

The equations for ensemble-averaged velocities and scalars can be obtained by averaging the equations (4.71a-d). This results in

$$\frac{\partial\langle\rho\rangle}{\partial t} + \overline{U}_i\frac{\partial\langle\rho\rangle}{\partial x_i} = -\langle\rho\rangle\overline{S}_{kk}, \tag{4.95a}$$

$$\frac{\partial\overline{U}_i}{\partial t} + \overline{U}_k\frac{\partial\overline{U}_i}{\partial x_k} = \langle\rho\rangle^{-1}\frac{\partial}{\partial x_k}\langle\rho\rangle\left[2\overline{\nu S^d_{ik}} - \overline{u_i u_k}\right] - \langle\rho\rangle^{-1}\frac{\partial\langle p\rangle}{\partial x_i} + \overline{F}_i, \tag{4.95b}$$

$$\frac{\partial\overline{m}_\alpha}{\partial t} + \overline{U}_k\frac{\partial\overline{m}_\alpha}{\partial x_k} = \langle\rho\rangle^{-1}\frac{\partial}{\partial x_k}\langle\rho\rangle\left[\overline{\frac{\nu}{Sc}\frac{\partial m_\alpha}{\partial x_k}} - \overline{u_k m_\alpha''}\right] + \overline{S}_\alpha. \tag{4.95c}$$

$$\frac{\partial\overline{T}}{\partial t} + \overline{U}_k\frac{\partial\overline{T}}{\partial x_k} = \langle\rho\rangle^{-1}\frac{\partial}{\partial x_k}\langle\rho\rangle\left[\overline{\frac{\nu}{Pr}\frac{\partial T}{\partial x_k}} - \overline{u_k T''}\right] + \overline{S}_T. \tag{4.95d}$$

The ensemble-averaged pressure <p> in (4.95b) is given by taking the mean of (4.63) multiplied by the density ρ,

$$\langle p\rangle = \langle\rho\rangle\overline{RT}. \tag{4.96}$$

For flows with minor variations of the viscosity ν, the molecular transport terms on the right-hand sides of (4.95b-d) appear in a closed form, this means they are given in terms of mean velocities and scalars that are calculated in terms of these equations. Compared to (4.71a-d), the equations (4.95a-d) reveal two significant differences. First, the diffusion terms are extended by the appearance of unknown velocity and scalar variances. The $\overline{u_i u_k}$ are called Reynolds stresses, and the $\overline{u_k m_\alpha''}$ and $\overline{u_k T''}$ are called the turbulent mass and heat fluxes, respectively. The second remarkable difference from (4.71a-d) is given by averaged source terms $\overline{F}_i$, $\overline{S}_\alpha$ and $\overline{S}_T$, which appear as unknowns in (4.95b-d). Some basic problems related to the parametrization of these unknowns will be addressed next.

4.6.2. The calculation of variances

The first problem to provide the unknown variances $\overline{u_i u_k}$, $\overline{u_k m_\alpha}''$ and $\overline{u_k T}''$ for (4.95b-d) is often tackled on the basis of transport equations for these quantities, which are implied by (4.71a-d). These equations can be obtained as shown in Appendix 4A. Nevertheless, the solution of the equations (4.95a-d) in combination with variance transport equations is still expensive. What one may expect in many cases is that the turbulence reaches local equilibrium states, where the production of variances is balanced locally by their dissipation. This assumption corresponds to significant simplifications of the variance transport equations, which reduce to algebraic relations between variances and gradients of mean velocities and scalars. Formally, the derivation of such relations corresponds with the methodology used to construct corresponding analytical approximations for the stress tensor and heat flux in section 4.3.

However, the point is that one needs several approximations to close the variance transport equations (4A.4a-c) given in Appendix 4A. The traditional way to address this question was to find suitable approximations for each of the unclosed terms, see for instance the review given by Launder (1990). This approach may lead to significant consistency problems because it is not assured in general that there exists a velocity-scalar PDF which has moments that evolve according to such turbulence models. Therefore, a better way to tackle this problem is to first construct a stochastic turbulence model and to then derive consistent variance transport equations as a consequence of the underlying PDF model (Durbin & Speziale 1994; Pope 1994a). This approach will be demonstrated in chapters 5 and 6.

4.6.3. The closure of source terms

The second problem related to the closure of (4.95a-d) basically concerns the calculation of $\overline{S}_\alpha$ and $\overline{S}_T$ since the treatment of $\overline{F}_i$ often poses no problem. To illustrate the requirements for the closures of these source rates we restrict attention to the source rate $\overline{S}_\alpha$ in the mass fraction equations. The treatment of $\overline{S}_T$ represents a similar problem that will be addressed in chapter 5.

The averaged chemical reaction rate $\overline{S}_\alpha$ is a mean over a very complicated function of mass fractions **m** and temperature T in general,

$$\overline{S}_\alpha = \overline{S_\alpha(\mathbf{m}, T)}. \tag{4.97}$$

Thus, the use of an approach in analogy to that described in section 4.6.2 is faced with two serious problems. First, the temperature dependence in (4.97), which arises via the variation of reaction parameters with temperature, is in general such that (4.97) cannot be written as an explicit function of moments of the mass

fraction-temperature PDF. Second, given the case that relation (4.97) can be approximated in terms of moments, there appears the problem that the use of variance transport equations (and required equations for higher-order moments) turns out to be unfeasible for flows that involve many reacting species. The consideration of n species for instance would imply the need to consider n (n + 1) / 2 (which is equal to 55 for n = 10) transport equations for variances.

Simple parametrizations for $\overline{S}_\alpha$ can only be found in the special cases of a very slow or fast chemistry. For example, the neglect of scalar fluctuations,

$$\overline{S}_\alpha \approx \overline{S}_\alpha(\overline{\mathbf{m}}, \overline{T}), \tag{4.98}$$

implies the assumption that mass fraction and temperature fluctuations decay much faster than reaction takes place, this means the species are perfectly mixed before chemical reactions occur. Obviously, such a neglect of influences of scalar fluctuations may result in serious overestimates of chemical conversion effects with regard to non-premixed combustion simulations. In the other limit case of a very fast chemistry (chemical reactions take place instantaneously), species cannot coexist such that one only finds areas where one of the species exist. Within such areas, the species behave as inert tracers, i.e., their reaction rate is equal to zero. In this case, one may introduce new variables as differences of species mass fractions, which obey equations where $\overline{S}_\alpha = 0$ (Baldyga & Bourne 1999; Durbin & Petterson 2001). In some cases it is possible to find appropriate values for $\overline{S}_\alpha$ by interpolation between the limit cases of a very slow and fast chemistry. However, this approach is restricted to the consideration of a few species, and such an interpolation between the limit cases of maximal and minimal $\overline{S}_\alpha$ may be related to significant errors (Baldyga & Bourne 1999).

For these reasons, the most promising approach to handle the closure of the chemical reaction rate $\overline{S}_\alpha$ is to combine (4.95a-d) with a stochastic model for mass fraction and temperature fluctuations. Such a model determines the mass fraction-temperature PDF, from which $\overline{S}_\alpha$ can be derived by integration. The fact that such scalar PDFs are coupled in general to velocity PDFs provides an additional reason for the consideration of stochastic velocity models. Such models for both velocities and scalars will be introduced in chapter 5.

Appendix 4A: Second and higher-order RANS equations

In extension to the consideration of transport equations for mean velocities and scalars in section 4.6, the corresponding equations for second-, third- and fourth-order moments implied by the basic equations will be presented here. To present these equations efficiently, this will be done by combining the mass fractions of N species and temperature to a scalar vector $\mathbf{\Phi}(\mathbf{x}, t) = \{\Phi_1, \ldots, \Phi_{N+1}\}$, and by

applying the following abbreviations for the right-hand sides of (4.71b-d),

$$\frac{DU_i}{Dt} = A_i, \qquad \frac{D\Phi_\alpha}{Dt} = A_\alpha. \tag{4A.1}$$

Fluctuations of A_i and A_α will be referred to by small variables,

$$a_i = A_i - \overline{A}_i, \qquad a_\alpha = A_\alpha - \overline{A}_\alpha. \tag{4A.2}$$

The equations for mean velocities and scalars can be derived then from (4A.1),

$$\frac{\partial \overline{U}_j}{\partial t} + \overline{U}_i \frac{\partial \overline{U}_j}{\partial x_i} + \langle\rho\rangle^{-1} \frac{\partial \langle\rho\rangle \overline{u_i u_j}}{\partial x_i} = \overline{A}_j, \tag{4A.3a}$$

$$\frac{\partial \overline{\Phi}_\alpha}{\partial t} + \overline{U}_i \frac{\partial \overline{\Phi}_\alpha}{\partial x_i} + \langle\rho\rangle^{-1} \frac{\partial \langle\rho\rangle \overline{u_i \phi_\alpha}}{\partial x_i} = \overline{A}_\alpha. \tag{4A.3b}$$

The combination of these equations with (4A.1) leads to transport equations for turbulent fluctuations of velocities $u_i = U_i - \overline{U}_i$ and scalars $\phi_\alpha = \Phi_\alpha - \overline{\Phi}_\alpha$, which may be used to obtain all the transport equations for higher-order moments.

4A.1. Second-order equations

The equations obtained in this way for the variances of velocities and scalars are the following ones,

$$\frac{\partial \overline{u_i u_j}}{\partial t} + \overline{U}_k \frac{\partial \overline{u_i u_j}}{\partial x_k} + \langle\rho\rangle^{-1} \frac{\partial \langle\rho\rangle \overline{u_k u_i u_j}}{\partial x_k} + \overline{u_k u_j} \frac{\partial \overline{U}_i}{\partial x_k} + \overline{u_k u_i} \frac{\partial \overline{U}_j}{\partial x_k} = \overline{a_i u_j} + \overline{a_j u_i}, \tag{4A.4a}$$

$$\frac{\partial \overline{u_i \phi_\alpha}}{\partial t} + \overline{U}_k \frac{\partial \overline{u_i \phi_\alpha}}{\partial x_k} + \langle\rho\rangle^{-1} \frac{\partial \langle\rho\rangle \overline{u_k u_i \phi_\alpha}}{\partial x_k} + \overline{u_i u_k} \frac{\partial \overline{\Phi}_\alpha}{\partial x_k} + \overline{u_k \phi_\alpha} \frac{\partial \overline{U}_i}{\partial x_k} = \overline{a_i \phi_\alpha} + \overline{a_\alpha u_i}, \tag{4A.4b}$$

$$\frac{\partial \overline{\phi_\alpha \phi_\beta}}{\partial t} + \overline{U}_k \frac{\partial \overline{\phi_\alpha \phi_\beta}}{\partial x_k} + \langle\rho\rangle^{-1} \frac{\partial \langle\rho\rangle \overline{u_k \phi_\alpha \phi_\beta}}{\partial x_k} + \overline{u_k \phi_\beta} \frac{\partial \overline{\Phi}_\alpha}{\partial x_k} + \overline{u_k \phi_\alpha} \frac{\partial \overline{\Phi}_\beta}{\partial x_k} = \overline{a_\alpha \phi_\beta} + \overline{a_\beta \phi_\alpha}. \tag{4A.4c}$$

A model that applies these equations to obtain the Reynolds stresses and turbulent scalar fluxes in equations for averaged variables is called a second-order RANS model. The first two terms in (4A.4a-c) represent the substantial derivatives of variances. The fourth and fifth terms describe the production of turbulence by gradients of the mean fields. The variances are then affected by turbulent transport (given by the third terms), and energy redistribution and dissipation processes, which are represented by the right-hand sides of (4A.4a-c).

4A.2. Third-order equations

To calculate the triple correlations that appear in the third terms of (4A.4a-c), one may apply their transport equations. With regard to velocity correlations, these equations are given by

$$\frac{\partial\overline{u_i u_j u_k}}{\partial t}+\overline{U}_m\frac{\partial\overline{u_i u_j u_k}}{\partial x_m}+\langle\rho\rangle^{-1}\frac{\partial\langle\rho\rangle\overline{u_m u_i u_j u_k}}{\partial x_m}+\frac{\partial\overline{U}_i}{\partial x_m}\overline{u_m u_j u_k}+\frac{\partial\overline{U}_j}{\partial x_m}\overline{u_m u_i u_k}$$

$$+\frac{\partial\overline{U}_k}{\partial x_m}\overline{u_m u_i u_j}-\langle\rho\rangle^{-1}\left(\frac{\partial\langle\rho\rangle\overline{u_i u_m}}{\partial x_m}\overline{u_j u_k}+\frac{\partial\langle\rho\rangle\overline{u_j u_m}}{\partial x_m}\overline{u_i u_k}+\frac{\partial\langle\rho\rangle\overline{u_k u_m}}{\partial x_m}\overline{u_i u_j}\right)=$$

$$=\overline{a_i u_j u_k}+\overline{a_j u_i u_k}+\overline{a_k u_i u_j}. \qquad (4A.5)$$

A RANS model that applies (4A.4a) and (4A.5) to calculate the Reynolds stresses $\overline{u_i u_k}$ is called a third-order RANS model. The corresponding transport equations for triple correlations that involve scalar fluctuations may be obtained by replacing u_k by ϕ_α, a_k by a_α and $\overline{U}_k$ by $\overline{\Phi}_\alpha$ in (4A.5).

4A.3. Fourth-order equations

The fourth-order moments that appear in (4A.5) can be calculated by means of their transport equations. They read

$$\frac{\partial\overline{u_i u_j u_k u_l}}{\partial t}+\overline{U}_m\frac{\partial\overline{u_i u_j u_k u_l}}{\partial x_m}+\langle\rho\rangle^{-1}\frac{\partial\langle\rho\rangle\overline{u_m u_i u_j u_k u_l}}{\partial x_m}+$$

$$+\frac{\partial\overline{U}_i}{\partial x_m}\overline{u_m u_j u_k u_l}+\frac{\partial\overline{U}_j}{\partial x_m}\overline{u_m u_i u_k u_l}+\frac{\partial\overline{U}_k}{\partial x_m}\overline{u_m u_i u_j u_l}+\frac{\partial\overline{U}_l}{\partial x_m}\overline{u_m u_i u_j u_k}-\langle\rho\rangle^{-1}\cdot$$

$$\cdot\left(\frac{\partial\langle\rho\rangle\overline{u_i u_m}}{\partial x_m}\overline{u_j u_k u_l}+\frac{\partial\langle\rho\rangle\overline{u_j u_m}}{\partial x_m}\overline{u_i u_k u_l}+\frac{\partial\langle\rho\rangle\overline{u_k u_m}}{\partial x_m}\overline{u_i u_j u_l}+\frac{\partial\langle\rho\rangle\overline{u_l u_m}}{\partial x_m}\overline{u_i u_j u_k}\right)$$

$$=\overline{a_i u_j u_k u_l}+\overline{a_j u_i u_k u_l}+\overline{a_k u_i u_j u_l}+\overline{a_l u_i u_j u_k}. \qquad (4A.6)$$

Equations for moments that involve scalar fluctuations can be obtained by adopting the replacements described above. The common use of (4A.4a), (4A.5) and (4A.6) to calculate the Reynolds stresses $\overline{u_i u_k}$ is called a fourth-order RANS model. Examples for the application of third- and fourth-order moment equations will be presented in chapter 5.

5. Stochastic models for large-scale turbulence

The closure problems related to the use of RANS equations pointed out in section 4.6 may be overcome by the construction of stochastic turbulence models. This approach will be addressed here with regard to both velocity and scalar models. In particular, this is done by generalizing (in analogy to the derivation of the fluid dynamic equations in chapter 4) the equations for the equilibrium dynamics of relevant variables derived in Appendix 3A. The most essential assumption related to stochastic models presented in this chapter is the consideration of large-scale fluctuations around ensemble means (see the discussion of averaging procedures in Appendix 1A). The alternative modeling of small-scale turbulence will be addressed in chapter 6.

Basics of the construction of stochastic velocity models will be presented in sections 5.1 – 5.4. Essential questions considered in this way are for instance: Which processes can be described by which equation structure of a stochastic model? How is it possible to determine the coefficients of stochastic models? What is the physical meaning of the coefficient C_0 (see below) that controls stochastic contributions in velocity models? To answer these questions, a hierarchy of stochastic velocity models for homogeneous, isotropic and stationary turbulence will be introduced in section 5.1. The extension of these models to the more realistic case of inhomogeneous, nonstationary and anisotropic flows will be considered in section 5.2, where the generalized Langevin model is presented. Nevertheless, this model only represents a frame for the construction of closed models, and one still has to parametrize ten unknown coefficients. Essential properties of different simplifications of this model will be investigated in section 5.3 with regard to the simulation of shear flows, which represent a cornerstone for the calculation of wall-bounded turbulent flows of engineering and environmental interest. In combination with the estimation of the coefficient C_0 that controls the stochastic forcing of velocity fluctuations, section 5.4 deals with a discussion of the physical meaning of various contributions in stochastic velocity models and their universality. In correspondence to the hierarchical consideration of the modeling of the evolution of velocities, the simulation of scalar transport will be addressed in section 5.5. Finally, sections 5.6 and 5.7 deal with conclusions about the application of stochastic methods for compressible flow simulations, which is in particular relevant to the calculation of turbulent combustion processes.

S. Heinz, *Statistical Mechanics of Turbulent Flows*

The concept used in sections 5.1 – 5.6 for the construction of stochastic models is to extend the stochastic model for the equilibrium dynamics of relevant variables presented in Appendix 3A. This line will be complemented in Appendix 5A by another one, which makes a direct use of the relations between stochastic models and the basic equations of fluid and thermodynamics. The main result obtained in this way is a unique relationship between the coefficients of stochastic models and the measurable statistics of acceleration fluctuations. Applications of this approach will be shown with regard to the construction of linear stochastic models in Appendix 5B, and regarding the construction of nonlinear stochastic models in Appendix 5C. The latter then allows us to assess the range of applicability of linear stochastic methods usually applied.

5.1. A hierarchy of stochastic velocity models

As done in chapter 4, we use the stochastic model for the dynamics of relevant variables as a basis for the construction of stochastic models for the fluid motion (Heinz 1997). For simplicity, we restrict the following explanations to the case of statistically homogeneous, isotropic and stationary turbulence (HIST).

5.1.1. An acceleration model

The relevant variable ξ_i considered is the velocity U_i^*. In contrast to the developments made in chapter 4, the assumption that U_i^* represents a Markov process cannot be seen to be justified in general here. As discussed in section 4.5, fluctuations of U_i^* are caused by eddies of the energy cascade which have finite correlation times. It was shown in Appendix 3A that such stochastic force correlations can be taken into account by considering a stochastic equation for the acceleration $dU_i^* / dt = A_i^*$. According to (3A.31), this equation reads

$$\frac{d}{dt} A_i^* = \frac{1}{\tau_f} \left\{ - A_i^* - \frac{1}{\tau_u} U_i^* + \sqrt{\frac{4k}{3\tau_u}} \frac{dW_i}{dt} \right\}. \tag{5.1}$$

For simplicity, mean velocities, which have to be constant for HIST, are set equal to zero here. As done in section 4.2.1, we used isotropic matrices $b_{in} = b_{mm} / 3\ \delta_{in}$ and $\sigma_{in} = 2\ k / 3\ \delta_{in}$ in this specification of (3A.31), and we introduced (in correspondence to the molecular time scale τ_m) the time scale $\tau_u = 12\ k / b_{mm}^2$, where k represents the turbulent kinetic energy.

The characteristic relaxation time scales of fluctuations of velocities and stochastic forces, τ_u and τ_f, respectively, can be related to measurable quantities as shown by Sawford (1991). The velocity autocorrelation function R(s) that is implied by the stochastic acceleration model (5.1) is given by

$$R(s) = \frac{3}{2k}\left\langle U_{(i)}{}^{*}(t+s)U_{(i)}{}^{*}(t)\right\rangle = \frac{\beta_2 \exp(\beta_1 |s|) - \beta_1 \exp(\beta_2 |s|)}{\beta_2 - \beta_1}. \tag{5.2}$$

Bracketed subscripts are excluded from the summation convention. β_1 and β_2 are parameters that are related to τ_u and τ_f via the expressions

$$2\beta_1\tau_f = -1 + \sqrt{1 - 4\frac{\tau_f}{\tau_u}}, \qquad 2\beta_2\tau_f = -1 - \sqrt{1 - 4\frac{\tau_f}{\tau_u}}. \tag{5.3}$$

The analysis of the small-time behaviour of (5.2) can be used to derive relations between β_1 and β_2 and turbulence parameters. By truncating the Taylor series of R(s) in the second order of approximation we obtain

$$R(s) = 1 - \beta_1\beta_2\frac{s^2}{2}. \tag{5.4}$$

Another expression for the small-time behaviour of R(s) is obtained if the consideration is restricted to motions within the inertial subrange (see Fig. 4.2), for which $\tau_u >> \tau_f$. The development of the expressions (5.3) into Taylor series of τ_f / τ_u reveals that β_2 becomes large and negative in this case. Hence, the velocity autocorrelation function reduces to $R(s) = \exp(\beta_1 |s|)$, which provides in the first order of approximation of the Taylor series

$$R(s) = 1 + \beta_1 |s|. \tag{5.5}$$

The comparison of (5.4) and (5.5) with the corresponding predictions of Kolmogorov's similarity theory (Monin & Yaglom 1975) leads to the following relations for β_1 and β_2,

$$\beta_1\beta_2 = \frac{3A_0}{2\tau\tau_\eta}, \qquad \beta_1 = -\frac{3C_0(\infty)}{4\tau}. \tag{5.6}$$

A_0 and $C_0(\infty)$ represent universal constant according to Kolmogorov's similarity theory, τ_η is the Kolmogorov time scale and $\tau = k / \varepsilon$ the dissipation time scale of turbulence. By adopting the relations (5.3) between β_1 and β_2 with τ_u and τ_f, the expressions (5.6) show that τ_f scales with the characteristic time scale of the smallest, dissipative eddies τ_η,

$$\frac{\tau_\eta}{\tau_f} = 2\frac{A_0}{C_0}, \tag{5.7}$$

and τ_u scales with the characteristic time scale of large-scale eddies τ,

$$\frac{\tau}{\tau_u} = \frac{3}{4} C_0 . \tag{5.8}$$

The relations (5.7) and (5.8) are presented here by adopting the abbreviation

$$C_0 = C_0(\infty) \left[1 + \frac{3 C_0^{\,2}(\infty)}{8 A_0 \, \mathrm{Re}_L^{\,1/2}} \right]^{-1} . \tag{5.9}$$

Obviously, C_0 tends towards $C_0(\infty)$, which is called the Kolmogorov constant, in the limit of high Reynolds numbers $\mathrm{Re}_L = \tau^2 / \tau_\eta^{\,2}$.

Nevertheless, to close the relations (5.7) and (5.8) between τ_u and τ_f and turbulence parameters one still has to estimate A_0 and $C_0(\infty)$. By comparing the predictions of the acceleration model (5.1) with the results of DNS of velocity fields performed by Yeung & Pope (1987), Sawford estimated A_0 as a function of the Taylor-scale Reynolds number Re_λ defined by (4.91),

$$A_0 = 0.13 \, \mathrm{Re}_\lambda^{\,0.64} . \tag{5.10}$$

The combination of (5.9), (5.10) and (4.91) to replace Re_L by Re_λ leads then to Sawford's parametrization for C_0,

$$C_0 = \frac{C_0(\infty)}{1 + 7.5 C_0^{\,2}(\infty) \, \mathrm{Re}_\lambda^{\,-1.64}} . \tag{5.11}$$

Sawford (1991) estimated $C_0(\infty) = 7$ on the basis of the DNS data of Yeung & Pope (1989). Recently, Sawford and Yeung (2001) derived a revised value $C_0(\infty) = 6$ on the basis of new DNS data.

5.1.2. A velocity model

To see the asymptotic features of the acceleration model (5.1), we write it according to equation (3.44) for discrete time steps (Δt is a time interval),

$$\frac{\tau_f}{\Delta t} \left[A_i^{\,*}(t + \Delta t) - A_i^{\,*}(t) \right] = -A_i^{\,*}(t) - \frac{1}{\tau_u} U_i^{\,*}(t) + \sqrt{\frac{4k}{3\tau_u}} \frac{\Delta W_i(t)}{\Delta t} . \tag{5.12}$$

This equation reveals that (5.1) reduces asymptotically (for time steps Δt that are much larger than the characteristic relaxation time scale τ_f of stochastic forces) to a velocity model. The left-hand side of (5.12) then vanishes compared to $A_i^{\,*}(t)$ on the right-hand side such that we obtain the equation

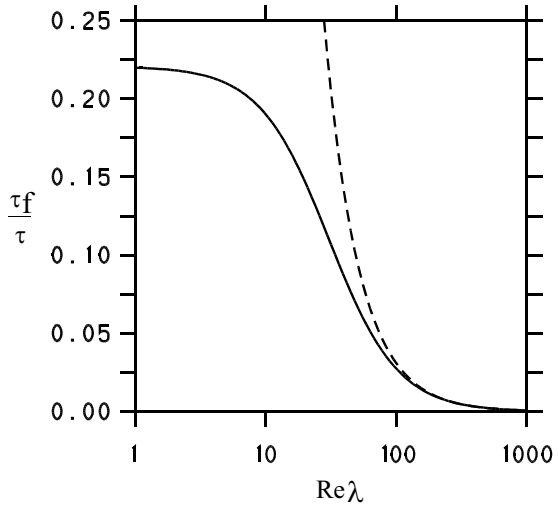

Fig. 5.1. The solid line gives τ_f / τ according to (5.7) against the Taylor-scale Reynolds number Re_λ. The dashed line shows the approximation $(12 / Re_\lambda)^{1.64}$ for the large-Re_λ behaviour of τ_f / τ.

$$\frac{d}{dt}U_i^* = -\frac{3C_0}{4\tau}U_i^* + \sqrt{C_0\varepsilon}\,\frac{dW_i}{dt}, \tag{5.13}$$

which is written in accordance with (5.1). To derive (5.13) one has to involve relation (5.8). This model represents the basic form of most of the models applied to turbulence simulations by means of stochastic methods. The mechanism of turbulent velocity fluctuations modeled in this way is very simple: the last term in (5.13) represents the stochastic generation of fluctuations, and the first term on the right-hand side acts such that these fluctuations relax. As shown in the next section, (5.13) is a specific formulation of the generalized Langevin model.

The difference between the velocity predictions of the acceleration model (5.1) and its asymptotic limit (5.13) depends essentially on the Reynolds number of the flow considered. To see this, we rewrite the factor $\tau_f / \Delta t$ of the acceleration difference in (5.12) by adopting τ as normalization quantity,

$$\frac{\tau_f}{\Delta t} = \frac{\tau_f / \tau}{\Delta t / \tau}. \tag{5.14}$$

The ratio τ_f / τ is shown in Fig. 5.1 in dependence on the Taylor-scale Reynolds number Re_λ. This figure reveals that the approximation $\tau_f / \tau = (12 / Re_\lambda)^{1.64}$ provides a very good estimate to τ_f / τ for $Re_\lambda > 100$. By adopting this approximation, one finds $\tau_f / \tau < 7\ 10^{-4}$ for high-Reynolds numbers $Re_\lambda > 1{,}000$. Hence, the acceleration model (5.1) reduces to the velocity model (5.13) in the case of high-Reynolds numbers. However, for lower Reynolds numbers one finds higher values for τ_f / τ. In this case, the use of the velocity model (5.13) corresponds with the neglect of Kolmogorov scale processes, which are then not resolved. In addition to this, a simple analysis of relation (5.14) reveals that inertial

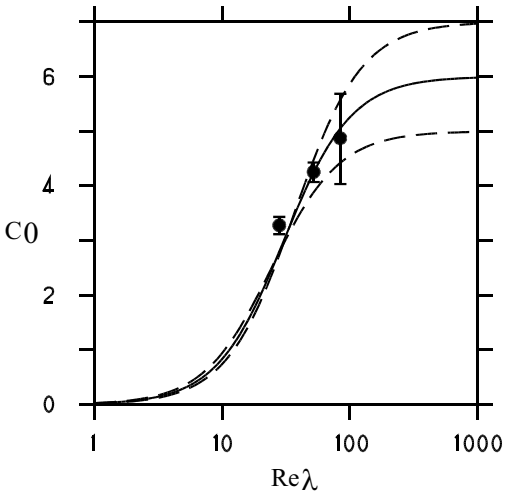

Fig. 5.2. The symbols show C_0 values for HIST according to the DNS data of Overholt & Pope (1996) against the Taylor-scale Reynolds number Re_λ. The error bars denote the accuracy of these values. The solid line gives the prediction of Sawford's formula (5.11) combined with $C_0(\infty) = 6$. The lower and upper dashed lines show predictions of this formula for $C_0(\infty) = 5$ and $C_0(\infty) = 7$, respectively.

subrange processes are not completely resolved by (5.13) if $Re_\lambda < 100$ (the choice $\Delta t = 10\ \tau_f$ at $Re_\lambda = 100$ corresponds with the use of $\Delta t = 0.3\ \tau$, but we find, for example, $\Delta t > \tau$ if $Re_\lambda < 34$). However, (5.13) then still represents a consistent model: it does not contain details of processes that take place within the interval Δt, but it provides the correct asymptotic behaviour of the acceleration model (5.1).

5.1.3. A position model

In some cases it is advantageous to model only the transport of scalars by means of stochastic methods whereas the velocity field is described by deterministic equations, see the discussion of hybrid methods in section 5.6. The scalars are then transported in physical space by a position model. The latter follows by writing (5.13) in correspondence to (5.12), and assuming that $\Delta t >> \tau_u$. Accordingly, equation (5.13) reduces to a model for the particle position x_i^*,

$$\frac{d}{dt} x_i^* = \sqrt{2\Gamma}\,\frac{dW_i}{dt}, \tag{5.15}$$

where $U_i^* = dx_i^* / dt$ is used. In (5.15), the turbulent diffusion coefficient Γ is introduced, which is given by

$$\Gamma = \frac{8k\tau}{9C_0}. \tag{5.16}$$

The velocity and position models (5.13) and (5.15) reveal that the Kolmogorov constant $C_0(\infty)$ is the only parameter in these equations, which indicates its high relevance. According to Kolmogorov's theory, this constant $C_0(\infty)$ is assumed to be universal. To prove this assumption, one has to investigate how $C_0(\infty)$ estimates are affected by the flow considered and the model applied. This question will be

addressed in section 5.4. To prepare this discussion, it will be shown here that the same $C_0(\infty)$ is obtained from the acceleration model (5.1) and its reduced form, the position model (5.15). This is done in terms of Fig. 5.2, which shows C_0 calculations on the basis of (5.16). All the details may be found elsewhere (Heinz 2002). These data reveal the excellent agreement of the Reynolds number dependence and the asymptotic value $C_0(\infty)$ given here with the corresponding findings obtained on the basis of the acceleration model (5.1), see Sawford (1991) and Sawford & Yeung (2001).

5.2. The generalized Langevin model for velocities

The hierarchy of stochastic models was presented in section 5.1 by considering the case of HIST. Extensions of these models, which are required to simulate more realistic flows, will be described next. This will be done by restricting the attention to high-Re flows, this means we consider generalizations of the velocity model (5.13). The incorporation of Reynolds number effects can be performed then by extending these models to acceleration models, see Pope (2002).

5.2.1. The generalized Langevin model

The stochastic velocity model considered is the following one,

$$\frac{d}{dt} x_i^* = U_i^*, \tag{5.17a}$$

$$\frac{d}{dt} U_i^* = -\frac{1}{\langle \rho \rangle} \frac{\partial < p >}{\partial x_i} + G_{ik} \left(U_k^* - \overline{U}_k \right) + \sqrt{C_0 \varepsilon} \frac{dW_i}{dt}. \tag{5.17b}$$

This model is called the generalized Langevin model (GLM). The name of this model refers to a suggestion of Langevin (1908), who reformulated an earlier idea of Einstein (1905). There are three differences compared to the velocity model (5.13). First, an additional systematic term (the pressure gradient term) is involved. This term describes the mean velocity change, which is nonzero in inhomogeneous flows. The justification for its appearance may be seen by means of the transport equation (5.20) for mean velocities presented below. The second difference is that turbulent velocities are written with reference to the mass density-averaged velocity $\overline{U}_k$. This explains the second term on the right-hand side of (5.17b) as a contribution related to fluctuations: this term vanishes in the mean, as the last term. The third difference is given by the consideration of an anisotropic coefficient G_{ik}, which may depend on time and position but not on actual velocities. The consideration of nine elements of G_{ik} and C_0 results in ten unknowns of the model (5.17a-b) that have to be determined.

5.2.2. The implied moment transport equations

Essential features of the GLM may be seen by comparing the moment transport equations derived in Appendix 4A from the basic equations with corresponding equations implied by (5.17a-b). The simplest way to obtain the latter equations is to consider the evolution equation for the velocity PDF

$$F(\mathbf{w},\mathbf{x},t)=\langle\rho(\mathbf{x},t)\rangle^{-1}\left\langle\rho(\mathbf{x},t)\,\delta\left(\mathbf{U}^{*}(\mathbf{x}^{*}(t),t)-\mathbf{w}\right)\right\rangle=\overline{\delta(\mathbf{U}(\mathbf{x},t)-\mathbf{w})}. \tag{5.18}$$

$\rho(\mathbf{x}, t) = M\,\delta(\mathbf{x}^{*}(t) - \mathbf{x})$ is the fluid mass density, where $M = \int d\mathbf{x} <\rho(\mathbf{x}, t)>$ describes the total mass of fluid within the domain considered. The last expression of (5.18) makes use of the definition (4.93) of mass-weighted means. $\mathbf{U}(\mathbf{x}, t)$ is the Eulerian instantaneous fluid velocity of that fluid particle which has the position $\mathbf{x}$ at the time t. As pointed out in detail in chapter 3, the model (5.17a-b) can be rewritten into an equivalent Fokker-Planck equation for the joint velocity-position PDF $<\rho>$ F / M. After multiplication by M this equation reads

$$\frac{\partial}{\partial t}\langle\rho\rangle F=-\frac{\partial}{\partial x_i}w_i\langle\rho\rangle F-\frac{\partial}{\partial w_i}\left[-\frac{1}{\langle\rho\rangle}\frac{\partial<p>}{\partial x_i}+G_{ik}\left(w_k-\overline{U}_k\right)\right]\langle\rho\rangle F+$$

$$+\frac{1}{2}C_0\varepsilon\frac{\partial^2}{\partial w_i\partial w_i}\langle\rho\rangle F. \tag{5.19}$$

The consistency of (5.19) with the conservation equation of mass (4.95a) may be seen by integration over the velocity sample space.

The multiplication of (5.19) with w_i and integration leads to the following equations for mean velocities, which are implied by (5.17a-b),

$$\frac{\partial\overline{U}_i}{\partial t}+\overline{U}_k\frac{\partial\overline{U}_i}{\partial x_k}=-\langle\rho\rangle^{-1}\frac{\partial\langle\rho\rangle\overline{u_iu_k}}{\partial x_k}-\langle\rho\rangle^{-1}\frac{\partial\langle p\rangle}{\partial x_i}. \tag{5.20}$$

The comparison of (5.20) with equation (4.95b) reveals that the model (5.17a-b) neglects (in consistency with the consideration of a high-Reynolds number flow) contributions due to molecular transport and external forces.

Equations for the Reynolds stresses $\overline{u_iu_k}$ can be obtained by multiplying (5.19) with $w_i\,w_j$ and integrating it over the sample space. These equations read

$$\frac{\partial\overline{u_iu_j}}{\partial t}+\overline{U}_k\frac{\partial\overline{u_iu_j}}{\partial x_k}+\langle\rho\rangle^{-1}\frac{\partial\langle\rho\rangle\overline{u_ku_iu_j}}{\partial x_k}+\overline{u_ku_j}\frac{\partial\overline{U}_i}{\partial x_k}+\overline{u_ku_i}\frac{\partial\overline{U}_j}{\partial x_k}=$$

$$=G_{ik}\overline{u_ku_j}+G_{jk}\overline{u_ku_i}+C_0\varepsilon\delta_{ij}. \tag{5.21}$$

The comparison of (5.21) with the equations (4A.4a) shows that the stochastic model (5.17a-b) implies models for the acceleration correlations on the right-hand side of (4A.4a). It is worth noting that the turbulent transport term (the third term on the left-hand side) of (5.21) agrees exactly with the corresponding term in (4A.4a). However, in contrast to direct closures of (4A.4a) there is no need for any assumptions on triple correlations in (5.17a-b).

5.2.3. Specifications of the generalized Langevin model

The problem to be solved now is to close the GLM (5.17a-b) by suitable parametrizations of G_{ik} and C_0. Usually, this problem is addressed by making sure that the predictions of (5.17a-b) agree with given (asymptotic) values of the normalized Reynolds stress tensor. To illustrate essential features of this approach, we rewrite the variance equations (5.21) into equations for the turbulent kinetic energy k and the standardized anisotropy tensor a_{ij}, which measures the deviation from isotropy. These two quantities are defined by

$$k = \frac{1}{2}\overline{u_i u_i}, \qquad a_{ij} = \frac{1}{2k}\left(\overline{u_i u_j} - \frac{2k}{3}\delta_{ij}\right). \tag{5.22}$$

The equation for k that follows from (5.21) reads

$$\frac{\partial k}{\partial t} + \overline{U}_k \frac{\partial k}{\partial x_k} + \frac{1}{2}\langle\rho\rangle^{-1}\frac{\partial \langle\rho\rangle \overline{u_k u_i u_i}}{\partial x_k} = P - \varepsilon + \frac{1}{\langle\rho\rangle}\Pi_d\,. \tag{5.23}$$

$P = -\,\overline{u_i u_k}\;\overline{S}_{ki}$ represents the production due to shear, and $\varepsilon = 2\overline{\nu}\,\overline{(S_{ik}{}^{d})''(S_{ki}{}^{d})''}$ is the dissipation rate of k. Regarding Π_d we assume

$$\frac{1}{\langle\rho\rangle}\Pi_d = G_{kn}\overline{u_n u_k} + \left(\frac{3}{2}C_0 + 1\right)\varepsilon\,. \tag{5.24}$$

The term Π_d is usually considered to be caused by correlations of pressure and dilatation fluctuations, this means compressibility effects in addition to modifications of the dissipation rate ε (Wilcox 1998). Here, Π_d is defined by the right-hand side of (5.24).

The transport equation for a_{ij} that follows from (5.21) is the following one,

$$\frac{\partial a_{ij}}{\partial t} + \overline{U}_k \frac{\partial a_{ij}}{\partial x_k} + \frac{1}{2k\langle\rho\rangle}\left[\frac{\partial \langle\rho\rangle \overline{u_k u_i u_j}}{\partial x_k} - \overline{u_i u_j}\frac{\partial \langle\rho\rangle \overline{u_k u_n u_n}}{\partial x_k}\right] = \frac{C_0\varepsilon}{2k}\delta_{ij} -$$

$$-\frac{\overline{u_i u_j}}{2k^2}\left(P - \varepsilon + \frac{\Pi_d}{\langle\rho\rangle}\right) - \frac{\overline{u_k u_j}}{2k}\left(\frac{\partial \overline{U}_i}{\partial x_k} - G_{ik}\right) - \frac{\overline{u_k u_i}}{2k}\left(\frac{\partial \overline{U}_j}{\partial x_k} - G_{jk}\right). \tag{5.25}$$

Model	ELM	LM	SLM
G =	$\begin{pmatrix} G_{11} & G_{12} & G_{13} \\ G_{12} & G_{22} & G_{23} \\ G_{13} & G_{23} & G_{33} \end{pmatrix}$ may represent any Reynolds stresses	$\begin{pmatrix} G_{11} & 0 & 0 \\ 0 & G_{22} & 0 \\ 0 & 0 & G_{33} \end{pmatrix}$ may represent shear flow stresses	$\begin{pmatrix} G & 0 & 0 \\ 0 & G & 0 \\ 0 & 0 & G \end{pmatrix}$ may approximately represent shear flow
C_0 =	unconstrained	constrained	constrained

Table 5.1. Different specifications of the GLM. Their mentioned characteristics are pointed out with regard to the modeling of shear flows in section 5.3.

For many flows it is reasonable to assume that the standardized anisotropy tensor a_{ij} evolves towards a local equilibrium state. This assumption corresponds to the neglect of the left-hand side of (5.25),

$$\frac{C_0\varepsilon}{2k}\delta_{ij} = \frac{\overline{u_i u_j}}{2k^2}\left(P - \varepsilon + \frac{\Pi_d}{\langle\rho\rangle}\right) + \frac{\overline{u_k u_j}}{2k}\left(\frac{\partial \overline{U}_i}{\partial x_k} - G_{ik}\right) + \frac{\overline{u_k u_i}}{2k}\left(\frac{\partial \overline{U}_j}{\partial x_k} - G_{jk}\right). \qquad (5.26)$$

The equations (5.26) provide six algebraic relations for the calculation of C_0 and the nine components of G_{ik}. In general, one is satisfied if a velocity model is capable of representing (in addition to the mean velocity field) the observed evolution of the Reynolds stress tensor correctly. This can be achieved by introducing an extended Langevin model (ELM), where G_{ik} is a symmetric matrix as the Reynolds-stress tensor. In this case, all the components of G_{ik} are determined by (5.26), where C_0 is left unconstrained. The latter could be found by adjusting the characteristic time scale for the relaxation into the asymptotic state to measurements. The possibility of a unconstrained choice of C_0 may be seen as an advantage, but in fact it also poses a non-trivial problem. One has to assess the dependence of C_0 on the Reynolds number (which may vary in time and space), and one has to provide C_0 with a comparable accuracy as the components of G_{ik}.

Under circumstances where one is mainly interested in stationary model predictions of a flow where two components of the Reynolds stress tensor vanish (as given for the shear flow considered in section 5.3), one may apply a Langevin model (LM) instead of the ELM, where G_{ik} is taken as a diagonal matrix. The special advantage of this model is that one obtains an estimate for C_0 with the same accuracy as given for the calculated components of G_{ik}. The latter is relevant regarding the significant variations of C_0 which are found if various measurements are involved, see section 5.4.

A third type of parametrization of G_{ik} is given by reducing the LM to the simplified Langevin model (SLM), where G_{ik} is assumed to be an isotropic tensor. This is the standard model used for most of the stochastic simulations of turbulent flows (Pope 2000). It has the significant advantage that it is extremely simple, which simplifies analyses and numerical simulations. Nevertheless, the SLM is related to assumptions that are only satisfied approximately, see the consideration of this question in section 5.3. Characteristic features of these three specifications of the GLM model are summarized in Table 5.1.

5.3. A hierarchy of Langevin models

The differences between the ELM, LM and SLM will be illustrated now by calculating their model coefficients for shear flows. This class of flows represents a cornerstone for the calculation of wall-bounded turbulent flows of engineering and environmental interest. The expressions presented here will be applied then in section 5.4 for the calculation of the Kolmogorov constant and in section 5.6 for the discussion of models for compressible reacting flow.

A shear flow is characterized by a mean velocity field that has gradients (shear) only in one direction,

$$\frac{\partial \overline{U}_i}{\partial x_j} = S\delta_{i1}\delta_{j2}. \tag{5.27}$$

The coordinate system is chosen such that x_1 is in the streamwise direction and x_2 is in the direction of the mean shear. Obviously, (5.27) implies $S = \partial \overline{U}_1 / \partial x_2$. It is worth noting that S is not considered as a constant, i.e., it may vary with x_2. According to the expression (5.27), the turbulence forcing does not produce correlations between turbulent motions in the x_1- x_2-plane and x_3-direction. Thus, $\overline{u_1u_3} = \overline{u_2u_3} = 0$, this means the Reynolds stress tensor is given by

$$\begin{pmatrix} \overline{u_1u_1} & \overline{u_1u_2} & 0 \\ \overline{u_1u_2} & \overline{u_2u_2} & 0 \\ 0 & 0 & \overline{u_3u_3} \end{pmatrix}. \tag{5.28}$$

For the shear flow considered, the production of k is given by $P = -S\ \overline{u_1u_2}$.

5.3.1. The extended Langevin model

As pointed out in section 5.2.3, the ELM is obtained by considering G_{ik} as a symmetric matrix. Equation (5.26) then provides six relations for six components of G_{ik}. Regarding the shear flow considered, one finds that G_{13} and G_{23} have to

vanish,

$$G_{13} = 0, \qquad G_{23} = 0. \tag{5.29}$$

By adopting the dissipation time scale $\tau = k / \varepsilon$ of turbulence for the normalization, the diagonal elements of G_{ik} are determined by the relations

$$\frac{\overline{u_1u_1}}{2k}\left[-2G_{11}\tau + \frac{P}{\varepsilon} - 1 + \frac{\Pi_d}{\langle\rho\rangle\varepsilon}\right] = \frac{1}{2}C_0 + \frac{P}{\varepsilon} + \frac{\overline{u_1u_2}}{k}G_{12}\tau, \tag{5.30a}$$

$$\frac{\overline{u_2u_2}}{2k}\left[-2G_{22}\tau + \frac{P}{\varepsilon} - 1 + \frac{\Pi_d}{\langle\rho\rangle\varepsilon}\right] = \frac{1}{2}C_0 + \frac{\overline{u_1u_2}}{k}G_{12}\tau, \tag{5.30b}$$

$$\frac{\overline{u_3u_3}}{2k}\left[-2G_{33}\tau + \frac{P}{\varepsilon} - 1 + \frac{\Pi_d}{\langle\rho\rangle\varepsilon}\right] = \frac{1}{2}C_0. \tag{5.30c}$$

The coefficient G_{12}, which appears in (5.30a-b) satisfies the relation

$$\frac{\overline{u_1u_1}}{k}G_{12}\tau\left(1 + \frac{\overline{u_1u_1}\ \overline{u_2u_2}}{\overline{u_1u_2}^2}\right) = \frac{1}{2}C_0 + \frac{P}{\varepsilon}\left(1 - \frac{\overline{u_1u_1}\ \overline{u_2u_2}}{\overline{u_1u_2}^2}\right)\left(1 + \frac{\overline{u_1u_1}}{\overline{u_2u_2}}\right)^{-1}. \tag{5.31}$$

As explained above, the use of the ELM is related to the problem of providing C_0.

5.3.2. The Langevin model

A simpler model is given by the LM, which assumes that G_{ik} is a diagonal matrix. Hence, we have $G_{12} = 0$ in this case. The diagonal elements of G_{ik} are then given by the equations (5.30a-c) with zero G_{12}. The advantage of the LM is that it determines C_0. By equating the right-hand side of (5.31) to zero one finds

$$C_0 = 2\frac{P}{\varepsilon}\left(\frac{\overline{u_1u_1}\ \overline{u_2u_2}}{\overline{u_1u_2}^2} - 1\right)\left(1 + \frac{\overline{u_1u_1}}{\overline{u_2u_2}}\right)^{-1}. \tag{5.32}$$

C_0 is determined in this way by properties of large-scale turbulence (the anisotropy and normalized time scale $S\,\tau$). A discussion of the idea of modeling turbulence by means of a stochastic forcing that is controlled by such a C_0 may be found in section 5.4.2.

5.3.3. The simplified Langevin model

A further simplification is given by the SLM, which corresponds to the choice of G_{ik} as an isotropic tensor, $G_{ik} = G\,\delta_{ik}$. The three relations (5.30a-c) for the

Re_τ	$\overline{u_1u_1}$	$\overline{u_2u_2}$	$\overline{u_3u_3}$	$\overline{u_1u_2}$	η_1	η_2
180	1.59	0.56	0.74	– 0.42	1.19	0.65
395	2.73	0.95	1.42	– 0.73	2.07	1.19
590	3.13	1.06	1.63	– 0.80	2.27	1.35

Table 5.2. Normalized channel flow DNS data of Moser et al. (1999), which allow the assessment of the approximations (5.33). Re_τ refers to the friction Reynolds number (5.40). The wall distance, which is defined by (5.38), is $y^+ = 98$ for these data.

diagonal elements of G_{ik} then determine G. Further, they provide two constraints for the statistics of the velocity field,

$$\overline{u_1u_1} = \eta_1, \qquad \overline{u_2u_2} = \overline{u_3u_3} = \eta_2, \tag{5.33}$$

where the following abbreviations are introduced,

$$\eta_1 = \overline{u_2u_2} + 2\frac{\overline{u_1u_2}^2}{\overline{u_2u_2}}, \qquad \eta_2 = \frac{1}{2}\left(\overline{u_2u_2} + \overline{u_3u_3}\right). \tag{5.34}$$

The DNS data presented in Table 5.2 reveal that the variance relations (5.33), which are implied by the SLM, are only satisfied approximately (the deviations are 13-27%).

The combination of (5.30a-c) with $G_{ik} = G\,\delta_{ik}$ enables the calculation of G, for which one obtains

$$-G\tau = \frac{3}{4}C_0 + \frac{1}{2} - \frac{1}{2}\frac{\Pi_d}{\langle\rho\rangle\varepsilon}. \tag{5.35}$$

For an incompressible flow where $\Pi_d = 0$, the difference from the corresponding turbulence frequency in (5.13) is given by the appearance of the contribution 1 / 2 on the right-hand side, which guarantees the decay of turbulent kinetic energy. Relation (5.32) for C_0 reduces now to

$$C_0 = \frac{2}{3}\frac{P}{\varepsilon}\frac{1+\sqrt{1-6\,\overline{u_1u_2}^2/k^2}}{1-\sqrt{1-6\,\overline{u_1u_2}^2/k^2}}. \tag{5.36}$$

To obtain (5.36), one has to replace the variances in (5.32) divided by $\overline{u_1u_2}$ as functions of $\overline{u_1u_2}$ / k. This can be done by adopting the variance relations (5.33), which follow from the SLM.

5.4. The Kolmogorov constant

The stochastic models considered above reveal the fundamental role of C_0, which represents the standardized intensity of the generation of turbulent velocity fluctuations. Within the frame of the SLM, C_0 determines (for an incompressible flow with $\Pi_d = 0$) both the production and relaxation of velocity fluctuations. Thus, the questions of how C_0 varies with the Reynolds number, and whether C_0 approaches to a universal value at high Reynolds numbers, as predicted by the theory of Kolmogorov, are clearly relevant. To address these questions, one has to investigate how C_0 estimates depend on the stochastic model applied and the flow considered. This will be done next by following closely a publication of the author (Heinz 2002).

5.4.1. C_0 for an equilibrium turbulent boundary layer

To calculate C_0 for a more complex flow than HIST, we consider a constant-density equilibrium turbulent boundary layer (ETBL), which is well investigated by DNS and experiments. This flow represents a shear flow with characteristics according to (5.27) and (5.28). In particular, the velocity is given by

$$\frac{\partial u^+}{\partial y^+} = \frac{1}{\kappa y^+}. \tag{5.37}$$

Here, $\kappa = 0.41\ (\pm\ 0.02)$ is the von Kármán constant. The scaled velocity $<U_1>$ and position x_2 are defined by

$$u^+ = \frac{<U_1>}{u_\tau}, \qquad y^+ = \frac{u_\tau x_2}{\nu}, \tag{5.38}$$

where u_τ denotes the friction velocity u_τ (Pope 2000)

$$u_\tau = \sqrt{\nu \left(\frac{\partial <U_1>}{\partial x_2} \right)_{x_2=0}}. \tag{5.39}$$

The variances normalized to u_τ are given in Table 5.2 in dependence on the friction Reynolds number (h being the channel height)

$$Re_\tau = \frac{u_\tau h}{2\nu}. \tag{5.40}$$

The flow considered is in an equilibrium state as given for HIST. However, P does not vanish here but it is in balance with the dissipation rate of k, $P = \varepsilon$.

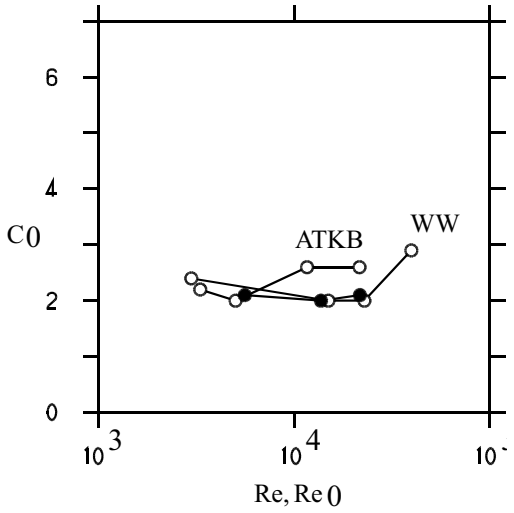

Fig. 5.3. The solid symbols show C_0 obtained for the LM in dependence on the Reynolds number Re according to the DNS data of Moser et al. (1999). The open symbols represent C_0 in dependence on the Reynolds number Re_0 according to the measurements of Wei & Willmarth (1989, referred to as WW) and Antonia et al. (1992, referred to as ATKB).

For reasons pointed out in section 5.2.3, we will use the LM to calculate C_0 for this flow. This model is capable of representing the Reynolds stresses of the ETBL correctly, where C_0 can be determined accurately. Compared to the ELM, the assumption that underlies the application of the LM is that turbulent velocity fluctuations interact primarily with their own means. A way to prove the suitability of this assumption is to study the influence of modeling assumptions on C_0 estimates. This question will be addressed in section 5.4.2.

Calculations of C_0 according to relation (5.32) combined with $P = \varepsilon$ are shown in Fig. 5.3, where both DNS and experimental data were applied. These C_0 values are presented in dependence on the Reynolds numbers

$$Re_0 = \frac{U_0 h}{2\nu}, \qquad Re = \frac{U_b h}{\nu}, \tag{5.41}$$

where U_0 denotes the centerline velocity and U_b the bulk velocity,

$$U_b = \frac{2}{h}\int_0^{h/2} dx_2 < U_1(x_2) >. \tag{5.42}$$

The friction Reynolds number Re_τ given in Table 5.2 was related to Re by means of the relation $Re_\tau = 0.09\ Re^{0.88}$, see Pope (2000, p. 279). The results shown in Fig. 5.3 reveal that the influence of the Reynolds number on these C_0 predictions is negligible (there is no observable trend of these values with the Reynolds number), and that the asymptotic value $C_0(\infty)$ is significantly less than 6. In particular, the DNS data provide a mean of $C_0 = 2.1 \pm 0.04$. This value agrees very well with the results of measurements: both provide $C_0 = 2.3 \pm 0.3$.

5.4.2. An explanation for the variations of C_0

$C_0(\infty)$ should be a universal constant according to Kolmogorov's theory, i.e., the same for each flow. However, the results obtained in sections 5.1.3 and 5.4.1 do not support this view: one finds $C_0(\infty) \approx 6$ for HIST whereas $C_0(\infty) \approx 2$ was found for the ETBL. It is worth emphasizing that the latter finding is very well supported by many results obtained for other flows than HIST: for decaying turbulence, evolving scalar fields and the atmospheric boundary layer one found values $1 \leq C_0(\infty) \leq 3$ (Du et al. 1995; Dreeben & Pope 1997; Heinz 1997, 1998a; Weinman & Klimenko 2000).

To understand the reasons for the observed variations of $C_0(\infty)$ estimates between 1 and 7 it is helpful to write the GLM (5.17a-b) for the incompressible flow considered in the following way,

$$U_i^* - \left\langle U_i^* \right\rangle = u_i^{ac} + u_i^{an} + u_i^{st}. \tag{5.43}$$

On the right-hand side, we have contributions due to acceleration fluctuations u_i^{ac}, anisotropy u_i^{an} and stochastic forcing u_i^{st}. These quantities are defined by

$$u_i^{ac} = G^{-1}\left(\frac{dU_i^*}{dt} - \left\langle \frac{dU_i^*}{dt} \right\rangle \right), \tag{5.44a}$$

$$u_i^{an} = \left[\delta_{ij} - G^{-1}G_{ij}\right]\left(U_j^* - \left\langle U_j^* \right\rangle\right), \tag{5.44b}$$

$$u_i^{st} = G^{-1}\sqrt{C_0\varepsilon}\,\frac{dW_i}{dt}. \tag{5.44c}$$

To obtain (5.43), one has to introduce the fluctuation of dU_i^* / dt and to split G_{ij} into its isotropic ($G = G_{nn} / 3$) and deviatoric part. According to (5.43), velocity fluctuations $U_i^* - < U_i^* >$ are caused by three contributions, u_i^{ac}, u_i^{an} and u_i^{st}. Therefore, the assumption of a universal $C_0(\infty)$ would correspond, basically, to the consideration of u_i^{st} as a contribution in (5.43) that is relatively independent of variations of u_i^{ac} and u_i^{an}. To prove this idea one has to study whether u_i^{ac} and u_i^{an} affect C_0 estimates or not.

This will be done for two flows, the ETBL and HIST, as pointed out in Table 5.3. The use of the LM involves both u_i^{an} and u_i^{ac} for the calculation of $C_0^{(I)}$, which is given by (5.32). The application of the SLM corresponds then with the neglect of u_i^{an}. For that case, $C_0^{(II)}$ is given by (5.36). The further reduction of the LM to a diffusion model (DM), which is given by the extension of the position model (5.15) to a model for inhomogeneous flows (see section 5.7), neglects both u_i^{an} and u_i^{ac}. Expression (5.16) for the diffusion coefficient has to be modified in this case

Model	ETBL	HIST
LM ($u_i^{an} \neq 0$; $u_i^{ac} \neq 0$)	$C_0^{(I)}$	($= C_0^{(IV)}$)
SLM ($u_i^{an} = 0$; $u_i^{ac} \neq 0$)	$C_0^{(II)}$	($= C_0^{(IV)}$)
DM ($u_i^{an} = 0$; $u_i^{ac} = 0$)	$C_0^{(III)}$	$C_0^{(IV)}$

Table 5.3. C_0 calculations for the ETBL and HIST by means of various models.

by $\Gamma = 2\ \eta_2^2 / (C_0\ \varepsilon)$. The combination of this relation with the result $\Gamma = \overline{u_1 u_2}^{\,2} / \varepsilon$ of measurements in the horizontally uniform neutral atmospheric surface layer implies then $C_0^{(III)} = 2\ \eta_2^2 / \overline{u_1 u_2}^{\,2}$ (Heinz 2002). Regarding the ETBL, C_0 is calculated here by the channel flow DNS data of Moser et al. (1999). Experimental data cannot be used for a comparison because $\overline{u_3 u_3}$ was not measured. With regard to HIST, contributions due to u_i^{ac} and u_i^{an} to the variance budget disappear. Thus, the values $C_0^{(IV)}$ obtained for HIST in section 5.1.3 have to be the same for all the three models considered. Evidence for this is given by the excellent agreement of the results presented above with those of Sawford's acceleration model, which is (for HIST) more complete than (5.43).

The results of these calculations are presented in Fig. 5.4. In contrast to Fig. 5.2, it is advantageous to present the data for HIST in dependence on Re_ℓ, which is based on a length scale that is defined in terms of the integral length scale (Overholt & Pope 1996). Equation (5.43) provides the key for the explanation of the behaviour of C_0 shown in Fig. 5.4. The fluctuations u_i^{ac}, u_i^{an} and u_i^{st} may be seen as "degrees of freedom" which may store turbulent kinetic energy. In particular, u_i^{ac} and u_i^{an} may be seen as "internal degrees of freedom" which bind kinetic energy by the appearance of flow structures (variations of turbulence statistics and anisotropy). In flows where u_i^{ac} and u_i^{an} take part in the energy budget (the ETBL) one has low values of C_0 near 2 (the energy is distributed to all available degrees of freedom). In flows where u_i^{ac} and u_i^{an} do not contribute to the energy budget (HIST) one finds high values of C_0 because all the energy is bounded in stochastic motions (u_i^{st}). The neglect of u_i^{ac} and u_i^{an} contributions in models (which results in the SLM and DM) provides again higher values of C_0. The Reynolds number dependence of C_0 estimates agrees very well with Sawford's parametrization (5.11) provided the corresponding values for $C_0(\infty)$ are applied (the second term in the denominator of (5.11) is for $C_0(\infty) = 2.1$ about one order of magnitude smaller than for $C_0(\infty) = 6$). Regarding the ETBL, a model that predicts C_0 as independent of the Reynolds number (as the LM) has to be seen as a model that involves all relevant contributions to velocity fluctuations (model deficiencies do not have to be compensated by variations of C_0). This fact provides additional support for the suitability of the application of the LM for the calculation of C_0.

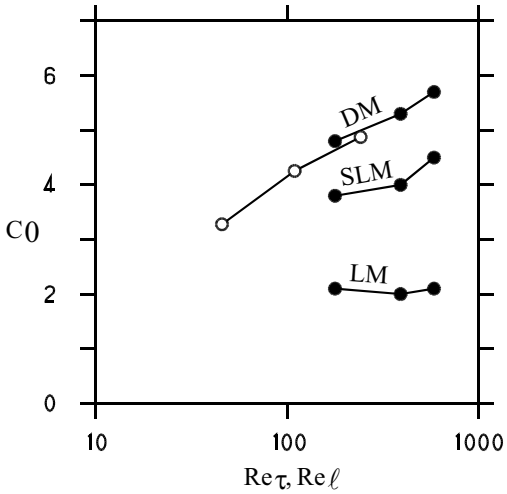

Fig. 5.4. The solid symbols are used to show the ETBL C_0 estimates related to the LM, SLM and DM according to the DNS data of Moser et al. (1999) in dependence on Re_τ. The open symbols show, according to the DNS data of Overholt & Pope (1996), the same C_0 data for HIST as given in Fig. 5.2, but now in dependence of Re_ℓ.

5.4.3. Landau's objection to universality

A relevant conclusion of these findings is that the Kolmogorov constant $C_0(\infty)$ is found to be non-universal: the use of the LM (or corresponding models) to the simulation of flows with a different relevance of u_i^{an} and u_i^{ac} (HIST and the ETBL) requires different C_0 values.

This result supports the objection of Landau to universality, see the detailed discussion of the ideas of Kolmogorov and Landau provided by Frisch (1995). Regarding the question about the universality of corresponding constants in the Eulerian velocity correlation (Pope 2000), Landau tried to show that these constants must depend on the detailed geometry of the production of turbulence. In particular, Landau and Lifshitz (1963, p. 126) state that the possibility exists in principle to obtain a universal formula for the relation of the corresponding instantaneous variables, i.e., if averaging is not involved. "When we average these expressions, however, an important part will be played by the law of variation of ε over times of the order of the periods of the large eddies, and this law is different for different flows. The result of averaging therefore cannot be universal." Contributions due to large-scale eddy motions are represented here by u_i^{ac} and u_i^{an}, which are found to be responsible for $C_0(\infty)$ variations. Therefore, the results presented here are fully consistent with the view of Landau and Lifshitz.

Nevertheless, it is worth noting that one finds relatively similar values near 2 for C_0 (which are hardly affected by Reynolds number effects) in many flows where all the "degrees of freedom" u_i^{ac}, u_i^{an} and u_i^{st} appear (Du et al. 1995; Dreeben & Pope 1997; Heinz, 1997, 1998a; Weinman & Klimenko 2000). This finding agrees very well with corresponding minor variations found for the Kolmogorov constant $C_K = 1.62 \pm 0.17$ (Sreenivasan 1995), which appears in the energy spectrum (4.86).

5.5. A hierarchy of stochastic models for scalars

The modeling of the dynamics of scalars will be addressed next. No attempt is made to compare a variety of existing scalar mixing models, which can be found elsewhere (Subramaniam & Pope 1998; Peters 2001), but the goal is a discussion of the hierarchical structure of scalar equations (which follows closely Heinz (2003a)) in analogy to the consideration of the hierarchical structure of velocity equations in section 5.1. This will be done again on the basis of the equations for the equilibrium dynamics of relevant variables presented in Appendix 3A. In this way, the attention is confined to the consideration of the transport of a passive, inert scalar in statistically homogeneous velocity and scalar fields. The more general case of scalar transport in inhomogeneous, nonstationary and anisotropic flows will be considered in section 5.7, where the modeling of compressible reacting flows is discussed.

5.5.1. The scalar dynamics

According to the structure of the equation (3A.31) for the equilibrium dynamics of relevant variables, the transport of a scalar Φ^* will be described by the equations

$$\frac{d\Phi^*}{dt} = \Psi^*, \tag{5.45a}$$

$$\frac{d\Psi^*}{dt} = -A\Psi^* - B\Phi^* + C\frac{dW}{dt}. \tag{5.45b}$$

Ψ^* refers to the scalar derivative, which is defined by (5.45a). A, B and C are any model parameters. dW / dt denotes one component of dW_i / dt that is given by (3.43a-b). The averages of Φ^* and Ψ^* have to be constant for the flow considered. For simplicity, they are set equal to zero.

Regarding the following explanations it is advantageous to rewrite the equations (5.45a-b) into a standardized form. For that, we introduce a characteristic scalar variance relaxation time scale τ_φ,

$$\frac{1}{\tau_\varphi} = -\frac{1}{2\overline{\Phi^{*2}}}\frac{d\overline{\Phi^{*2}}}{dt}. \tag{5.46}$$

Next, we define a dimensionless time scale $T = 2\int_0^t ds\, \tau_\varphi^{-1}$. The integration of the scalar variance equation (5.46) provides then the scalar variance as a function of T,

$$\overline{\Phi^{*2}} = \overline{\Phi^{*2}}(0)\, e^{-T}. \tag{5.47}$$

By adopting this relation, the scalar equations (5.45a-b) can be rewritten into

$$\frac{d\phi}{dT} = \psi, \tag{5.48a}$$

$$\frac{d\psi}{dT} = a\left\{ -\psi - b\phi + c\frac{dW}{dT} \right\}. \tag{5.48b}$$

The model parameters a, b and c and standardized scalar variables ϕ and ψ are defined in the following way,

$$a = \frac{1}{2}\left(\tau_\varphi A - \frac{d\tau_\varphi}{dt} \right) - 1, \qquad b = \frac{1}{4a}\left(\tau_\varphi{}^2 B - 2A + 1 \right), \qquad c = \frac{C}{a}\sqrt{\frac{\tau_\varphi}{2\overline{\Phi^{*2}}}},$$

$$\phi = \frac{\Phi^*}{\sqrt{\overline{\Phi^{*2}}}}, \qquad \psi = \frac{\Phi^* + \tau_\varphi \Psi^*}{2\sqrt{\overline{\Phi^{*2}}}}. \tag{5.49}$$

The transport equations for the variances $\overline{\phi\phi}$, $\overline{\phi\psi}$ and $\overline{\psi\psi}$ which are implied by (5.48a-b) can be obtained by rewriting these equations into the corresponding Fokker-Planck equation, multiplication with the corresponding variables and integration, see chapter 3. This leads to

$$0 = \overline{\phi\psi}, \tag{5.50a}$$

$$0 = \overline{\psi\psi} - a\,b, \tag{5.50b}$$

$$\frac{d\overline{\psi\psi}}{dT} = -2a\,\overline{\psi\psi} + a^2\overline{c^2}. \tag{5.50c}$$

Relation (5.50a) follows from the normalization $\overline{\phi\phi}$ = 1. Relation (5.50b) provides a constraint for the calculation of b in terms of model statistics such that only the coefficients a and c appear as independent model parameters. In particular, the standardized frequency a will be considered as a constant, but c has to be taken as a function of scalars, as explained in section 5.5.3.

5.5.2. A hierarchy of scalar equations

The consideration of the model (5.45a-b) in the standardized form (5.48a-b) simplifies the explanation of its physics. To do this, we rewrite (5.48a-b) into an equation for the scalar ϕ. First, we solve (5.48b) formally, which results in

$$\psi = -\int_0^T dT' \exp\{-a(T-T')\}\,\overline{\psi\psi}(T')\,\phi(T') + f(T). \tag{5.51}$$

To obtain (5.51), we applied $\psi(0) = 0$ to assure (5.50a), and we used (5.50b). The abbreviation f(T) is defined by

$$f(T) = a\int_0^T dT' \exp\{-a(T-T')\}\, c(T')\, \frac{dW}{dT'}(T'). \tag{5.52}$$

The function f(T) vanishes in the mean, and its correlation function is given according to (5.52) by

$$\overline{f(T)f(T')} = \overline{\psi\psi}(T') \exp\{-a(T-T')\}, \tag{5.53}$$

where $T \geq T'$ is assumed. The consistency of (5.53) at $T = T'$ is given by the fact that both sides vanish initially at $T = 0$ and satisfy the same transport equation. The use of (5.51) combined with (5.53) in (5.48a) results then in the following form of the scalar model (4.48a-b),

$$\frac{d\phi}{dT} = -\int_0^T dT' \, \overline{f(T)f(T')}\, \phi(T') + f(T), \tag{5.54a}$$

$$\frac{df}{dT} = -af + ac\frac{dW}{dT}, \tag{5.54b}$$

where (5.52) is differentiated to obtain equation (5.54b). To be consistent with (5.52), we have to demand that f(0) = 0. The model (5.54a-b) in conjunction with the specification of the coefficient c derived in section 5.5.3 will be referred to as "refined interaction by exchange with the mean" (RIEM) model (Heinz 2003a). It may be seen that the scalar equation (5.54a) is fully determined by the properties of the stochastic force f. According to (5.54b), which represents a specification of equation (3A.28), this stochastic force f simulates stochastic motions that appear randomly and disappear with a characteristic time scale a^{-1}.

Asymptotically, the RIEM model (5.54a-b) reduces to an extension of the often applied "interaction by exchange with the mean" (IEM) model. In the limit of a vanishing correlation time $a^{-1} \to 0$, the force f becomes delta-correlated,

$$\overline{f(T)f(T')} = \frac{2}{a}\overline{\psi\psi}(T')\, \delta(T-T') = \overline{c^2}(T)\, \delta(T-T'). \tag{5.55}$$

The last expression is found by adopting relation (5.50c) in the limit $a^{-1} \to 0$, which is equivalent to neglecting the derivative on the left-hand side. The use of (5.55) in (5.54a) leads then to

$$\frac{d\phi}{dT} = -\frac{\overline{c^2}}{2}\phi + c\frac{dW}{dT}. \tag{5.56}$$

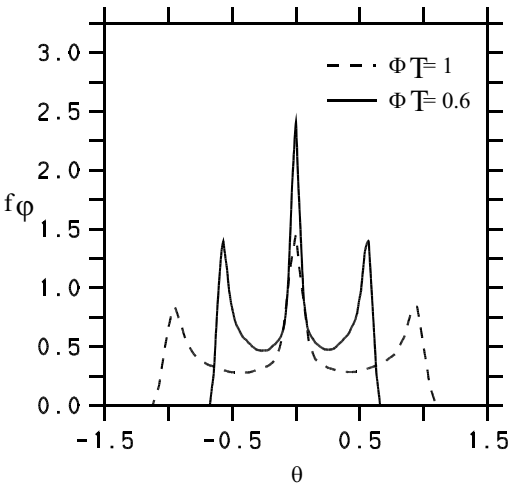

Fig. 5.5. The evolution of a scalar PDF, as predicted by the IEM model. The dashed line presents an initial ($\Phi_T = 1$) PDF of a (scalar-1) test case described in detail in section 5.5.4. The solid line presents the scalar PDF at a later time ($\Phi_T = 0.6$), which follows from the use of the IEM model (5.57).

The last contribution follows by taking (5.54b) in the limit $a^{-1} \to 0$ (the derivative of f vanishes). The model (5.56) generalizes the IEM model by the consideration of a nonzero c. This model will be referred to as "stochastic interaction by exchange with the mean" (SIEM) model.

The neglect of c in equation (5.56) finally recovers the IEM model, which is given by

$$\frac{d\phi}{dT} = 0. \tag{5.57}$$

The assumption (5.57) implies that information about the initial scalar PDF does not disappear in time, which is the well known drawback of the IEM model (Pope 1985). An example for the poor performance of the IEM model is given in Fig. 5.5. One observes that the scalar variance changes in time but the PDF structure never changes, which contradicts to corresponding DNS results presented in section 5.5.4.

5.5.3. The boundedness of scalars

An important property of scalars is their characteristic boundedness. Mass fractions for example are bounded by zero from below and unity from above. A weak formulation of the boundedness constraint is the following: if the initial and boundary values of a scalar lie within a certain range, then all the scalar values at later times have also to be within that range (Pope 2000, p. 21). A generalization of this constraint is that the convex region in the scalar sample space occupied by the scalar must decrease with time (Pope 2000, p. 554).

Whether the RIEM and SIEM models satisfy the boundedness constraint or not depends on the modeling of c: the application of a coefficient c that is independent

of the actual scalar value can result in the appearance of unphysical scalar values outside of bounds. The boundedness constraint could be satisfied within the frame of Fokker-Planck equations by adopting boundary conditions (Gardiner 1983; Risken 1984; Fox 1992, 1994). However, one may prove by means of the equations given above that this approach results in unphysical peaks of scalar PDFs near boundaries. Another way to guarantee the boundedness of scalar values consists in an appropriate specification of the coefficient c. This approach will be applied here.

We assume that c is nonzero only inside the lower and upper bounds, ϕ_- and ϕ_+, respectively, of the scalar space and given by the relation

$$c^2 = C_{\varphi 0}{}^* \left[(\phi - \phi_-)(\phi_+ - \phi) \right]^n . \tag{5.58}$$

$C_{\varphi 0}{}^*$ is a proportionality factor that will be calculated in section 5.5.4. The power n can be determined by means of the following arguments. One may easily check that the maximum of $c^2(\phi)$ is given by

$$c^2{}_{max} = C_{\varphi 0}{}^* \left[\frac{\phi_+ - \phi_-}{2} \right]^{2n} . \tag{5.59}$$

The asymptotic model (5.56) reveals that $\overline{cc}$ represents a scalar relaxation frequency. One has to expect this frequency as the sum of independent contributions related to lower and upper bounds. This implies n = 0.5 such that

$$c^2 = C_{\varphi 0}{}^* \sqrt{(\phi - \phi_-)(\phi_+ - \phi)} . \tag{5.60}$$

The remaining question is the modeling of the evolution of bounds ϕ_- and ϕ_+. They have to satisfy deterministic equations, which should be linear in ϕ_- and ϕ_+ according to the linear deterministic contributions in (5.48a-b). Thus, we postulate

$$\frac{d}{dT}\phi_+ = \lambda \phi_+ , \qquad \frac{d}{dT}\phi_- = \lambda \phi_- , \tag{5.61}$$

where λ is a constant that has to be determined. The integration of the relations (5.61) provides then

$$\phi_+(T) = \phi_+(0)\exp(\lambda T) , \qquad \phi_-(T) = \phi_-(0)\exp(\lambda T) . \tag{5.62}$$

The RIEM model (5.54a-b) combined with (5.58) and (5.62) guarantees the boundedness of scalars statistically: some scalar values may be found outside the bounds but the probability for such events is very small. This will be demonstrated by comparisons with DNS data in section 5.5.4.

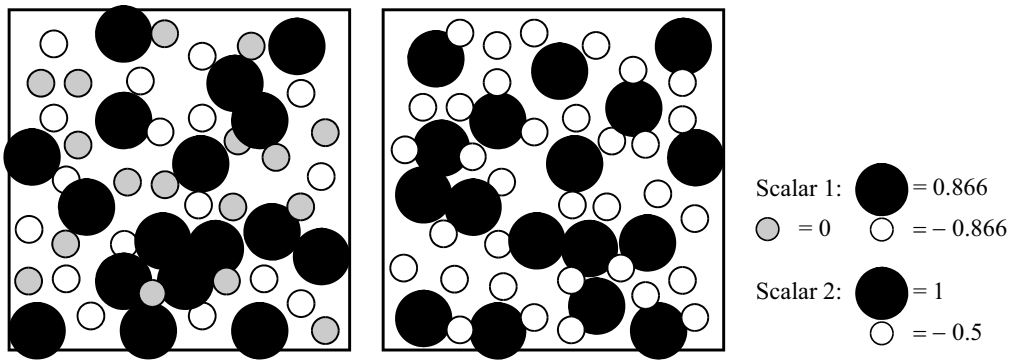

Fig. 5.6. An illustration of scalar PDFs. The left figure shows the initial scalar-1 PDF and the right figure the initial scalar-2 PDF according to (5.63). The different scalar values of fluid particles have a relative character. Regarding the scalar-1 PDF, they can be interpreted such that particles with the values (0.866; 0; – 0.866) have a maximum, middle or minimum value of any substance, respectively.

5.5.4. Comparisons with DNS

The RIEM model can be tested by the comparison of its predictions with the R92A-DNS data of scalar mixing in statistically stationary, homogeneous and isotropic turbulence obtained by Juneja and Pope (1996). The Taylor-scale Reynolds number is $Re_\lambda = 92$ in this simulation. Two initial PDFs $f_\varphi(\theta, t) = \overline{\delta(\Phi^*(t) - \theta)}$ were considered, which are close to

$$f_\varphi = \frac{1}{3}\begin{cases} \delta\left(\theta - \frac{1}{2}\sqrt{3}\right) + \delta\left(\theta + \frac{1}{2}\sqrt{3}\right) + \delta(\theta) & \text{(Scalar 1)} \\ \delta(\theta - 1) + 2\delta\left(\theta + \frac{1}{2}\right) & \text{(Scalar 2)} \end{cases} . \qquad (5.63)$$

The initial PDFs are illustrated in Fig. 5.6. The prediction of the evolution of these scalar fields is remarkably more challenging than previous comparisons with the DNS data of Eswaran & Pope (1988): the symmetric scalar-1 PDF contains modes which decay differently and the scalar-2 PDF is strongly asymmetric.

The PDF evolution was considered in terms of the normalized scalar variance $\Phi_T = e^{-T/2}$, see (5.47). The progress variable Φ_T is bounded, $0 \le \Phi_T \le 1$. The initial values for φ were chosen according to the DNS data for $\Phi_T = 1$. The ψ-values were set equal to zero initially to satisfy $\overline{\phi\psi} = 0$. The equations (5.48a-b) were solved numerically by adopting $5\ 10^5$ particles and a time step $dT = 0.002$. At the corresponding Φ_T, the scalar PDF $f_\varphi(\theta)$ was calculated where intervals $\Delta\theta = 0.025$ were applied to obtain the value of f_φ at θ. The parameters of the bound model (5.62) were found by means of the DNS-data,

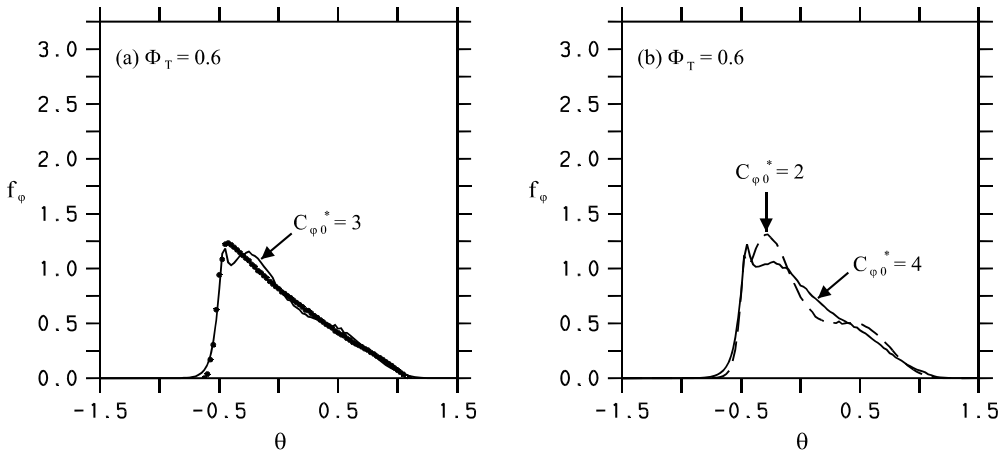

Fig 5.7. The RIEM model prediction (line) with $C_{\varphi 0}^* = 3$ is compared to Juneja and Pope's (1996) DNS data of the scalar-2 PDF (dots) at $\Phi_T = 0.6$ in (a). The effect of $C_{\varphi 0}^*$ variations is shown in (b).

$$\lambda = 0.3; \qquad \phi_-(0) = \begin{cases} -1.90 & \text{(Scalar 1)} \\ -0.93 & \text{(Scalar 2)} \end{cases}; \qquad \phi_+(0) = \begin{cases} 1.90 & \text{(Scalar 1)} \\ 2.08 & \text{(Scalar 2)} \end{cases}. \quad (5.64)$$

The parameters a and $C_{\varphi 0}^*$ were fitted to achieve the best agreement with the DNS data. The value a = 1 was found as an optimal value. Fig. 5.7a demonstrates the good performance of PDF simulations where $C_{\varphi 0}^* = 3$ was used. The effect of $C_{\varphi 0}^*$ variations is shown in Fig. 5.7b. Only the scalar-2 DNS data were used to determine the model parameters.

Figures 5.8 and 5.9 show that the results of these PDF simulations agree well with the corresponding DNS data. The most difficult task is the simulation of the nonequilibrium processes within the first stage of mixing, $0.7 \le \Phi_T \le 1$. The results of the PDF simulations are very similar here to the DNS data; there are only minor differences. The mixing processes may be seen to be in a near-equilibrium stage for $\Phi_T \le 0.6$, where $T > a^{-1} = 1$. Here, the RIEM model predicts approximately the same PDF as found by DNS. The relevance of memory effects can be assessed by a comparison with the performance of the SIEM model combined with a constant c. For the latter, one finds an optimal value c = 0.65, which provides the best agreement between model predictions and the scalar-2 DNS data at $\Phi_T = 0.6$. The resulting scalar PDF calculations are also shown in Figs. 5.8 and 5.9. These figures reveal significant deviations between the predictions of the RIEM and SIEM models in the early stage of mixing ($0.7 \le \Phi_T \le 1$). For $\Phi_T \le 0.6$, one finds that the predictions of both models are very similar, in particular for the scalar-1 case. This shows that memory effects are of minor relevance to this stage of mixing.

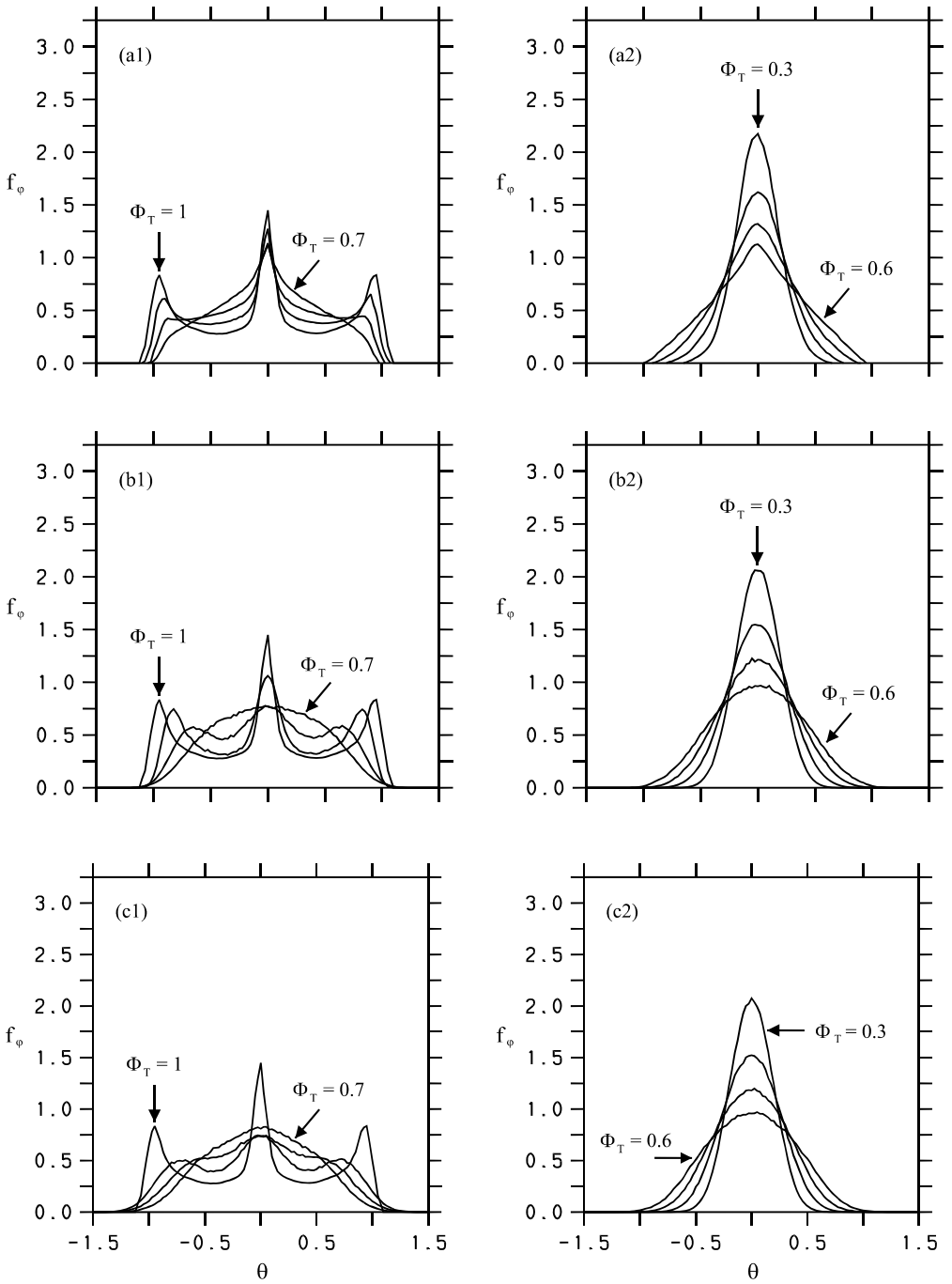

Fig. 5.8. The scalar-1 PDF evolution in statistically stationary, homogeneous and isotropic turbulence is given in (a1) and (a2) according to the DNS data of Juneja & Pope (1996). The corresponding predictions of the RIEM model are shown in (b1) and (b2), where $C_{\varphi 0}^{*} = 3$ is applied. The figures (c1) and (c2) show the predictions of the SIEM model (5.56) combined with c = 0.65.

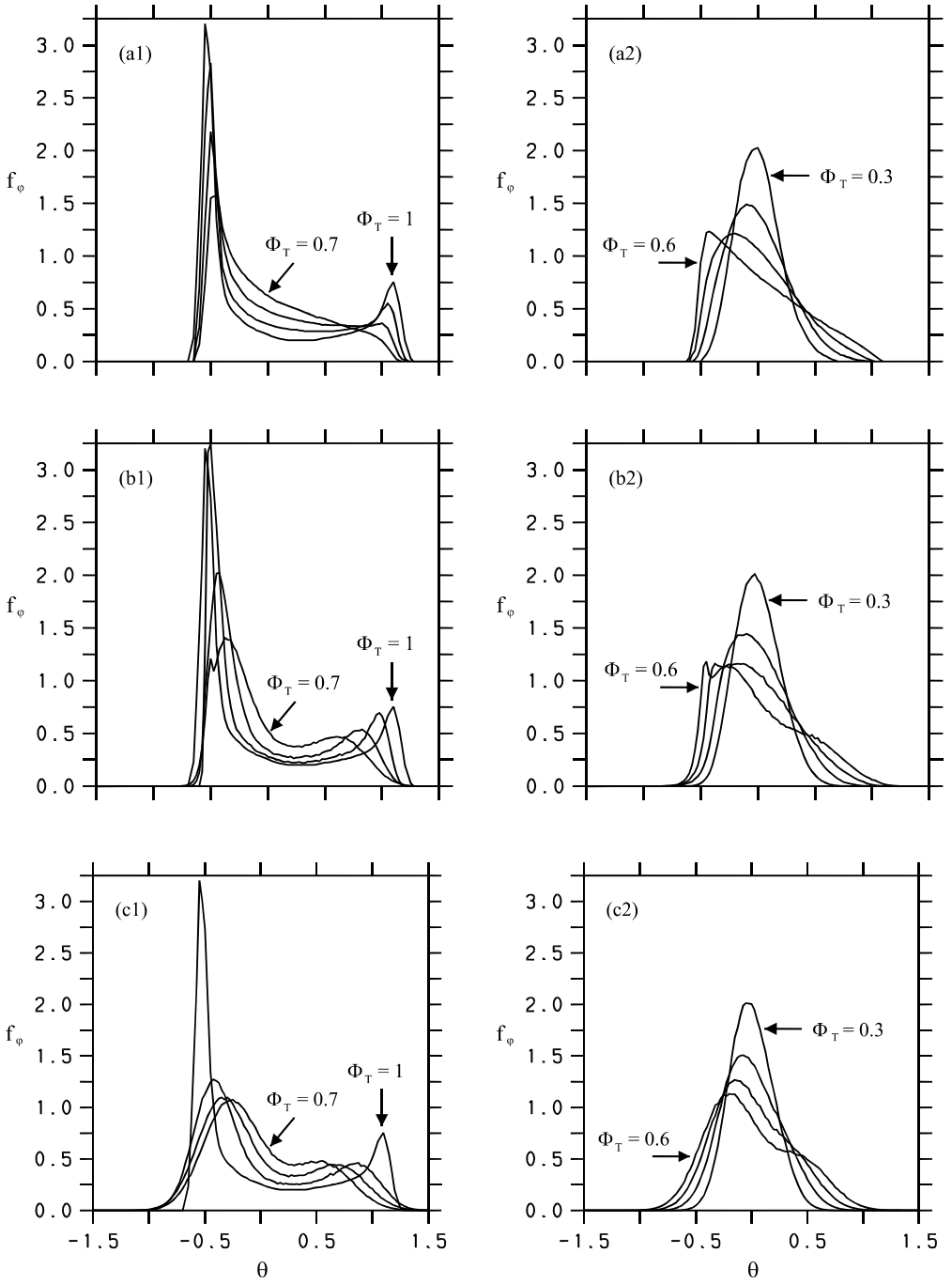

Fig. 5.9. The same comparison of predictions of the RIEM and SIEM models with DNS data as given in Fig. 5.8, but now regarding the scalar-2 PDF.

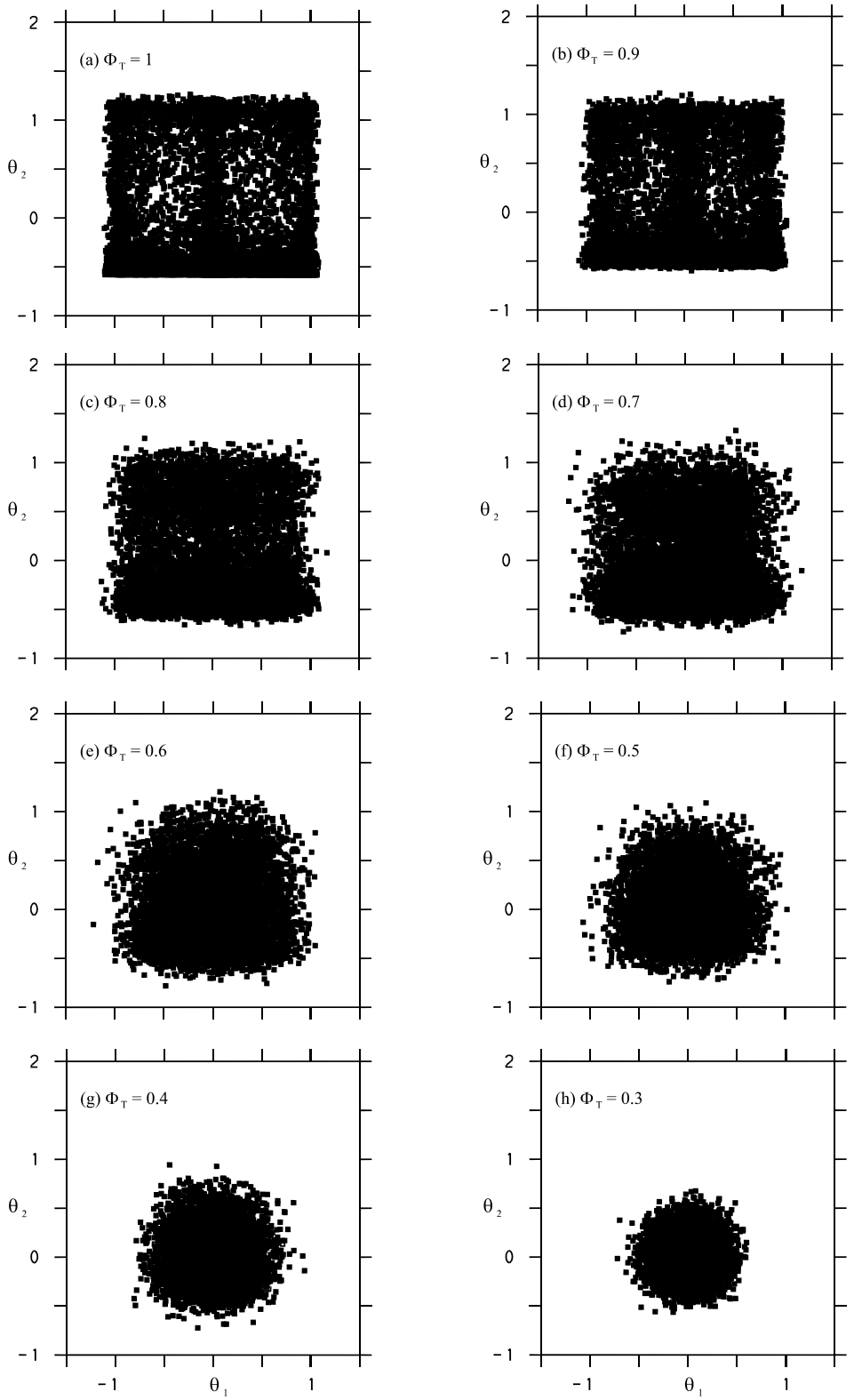

Fig. 5.10. The evolution of the joint PDF of both scalars.

Fig. 5.10 reveals that the joint scalar PDF predicted by the RIEM model satisfies the boundedness constraint: the convex region in sample space occupied by the scalars decreases with time. This simulation cannot be performed by using the same initial conditions as considered in the DNS of Juneja & Pope (1996) because a sufficiently accurate assignment between the scalar-1 and scalar-2 values cannot be established. Therefore, it is assumed that there is no assignment between these scalar values. This case enables the study of the transition of a rectangular initial joint PDF to a circular asymptotic joint PDF. This is very similar to the consideration of the transition from a triangular to a circular joint PDF, which was investigated by Juneja & Pope (1996). Within the first stage of mixing ($0.7 \leq \Phi_T \leq 1$), the form of the rectangular joint PDF is preserved. After a transitional stage ($0.3 \leq \Phi_T \leq 0.6$), the form of the joint PDF changes to a circular joint PDF. The latter characterizes a joint Gaussian PDF for the case considered that both scalars have about the same variance. These features of the RIEM model agree well with those observed by DNS. The DNS data show a somewhat slower decay of the initial joint PDF structure in the transitional stage, but such small differences have to be expected.

5.6. Compressible reacting flow: velocity models

In the previous sections of this chapter we discussed stochastic models for incompressible flows. However, the most essential advantage of the use of stochastic turbulence models is given by applying them to reacting flows, which are compressible in general. Thus, the question of how stochastic models for incompressible flows can to be extended to models for compressible flows will be considered next. The development of such simulation methods is highly relevant, for instance, to improve combustion engines (ramjet, scramjet, conventional gas turbine and internal combustion engines), see Lele (1994), Friedrich (1999), Adumitroaie et al. (1999) and Chassaing et al. (2002).

5.6.1. Compressibility effects on velocity fields

To prepare the consideration of stochastic velocity models for compressible flows in section 5.6.2, one needs to know which effects compressibility may have on velocity fields. Apart from the approximative treatment of compressibility effects in terms of the Boussinesq approximation (see the explanations given in section 4.4.6), such effects may be differentiated into two basic groups: dilatational and structural compressibility effects.

Dilatational compressibility effects are related to variations of the mean mass density (a nonzero mean dilatation $\overline{S}_{kk}$), or variations of the instantaneous mass density (nonzero dilatation fluctuations S_{kk}''). The mean dilatation $\overline{S}_{kk}$ controls for

instance temperature changes due to compression or expansion, see equation (4.72) for the temperature source rate S_T. As shown in section 4.4.5, $\overline{S}_{kk}$ effects scale with the squared Mach number. Dilatation fluctuations S_{kk}" imply a nonzero term Π_d in the turbulent kinetic energy equation (5.23), which is given by

$$\Pi_d = \overline{(p/\rho)"S_{kk}"}. \tag{5.65}$$

Further, dilatation fluctuations may cause an additional contribution to the dissipation rate ε. This quantity is assumed to be given by (Wilcox 1998)

$$\varepsilon = \varepsilon_s + \varepsilon_d, \tag{5.66}$$

where ε_s is the solenoidal dissipation (the incompressible part of the dissipation) and ε_d the dilatational dissipation (the part which is caused by compressibility). The latter quantity is proportional to the dilatation variance,

$$\varepsilon_d = \frac{4}{3}\overline{\nu}\,\overline{S_{kk}"S_{kk}"}. \tag{5.67}$$

Such S_{kk}" effects are assumed to scale with the turbulence Mach number (Wilcox 1998; Friedrich 1999; Chassaing et al. 2002)

$$M_t = \sqrt{\frac{2k}{\overline{a^2}}}, \tag{5.68}$$

where $\overline{a^2} = \overline{\gamma p/\rho} = \overline{\gamma RT}$ denotes the mass-weighted mean of the squared speed of sound and k the turbulent kinetic energy. Available experience seems to indicate that the influence of dilatational compressibility effects is small in flows that do not involve shocks (which may be produced by sharp-edged obstacles as they often appear in technological applications, see Fig. 5.11 for an illustration). $\overline{S}_{kk}$, ε_d and Π_d are negligibly small, in particular in wall-bounded supersonic flows (Friedrich & Bertolotti 1997; Friedrich 1999; Freund 1997; Freund et al. 2000a-b). Only in homogeneous shear flows ($\overline{S}_{kk}$ = 0), where the turbulent kinetic energy constantly grows, does one find small additional contributions near 9-12% due to ε_d and Π_d (Blaisdell et al. 1993; Sarkar 1995). However, dilatational compressibility effects may be much more important in flows that involve shocks, but clear evidence for this is unavailable at present (Friedrich & Bertolotti 1997).

In contrast to dilatational effects, structural compressibility effects may have a significant influence on the structure of turbulent flows (Sarkar 1995; Pantano & Sarkar 2002). To study these effects, one needs a parameter that measures the strength of compressibility. With regard to compressible turbulent shear flow, Sarkar (1995) suggested the use of the gradient Mach number M_g for this, which is defined by

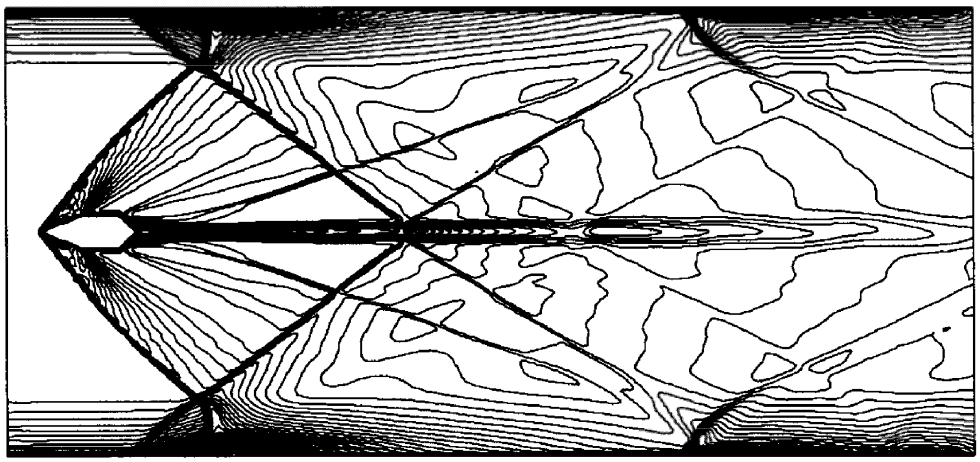

Fig. 5.11. Isolines of the mean streamwise velocity $\overline{U}_1$, which were calculated by means of FLUENT (2003), for a flow around a pylon (the sharp-edged obstacle in the center). The domain considered is 55 mm (x_1-direction) $*$ 27.5 mm (x_2-direction). $\overline{U}_1 \approx 1120$ m / s in front of the pylon. The interaction of the flow with the pylon leads to the appearance of a shock, which decelerates the flow ($\overline{U}_1 \approx 700$ m / s in the area near the pylon behind the shock). The shock is then reflected at the wall, which results in the appearance of a shock system. Near the boundaries one observes complex shock-boundary layer interactions.

$$M_g = \frac{S\ell_{12}}{\sqrt{\overline{a^2}}}. \tag{5.69}$$

$S = \partial \overline{U}_1 / \partial x_2$ is a constant shear rate, see section 5.3, and ℓ_{12} is the correlation length of u_1-fluctuations in the direction of shear x_2,

$$\ell_{12} = \frac{1}{\overline{u_1(x_2)\, u_1(x_2)}} \int dr_2 \; \overline{u_1(x_2 + r_2)\, u_1(x_2)}. \tag{5.70}$$

Obviously, the structure of M_g is similar to that of M_t, but there is an essential difference: ℓ_{12} is bounded from above since $\ell_{12} \le L_0$, where L_0 is the extension of the domain considered in the direction of shear. Accordingly, Sarkar (1995) found in his compressible turbulent shear flow DNS that ℓ_{12} evolves in time from a small value (corresponding to an approximately laminar state with $Re_\lambda = 14$) to an equilibrium value (where $Re_\lambda \approx 40$) of order L_0. As a consequence of this behaviour of ℓ_{12}, M_g shows a trend to become asymptotically constant, such that M_g can be used to characterize the asymptotic state of the flow. In contrast to this, M_t seems constantly to grow, which does not provide support for the assumption that the asymptotic state of the flow is controlled by M_t.

Variances	Production-to-dissipation ratio
$\frac{\overline{u_1u_1}}{2k} = 1 - 0.40\exp(-0.3\,M_g) \pm 0.01$	$\frac{\varepsilon_s}{P} = 0.52 \pm 0.04$
$\frac{\overline{u_2u_2}}{2k} = 0.17\exp(-0.3\,M_g) \pm 0.01$	$\frac{\varepsilon_s}{P} + \frac{\varepsilon_d}{P} - \frac{\Pi_d}{<\rho>P} = 0.64 \pm 0.02$
$\frac{\overline{u_1u_2}}{2k} = -0.17\exp(-0.2\,M_g) \pm 0.005$	

Table 5.4. The asymptotic statistics of Sarkar's (1995) A1-A4 compressible turbulent shear flow DNS in dependence on the gradient Mach number M_g. The Taylor-scale Reynolds number $Re_\lambda \approx 40$. The analytical variance profiles given here present fitting curves to the corresponding DNS data points, see Fig. 5.12.

Typical asymptotic features of Sarkar's (1995) compressible turbulent shear flow DNS are presented in Table 5.4. Contributions related to ε_d and $\Pi_d / <\rho>$ are not separately given in this way. However, according to Blaisdell et al. (1993), one knows that ε_d and $-\Pi_d / <\rho>$ affect the production of k in the same direction and approximately by the same amount. According to the data given in Table 5.4, one may conclude then that $\varepsilon_d / P \approx 0.06$, which implies $\varepsilon_d / \varepsilon_s \approx 0.12$ and $P / \varepsilon \approx 1.72$. By adopting $P = -S\,\overline{u_1u_2}$, see section 5.3, we find for the production and dissipation normalized to the characteristic shear flow parameters k and S

$$\frac{P}{Sk} = -\frac{\overline{u_1u_2}}{k} = 0.34\exp(-0.2\,M_g), \tag{5.71a}$$

$$\frac{\varepsilon}{Sk} = -\frac{\varepsilon}{P}\frac{\overline{u_1u_2}}{k} = 0.20\exp(-0.2\,M_g). \tag{5.71b}$$

Thus, the production-to-dissipation ratio P / ε remains approximately unaffected by M_g, but both P and ε vanish with growing compressibility. In particular, we see that the mixing frequency $(S\,\tau)^{-1} = \varepsilon / (S\,k)$ vanishes according to equation (5.71b). This implies that the redistribution of turbulent kinetic energy is strongly reduced, such that the features presented in Fig. 5.12 are found (Sarkar 1995): the turbulence in the x_2- and x_3-directions vanishes and all the turbulent kinetic energy is directed into the streamwise direction x_1. Hence, the shear stress $\overline{u_1u_2}$ must also vanish then with growing M_g. According to the relations (5.71a-b), the $\overline{u_1u_2}$-curve shown in Fig. 5.12 describes the $P / (S\,k)$ and $\varepsilon / (S\,k)$ variation with M_g.

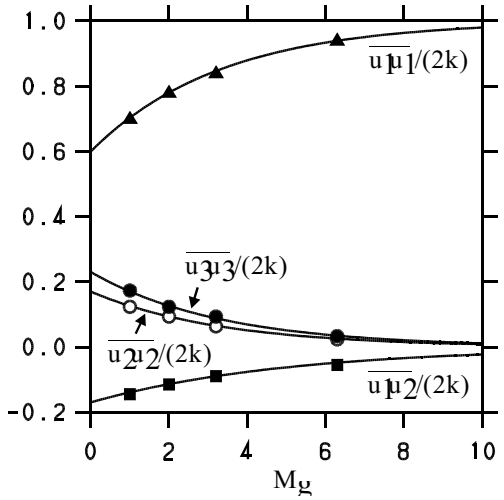

Fig. 5.12. The symbols present the normalized asymptotic variances of Sarkar's (1995) compressible shear flow DNS in dependence on the gradient Mach number M_g. The solid lines present corresponding fitting curves that are given in Table 5.4.

The gradient Mach number M_g was introduced above as an appropriate parameter to assess the relevance of structural compressibility effects - but which characteristic flow properties are controlled by M_g? The answer to this question is not as obvious as given, for example, in the case of the gradient Richardson number Ri, which controls the thermal stability of a flow. According to Table 5.4, M_g may be seen as a measure for $\overline{u_1u_1}\ /\ (2\ k)$. By introducing $r_{32} = \overline{u_3u_3}\ /\ \overline{u_2u_2}$ and taking reference to the fact that the normalized diagonal elements of the variance matrix sum to unity, $\overline{u_2u_2}$ and $\overline{u_3u_3}$ are related to $\overline{u_1u_1}\ /\ (2\ k)$ by

$$\frac{\overline{u_2u_2}}{2k} = \frac{1}{1+r_{32}}\left(1-\frac{\overline{u_1u_1}}{2k}\right), \qquad \frac{\overline{u_3u_3}}{2k} = \frac{r_{32}}{1+r_{32}}\left(1-\frac{\overline{u_1u_1}}{2k}\right). \tag{5.72}$$

The data given in Table 5.4 reveal that $r_{32} = 1.35$ independent of M_g. Hence, the diagonal elements of $\overline{u_iu_k}\ /\ (2\ k)$ are controlled by $\overline{u_1u_1}\ /\ (2\ k)$, which is uniquely related to M_g. Correspondingly, the physical meaning of M_g is that it represents, for the flow considered, a unique measure for the spatial distribution of turbulence (the diagonal elements of $\overline{u_iu_k}\ /\ (2\ k)$).

5.6.2. Stochastic velocity models

Next, we address the question of how modifications of turbulence structures which are caused by compressibility can be explained in terms of a stochastic velocity model. In particular, this question will only be addressed with regard to the incorporation of structural compressibility effects. Unfortunately, mainly due to the unavailability of suitable DNS data, one can only speculate at present about the structure of stochastic dilatation equations and their coupling to velocity models (Kollmann 1990; Eifler & Kollmann 1993).

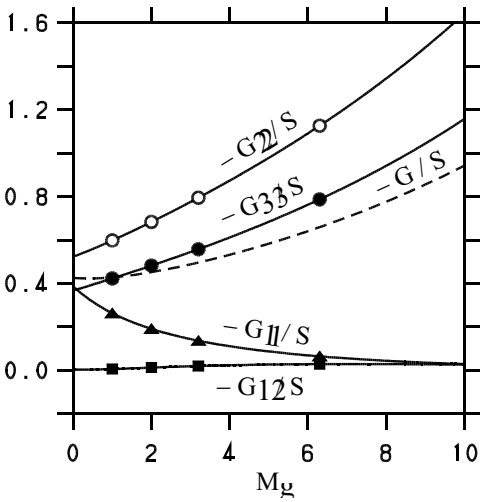

Fig. 5.13. The ELM coefficients normalized to S are shown in dependence on M_g. For this, (5.30a-c) and (5.31) are used. The required data are taken from Table 5.4, and $C_0 = 2.0$ is used according to the results given in section 5.4. The symbols present the data points according to Sarkar's (1995) DNS data. The dashed line shows $-G / S = -(G_{11} + G_{22} + G_{33}) / (3\,S)$ for a comparison.

A stochastic model for compressible flows without shocks (where dilatational compressibility effects are negligible) can be developed by the calculation of the coefficients G_{ij} of the GLM (5.17a-b). One should expect that C_0, which controls the stochastic forcing, is independent of M_g (such a dependence would mean that C_0 depends for instance on the extension L_0 of the domain considered, see section 5.6.1). Therefore, we will apply the ELM introduced in section 5.3.1. This model is characterized by a unique relationship between its coefficients and Reynolds stresses while C_0 is left unconstrained.

The results are shown in Fig. 5.13, where the flow statistics presented in Table 5.4 and $C_0 = 2.0$ (see section 5.4) are applied to calculate the coefficients G_{ij} according to (5.30a-c) and (5.31). For an incompressible flow ($M_g = 0$), the coefficients G_{11}, G_{22} and G_{33} have comparable values (G_{11}, G_{22}, G_{33}) = – (0.39, 0.52, 0.37) S. However, with growing compressibility they show a different behaviour: G_{11} vanishes whereas G_{22} and G_{33} go to minus infinity (in a ratio $G_{33} / G_{22} = 0.7$, the deviations from this value are below 1%). A relevant finding is that G_{12} obviously vanishes (its maximum is $G_{12} = -0.029$ S). This behaviour is fully consistent with the explanations given in sections 5.2 and 5.3: the LM, where only the diagonal components of G_{ik} are nonzero, represents a sufficiently general model with regard to the flow considered. It is worth noting that the suitability of the LM also provides further evidence for the suitability of the value chosen for C_0 here since C_0 is constrained by the LM, see section 5.2.

Compared to existing methods, one has to conclude that a reduction of the ELM to the SLM with an isotropic coefficient matrix $G_{ik} = G\,\delta_{ik}$ does not enable accurate simulations of compressible flows in general. As may be seen in Fig. 5.13, the approximation $G_{ik} = G\,\delta_{ik}$ is related to significant errors regarding the modeling of G_{22} and G_{33}, and a qualitatively wrong behaviour of G_{11}.

As shown above, one question related to the use of stochastic equations for velocities is a proper consideration of dilatational and structural compressibility effects. Another problem concerns the numerical solution of these equations. The most natural way to solve such equations is their self-consistent solution. This is realized in the PDF2DV code where mean fields are derived from particle properties (Pope 1994b; Delarue & Pope 1997, 1998). However, the use of mean particle velocities as flow velocities in particle equations has been found to lead to substantial deterministic errors (Muradoglu et al. 1999). A way that has recently been proved to be superior to the stand-alone particle method realized in PDF2DV is the solution of stochastic equations in such a way that mean fields and fluctuations are calculated consistently by finite-volume and particle methods, respectively (Muradoglu et al. 1999; Muradoglu et al. 2001; Jenny et al. 2001a-b). However, this development required the assumption of small Mach numbers (Muradoglu et al. 2001). One of the problems related to the extension of the latter numerical method to compressible flows that involve shocks is to treat shock-turbulence interactions sufficiently accurate.

5.6.3. Deterministic velocity models: the k-ε model

A way to avoid these problems is the reduction of stochastic equations to deterministic equations for mean velocities. The advantage of this approach is that (presently unknown) details of stochastic velocity equations for compressible flows that involve shocks do not have to be specified. Further, one avoids the numerical solution of such stochastic equations, such that well-developed methodologies for the solution of mean velocity equations (e.g., existing shock-capturing techniques) can be used.

The basic problem that has to be solved in order to close the mean velocity equation (4.95b) is the derivation of a model for the Reynolds stresses $\widetilde{u_i u_k}$. These quantities are determined by their transport equation (5.21) combined with a suitable model for triple correlations (in correspondence to (5.81)). However, it will be shown in section 5.7 that the decoupling of stochastic velocity and scalar equations, which is performed by the reduction of stochastic velocity equations to equations for mean velocities, implies an algebraic model for the turbulent scalar fluxes. In consistency with that, we look for an algebraic model for $\widetilde{u_i u_k}$. This is given by the rewritten equation (5.26)

$$\left(\frac{P}{\varepsilon}-1+\frac{\Pi_d}{\langle\rho\rangle\varepsilon}\right)a_{ij}=\frac{\widetilde{u_k u_j}}{2k}\tau\left(G_{ik}-\frac{\partial\widetilde{U}_i}{\partial x_k}\right)+\frac{\widetilde{u_k u_i}}{2k}\tau\left(G_{jk}-\frac{\partial\widetilde{U}_j}{\partial x_k}\right)-$$

$$-\frac{\widetilde{u_k u_n}}{3k}\tau\left(G_{nk}-\frac{\partial\widetilde{U}_n}{\partial x_k}\right)\delta_{ij}, \qquad (5.73)$$

where (5.24) is applied to replace C_0. This algebraic equation for $\overline{u_i u_k}$ can be solved exactly (Pope 1975; Gatski & Speziale 1993), but one obtains complicated functions of growing order in shear (velocity gradients) in this way, see chapter 6. In the first order of approximation, the solution to equation (5.73) is given by replacing the variances in the production terms (the terms multiplied by velocity gradients) by their isotropic parts,

$$\left(\frac{P}{\varepsilon}-1+\frac{\Pi_d}{\langle\rho\rangle\varepsilon}\right)a_{ij}=\frac{\overline{u_k u_j}}{2k}\tau\,G_{ik}+\frac{\overline{u_k u_i}}{2k}\tau\,G_{jk}-\frac{\overline{u_k u_n}}{3k}\tau\,G_{nk}\delta_{ij}-\frac{2}{3}\tau\overline{S}_{ij}^{\,d}, \qquad (5.74)$$

where the deviatoric part S_{ij}^{d} of the rate-of-strain tensor is given by (4.20). The Reynolds stresses then depend on the specification of G_{ij}. In accord with the isotropization of variances in the production terms of (5.73), we consider G_{ij} as isotropic, $G_{ij} = G\,\delta_{ij}$. The suitability of this assumption will be discussed below. In this case, relation (5.74) reduces to

$$a_{ij}=-C_\mu\tau\overline{S}_{ij}^{\,d}, \qquad (5.75)$$

where the parameter C_μ is introduced, which is given by

$$C_\mu=\frac{2}{3}\left(\frac{P}{\varepsilon}-1+\frac{\Pi_d}{\langle\rho\rangle\varepsilon}-2\tau\,G\right)^{-1}. \qquad (5.76)$$

The most convenient way to determine C_μ is to assure that the production P in the turbulent kinetic energy equation is correctly represented. Regarding the shear flow considered in section 5.6.1, this corresponds to the following relation for C_μ,

$$C_\mu=4\frac{a_{12}^{\,2}}{P/\varepsilon}=0.07\exp(-0.4\,M_g). \qquad (5.77)$$

The values of C_μ are presented in Fig. 5.14 according to Sarkar's (1995) DNS data. The value $C_\mu = 0.07$, which follows from the extrapolation of these DNS data to the limit $M_g = 0$, is comparable to the standard value $C_\mu = 0.09$, which follows for an equilibrium turbulent boundary layer by adopting $P / \varepsilon = 1$ and $a_{12} = -0.15$ (Pope 2000). The difference between these values $C_\mu = 0.07$ and $C_\mu = 0.09$ may be caused by Reynolds number effects. The most relevant finding presented in Fig. 5.14 is the significant reduction of C_μ due to compressibility, which assures the corresponding reduction of the production. This fact reveals that the approximation $G_{ij} = G\,\delta_{ij}$ that is used to calculate the anisotropy tensor a_{ij} differs significantly from the use of the SLM in stochastic equations for velocities. It was pointed out above that the latter neglects structural compressibility effects, whereas these effects are involved by adopting $G_{ij} = G\,\delta_{ij}$ at the level of Reynolds stress models.

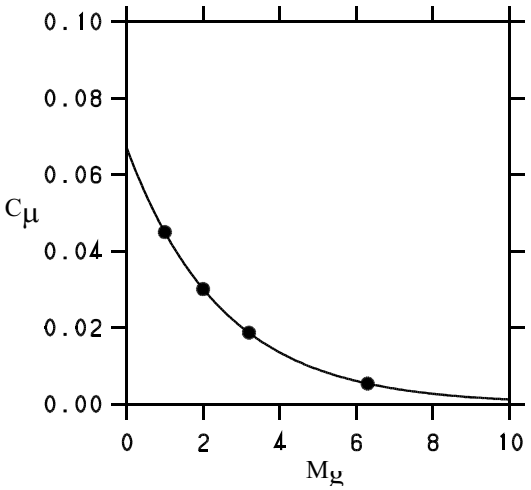

Fig 5.14. The solid line presents C_μ in dependence on the gradient Mach number M_g according to (5.77). The data for this are taken from Table 5.4. The symbols give the corresponding DNS data of Sarkar (1995).

Nevertheless, it is obvious that the model (5.75) is not very accurate in general: the energy transport may be treated conveniently by adopting it, but the values of a_{ij} are often inaccurately represented. However, it is worth emphasizing that the latter is not a necessary condition to perform flow computations successfully: only the gradients of Reynolds stresses enter the mean velocity equation (4.95b), and a correct treatment of the energy transport is the most essential requirement. Therefore, the approximation (5.75) is widely used, see for instance Wilcox (1998), Pope (2000) and Durbin & Petterson (2001).

To apply (5.74) in the mean velocity equation (4.95b), one has to rewrite it into a relation for the Reynolds stresses,

$$\overline{u_i u_j} - \frac{2k}{3}\delta_{ij} = -2\nu_T \overline{S}_{ij}^{\,d}, \tag{5.78}$$

where the turbulent viscosity ν_T is defined by

$$\nu_T = C_\mu k \tau. \tag{5.79}$$

Expression (5.78) shows that one still needs the turbulent kinetic energy k and dissipation rate $\varepsilon = k / \tau$ in order to close this model for the Reynolds stresses. The turbulent kinetic energy k is determined by its transport equation (5.23), where the production term P and triple correlation term appear as unknowns. P can be closed by means of (5.78),

$$P = -\overline{u_k u_i}\frac{\partial \overline{U}_i}{\partial x_k} = -\frac{2}{3}k\,\overline{S}_{nn} + 2\nu_T \overline{S}_{ki}^{\,d}\overline{S}_{ik}^{\,d}. \tag{5.80}$$

The triple correlation term can be obtained analogously to the heat flux calculation in section 4.3.2 (one just has to reinterpret the variables). This leads to

$$\frac{1}{2}\overline{u_i u_n u_n} = -\frac{\nu_T}{Pr_k}\frac{\partial k}{\partial x_i}, \tag{5.81}$$

where the Prandtl number Pr_k in the energy equation is introduced by

$$Pr_k = -\frac{27 C_\mu G\tau}{10} = \frac{9}{10}\left(1 + \frac{3C_\mu}{2}\left[1 - \frac{P}{\varepsilon} - \frac{\Pi_d}{\langle\rho\rangle\varepsilon}\right]\right). \tag{5.82}$$

Hence, in correspondence to (4.38), $Pr_k = 0.9$ for an incompressible equilibrium flow. Obviously, the finding (5.82) agrees well with the use of the standard value $Pr_k = 1.0$ (Wilcox 1998). The application of (5.80) and (5.81) in (5.23) for the turbulent kinetic energy k results then in

$$\frac{\partial k}{\partial t} + \overline{U}_k\frac{\partial k}{\partial x_k} = \frac{1}{\langle\rho\rangle}\frac{\partial}{\partial x_k}\langle\rho\rangle\frac{\nu_T}{Pr_k}\frac{\partial k}{\partial x_k} + 2C_\mu\frac{k^2}{\varepsilon}\overline{S}_{ki}{}^d\overline{S}_{ik}{}^d - \varepsilon + \frac{\Pi_d}{\langle\rho\rangle} - \frac{2}{3}k\overline{S}_{nn}. \tag{5.83}$$

The transport equation for ε can be constructed in a formal correspondence to the turbulent kinetic energy equation. By replacing k by ε in the transport terms of (5.83) and multiplying the source terms (the last four terms) with ε / k, one finds

$$\frac{\partial \varepsilon}{\partial t} + \overline{U}_k\frac{\partial \varepsilon}{\partial x_k} = \frac{1}{\langle\rho\rangle}\frac{\partial}{\partial x_k}\langle\rho\rangle\frac{\nu_T}{Pr_\varepsilon}\frac{\partial \varepsilon}{\partial x_k} + 2C_{\varepsilon1}C_\mu k\overline{S}_{ki}{}^d\overline{S}_{ik}{}^d - C_{\varepsilon2}\frac{\varepsilon^2}{k} + C_{\varepsilon3}\frac{\Pi_d\varepsilon}{\langle\rho\rangle k} -$$

$$-\frac{2}{3}C_{\varepsilon4}\varepsilon\overline{S}_{nn}, \tag{5.84}$$

where several new constants are introduced in order to handle this approach in a more flexible way. With regard to Pr_ε, $C_{\varepsilon1}$ and $C_{\varepsilon2}$, one applies the standard values (Pr_ε, $C_{\varepsilon1}$, $C_{\varepsilon2}$) = (1.3, 1.44, 1.92), see for instance Wilcox (1998), Pope (2000) and Durbin & Petterson (2001). For $C_{\varepsilon3}$ and $C_{\varepsilon4}$ related to compressibility effects, one uses ($C_{\varepsilon3}$, $C_{\varepsilon4}$) = (1.0, $C_{\varepsilon1}$ + 1.5), but there is no general agreement regarding the suitability of these choices (Chassaing et al. 2002). An alternative is to split ε according to (5.66) into solenoidal and dilatational contributions in (5.83), and to use the incompressible version of equation (5.84) for the calculation of the solenoidal dissipation ε_s. The dilatational dissipation can be parametrized as described by Wilcox (1998) and Chassaing et al. (2002).

The equations (5.83) and (5.84) differ from standard methods (Wilcox 1998) by the neglect of the viscous transport term. The latter may be involved by adding the mean viscosity $\overline{\nu}$ to ν_T / Pr_k and ν_T / Pr_ε, respectively. The inclusion of buoyancy effects in (5.83) and (5.84) will be pointed out next.

5.6.4. The inclusion of buoyancy effects

The approximative treatment of compressibility effects in terms of the Boussinesq approximation is often very helpful, in particular regarding the simulation of environmental flows. To involve buoyancy effects in (5.83) and (5.84), one has to add terms B and $C_{\varepsilon 5}$ B on the right-hand sides of these equations, respectively. By adopting a body force F_i on the right-hand side of the GLM (5.17b) and repeating the derivation of the turbulent kinetic energy equation, one may prove that $B = \overline{F_k'' u_k}$. Due to the fact that there is currently no agreement regarding the choice of the parameter $C_{\varepsilon 5}$ that controls the buoyancy term $C_{\varepsilon 5}$ B in the dissipation equation, this coefficient will be estimated here.

According to the Boussinesq approximation pointed out in section 4.4.6, we have $F_i = \beta\, g\, T''\, \delta_{i3}$, such that $B = \beta\, g\, \overline{T'' u_3}$. Here, x_3 is chosen in the direction of gravity, β is the thermal expansion exponent and g the acceleration due to gravity. As pointed out in detail in Appendix 6B, the heat flux can be parametrized by

$$\overline{T'' u_3} = -K_{3n} \frac{\partial \overline{T}}{\partial x_n}. \tag{5.85}$$

The use of (5.97) for K_{ij} in this expression leads then to the result

$$B = -\frac{\nu_T}{Sc_t} |\overline{S}|^2 \, Ri. \tag{5.86}$$

$|\overline{S}| = (2\overline{S}_{kn}\overline{S}_{nk})^{1/2}$ is a characteristic strain rate, $Ri = \beta\, g\, |\overline{S}|^{-2}\, \partial \overline{T} / \partial x_3$ the gradient Richardson number, and Sc_t is the turbulence Schmidt number, see (5.98).

To calculate the coefficient $C_{\varepsilon 5}$, we consider a homogeneous stratified shear flow with a constant shear rate $|\overline{S}| = S$. For that case, (5.83) and (5.84) reduce to

$$\frac{dk}{dt} = \frac{k}{\tau}\left[\left(1 - \frac{Ri}{Sc_t}\right) C_\mu \tau^2 S^2 - 1\right] = \frac{k}{\tau}\left[\frac{P}{\varepsilon} - 1\right], \tag{5.87a}$$

$$\frac{d\varepsilon}{dt} = \frac{\varepsilon}{\tau}\left[\left(C_{\varepsilon 1} - C_{\varepsilon 5}\frac{Ri}{Sc_t}\right) C_\mu \tau^2 S^2 - C_{\varepsilon 2}\right]. \tag{5.87b}$$

The dimensionless quantities P / ε and τS inside the brackets become stationary, as all the other flow statistics that are standardized by means of the imposed constant shear S and turbulent kinetic energy k(t). This stationary values of P / ε and τS are then given as functions of the constant gradient Richardson number Ri,

$$\frac{P}{\varepsilon} = \frac{(C_{\varepsilon 2} - 1)(1 - Ri / Sc_t)}{C_{\varepsilon 1} - 1 + (1 - C_{\varepsilon 5})\, Ri / Sc_t}, \tag{5.88a}$$

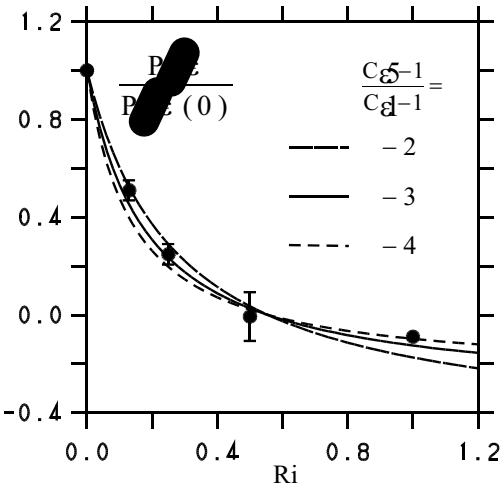

Fig 5.15. The normalized production-to-dissipation ratio P / ε according to (5.88a) for different $C_{\varepsilon 5}$. The symbols present the corresponding DNS data of Kaltenbach et al. (1994). The error bars denote the accuracy of these values (the accuracy of the value at Ri = 1 cannot be assessed). Ri refers to the gradient Richardson number.

$$\tau S = \sqrt{\frac{C_{\varepsilon 2} - 1}{C_\mu \left(C_{\varepsilon 1} - 1 + (1 - C_{\varepsilon 5}) \mathrm{Ri} / \mathrm{Sc}_t \right)}}. \tag{5.88b}$$

To assess such Ri effects, there are DNS and LES data available (Gerz et al. 1989; Kaltenbach et al. 1994). These data basically agree for weakly and moderately stratified flows ($0 < \mathrm{Ri} < 0.5$). However, for strongly stratified flows ($\mathrm{Ri} > 0.5$) one observes significant differences, for instance regarding the variation of P / ε with Ri (Gerz et al. 1989; Kaltenbach et al. 1994). The authors state that a severe limitation of LES is given by the fact that vertical turbulent diffusivities become smaller than the molecular or subgrid scale diffusivity when the gradient Richardson number Ri exceeds 0.5 in the LES (Kaltenbach et al. 1994). Thus, the 96^3 DNS data of Kaltenbach et al. are used here to assess the Ri variation of P / ε (corresponding τ S data are unavailable). The predictions of (5.88a) are compared to these DNS data in Fig. 5.15 for different $C_{\varepsilon 5}$. For Sc_t, we used $\mathrm{Sc}_t = 5 / 9$, see (5.98). We see that the model predictions provide for $C_{\varepsilon 5} = 5 - 3\, C_{\varepsilon 1}$ the best agreement with the DNS data. The small differences for a very strong stratification (Ri = 1) may be attributed to the significant variations of the DNS data in time. The characteristic gradient Richardson number Ri_c which determines a local equilibrium P = ε is given according to (5.88a) by

$$\mathrm{Ri}_c = \mathrm{Sc}_t \frac{C_{\varepsilon 2} - C_{\varepsilon 1}}{C_{\varepsilon 2} - C_{\varepsilon 5}}. \tag{5.89}$$

The application of $C_{\varepsilon 1} = 1.56$ and $C_{\varepsilon 2} = 1.9$ for a homogeneous shear flow at Ri = 0 (Pope 1994a) in conjunction with $C_{\varepsilon 5} = 5 - 3\, C_{\varepsilon 1}$ implies then $\mathrm{Ri}_c = 0.07$. This value is also in accord with DNS data (Gerz et al. 1989; Kaltenbach et al. 1994).

5.7. Compressible reacting flow: scalar models

The consideration of stochastic velocity models for compressible reacting flows in section 5.6 will be complemented now by a discussion of the inclusion of scalar models. This will be done on the basis of the explanations given in section 5.5.

5.7.1. Stochastic velocity-scalar models

First, we combine the GLM for velocities with stochastic equations for scalars that have a corresponding structure. The equations considered for particle positions $\mathbf{x}^* = (x_1^*, x_2^*, x_3^*)$, velocities $\mathbf{U}^* = (U_1^*, U_2^*, U_3^*)$, temperature T^* and mass fractions $\mathbf{m}^* = (m_1^*, \ldots, m_N^*)$ read

$$\frac{d}{dt}x_i^* = U_i^*, \tag{5.90a}$$

$$\frac{d}{dt}U_i^* = \overline{\Gamma}_i + G_{ij}\left(U_j^* - \overline{U}_j\right) + F_i + \sqrt{C_0\varepsilon}\,\frac{dW_i}{dt}, \tag{5.90b}$$

$$\frac{d}{dt}T^* = \overline{\Omega}_T - \frac{C_\varphi}{2\tau}\left(T^* - \overline{T}\right) + G_{Tk}\left(U_k^* - \overline{U}_k\right) + S_T + \sqrt{\frac{C_T}{\tau}\overline{T''T''}}\,\frac{dW}{dt}, \tag{5.90c}$$

$$\frac{d}{dt}m_\alpha^* = \overline{\Omega}_\alpha - \frac{C_\varphi}{2\tau}\left(m_\alpha^* - \overline{m}_\alpha\right) + G_{\alpha k}\left(U_k^* - \overline{U}_k\right) + S_\alpha + \sqrt{\frac{C_\alpha}{\tau}\overline{m_{(\alpha)}''m_{(\alpha)}''}}\,\frac{dW}{dt}. \tag{5.90d}$$

The first terms on the right-hand sides of (5.90b-d) are fully determined by the constraint that these equations have to be consistent with the transport equations (4.95b-d) for mean velocities and scalars,

$$\overline{\Gamma}_i = 2\langle\rho\rangle^{-1}\frac{\partial}{\partial x_k}\langle\rho\rangle\overline{\nu S_{ik}^{\,d}} - \langle\rho\rangle^{-1}\frac{\partial\langle p\rangle}{\partial x_i}, \qquad \overline{\Omega}_\alpha = \langle\rho\rangle^{-1}\frac{\partial}{\partial x_i}\langle\rho\rangle\overline{\frac{\nu}{Sc}\frac{\partial m_\alpha}{\partial x_i}},$$

$$\overline{\Omega}_T = \langle\rho\rangle^{-1}\frac{\partial}{\partial x_i}\langle\rho\rangle\overline{\frac{\nu}{Pr}\frac{\partial m_\alpha}{\partial x_i}}. \tag{5.91}$$

The second terms on the right-hand sides of (5.90b-d) represent the relaxation of fluctuations. The structure of G_{ij} was investigated in detail in sections 5.2 and 5.3. C_φ represents the ratio of τ to the time scale of the relaxation of scalar fluctuations. DNS estimates for C_φ are given in Fig. 5.16, which presents the findings of Overholt & Pope's (1996) investigations of passive scalar mixing in homogeneous isotropic stationary turbulence with imposed constant mean scalar gradient. These data represent the temporal average values of C_φ obtained for the

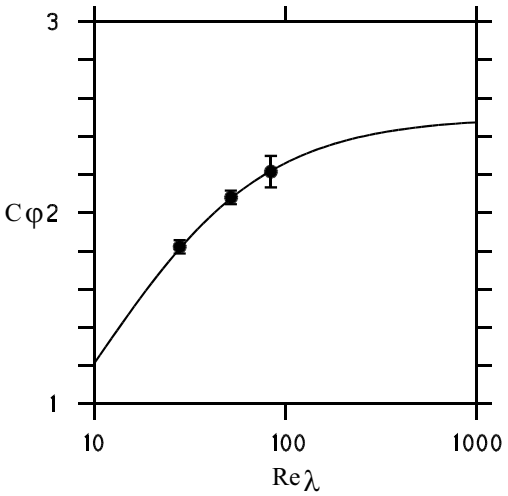

Fig. 5.16. The calculation of C_φ in dependence on Re_λ according to the DNS data of Overholt & Pope (1996). The error bars denote the accuracy of these data. The solid curve shows the prediction of relation (5.92) combined with $C_\varphi(\infty) = 2.5$.

stationary portion of each simulation. A value at $Re_\lambda = 185$ is not considered here because it is strongly influenced by the forcing energy input (Overholt & Pope 1996). The solid curve in Fig. 5.16 represents a parametrization of the dependence of C_φ on Re_λ,

$$C_\varphi = \frac{C_\varphi(\infty)}{1 + 1.7 C_\varphi^{\,2}(\infty)\, Re_\lambda^{\,-1}}. \tag{5.92}$$

The structure of this formula is chosen according to the parametrization (5.11) of C_0 suggested by Sawford (1991). Support for such a variation of C_φ with Re_λ is provided by recent results of Heinz & Roekaerts (2001). The parameters in (5.92) are estimated such that the predictions of (5.92) agree with the DNS data. This leads to the asymptotic value $C_\varphi(\infty) = 2.5$.

The third terms on the right-hand sides of (5.90b-d) involve couplings of instantaneous velocities and scalars. F_i may represent for instance buoyancy effects according to the Boussinesq approximation (Heinz 1997, 1998a; Heinz & van Dop 1999). $G_{\alpha k}$ and G_{Tk} are coefficients that involve the effect of velocities on the dynamics of scalars (Fox 1992, 1994, 1996). They are given by the expressions

$$G_{\alpha m} = \frac{C_\varphi}{2\tau}\, \overline{m_\alpha'' u_i} V^{-1}{}_{im}, \qquad G_{Tm} = \frac{C_\varphi}{2\tau}\, \overline{T'' u_i} V^{-1}{}_{im}. \tag{5.93}$$

V^{-1} is the inverse velocity variance matrix V, which has elements $V_{ik} = \overline{u_i u_k}$. The expressions (5.93) can be found by means of the constraint that the turbulent scalar flux has to be independent of the scalar mixing frequency $C_\varphi\, \tau^{-1}$ for a high-Reynolds number flow, see the explanations given in Appendix 5B. One may prove that the terms related to $G_{\alpha k}$ and G_{Tk} compensate terms related to the mixing frequency $C_\varphi\, \tau^{-1}$ in the turbulent scalar flux equation that follows from (5.90a-d). In the equations (5.90c-d), S_α is a chemical reaction rate, and S_T is given by (4.72).

The last terms in the equations (5.90b-d) represent the generation of velocity and scalar fluctuations by stochastic sources. dW_i /dt is a Gaussian noise process with vanishing means and uncorrelated values at different times, see (3.43a-b). C_T and C_α have to be chosen according to the results presented in section 5.5. Compared to the RIEM model for the transport of scalars presented there, the assumption of the structure of the scalar equations (5.90c-d) corresponds with the neglect of memory effects. This is in accord with the analogous consideration of the velocity equation (5.90b). It was shown in section 5.1 that an equation as given by (5.90b) represents the asymptotic limit of an acceleration model, which resolves processes in the order of the Kolmogorov microscale. Regarding the stochastic force terms in (5.90c-d), it is worth emphasizing that their consideration is still a requirement in general, although contributions due to velocity fluctuations also involve stochastics. It will be shown in Appendix 5A and (in more detail) in chapter 6, that the effect of velocity-induced contributions on the evolution of scalar variances is very different to that of stochastic force terms: velocity-induced contributions only modify the characteristic scalar time scale in such equations.

5.7.2. Hybrid methods

It was pointed out in section 5.6.3 that the reduction of stochastic equations for velocities to equations for mean velocities may be related to significant advantages with regard to various applications. This reduction requires the decoupling of the stochastic scalar equations (5.90c-d) from the equations (5.90a-b). Hybrid methods obtained in this way combine RANS equations for the velocity field with scalar PDF transport equations, see Fig. 5.17 for an illustration. These methods were often used successfully to calculate weakly compressible (Roekaerts 1991; Wouters et al. 1996; Nooren et al. 1997; Nooren 1998; Wouters 1998; Krieger et al. 1997; Hinz et al. 1999; Repp et al. 2002) and compressible reacting flows (Eifler & Kollmann 1993; Hsu et al. 1994; Möbus et al. 1998, 1999).

The reduction of the equations (5.90a-d) to a closed stochastic model for scalars can be performed as pointed out in Appendix 6B. The equations obtained read

$$\frac{d}{dt}x_i^* = \overline{U}_i + \omega^{-1}{}_{ij}F_j'' + \frac{1}{\langle\rho\rangle}\frac{\partial\langle\rho\rangle K_{ij}}{\partial x_j} + \sqrt{2K_{ij}}\frac{dW_j}{dt}, \tag{5.94a}$$

$$\frac{d}{dt}T^* = \overline{\Omega}_T - \frac{C_\varphi}{2\tau}\left(T^* - \overline{T}\right) + D_T + S_T + \sqrt{\frac{C_T}{\tau}\overline{T''T''}}\frac{dW}{dt}, \tag{5.94b}$$

$$\frac{d}{dt}m_\alpha^* = \overline{\Omega}_\alpha - \frac{C_\varphi}{2\tau}\left(m_\alpha^* - \overline{m}_\alpha\right) + D_\alpha + S_\alpha + \sqrt{\frac{C_\alpha}{\tau}\overline{m_{(\alpha)}''m_{(\alpha)}''}}\frac{dW}{dt}. \tag{5.94c}$$

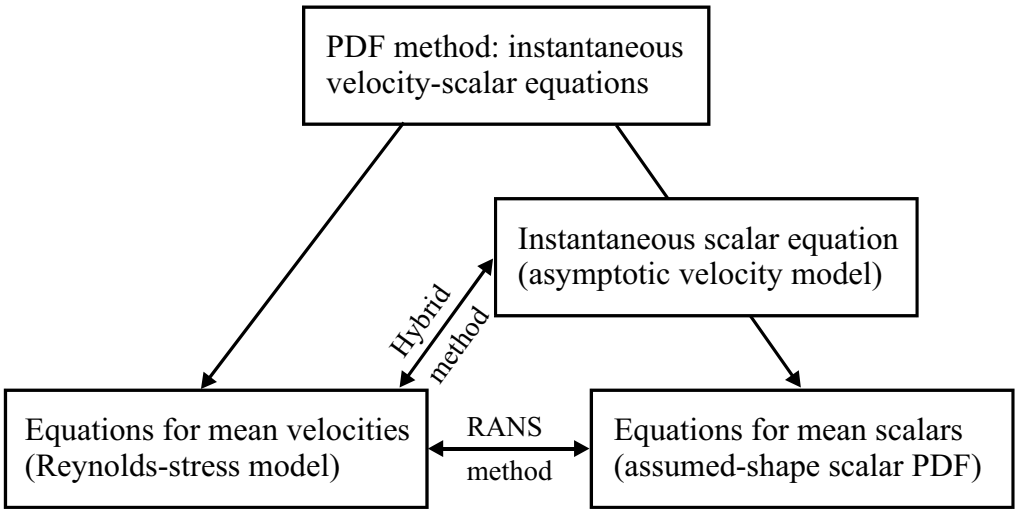

Fig. 5.17. An illustration of the reduction of PDF methods (stochastic equations for velocities and scalars) to RANS and hybrid methods. Equations for mean velocities must be closed by algebraic or transport equation models for Reynolds stresses. The direct use of equations for mean scalars requires (assumed-shape) models for scalar PDFs to close mean reaction rates, see section 5.7.3. A hybrid method is given by combining RANS equations for velocities with stochastic equations for scalars. The latter involve the asymptotic velocity model (5.94a) to calculate the transport of scalars in space. Consistent with that, one has to use an algebraic Reynolds stress model (the k-ε model) in RANS equations for velocities.

ω^{-1} refers to the inverse matrix of ω, which has elements $\omega_{ij} = \partial \overline{U}_i / \partial x_j - G_{ij}$. The diffusion coefficient $K_{ik} = \omega^{-1}{}_{in} \, \overline{u_n u_k}$, and the following abbreviations are applied,

$$D_T = G_{Tk}\left(\frac{dx_k^*}{dt} - \overline{U}_k\right) + \frac{\partial G_{Tk}}{\partial x_j} K_{kj}, \; D_\alpha = G_{\alpha k}\left(\frac{dx_k^*}{dt} - \overline{U}_k\right) + \frac{\partial G_{\alpha k}}{\partial x_j} K_{kj}. \quad (5.95)$$

The essential result of the reduction of the equations (5.90a-d) to the equations (5.94a-c) is given by equation (5.94a), which represents the asymptotic form of the velocity equation (5.90b). Apart from the inclusion of the mean velocity $\overline{U}_i$, there are three differences of (5.94a) compared to the corresponding equation (5.15) derived in section 5.1 for HIST. The first one is given by the second term on the right-hand side, which involves buoyancy processes. The relevance of such terms (which act as counter-gradient terms in algebraic models for the turbulent heat or mass flux) is well investigated (Schumann 1987; Holtslag & Moeng 1991; Canuto 1992). Recent simulations of buoyant plume rise also provide evidence for the requirement to involve such terms in simulations of flows that are driven by temperature differences (Heinz & van Dop 1999). The second difference is given

by the derivation of K_{ij} as an anisotropic tensor. This is in accord with the results of various studies (Rogers et al. 1989; Kaltenbach et al. 1994). The third difference is the appearance of an additional drift velocity due to spatial gradients of K_{ij}.

To see the properties of $K_{ik} = \omega^{-1}{}_{in}\ \overline{u_n u_k}$ in more detail we apply $G_{ij} = G\,\delta_{ij}$ and relation (5.78) for $\overline{u_i u_k}$ as in section 5.6.3. This leads to

$$\left(\frac{\partial \overline{U}_i}{\partial x_n} - G\,\delta_{in}\right) K_{nk} = \frac{2k}{3}\delta_{ik} - 2\nu_T \overline{S}_{ik}{}^{d}. \tag{5.96}$$

This expression can be developed in different orders of contributions due to shear. By neglecting velocity gradients at all, one obtains for instance

$$K_{ik} = \frac{\nu_T}{Sc_t}\delta_{ik}, \tag{5.97}$$

where the turbulence Schmidt number is given by

$$Sc_t = \frac{5}{9}Pr_k = \frac{1}{2}\left(1 + \frac{3C_\mu}{2}\left[1 - \frac{P}{\varepsilon} - \frac{\Pi_d}{\langle\rho\rangle\varepsilon}\right]\right). \tag{5.98}$$

To obtain this expression one has to involve the definitions (5.79) and (5.82) of ν_T and Pr_k. The use of $Pr_k = 1$ implies then $Sc_t = 0.56$. This is in accord with the finding $Sc_t = 0.7 \pm 0.5$ obtained by Rogers et al. (1989).

Nevertheless, the scalar model (5.94a-c) is still unclosed due to the appearance of instantaneous velocity gradients in S_T, which is given according to (4.72) by

$$S_T = -(\gamma-1)S_{kk}T + \frac{2}{R}(\gamma-1)\nu S_{jk}{}^{d}S_{kj}{}^{d} - \frac{1}{c_v}\sum_{\alpha=1}^{N_S} e_\alpha S_\alpha + \frac{Q_B + Q_R}{c_v}. \tag{5.99}$$

It is essential to note that the hybrid approach provides a simple solution for this question. To see this, we may consider (5.94a) for a homogeneous flow without buoyancy. Velocity fluctuations are then proportional to d**W** / dt. Hence, their correlation time vanishes, this means they decay much faster than temperature and mass fraction fluctuations which relax with time scales proportional to τ. An approximation that is consistent with this velocity model is to replace the instantaneous velocity gradients in (5.99) by their means. In conjunction with the simplifying assumption that ν is uncorrelated with velocity gradients, this results in

$$S_T = -(\gamma-1)\overline{S}_{kk}T + \frac{\gamma-1}{R}\left(\varepsilon + E\right) - \frac{1}{c_v}\sum_{\alpha=1}^{N_S} e_\alpha S_\alpha + \frac{Q_B + Q_R}{c_v}, \tag{5.100}$$

where $\varepsilon = 2\overline{\nu}\,\overline{(S_{ik}{}^{d})''(S_{ki}{}^{d})''}$ and $E = 2\overline{\nu}\,\overline{S}_{ik}{}^{d}\overline{S}_{ki}{}^{d}$ are used for the representation of the averaged second term on the right-hand side of (5.99). The influence of

compressibility may be better seen by defining an instantaneous turbulence Mach number $\widetilde{M}_t = (2k)^{1/2}/a$, which enables, combined with the definition $a^2 = \gamma R T$ of the speed of sound, the following rewriting of the term involving ε in (5.100),

$$S_T = -(\gamma-1)\overline{S}_{kk}T + \gamma(\gamma-1)\frac{\widetilde{M}_t^{\,2}}{2\tau}T + \frac{\gamma-1}{R}E - \frac{1}{c_v}\sum_{\alpha=1}^{N_S} e_\alpha S_\alpha + \frac{Q_B + Q_R}{c_v}. \qquad (5.101)$$

We note that the term that involves E becomes small for high Reynolds number flows since E is then small compared to ε in (5.100).

5.7.3. Assumed-shape PDF methods

Compared to the use of a hybrid method, a simpler approach is given by the direct consideration of equations for mean mass fractions and temperature, where mean reaction rates are closed by assumption on scalar PDFs, see Fig. 5.17 for an illustration. Such methods are called assumed-shape (or presumed) PDF methods (Baldyga & Bourne 1999). In this way, scalar PDFs are standardized in terms of scalar means and variances. These means and variances are then calculated by transport equations, and the standardized scalar PDF is provided by an analytical function (e.g., the beta PDF considered in section 2.6.2).

The notable advantage of this approach is its simplicity. Nevertheless, there are also significant disadvantages. It will be shown in Appendix 6C that the most important problem related to the application of assumed-shape PDF methods is given by the neglect of velocity-scalar correlations (their consideration would result in changes of the standardized scalar PDF in time). The neglect of such correlations is only justified for homogeneous scalar fields, this means for premixed combustion problems. Another problem is the treatment of scalar correlations (Baurle & Girimaji 1999). In existing methods one assumes that all the mass fractions of species are perfectly correlated, have the same variance and are uncorrelated with the temperature (Gerlinger et al. 2001). These assumptions are not satisfied for instance regarding the turbulent mixing of different species streams, and under conditions where chemical reactions produce significant temperature changes. Thus, the application of assumed-shape PDF methods may result in erroneous calculations (Baldyga & Bourne 1999).

Appendix 5A: Stochastic models and basic equations

The discussion of some relevant questions related to the modeling of any stochastic processes in section 3.5 was based on the consideration of the stochastic differential equation (3.42) for a set of variables $\xi(t)$ considered,

$$\frac{d\xi_i}{dt} = a_i(\xi,t) + b_{ik}(\xi,t)\frac{dW_k}{dt}. \tag{5A.1}$$

It was pointed out there that suitable concepts for the modeling of b_{ik} are available in general, such that the remaining question is to provide a_i as function of $\xi(t)$.

The concept used before in this chapter for the construction of stochastic models was to provide the term a_i as an extension of the stochastic model for the equilibrium dynamics of relevant variables presented in Appendix 3A. However, this heuristic approach does not explain in which way a_i is related to the basic equations of fluid and thermodynamics. This question will be addressed now on the basis of a publication of the author (Heinz 2003a), this means we ask how a_i can be calculated from the basic equations. Examples for the relevance of these relationships between stochastic models and the basic equations will be given in the Appendices 5B and 5C regarding the development of linear and nonlinear stochastic turbulence models, respectively.

5A.1. A nonlinear stochastic model

To study the relationships between stochastic models and basic equations we consider a general nonlinear stochastic model for particle positions x_i^*, velocities U_i^* and scalars Φ_α^* (the vector of mass fractions of species and temperature),

$$\frac{d}{dt}x_i^* = U_i^*, \tag{5A.2a}$$

$$\frac{d}{dt}U_i^* = \Gamma_i\left[\mathbf{U}^*,\mathbf{\Phi}^*\right] + F_i + b_{ik}\frac{dW_k}{dt}, \tag{5A.2b}$$

$$\frac{d}{dt}\Phi_\alpha^* = \Omega_\alpha\left[\mathbf{U}^*,\mathbf{\Phi}^*\right] + S_\alpha + c_{\alpha\beta}\frac{dW_\beta}{dt}. \tag{5A.2c}$$

Γ_i, Ω_α, b_{ik} and $c_{\alpha\beta}$ are any unknown functions of $\mathbf{x}^*$, $\mathbf{U}^*$, $\mathbf{\Phi}^*$ and t. F_i and S_α represent known source terms. dW_i / dt and dW_β / dt are uncorrelated Gaussian noise processes with vanishing mean values and uncorrelated values at different times, see the relations (3.43a-b). As shown in chapter 3, the stochastic Itô-equations (5A.2a-c) may be rewritten into the following Fokker-Planck equation

$$\frac{\partial}{\partial t}\langle\rho\rangle F + \frac{\partial}{\partial x_i}\langle\rho\rangle w_i F = -\frac{\partial}{\partial w_i}\langle\rho\rangle(\Gamma_i + F_i)F + \frac{1}{2}\frac{\partial^2}{\partial w_i \partial w_j}\langle\rho\rangle b^2{}_{ij}F$$

$$-\frac{\partial}{\partial\theta_\alpha}\langle\rho\rangle(\Omega_\alpha + S_\alpha)F + \frac{1}{2}\frac{\partial^2}{\partial\theta_\alpha\partial\theta_\beta}\langle\rho\rangle c^2{}_{\alpha\beta}F \tag{5A.3}$$

for the joint velocity-scalar PDF F, which is defined by

$$F(\mathbf{w},\boldsymbol{\theta},\mathbf{x},t)=\frac{1}{\langle\rho(\mathbf{x},t)\rangle}\left\langle\rho(\mathbf{x},t)\,\delta(\mathbf{U}^*(\mathbf{x}^*(t),t)-\mathbf{w})\,\delta(\boldsymbol{\Phi}^*(\mathbf{x}^*(t),t)-\boldsymbol{\theta})\right\rangle$$

$$=\overline{\delta(\mathbf{U}(\mathbf{x},t)-\mathbf{w})\,\delta(\boldsymbol{\Phi}(\mathbf{x},t)-\boldsymbol{\theta})}. \qquad (5A.4)$$

In (5A.3), we used $b^2_{ij} = b_{ik}\, b_{jk}$ and $c^2_{\alpha\beta} = c_{\alpha\mu}\, c_{\beta\mu}$. The last expression in (5A.4) is implied by the required consistency between the PDF that follows from the model (5A.2a-c) and the PDF of fluid variables $\mathbf{U}(\mathbf{x}, t)$ and $\boldsymbol{\Phi}(\mathbf{x}, t)$.

5A.2. The consistency with basic equations

A PDF transport equation that corresponds to equation (5A.3) may also be derived from the basic equations of fluid and thermodynamics. To do this, we apply as in Appendix 4A the following abbreviations for the right-hand sides of the equations (4.71b-d),

$$\frac{DU_i}{Dt}=A_i, \qquad \frac{D\Phi_\alpha}{Dt}=A_\alpha. \qquad (5A.5)$$

The transport equation for the velocity-scalar PDF F that follows from (5A.5) can be derived by means of standard methods. It reads (Gardiner 1983; Risken 1984; Pope 1985, 2000)

$$\frac{\partial}{\partial t}\langle\rho\rangle F+\frac{\partial}{\partial x_i}\langle\rho\rangle w_i F=-\frac{\partial}{\partial w_i}\langle\rho\rangle\overline{A_i|\,\mathbf{w},\boldsymbol{\theta}}\;F-\frac{\partial}{\partial\theta_\alpha}\langle\rho\rangle\overline{A_\alpha|\,\mathbf{w},\boldsymbol{\theta}}\;F, \qquad (5A.6)$$

where the conditional accelerations are defined by the relations

$$\overline{A_i|\,\mathbf{w},\boldsymbol{\theta}}=\frac{1}{F}\overline{A_i\,\delta(\mathbf{U}-\mathbf{w})\,\delta(\boldsymbol{\Phi}-\boldsymbol{\theta})}, \quad \overline{A_\alpha|\,\mathbf{w},\boldsymbol{\theta},}=\frac{1}{F}\overline{A_\alpha\,\delta(\mathbf{U}-\mathbf{w})\,\delta(\boldsymbol{\Phi}-\boldsymbol{\theta})}. \qquad (5A.7)$$

Obviously, the modeled Fokker-Planck equation (5A.3) should be consistent with the basic Fokker-Planck equation (5A.6). This is assured provided the equation

$$0=\frac{\partial F h_i}{\partial w_i}+\frac{\partial F h_\alpha}{\partial\theta_\alpha} \qquad (5A.8)$$

is satisfied, where we introduced the abbreviations

$$h_i=\Gamma_i+F_i-\frac{1}{2F}\frac{\partial b^2{}_{ij}F}{\partial w_j}-\overline{A_i|\,\mathbf{w},\boldsymbol{\theta}}, \qquad h_\alpha=\Omega_\alpha+S_\alpha-\frac{1}{2F}\frac{\partial c^2{}_{\alpha\beta}F}{\partial\theta_\beta}-\overline{A_\alpha|\,\mathbf{w},\boldsymbol{\theta}}. \qquad (5A.9)$$

The relations (5A.9) relate the stochastic model coefficients Γ_i, Ω_α, b_{ik} and $c_{\alpha\beta}$ to the measurable conditional accelerations (5A.7) and the unknown h_i and h_α. To assess the relevance of h_i and h_α, we multiply (5A.8) with any function Q of velocities and scalars and integrate it over the sample space. After applying partial integration we obtain

$$0 = \overline{\frac{\partial Q(\mathbf{U},\mathbf{\Phi})}{\partial U_i} h_i} + \overline{\frac{\partial Q(\mathbf{U},\mathbf{\Phi})}{\partial \Phi_\alpha} h_\alpha}. \tag{5A.10}$$

The components h_i and h_α could be combined to a joint vector $\mathbf{h} = (h_i, h_\alpha)$, and, correspondingly, the velocities and scalars to a joint process. The use of suitable choices of Q reveals then that the means of h_i and h_α are zero, and that h_i and h_α are uncorrelated with any functions of velocities. Thus, h_i and h_α can be neglected such that the relations (5A.9) reduce to

$$\overline{A_i \,|\, \mathbf{w},\boldsymbol{\theta}} = \Gamma_i + F_i - \frac{1}{2F}\frac{\partial b^2{}_{ij} F}{\partial w_j}, \qquad \overline{A_\alpha \,|\, \mathbf{w},\boldsymbol{\theta}} = \Omega_\alpha + S_\alpha - \frac{1}{2F}\frac{\partial c^2{}_{\alpha\beta} F}{\partial \theta_\beta}. \tag{5A.11}$$

These relations provide the formal solution to the problem described above: they explain how Γ_i and Ω_α can be calculated in principle from basic equations by adopting the measurable conditional accelerations (5A.7). However, the direct application of this concept requires us to provide the conditional accelerations as functions of velocities and scalars, which poses a non-trivial question. A method to overcome this problem will be described next.

5A.3. The determination of model coefficients

First, we split (5A.11) into relations for means and fluctuations of Γ_i and Ω_α. By multiplying these relations with F and integration, $\overline{\Gamma}_i$ and $\overline{\Omega}_\alpha$ are found to obey

$$\overline{A}_i = \overline{\Gamma}_i + \overline{F}_i, \qquad \overline{A}_\alpha = \overline{\Omega}_\alpha + \overline{S}_\alpha. \tag{5A.12}$$

These relations assure that the transport equations for mean velocities and scalars that are implied by the basic equations agree with the corresponding equations that are implied by the stochastic model (5A.2a-c). By adopting (5A.12), the relations (5A.11) can be rewritten into the following relations for Γ_i" and Ω_α",

$$\overline{a_i - F_i" \,|\, \mathbf{w},\boldsymbol{\theta}} = \Gamma_i" - \frac{1}{2F}\frac{\partial b^2{}_{ij} F}{\partial w_j}, \quad \overline{a_\alpha - S_\alpha" \,|\, \mathbf{w},\boldsymbol{\theta}} = \Omega_\alpha" - \frac{1}{2F}\frac{\partial c^2{}_{\alpha\beta} F}{\partial \theta_\beta}. \tag{5A.13}$$

The equations (5A.13) can also be written as relations for all the moments of the conditional accelerations. To see this, we multiply (5A.13) with F Q, where Q is

again any function of velocities or scalars. By adopting partial integration, the resulting relations are found to be

$$\overline{Q(a_i - F_i'')} = \overline{Q\Gamma_i''} + \frac{1}{2}\overline{\frac{\partial Q}{\partial w_j} b^2{}_{ij}}, \quad \overline{Q(a_\alpha - S_\alpha'')} = \overline{Q\Omega_\alpha''} + \frac{1}{2}\overline{\frac{\partial Q}{\partial \theta_\beta} c^2{}_{\alpha\beta}}. \qquad (5A.14)$$

These expressions (5A.14) can be used in the following way for the calculation of Γ_i'' and Ω_α'':

(i) The first step is the specification of the order of a RANS model (e.g., by the choice of a second-, third- or fourth-order model), which may be considered to provide a suitable frame for the simulation of a problem considered. It is worth noting that this approach may be seen as the dynamic version of the concept to construct SML PDFs, see the explanations given in section 2.4.

(ii) The second step is the extension of this RANS model to a corresponding PDF model. One may easily prove that the consideration of second-, third- or fourth-order RANS models implies the need to consider Γ_i'' and Ω_α'' as linear, quadratic or cubic functions of velocities and scalars, respectively.

(iii) The third step is to specify Q in (5A.14) such that unique relations between the coefficients of the linear, quadratic or cubic terms of Γ_i'' and Ω_α'' with turbulence statistics are obtained. These relations then permit the calculation of the coefficients of Γ_i'' and Ω_α''.

To illustrate this approach, let us assume that we have chosen the means and variances of velocities and scalars as relevant variables. Correspondingly, we have to specify Γ_i and Ω_α as linear functions of velocities and scalars,

$$\Gamma_i = \overline{\Gamma}_i + G_{im}\left(U_m^* - \overline{U}_m\right) + G_{i\mu}\left(\Phi_\mu^* - \overline{\Phi}_\mu\right),$$
$$\Omega_\alpha = \overline{\Omega}_\alpha + G_{\alpha\mu}\left(\Phi_\mu^* - \overline{\Phi}_\mu\right) + G_{\alpha m}\left(U_m^* - \overline{U}_m\right). \qquad (5A.15)$$

The relevance of considering these terms will be discussed in Appendix 5B. We apply these specification of Γ_i and Ω_α in (5A.14) and set $Q = u_j$ and $Q = \phi_\alpha$. This results in the following four relations,

$$\overline{(a_i - F_i'')u_j} = G_{im}\overline{u_m u_j} + G_{i\mu}\overline{\phi_\mu u_j} + \frac{1}{2}\overline{b^2{}_{ij}},$$

$$\overline{(a_\alpha - S_\alpha'')\phi_\beta} = G_{\alpha m}\overline{u_m \phi_\beta} + G_{\alpha\mu}\overline{\phi_\mu \phi_\beta} + \frac{1}{2}\overline{c^2{}_{\alpha\beta}},$$

$$\overline{(a_i - F_i'')\phi_\alpha} = G_{im}\overline{u_m \phi_\alpha} + G_{i\mu}\overline{\phi_\mu \phi_\alpha},$$

$$\overline{(a_\alpha - S_\alpha'')u_i} = G_{\alpha m}\overline{u_m u_i} + G_{\alpha\mu}\overline{\phi_\mu u_i}. \qquad (5A.16)$$

The relations (5A.16) represent for specified noise coefficients b^2_{ij} and $c^2_{\alpha\beta}$ a unique relationship between a second-order RANS model, which is given by (4A.4a-c), and a linear stochastic model, which is given by (5A.2a-c) combined with (5A.15)). The coefficients G_{im}, $G_{i\mu}$, $G_{\alpha\mu}$ and $G_{\alpha m}$ of the stochastic model can be obtained for specified acceleration correlations. Conversely, the acceleration correlations of the RANS model are determined if the coefficients of the stochastic model are provided.

The relations (5A.16) can be used in different ways to calculate the coefficients of the stochastic model. One way is to parametrize these coefficients and to estimate the open parameters by means of the acceleration correlations. This way will be described in Appendix 5B. Another way is to apply measurements of the acceleration correlations to calculate stochastic model coefficients. This will be demonstrated in Appendix 5C.

Appendix 5B: Consistent turbulence models

Second-order RANS models are applied as standard methods for simulations of industrial flows. However, the direct parametrization of the unclosed acceleration correlations in (4A.4a-c) does not assure the consistency of these models in general: it is possible that a stochastic process with moments that evolve according to such RANS equations cannot exist. This question can be solved by deriving a consistent RANS model as consequence of a stochastic model. As shown next, the coefficients of the stochastic model can then be obtained by means of (5A.16).

5B.1. The model considered

We specify the expressions (5A.15) for the coefficients of the stochastic model (5A.2a-c) in the following way,

$$\Gamma_i = \overline{\Gamma}_i - \left[\frac{c_1^*}{2\tau}\delta_{ik} - c_2^*\frac{\partial \overline{U}_i}{\partial x_k}\right]\left(w_k - \overline{U}_k\right) - c_3^* F_i'', \tag{5B.1a}$$

$$\Omega_\alpha = \overline{\Omega}_\alpha - \frac{c_{\varphi 1}^*}{2\tau}\left(\theta_\alpha - \overline{\Phi}_\alpha\right) + \frac{c_{\varphi 2}^*}{2\tau}\overline{\phi_\alpha u_i} V^{-1}{}_{ik}\left(w_k - \overline{U}_k\right). \tag{5B.1b}$$

Relation (5B.1a) assumes that G_{ik} in (5A.15) depends on two frequencies: the shear $\partial \overline{U}_i / \partial x_k$, which determines the production of turbulence, and the inverse dissipation time scale $\tau = k / \varepsilon$, where k is the turbulent kinetic energy and ε the dissipation rate of k. More general forms of G_{ik} (which may be seen to involve shear of higher than first-order) may be considered (Pope 2000). However, their introduction results in the need for additional constraints, as pointed out below.

Further, we specified $G_{i\mu}\ (\Phi_\mu^* - \overline{\Phi}_\mu) = -\ c_3^*\ F_i''$, where F_i'' may represent the influence of buoyancy (Heinz 1998a; Heinz & van Dop 1999). In this case, F_i'' is given by $F_i'' = \beta\ g\ T''\ \delta_{i3}$, see section 5.6.4. In (5B.1b), the second term on the right-hand side appears in correspondence to the modeling of the velocity term in (5B.1a). The suitability of the specification of the coefficient of the velocity term in (5B.1b) will be shown below, see (5B.2c). The effects of scalar gradients are involved in this way by the consideration of velocity-scalar correlations. V^{-1} denotes the inverse velocity variance matrix V, which has elements $V_{ik} = \overline{u_i u_k}$. The parameters c_1^*, c_2^*, c_3^* and $c_{\varphi 1}^*$, $c_{\varphi 2}^*$ will be estimated below. We complement the relations (5B.1a-b) by again adopting for the coefficient b_{ij} the parametrization $b_{ij} = (C_0\ \varepsilon)^{1/2}\ \delta_{ij}$. There is no need to specify $c_{\alpha\beta}$ for the following analysis.

5B.2. Coefficient relations

By adopting (5B.1a-b) for the coefficients of the stochastic model (5A.2a-c) and $b_{ij} = (C_0\ \varepsilon)^{1/2}\ \delta_{ij}$ in the relations (5A.16), one finds for the acceleration correlations in the variance equations (4A.4a-c) the expressions

$$\overline{(a_i - F_i'')u_j} = -\frac{c_4^*}{3}\varepsilon\delta_{ij} - \frac{c_1^*}{2\tau}\left(\overline{u_i u_j} - \frac{2}{3}k\delta_{ij}\right) + c_2^*\left(\frac{\partial\overline{U}_i}{\partial x_k}\overline{u_k u_j} + \frac{P}{3}\delta_{ij}\right) - c_3^*\left(\overline{F_i'' u_j} - \frac{B}{3}\delta_{ij}\right), \tag{5B.2a}$$

$$\overline{(a_i - F_i'')\phi_\beta} = -\frac{c_1^*}{2\tau}\overline{u_i\phi_\beta} + c_2^*\frac{\partial\overline{U}_i}{\partial x_k}\overline{u_k\phi_\beta} - c_3^*\overline{F_i''\phi_\beta}, \tag{5B.2b}$$

$$\overline{(a_\alpha - S_\alpha'')u_i} = \frac{c_{\varphi 2}^* - c_{\varphi 1}^*}{2\tau}\overline{\phi_\alpha u_i}, \tag{5B.2c}$$

$$\overline{(a_\alpha - S_\alpha'')\phi_\beta} = -\frac{c_{\varphi 1}^*}{2\tau}\overline{\phi_\alpha\phi_\beta} + \frac{c_{\varphi 2}^*}{2\tau}\overline{\phi_\alpha u_k}V^{-1}{}_{ki}\overline{u_i\phi_\beta} + \frac{1}{2}\overline{c^2{}_{\alpha\beta}}. \tag{5B.2d}$$

$P = -\,\partial\overline{U}_m / \partial x_k\ \overline{u_k u_m}$ and $B = \overline{F_k'' u_k}$ refer again to the production due to shear and body forces, respectively, in the equation for the turbulent kinetic energy. The abbreviation c_4^* in (5B.2a) is given by the expression

$$c_4^* = c_1^* + c_2^*\frac{P}{\varepsilon} + c_3^*\frac{B}{\varepsilon} - \frac{3}{2}C_0. \tag{5B.3}$$

The use of (5B.2a) in the transport equation for k, which follows from (4A.4a), reveals the constraint $c_4^* = 1$ as a consequence of the definition of ε. According to (5B.3), this implies then for c_1^* the relation

$$c_1^* = 1 + \frac{3}{2} C_0 - c_2^* \frac{P}{\varepsilon} - c_3^* \frac{B}{\varepsilon}. \qquad (5B.4)$$

By adopting this expression, we have for specified C_0 and $c_{\alpha\beta}$ a unique relationship between the stochastic model that applies (5B.1a-b) and the corresponding second-order RANS model: the acceleration correlations can be used to calculate the parameters c_2^*, c_3^* and $c_{\varphi 1}^*$, $c_{\varphi 2}^*$ of the stochastic model, and the right-hand sides of (5B.2a-d) determine the acceleration correlations on the left-hand sides.

5B.3. The determination of stochastic model coefficients

The advantage of the relations (5B.2a-d) with regard to the calculation of the parameters c_2^*, c_3^* and $c_{\varphi 1}^*$, $c_{\varphi 2}^*$ of the stochastic model is given by the possibility of calculating these parameters by measurements of the acceleration correlations given on the left-hand sides of (5B.2a-d). This will be demonstrated in Appendix 5C. Here, we use standard values applied in second-order RANS models to obtain the coefficients of the stochastic model. Such experience provides support for the use of the values $c_2^* = c_3^* = 0.5$ and $c_{\varphi 1}^* = 2.0$ (Launder 1990; Pope 1985, 2000). Further, according to the hypothesis of Taylor (1921), the turbulent flux of a passive scalar should be determined by the motion of fluid particles and independent of molecular transport (the details of the scalar mixing model) at high Reynolds numbers, see Pope (1998). To assure this, one has to set $c_{\varphi 2}^* = c_{\varphi 1}^*$ such that the acceleration correlation in (5B.2c) disappears in (4A.4b). In this way, all the stochastic model coefficients c_2^*, c_3^* and $c_{\varphi 1}^*$, $c_{\varphi 2}^*$ are given.

5B.4. A consistent RANS model

A significant advantage that arises from the derivation of the stochastic model in the sections 5B.1 – 5B.3 is the consistency of the second-order RANS model which is implied by the stochastic model. The latter is not the case in general if RANS models are obtained by direct parametrizations of unclosed terms in the variance equations (4A.4a-c). This may be seen by comparing the second-order RANS model obtained here with existing second-order RANS models. Instead of (5B.4) found for c_1^*, one usually assumes c_1^* to be constant in RANS models. In the velocity variance equation (4A.4a), one applies the value $c_1^* = 1.8$, whereas the value $c_1^* = 5.8$ (Launder 1990) is used in the turbulent scalar flux equation (4A.4b). Similarly, one applies $c_2^* = c_3^* = 0.6$ in (5B.2a) and $c_2^* = c_3^* = 0.4$ in (5B.2b), see Launder (1990). Such second-order RANS models do not represent consistent methods because one applies different models for acceleration fluctuations a_i and a_α on the right-hand sides of (4A.4a-c). The relevance of such imbalances is known (Durbin & Speziale 1994; Pope 1994a).

Appendix 5C: Nonlinear stochastic models

The discussions in the previous sections of this chapter were based on the consideration of linear stochastic models, but the limits of the applicability of this approach were not explained until now. This will be done next. It will be shown under which conditions linear stochastic models become inaccurate and have to be generalized by the consideration of nonlinear stochastic models. The latter models will then be introduced on the basis of the concept pointed out in Appendix 5A.3. This leads to the question of how these nonlinear methods obtained differ from previously developed nonlinear stochastic models.

5C.1. The limitations of the applicability of linear stochastic equations

The question of the range of applicability of linear stochastic equations cannot be seen to be trivial. It is essential to note that their use is not restricted to flows with Gaussian PDFs. The consideration of spatial variations of the coefficients in stochastic equations implies variance gradients which produce triple correlations (this may be seen in terms of the transport equations for second- and third-order moments). However, such deviations from Gaussian PDF shapes are usually found to be small, and an accurate simulation of the skewness of the velocity PDF of flows that involve coherent structures is impossible in this way. This may be seen by adopting linear stochastic equations for the simulation of convective boundary-layer (CBL) turbulence, which results in significant shortcomings (Heinz 1998b). The reason for this is related to the fact that the bimodal structure of this flow cannot be simulated. The mixing frequency (the negative coefficient of the velocity term in (5B.1a)) is considered to be independent of the actual value of the velocity, such that differences between the turbulent mixing of updrafts and downdrafts in the CBL are neglected.

The conclusion that linear stochastic equations are (in general) inapplicable to perform accurate simulations of flows that involve coherent structures is supported by previous applications of PDF and RANS methods to such flows. There exists broad evidence that nonlinear stochastic models are required to calculate the diffusion of species in the convective atmospheric boundary layer, see Sawford (1993, 1999), Luhar et al. (1996), Wilson & Sawford (1996) and the references therein. These models were constructed so that the second-, third- and fourth-order moments of the modeled velocity PDF agree with measurements. Particularly, information about third- and fourth-order moments was used to characterize the bimodality of the PDF structure. In accord with the explanations given above regarding the relations between stochastic and RANS models, this experience was confirmed by the application of RANS methods to such flows. Second-order RANS methods (which correspond to the use of linear stochastic equations) were

found to perform poorly in the prediction of even basic turbulent flows that are far from equilibrium (Speziale & Xu 1996; Kassinos et al. 2001). The consideration of transport equations for third- and fourth-order moments for convective and stratified flow simulations was found to be a suitable way to improve the performance of second-order RANS methods significantly, see for instance Canuto (1992), Canuto et al. (1994), Kawamura et al. (1995), Craft et al. (1997), Ilyushin & Kurbatski (1997), Craft (1998) and the references therein.

5C.2. A cubic stochastic model

As explained in Appendix 5A, the construction of a stochastic model in consistency with transport equations for third- and fourth-order moments requires the extension of the expression (5B.1a) for $\boldsymbol{\Gamma}$ to a cubic model. This model reads

$$\Gamma_i = \overline{\Gamma}_i - G_{ikm}\overline{u_k u_m} - G_{iklm}\overline{u_k u_l u_m} - M_{im}\left(w_m - \overline{U}_m\right). \tag{5C.1}$$

$\overline{\Gamma}_i$ is determined by the first part of (5A.12) combined with (4A.3a). The way of writing the cubic model reveals the extension of linear stochastic methods by the consideration of a mixing frequency M_{im} that is a quadratic function of velocities,

$$M_{im} = -G_{im} - G_{ikm}\left(w_k - \overline{U}_k\right) - G_{iklm}\left(w_k - \overline{U}_k\right)\left(w_l - \overline{U}_l\right). \tag{5C.2}$$

The second and third term in (5C.1) compensate the average of the last term. The model that applies (5C.1) in (5A.2b) will be referred to as cubic stochastic model (Heinz 2003a).

The need to introduce M_{im} as a quadratic function of velocities becomes obvious by considering the relationships between the moment transport equations for second-, third- and fourth-order moments that follow from the stochastic model with the corresponding equations that follow from (5A.5). By specifying the relations (5A.14) appropriately we find

$$\overline{(a_i - F_i'')u_j} = G_{ik}V_{kj} + G_{ikl}\overline{u_k u_l u_j} + G_{iklm}\overline{u_k u_l u_m u_j} + \frac{1}{2}\overline{b^2}_{ij}, \tag{5C.3a}$$

$$\overline{(a_i - F_i'')u_j u_n} = G_{ik}\overline{u_k u_j u_n} + G_{ikl}\left[\overline{u_k u_l u_j u_n} - V_{kl}V_{jn}\right] + G_{iklm}\left[\overline{u_k u_l u_m u_j u_n} - \overline{u_k u_l u_m}V_{jn}\right], \tag{5C.3b}$$

$$\overline{(a_i - F_i'')u_j u_n u_m} = G_{ik}\overline{u_k u_j u_n u_m} + G_{ikl}\left[\overline{u_k u_l u_j u_n u_m} - V_{kl}\overline{u_j u_n u_m}\right] + G_{iklm'}\left[\overline{u_k u_l u_m, u_j u_n u_m} - \overline{u_k u_l u_m, u_j u_n u_m}\right] + \frac{1}{2}\left(V_{nm}\overline{b^2}_{ij} + V_{jn}\overline{b^2}_{im} + V_{jm}\overline{b^2}_{in}\right). \tag{5C.3c}$$

For given b_{ij}, the equations (5C.3a-c) reveal a unique relationship between a fourth-order RANS model with the stochastic model that applies (5C.1): the stochastic model provides the acceleration correlations that are needed to close the fourth-order RANS model, and, vice versa, the coefficients that appear in (5C.1) can be determined for every choice of acceleration correlations. This relationship reveals the physical relevance of G_{ij}, G_{ijk} and G_{ijkl}: they provide information about the dynamics of second-, third- and fourth-order moments, respectively, in stochastic models.

5C.3. Comparisons with other methods

Compared to methods used previously for simulations of flows that involve coherent structures, see the references given in Appendix 5C.1, the cubic stochastic model reveals an essential agreement given by the inclusion of the dynamics of third- and fourth-order moments. However, there are also significant differences.

Nonlinear stochastic models that differ from the cubic model can be constructed by specifying a solution to a Fokker-Planck equation (Risken 1984; Thomson 1987). To illustrate this, we consider the nonlinear stochastic model (5A.2a-c) without scalars. The Fokker-Planck equation for the velocity PDF $F_u(\mathbf{w}, \mathbf{x}, t) = \overline{\delta(\mathbf{U}(\mathbf{x},t)-\mathbf{w})}$ is given by (5A.3) if F is replaced there by F_u and the second line is neglected. The assumed knowledge of F_u then enables the calculation of $\mathbf{\Gamma}$ by

$$\Gamma_i = \frac{1}{2F_u}\frac{\partial b^2{}_{ij}F_u}{\partial w_j} + \frac{\varphi_i}{F_u} - F_i, \tag{5C.4}$$

provided that singularities do not arise from this assumed solution and the boundary conditions applied (Risken 1984). φ_i satisfies the equation

$$\frac{\partial\langle\rho\rangle\varphi_i}{\partial w_i} = -\frac{\partial}{\partial t}\langle\rho\rangle F_u - \frac{\partial}{\partial x_i}\langle\rho\rangle w_i F_u \tag{5C.5}$$

in conjunction with the boundary condition $\boldsymbol{\varphi} \to 0$ for $|\mathbf{w}| \to \infty$ (Thomson 1987). The comparison of (5C.4) with (5A.11) reveals the relationship between φ_i and the conditional acceleration,

$$\varphi_i = \overline{A_i\big|\mathbf{w}}\, F_u. \tag{5C.6}$$

By comparing the cubic stochastic model with a model that applies (5C.4) for $\mathbf{\Gamma}$ in conjunction with a specification of the (asymptotic) limiting PDF F_u for instance as a fourth-order SML PDF, one observes essential differences. First, due to changes in space and time, buoyancy or chemical reactions (if scalars are involved), the limiting PDF which results from the cubic model has a non-analytical form in

general. Just these effects on the velocity field have to be neglected if any analytical PDF shape is assumed for the limiting PDF F_u. Consequently, the cubic stochastic model is more flexible than a model based on the use of (5C.4). The differences between these two model types will be shown in the next subsection.

In comparison to existing third- or fourth-order RANS models it is essential to note that the dynamics of third- or fourth-order moments were not considered previously (according to the author's knowledge) in acceleration models but only in conjunction with the treatment of turbulent transport. The need to consider such contributions results from the explanations given above. They simulate the influence of coherent (bimodal) structures on the dissipation in the variance transport equations, as may be seen in terms of (5C.3a). Simple parametrizations of G_{ijk} and G_{ijkl} in (5C.3a-c) could be applied to improve the performance of closure models for such flows.

5C.4. An application to CBL turbulence simulations

The cubic stochastic model could be used for three-dimensional flow simulations, but it will be particularly useful for computations of quasi one-dimensional (wall-bounded, buoyancy-driven, stratified boundary layer) flows, which are highly relevant (Kerstein 1999). An important example for such a flow is given by complex chemical processes in the convective atmospheric boundary layer. The special challenge related to such flow calculations is the simulation of the skewness of the velocity PDF, which has significant effects on the transport of reacting species (Luhar et al. 1996). This will be done now to demonstrate the performance of the cubic stochastic model. Previously, nonlinear stochastic models were developed for the convective atmospheric boundary layer on the basis of (5C.4), see Sawford (1993, 1999), Luhar et al. (1996), Wilson & Sawford (1996) and the references therein. This was done by adopting a superposition of two Gaussian modes as limiting PDF. However, as pointed out in section 2.4, the use of a SML PDF as limiting PDF appears to be a better way. The latter was also suggested by Du et al. (1994a-b), but not applied. Thus, the performance of the cubic stochastic model will be compared to that of a corresponding fourth-order SML PDF.

According to (5A.2b) combined with (5C.1) for $\mathbf{\Gamma}$, the stochastic model for the vertical velocity U_3^* may be written

$$\frac{d}{dt} x_3^* = U_3^*, \tag{5C.7a}$$

$$\frac{d}{dt} U_3^* = G_0 - G_2 \overline{u_3^2} - G_3 \overline{u_3^3} - M U_3^* + b_{33} \frac{dW}{dt}, \tag{5C.7b}$$

x_3	G_0	G_1	G_2	G_3	$\overline{u_3^2}$	$\overline{u_3^3}$
0.06	2.36	$0.78 - 1.08\ C_0$	$-3.12 + 0.31\ C_0$	$2.23 + 0.12\ C_0$	0.22	0.05
0.19	0.89	$0.80 - 0.52\ C_0$	$-1.01 + 0.47\ C_0$	$0.43 - 0.17\ C_0$	0.37	0.16
0.31	0.22	$0.18 - 0.40\ C_0$	$-0.20 + 0.49\ C_0$	$0.13 - 0.20\ C_0$	0.44	0.22
0.44	− 0.15	$-0.20 - 0.44\ C_0$	$0.27 + 0.47\ C_0$	$0.04 - 0.17\ C_0$	0.43	0.22
0.56	− 0.38	$-0.48 - 0.53\ C_0$	$0.42 + 0.45\ C_0$	$-0.03 - 0.13\ C_0$	0.40	0.22
0.69	− 0.64	$-0.78 - 0.72\ C_0$	$0.43 + 0.38\ C_0$	$-0.15 - 0.05\ C_0$	0.33	0.16
0.81	− 0.79	$-0.81 - 1.06\ C_0$	$0.27 + 0.25\ C_0$	$-0.25 + 0.13\ C_0$	0.24	0.09
0.94	− 1.51	$-1.51 - 2.15\ C_0$	$-0.69 - 0.01\ C_0$	$-0.18 + 0.70\ C_0$	0.13	0.04

Table 5.5. The coefficients of the cubic stochastic model (5C.7a-b) according to the water tank data of Luhar et al. (1996).

where the mixing frequency M is considered as a quadratic function of velocities,

$$M = -G_1 - G_2 U_3^* - G_3 \left(U_3^*\right)^2. \tag{5C.8}$$

All the variables involved here are made dimensionless by means of the convective velocity scale w_* and mixing layer height H. For simplicity, this normalization is not indicated. The coefficients G_0, G_1, G_2, G_3 and normalized moments $\overline{u_3 u_3}$ and $\overline{u_3 u_3 u_3}$ were derived from the water tank data of Luhar et al. (1996). This was done by means of (5A.12) and (5C.3a-c), where the mean acceleration and acceleration correlations were calculated by means of the moment transport equations (4A.3a), (4A.4a), (4A.5) and (4A.6). The values obtained are given at the available vertical positions $0 \le x_3 \le 1$ in Table 5.5. Analytical functions were obtained on the basis of these data by linear interpolation. These functions were applied in equation (5C.7b) by replacing x_3 by the actual particle position x_3^*. For b_{33}, the usual parametrization

$$b_{33} = \sqrt{C_0 \varepsilon} \tag{5C.9}$$

was applied, where the dimensionless dissipation rate of turbulent kinetic energy was taken to be $\varepsilon = 0.4$ (Luhar et al. 1996). The only unknown is then the constant C_0, which will be estimated below.

Boundary conditions for the particle motion were applied according to the analysis of Thomson & Montgomery (1994). A particle that would leave the computational domain due to its velocity was transported over a part of the time step until it reached the boundary. The incident velocity v_i at the boundary was

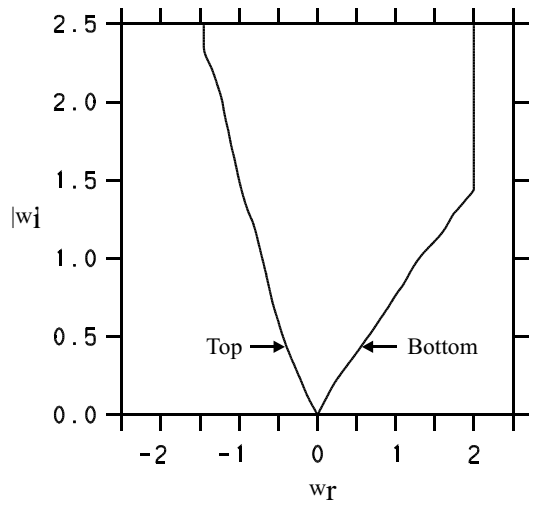

Fig. 5.18. The reflected velocity w_r in dependence on the incident velocity w_i at the lower and upper boundaries according to equation (5C.10).

then replaced by the reflected velocity v_r. The latter velocity satisfies the equation

$$0 = \int_{w_r}^{\infty} dw_3 F_3 w_3 + \int_{-\infty}^{w_i} dw_3 F_3 w_3. \qquad (5C.10)$$

w_3 is the normalized vertical sample space velocity and $F_3 = \overline{\delta(u_3 - w_3)}$ its PDF. All the details on this equation, which assures the correct PDF at the boundaries, may be found elsewhere (Thomson & Montgomery 1994). The relationship between the incident and reflected velocity is shown in Fig. 5.18, where the measured vertical velocity PDF was applied in (5C.10). After replacing the particle velocity at the boundary, the particle was transported over the remaining part of the time step with the new velocity.

The equations (5C.7a-b) were solved numerically with boundary conditions according to (5C.10). For that, 5 10^5 particles and a time step dt = 0.003 were applied. According to the measurements, the PDF was obtained by means of the particles which were found within 8 intervals in the x_3-domain. For each of these intervals, intervals $dw_3 = 0.1$ were applied to calculate the value of F_3 at w_3. The lower and upper boundaries were taken at $x_3 = 1 / 16$ and $x_3 = 15 / 16$, respectively.

To find an optimal value for the constant C_0 in (5C.7a-b), it is helpful to have a closer look at the mixing frequency M, which may be written

$$M = -G_1 \left\{ \left(1 + \frac{G_2}{2G_1} U_3^* \right)^2 + \left[4G_1 G_3 - G_2^2 \right] \left(\frac{U_3^*}{2G_1} \right)^2 \right\}. \qquad (5C.11)$$

We have to demand that M is positive so that velocity fluctuations relax. The coefficient G_1 is negative if we choose $C_0 \geq 1.54$, see Table 5.5. Hence, $M \geq 0$ provided $4 G_1 G_3 \geq G_2^2$. One may prove by means of the data given in Table 5.5

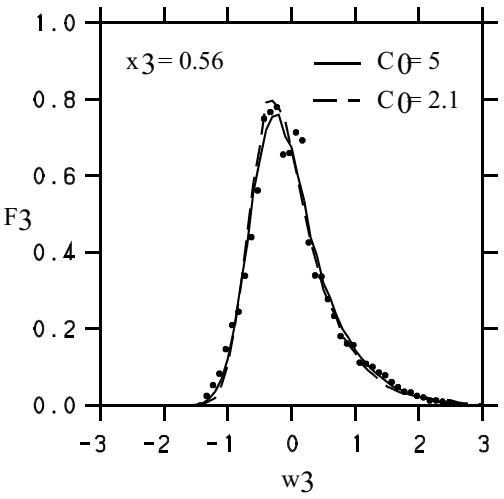

Fig. 5.19. The predictions of the cubic stochastic model (5C.7a-b) for the PDF F_3 of normalized vertical velocities w_3 at $x_3 = 0.56$, where different values for C_0 are applied. The results of the water tank experiments (Luhar et al. 1996) are given as dots.

that the latter constraint is satisfied for the bulk of the CBL ($0.19 \leq x_3 \leq 0.69$) provided that $C_0 \geq 3$. For values $C_0 > 3$, we have inside the bracket of (5C.11) two independent, positive contributions which cannot vanish simultaneously. Thus, $M > 0$ in this case. The choice $C_0 = 3$ implies that the last term in (5C.11) is small for the bulk of the CBL. The minimum of M is then zero, which is a plausible assumption. Hence, this consideration suggests the choice $C_0 = 3$. The suitability of choosing this value for C_0 is confirmed by Fig. 5.19, where the influence of C_0 variations on the vertical velocity PDF is shown. It is also worth noting that the choice $C_0 = 3$ agrees very well with the C_0 findings and corresponding conclusions presented in section 5.4.

The stationary predictions of the cubic stochastic model (5C.7a-b) and corresponding fourth-order SML PDF model (2.55) are compared to the results of the water tank measurements of Luhar et al. (1996) in Fig. 5.20. As may be seen, there is a good agreement between the calculated PDFs and measurements. In particular, the typical skewness of the velocity PDF is well represented. The appearance of this skewness is explained in terms of the cubic stochastic model by a significant difference of the mixing intensity for negative and positive velocities. M is approximately given by $M = 1.8\ (1 - 0.5\ U_3^*)^2$ in the middle of the CBL. Thus, we find for instance $M(U_3^* = -1) = 9\ M(U_3^* = 1)$. All the modeled PDFs underpredict somewhat the probability of the appearance of very small velocities in the upper CBL, see Fig. 5.20f. The predictions of the fourth-order SML PDF model agree, basically, with those obtained by means of a superposition of two Gaussian PDFs (Luhar et al. 1996). This is of interest because there is one fitting parameter more available in the latter model, and confirms the reasoning for the choice of a SML PDF as limiting PDF. As expected, the performance of the cubic stochastic model is somewhat better than that of the fourth-order SML PDF model (with the exception at $x_3 = 0.19$ where the model coefficients change strongly).

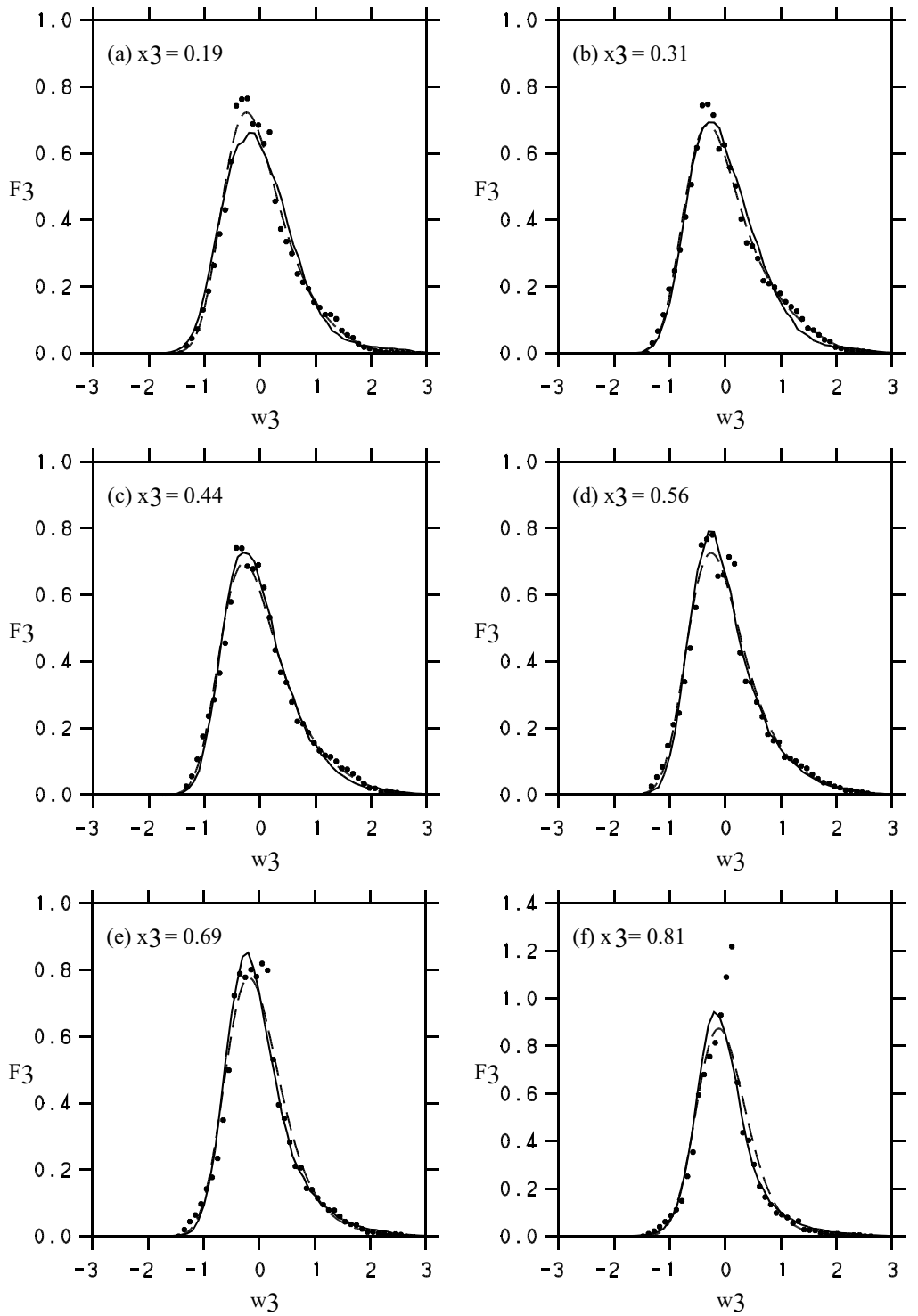

Fig. 5.20. The same comparison as in Fig. 5.19, but now for different heights x_3. For the constant C_0, the value $C_0 = 3$ is applied. The dashed line represents here the corresponding prediction of the fourth-order SML PDF model.

6. Stochastic models for small-scale turbulence

It was explained in section 4.5 that the calculation of turbulent reacting flows by means of DNS is found to be unfeasible for many relevant flows. The simplest way to overcome this problem is the use of RANS equations for ensemble-averaged variables. The problems related to the application of RANS equations to reacting flow simulations were pointed out in section 4.6. They can be solved by extending RANS to PDF methods, which was discussed in chapter 5. However, the complexity of PDF methods and their related RANS methods was found to be correlated with the complexity of the flow considered: the simulation of binary mixing requires the inclusion of memory effects in scalar equations, the calculation of compressible flows requires the parametrization of the reduction of the energy redistribution due to structural compressibility effects, and the simulation of coherent structures requires the introduction of nonlinear stochastic models. The reason for the need to consider complex models for complex flows was explained in the introduction: it is given by the reference to ensemble-averaged fluid dynamic variables. The latter represent fluid properties on a relatively coarser scale such that fluctuations may be large and may reveal a complicated behaviour.

The need to use specific models for specific phenomena implies the requirement to provide evidence for such extensions of simple standard models. This is expensive and often complicated due to the lack of suitable data for comparisons. A convenient way to tackle this problem is to construct equations for spatially-filtered variables as an alternative to RANS equations. This is done in large eddy simulation (LES) methods (Piomelli 1999; Pope 2000; Menevau & Katz 2000; Sagaut 2002). The motivation for this approach is the hope that simple standard models turn out to be well applicable for a wide range of flows since large-scale processes are resolved without additional approximations. Nevertheless, the use of LES requires the modeling of small-scale, subgrid scale (SGS) processes. Thus, the application of LES to reacting flows is faced with the same problem as RANS methods: such equations are characterized by the appearance of unknown filtered reaction rates for which accurate parametrizations are unavailable in general.

A way to overcome this problem is the use of the PDF methodology to extend LES equations to equations for instantaneous velocities and scalars. This was suggested by Givi (1989) and applied first by Madnia & Givi (1993). Pope (1990) introduced the concept of a filter density function (FDF), which is essentially the

S. Heinz, *Statistical Mechanics of Turbulent Flows*

PDF of SGS variables. He showed that the use of this methodology offers for reacting flow simulations the same advantage as the use of PDF methods: chemical reactions appear in a closed form. Gao & O'Brien (1993) developed a transport equation for the scalar FDF and offered suggestions for modeling of the unclosed terms in this equation. Basically, until now FDF methods have been used by applying them as hybrid methods where the velocity field is calculated by means of conventional LES equations and scalar transport by a FDF transport equation (Colucci et al. 1998; Réveillon & Vervisch 1998; Jaberi et al. 1999; Zhou & Pereira 2000). A more general method is the stochastic simulation of both velocity and scalar fields. Such calculations are feasible, as shown by Gicquel et al. (2002) who performed FDF simulations of velocity fields. Nevertheless, it turned out that a very large effort is needed to use velocity-scalar FDF methods: the simulation of velocity fields is six times less expensive than DNS, but it requires 15 - 30 times more effort than LES methods (Gicquel et al. 2002). This fact also has consequences for the investigation of the performance of FDF equations, which could be studied previously only by simulations of one type of a three-dimensional flow: a temporally developing mixing layer with a Reynolds number Re = 50 - 400 (Colucci et al. 1998; Jaberi et al. 1999; Gicquel et al. 2002).

A more general way to address the suitability of FDF models is to investigate their consequences analytically. This will be done here by following closely a publication of the author (Heinz 2003b). We consider the simplest model for the dynamics of SGS fluctuations, which may be seen as the analysis of a limiting case. Then, we compare the analytical implications of this FDF model with well-investigated standard SGS models. One may expect to obtain generalizations of existing methods in this way (the FDF model considered would be too simple in the other case), which can be used to assess the range of applicability of standard models. In particular, one obtains generalizations on the basis of a consistent model for the dynamics of SGS fluctuations, which is relevant as pointed out in Appendix 5B. On the other hand, such comparisons enable conclusions on the structure of FDF equations. As demonstrated below, they can be used for instance for the solution of the important problem of the parametrization of the model coefficients (which includes the model parameter choice).

The organization of this chapter is such that existing models for velocities and scalars will be combined to a model for the joint velocity-scalar FDF in section 6.1. This model will be used in section 6.2 to derive closed LES equations for the velocity field. The consideration of filtered velocities instead of the instantaneous ones implies then the need to decouple the scalar dynamics from the joint velocity-scalars dynamics. This reduction will be performed in section 6.3. The findings obtained will be summarized in section 6.4 with regard to the questions of the generalization of standard models and suitability of the FDF model considered.

6.1. The generalization of LES by FDF methods

First, let us consider LES equations in order to explain the need for their generalization by FDF methods. To obtain these equations, one has to introduce a spatial filter operation. We define the mass density-weighted filtered value of an arbitrary function Q of velocities $\mathbf{U}(\mathbf{x}, t) = (U_1, U_2, U_3)$ and scalars (the mass fractions of N species and temperature) $\mathbf{\Phi}(\mathbf{x}, t) = (\Phi_1, \ldots, \Phi_{N+1})$ by

$$\overline{Q} = \langle\rho\rangle^{-1}\langle\rho Q\rangle. \tag{6.1}$$

$\rho(\mathbf{x}, t)$ is the instantaneous mass density, and $<\cdots>$ refers here to a spatial filtering,

$$\langle\rho(\mathbf{x},t)Q(\mathbf{x},t)\rangle = \int d\mathbf{r}\ \rho(\mathbf{x}+\mathbf{r},t)\,Q(\mathbf{x}+\mathbf{r},t)\,G(\mathbf{r}). \tag{6.2}$$

The filter function G is assumed to be homogeneous, i.e., independent of $\mathbf{x}$. We assume $\int d\mathbf{r}\ G(\mathbf{r}) = 1$ and $G(\mathbf{r}) = G(-\mathbf{r})$. Moreover, only positive filter functions (Vreman et al. 1994) are considered, for which all the moments $\int d\mathbf{r}\ r^m\ G(\mathbf{r})$ exist for $m \geq 0$ (Colucci et al. 1998). It is worth noting that the definition (6.2) provides a bridge between non-filtered and ensemble-averaged variables. The second moment of G is typically used to determine the filter width Δ. For $\Delta \to 0$, G becomes a delta function so that $<\rho\ Q> = \rho\ Q$. The other limit case $\Delta \to \infty$ is given if G is chosen to be independent of $\mathbf{r}$, $G^{-1} = \int d\mathbf{r}$. Then, the box volume used for the spatial filtering is much larger than the characteristic eddy volume, which is one way to define the ensemble average, see the explanations given in chapter 1.

6.1.1. The unclosed LES equations

The filtering of the basic equations (4.71a-d) results in the following LES equations for the filtered mass density $<\rho>$, velocities $\overline{U}_i$ and scalars $\overline{\Phi}_\alpha$,

$$\frac{\partial\langle\rho\rangle}{\partial t} + \overline{U}_k\frac{\partial\langle\rho\rangle}{\partial x_k} = -\langle\rho\rangle\overline{S}_{kk}, \tag{6.3a}$$

$$\frac{\partial\overline{U}_i}{\partial t} + \overline{U}_k\frac{\partial\overline{U}_i}{\partial x_k} + \langle\rho\rangle^{-1}\frac{\partial\langle\rho\rangle\overline{u_k u_i}}{\partial x_k} = \frac{2}{\langle\rho\rangle}\frac{\partial}{\partial x_k}\langle\rho\rangle\nu\overline{S}_{ik}^{\,d} - \frac{1}{\langle\rho\rangle}\frac{\partial\langle p\rangle}{\partial x_i} + \overline{F}_i, \tag{6.3b}$$

$$\frac{\partial\overline{\Phi}_\alpha}{\partial t} + \overline{U}_k\frac{\partial\overline{\Phi}_\alpha}{\partial x_k} + \langle\rho\rangle^{-1}\frac{\partial\langle\rho\rangle\overline{u_k\phi_\alpha}}{\partial x_k} = \frac{1}{\langle\rho\rangle}\frac{\partial}{\partial x_k}\langle\rho\rangle\nu_{(\alpha)}\frac{\partial\overline{\Phi}_\alpha}{\partial x_k} + \overline{S}_\alpha. \tag{6.3c}$$

Repeated indices imply summation with the exception of subscripts in parentheses. F_i is any external force (the acceleration due to gravity), $p = p(\rho, \mathbf{\Phi})$ the pressure

that is defined via the thermal equation of state, and S_α denotes a known source rate. S_{ik}^d is the deviatoric part of the rate-of-strain tensor and ν the kinematic viscosity, which is considered to be constant for simplicity. $\nu_{(\alpha)}$ is the molecular or thermal diffusivity in dependence on α. To derive the first term on the right-hand side of (6.3b), we assumed that $\overline{\partial U_i/\partial x_k} = \partial\overline{U}_i/\partial x_k$. A corresponding relation is used regarding the derivation of the first term on the right-hand side of (6.3c). The expressions $\overline{u_k u_i}$ and $\overline{u_k \phi_\alpha}$ on the left-hand sides of (6.3b-c) are called the SGS stress tensor and SGS scalar flux, respectively. As before, $\overline{u_k u_i}$ and $\overline{u_k \phi_\alpha}$ denote elements of variance matrices of velocities and scalars (e.g., the velocity variance matrix V applied below has elements $V_{ik} = \overline{u_i u_k}$). These quantities are defined by the following right-hand sides,

$$\overline{u_k u_i} = \overline{U_k U_i} - \overline{U}_k \overline{U}_i, \qquad \overline{u_k \phi_\alpha} = \overline{U_k \Phi_\alpha} - \overline{U}_k \overline{\Phi}_\alpha. \tag{6.4}$$

It is relevant to emphasize that the right-hand sides of (6.4) do not involve double-filtering operations. Thus, they cannot be obtained in general by considering u_i and ϕ_α as fluctuations of U_i and Φ_α, and applying the filter operation (6.1) on $u_k u_i$ and $u_k \phi_\alpha$, respectively. The latter recovers the right-hand sides of (6.4) only in the case that a filtered variable is unchanged by filtering it once more, as it is given for instance for ensemble means.

The problem that has to be solved in order to use (6.3a-c) for turbulent reacting flow simulations is to provide closures for the unknowns $\overline{u_k u_i}$ and $\overline{u_k \phi_\alpha}$ and $\overline{S}_\alpha$. To calculate these terms, one needs a model for fluctuations of SGS variables.

6.1.2. The stochastic model considered

Such a model is given by the following stochastic equations for the dynamics of particle positions x_i^*, velocities U_i^* and scalars Φ_α^* (the vector of mass fractions of species and temperature),

$$\frac{d}{dt} x_i^* = U_i^*, \tag{6.5a}$$

$$\frac{d}{dt} U_i^* = \overline{\Gamma}_i - \frac{1}{\tau_L}\left(U_i^* - \overline{U}_i\right) + \overline{F}_i + \sqrt{C_0 \varepsilon_r}\,\frac{dW_i}{dt}, \tag{6.5b}$$

$$\frac{d}{dt} \Phi_\alpha^* = \overline{\Omega}_\alpha - \frac{1}{\tau_\varphi}\left(\Phi_\alpha^* - \overline{\Phi}_\alpha\right) + G_{\alpha m}\left(U_m^* - \overline{U}_m\right) + S_\alpha. \tag{6.5c}$$

$\overline{\Gamma}_i + \overline{F}_i$ and $\overline{\Omega}_\alpha + \overline{S}_\alpha$ determine the dynamics of resolved velocities $\overline{U}_i$ and scalars $\overline{\Phi}_\alpha$, as may be seen by filtering these equations. In correspondence to the relations (5.91), they are given by

$$\overline{\Gamma}_i = 2\langle\rho\rangle^{-1}\frac{\partial}{\partial x_k}\langle\rho\rangle\nu\overline{S}_{ik}{}^{d} - \langle\rho\rangle^{-1}\frac{\partial\langle p\rangle}{\partial x_i}, \qquad \overline{\Omega}_\alpha = \langle\rho\rangle^{-1}\frac{\partial}{\partial x_k}\langle\rho\rangle\nu_{(\alpha)}\frac{\partial\overline{\Phi}_\alpha}{\partial x_k}. \quad (6.6)$$

The second terms on the right-hand sides of (6.5b-c) involve the most relevant assumptions. They model the relaxation of velocity and scalar fluctuations. It is assumed that all the velocity fluctuations relax with the same frequency. τ_L and τ_φ are characteristic relaxation times that have to be estimated. The body force in the velocity equation (6.5b) is assumed to be independent of actual velocities and scalars, $F_i = \overline{F}_i$. This simplifies the explanations given in section 6.2 because $\overline{F}_i$ does not affect the calculation of the SGS stress tensor. The Boussinesq approximation described in section 4.4.6 is not covered in this way. Instead, compressibility effects can be taken into account as explained in section 6.2. The appearance of the term related to velocity fluctuations in the scalar equation (6.5c) is a consequence of assuming a locally isotropic dissipation of the scalar field. According to the explanations given in Appendix 5B, $G_{\alpha m}$ is determined by

$$G_{\alpha m} = \frac{1}{\tau_\varphi}\,\overline{\phi_\alpha u_i}V^{-1}{}_{im}. \quad (6.7)$$

V^{-1} refers to the inverse velocity variance matrix V with elements $V_{ik} = \overline{u_i u_k}$. The last term in (6.5b) generates velocity fluctuations. dW_i / dt is a Gaussian process with vanishing means and uncorrelated values at different times, see (3.43a-b). The coefficient of dW_i / dt has the same structure as in PDF methods. The residual dissipation rate of turbulent kinetic energy ε_r will be defined below, and C_0 is a constant that has to be estimated. A corresponding stochastic source term in the scalar equation (6.5c) is not considered. Such a term is needed within the frame of PDF methods to simulate the loss of information about the initial PDF in time, see the discussion in section 5.5. However, most of the scalar spectrum is resolved here so that there is no need to involve such a term. No assumption has to be made regarding the source term S_α in the scalar equation (6.5c).

The equations (6.5a-c) for the dynamics of SGS fluctuations were validated by simulations of various two-dimensional jets and mixing layers and a three-dimensional temporally developing mixing layer. The good performance of the velocity equation (6.5b) (without body force) was proved by Gicquel et al. (2002). The performance of the scalar equation (6.5c) combined with a conventional LES equation for the velocity field was investigated by Colucci et al. (1998), Jaberi et al. (1999) and Zhou & Pereira (2000). The term that involves velocity fluctuations in (6.5c) had to be neglected in these simulations because velocity fluctuations were not involved. The consideration of (6.5a-c) can also be justified with the argument that their analysis is equivalent to the consideration of a limiting case:

these equations (6.5a-c) represent the most simple model for the dynamics of SGS fluctuations that can be applied.

It is worth noting that the solution of the equations (6.5a-c) overcomes the closure problems related to the LES equations (6.3a-c). The equations (6.5a-c) are closed for specified τ_L, τ_φ and C_0 (which will be determined below), and the expressions (6.6) assure that the transport of filtered variables is calculated in full consistency with the LES equations (6.3a-c).

6.1.3. The closure of LES equations

According to the concept pointed out in the beginning of this chapter, we will use the stochastic model (6.5a-c) to provide closures for unknown terms in the LES equations (6.3a-c). This can be done in the following way. The stochastic model determines the joint velocity-scalar FDF that is defined by

$$F(\mathbf{w},\boldsymbol{\theta},\mathbf{x},t)=\overline{\delta(\mathbf{U}(\mathbf{x},t)-\mathbf{w})\delta(\boldsymbol{\Phi}(\mathbf{x},t)-\boldsymbol{\theta})}. \tag{6.8}$$

Its transport equation can be derived from the equations (6.5a-c) by means of standard methods. It reads (Gardiner 1983; Risken 1984; Pope 2000)

$$\frac{\partial}{\partial t}\langle\rho\rangle F+\frac{\partial}{\partial x_i}\langle\rho\rangle w_i F=-\frac{\partial}{\partial w_i}\langle\rho\rangle\left[\overline{\Gamma}_i-\frac{1}{\tau_L}\left(w_i-\overline{U}_i\right)+\overline{F}_i\right]F+\frac{1}{2}\frac{\partial^2\langle\rho\rangle C_0\varepsilon_r F}{\partial w_j\partial w_j}$$

$$-\frac{\partial}{\partial\theta_\alpha}\langle\rho\rangle\left[\overline{\Omega}_\alpha-\frac{1}{\tau_\varphi}\left(\theta_\alpha-\overline{\Phi}_\alpha\right)+G_{\alpha m}\left(w_m-\overline{U}_m\right)+S_\alpha\right]F. \tag{6.9}$$

The closure of the velocity equation (6.3b) requires the calculation of the SGS stress tensor. An equation for it can be obtained by multiplying (6.9) with w_i w_j and integrating it over the velocity-scalar space,

$$\frac{\partial\overline{u_iu_j}}{\partial t}+\overline{U}_k\frac{\partial\overline{u_iu_j}}{\partial x_k}+\frac{1}{\langle\rho\rangle}\frac{\partial\langle\rho\rangle\overline{u_ku_iu_j}}{\partial x_k}+\overline{u_ku_j}\frac{\partial\overline{U}_i}{\partial x_k}+\overline{u_ku_i}\frac{\partial\overline{U}_j}{\partial x_k}=-\frac{2}{\tau_L}\overline{u_iu_j}+C_0\varepsilon_r\delta_{ij}. \tag{6.10}$$

In correspondence to the definition of the SGS stress tensor, $\overline{u_ku_iu_j}$ is defined by

$$\overline{u_ku_iu_j}=\overline{U_kU_iU_j}-\overline{U}_k\overline{U}_i\overline{U}_j-\overline{U}_k\overline{u_iu_j}-\overline{U}_i\overline{u_ku_j}-\overline{U}_j\overline{u_ku_i}, \tag{6.11}$$

where the first part of (6.4) has to be applied on the right-hand side. $\overline{u_ku_iu_j}$ can be calculated in analogy to the treatment of the heat flux vector in section 4.3.2 (only the variables have to be reinterpreted), such that (6.10) provides a closed equation

for the SGS stress tensor. It will be shown in section 6.2 how an algebraic expression for the SGS stress tensor can be obtained on the basis of this equation.

The SGS scalar flux $\overline{u_i\phi_\alpha}$, which is needed to close the filtered scalar equation (6.3c), can be calculated analogously. However, this methodology cannot be applied in general to obtain a suitable expression for the source rate $\overline{S}_\alpha$, see the explanations in section 4.6.3 with regard to the corresponding problem in RANS equations. A closure model for the filtered source rate $\overline{S}_\alpha$ in (6.3c) requires the knowledge of the scalar FDF F_φ. Having this, $\overline{S}_\alpha$ could be obtained by integration,

$$\overline{S}_\alpha = \int d\boldsymbol{\theta}\, S_\alpha(\boldsymbol{\theta})\, F_\varphi(\boldsymbol{\theta}, \mathbf{x}, t). \tag{6.12}$$

One way to provide F_φ is its direct parametrization by an analytical shape, see section 6.3. However, it will be shown there that this assumed-shape FDF approach is related to relatively strong assumptions, which are not satisfied in general. A much more flexible approach is to calculate the scalar FDF by means of a transport equation. Because we only consider filtered instead of instantaneous velocities here, this implies the need to decouple the scalar dynamics from the dynamics of velocity fluctuations. This can be done as pointed out next.

6.1.4. Hybrid methods

The transport equation for the scalar FDF $F_\varphi(\boldsymbol{\theta}, \mathbf{x}, t) = \overline{\delta(\boldsymbol{\Phi}(\mathbf{x},t) - \boldsymbol{\theta})}$ can be obtained by integrating (6.9) over the velocity space. This results in

$$\frac{\partial}{\partial t}\langle\rho\rangle F_\varphi = -\frac{\partial\langle\rho\rangle\left(\overline{U}_i + \overline{u_i|\,\boldsymbol{\theta}}\right)F_\varphi}{\partial x_i} - \frac{\partial}{\partial\theta_\alpha}\langle\rho\rangle\left[\overline{\Omega}_\alpha - \frac{\theta_\alpha - \overline{\Phi}_\alpha}{\tau_\varphi} + G_{\alpha m}\overline{u_m|\,\boldsymbol{\theta}} + S_\alpha\right]F_\varphi. \tag{6.13}$$

The closure of this equation requires the determination of the scalar-conditioned convective flux

$$\overline{u_i|\,\boldsymbol{\theta}} = F_\varphi^{-1}\overline{U_i\delta(\boldsymbol{\Phi} - \boldsymbol{\theta})} - \overline{U}_i. \tag{6.14}$$

This scalar-conditioned convective flux can be calculated on the basis of its transport equation which follows from (6.9). This will be shown in section 6.3. One obtains in this way a hybrid method where the velocity field is calculated via a transport equation for filtered velocities and the transport of scalars by stochastic equations that correspond to (6.13). This hybrid approach represents a step in between the consideration of a velocity-scalar FDF transport equation and its implied velocity-scalar LES equations, see Fig. 6.1 for an illustration.

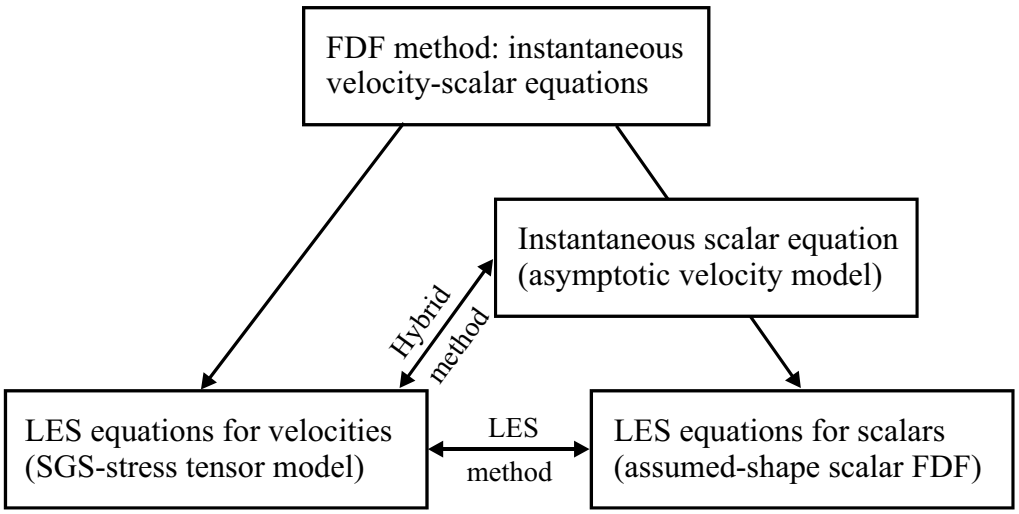

Fig. 6.1. An illustration of the reduction of velocity-scalar FDF methods to LES and hybrid methods (in analogy to the corresponding reduction of velocity-scalar PDF methods, see the explanations of Fig. 5.17).

6.2. The closure of the equation for filtered velocities

First, we follow the concept for the closure of the velocity LES equation (6.3b) by a parametrization of the SGS stress tensor $\overline{u_k u_i}$, see section 6.1.3.

6.2.1. The transport equation for the SGS stress tensor

For that, it is convenient to split $\overline{u_k u_i}$ into the anisotropic residual stress tensor

$$\tau_{ij} = \overline{u_i u_j} - \frac{2}{3} k_r \delta_{ij} \tag{6.15}$$

and isotropic part $2k_r / 3\ \delta_{ij}$. Here, $k_r = \overline{u_i u_i} / 2$ refers to the residual turbulent kinetic energy. The equations for τ_{ij} and k_r are given by (6.10). They read

$$\frac{\partial \tau_{ij}}{\partial t} + \overline{U}_k \frac{\partial \tau_{ij}}{\partial x_k} + \langle \rho \rangle^{-1} \frac{\partial \langle \rho \rangle \overline{u_k (u_i u_j - u_l u_l \delta_{ij}/3)}}{\partial x_k} = -\frac{\partial \overline{U}_i}{\partial x_k} \tau_{kj} - \frac{\partial \overline{U}_j}{\partial x_k} \tau_{ki} - \frac{4}{3} k_r \overline{S}_{ij} -$$

$$- \frac{2}{\tau_L} \tau_{ij} - \frac{2}{3} P_r \delta_{ij}, \tag{6.16a}$$

$$\frac{\partial k_r}{\partial t} + \overline{U}_k \frac{\partial k_r}{\partial x_k} + \frac{1}{2} \langle \rho \rangle^{-1} \frac{\partial \langle \rho \rangle \overline{u_k u_l u_l}}{\partial x_k} = P_r - \varepsilon_r. \tag{6.16b}$$

$P_r = -\overline{u_k u_i}\ \overline{S}_{ki}$ denotes the production of residual turbulent kinetic energy, and the dissipation rate ε_r is given by $\varepsilon_r = 2\ k_r / [(1 + 1.5\ C_0)\ \tau_L]$. The model (6.16a-b) determines the SGS stress tensor provided τ_L and C_0 are given, and the triple correlations are parametrized as described for instance in section 4.3.2.

6.2.2. The general algebraic expression for the SGS stress tensor

To derive an algebraic expression for the SGS stress tensor we neglect the left-hand sides of the equations (6.16a-b) in comparison to the terms on the right-hand sides. This results in

$$B^*_{ik}\left(S^*_{kj} - \Sigma^*_{kj} + \frac{1}{2}\delta_{kj}\right) + B^*_{jk}\left(S^*_{ki} - \Sigma^*_{ki} + \frac{1}{2}\delta_{ki}\right) = -S^*_{ij} + \frac{2}{3}B^*_{kl}S^*_{lk}\delta_{ij}, \quad (6.17a)$$

$$B^*_{kl}S^*_{lk} = -\frac{3}{4}\left(1 - \frac{1}{1+\tau_L\overline{S}_{nn}/3}\ \frac{C_0}{C_0 + 2/3}\right), \quad (6.17b)$$

where the following abbreviations are used,

$$B^*_{ij} = \frac{3}{4}\frac{\tau_{ij}}{k_r}, \quad S^*_{ij} = \frac{\tau_L}{2}\ \frac{1}{1+\tau_L\overline{S}_{nn}/3}\left(\overline{S}_{ij} - \frac{1}{3}\overline{S}_{nn}\delta_{ij}\right), \quad \Sigma^*_{ij} = \frac{\tau_L}{2}\ \frac{1}{1+\tau_L\overline{S}_{nn}/3}\overline{\Sigma}_{ij}. \quad (6.18)$$

$\Sigma_{ij} = ½\ [\partial U_i / \partial x_j - \partial U_j / \partial x_i]$ refers to the rate-of-rotation tensor. Relation (6.17b) follows from the definition $P_r = -\ \overline{u_i u_k}\ \overline{S}_{ki}$ and $P_r = \varepsilon_r = 2\ k_r / [(1 + 1.5\ C_0)\ \tau_L]$, which is implied by (6.16b).

There are different ways to solve the algebraic equation (6.17a) exactly (see Risken 1984 p. 155), but the presentation of its solution by means of an integrity basis is the most convenient way because it allows explicit comparisons with other methods. For that, we restrict the development to the consideration of an incompressible flow. This allows the use of a technique that was developed by Pope (1975) and applied by Gatski & Speziale (1993). Nevertheless, the explanations given below show that the incorporation of compressibility effects is straightforward. Correspondingly, the general solution to (6.17a) may be written

$$B^* = \sum_{\lambda=1}^{9} G^{(\lambda)}T^{(\lambda)}. \quad (6.19)$$

The integrity basis $T^{(\lambda)}$ and coefficients $G^{(\lambda)}$ are given in Table 6.1. In the relations for the coefficients $G^{(\lambda)}$ one finds the following irreducible invariants of S^* and Σ^*,

$$\eta_1 = \left\{S^{*2}\right\}, \quad \eta_2 = \left\{\Sigma^{*2}\right\}, \quad \eta_3 = \left\{S^{*3}\right\}, \quad \eta_4 = \left\{S^*\Sigma^{*2}\right\}, \quad \eta_5 = \left\{S^{*2}\Sigma^{*2}\right\}. \quad (6.20)$$

λ	$T^{(\lambda)}$	$G^{(\lambda)}$
1	S^*	$-(6-3\eta_1-21\eta_2-2\eta_3+30\eta_4)/(2D)$
2	$S^*\Sigma^*-\Sigma^*S^*$	$-(3+3\eta_1-6\eta_2+2\eta_3+6\eta_4)/D$
3	$S^{*2}-\{S^{*2}\}I/3$	$(6-3\eta_1-12\eta_2-2\eta_3-6\eta_4)/D$
4	$\Sigma^{*2}-\{\Sigma^{*2}\}I/3$	$-3(3\eta_1+2\eta_3+6\eta_4)/D$
5	$\Sigma^*S^{*2}-S^{*2}\Sigma^*$	$-9/D$
6	$\Sigma^{*2}S^*+S^*\Sigma^{*2}-2\{S^*\Sigma^{*2}\}I/3$	$-9/D$
7	$\Sigma^*S^*\Sigma^{*2}-\Sigma^{*2}S^*\Sigma^*$	$9/D$
8	$S^*\Sigma^*S^{*2}-S^{*2}\Sigma^*S^*$	$9/D$
9	$\Sigma^{*2}S^{*2}+S^{*2}\Sigma^{*2}-2\{S^{*2}\Sigma^{*2}\}I/3$	$18/D$

Table 6.1. The integrity basis and coefficients that appear in the general algebraic SGS stress tensor model (6.19). $\{\cdots\}$ denotes the trace and I is the unity tensor. The invariants η_1 - η_5 are given by (6.20) and D by (6.21).

The denominator D in the expressions for $G^{(\lambda)}$ is a function of these invariants,

$$D = 3-3.5\eta_1+{\eta_1}^2-7.5\eta_2-8\eta_1\eta_2+3{\eta_2}^2-\eta_3+1.5\eta_1\eta_3-2\eta_2\eta_3+21\eta_4 + 24\eta_5+2\eta_1\eta_4-6\eta_2\eta_4. \tag{6.21}$$

A consequence of the algebraic approximation considered is that relation (6.17b), which represents the algebraic version of the k_r equation (6.16b), provides an equation of 6th-order for τ_L,

$$\frac{D}{C_0+2/3}=\eta_1(6-3\eta_1-21\eta_2+4\eta_3+12\eta_4)-4\eta_3(3-\eta_3-6\eta_4)+36({\eta_4}^2+\eta_5), \tag{6.22}$$

whereas k_r remains unconstrained. Therefore, we have to define τ_L as a function of k_r in order to transform (6.22) into an equation for k_r. This is done by assuming

$$\tau_L=\frac{\ell}{\sqrt{k_r}}=\frac{\ell_*\Delta}{\sqrt{k_r}}, \tag{6.23}$$

where a length scale $\ell = \ell_* \Delta$ is introduced. Here, ℓ_* is any number and Δ the filter width. Hence, we find the SGS stress tensor in dependence on the dimensionless parameters C_0 and ℓ_*. The relation of the algebraic model (6.19) to models usually applied will be considered next.

6.2.3. Linear and quadratic algebraic SGS stress tensor models

First, we consider the simplest version of (6.19) where only shear of first order is taken into account. In this first approximation we find $B^*_{(1)} = - S^*$. In terms of τ_{ij}, the latter may be written

$$\tau_{ij}^{(1)} = -2\nu_r \overline{S}_{ij}, \tag{6.24}$$

where the residual eddy viscosity $\nu_r = k_r \tau_L / 3$ is introduced. Relation (6.24) may also be obtained by neglecting the production in (6.17a), i.e., the first, second, fourth and fifth term on the left-hand side, and the last term on the right-hand side. Equation (6.22) then provides

$$k_r^{(1)} = \frac{1+1.5C_0}{6} \ell_*^{\,2} \Delta^2 |\,\overline{S}\,|_r^{\,2}, \tag{6.25}$$

where we introduced $|\,\overline{S}\,|_r = (2\overline{S}_{kl}\overline{S}_{lk})^{1/2}$. This expression for k_r may be proved by equating ε_r with the production P_r that follows from the use of (6.24). The use of (6.25) in (6.24) then provides

$$\tau_{ij}^{(1)} = -2c_S \Delta^2 |\,\overline{S}\,|_r \overline{S}_{ij}. \tag{6.26}$$

Here, we introduced the parameter c_S, which is given by

$$c_S = \sqrt{\frac{1+1.5C_0}{54} \ell_*^{\,2}}\, \ell_*. \tag{6.27}$$

The comparison of (6.26) with the Smagorinsky model discussed in detail by Pope (2000) reveals that c_S corresponds to the Smagorinsky coefficient.

Two basic methods were applied previously to provide c_S to (6.26): the assumption of a constant c_S, see the corresponding discussion in section 6.2.5, and the dynamic procedure for the determination of c_S (Pope 2000; Sagaut 2002), which is described in Appendix 6A. The idea of the dynamic procedure, which was developed by Germano et al. (1991) and modified by Lilly (1992), is the following. By applying a new filtering (with another filter width) to equation (6.3b) for filtered velocities, one may derive a transport equation for double-filtered velocities. This transport equation contains a correlation that corresponds to τ_{ij}. By assuming that this term can be parametrized in a formal equivalence to (6.26) (and adopting some simplifying assumptions), one can relate c_S to quantities that are known. This offers several methods for its calculation. The point is that c_S found in this way may have negative values. Their appearance is interpreted as backscatter, which describes an energy transfer from the residual motions to the filtered velocity field (the production $P_r = - \tau_{ik}^{(1)} \overline{S}_{ki} = c_S \Delta^2 |\,\overline{S}\,|_r^3$ in the equation

for k_r becomes negative for negative values of c_S), see Piomelli et al. (1991), Liu et al. (1994), Menevau & Katz (2000) and Sagaut (2002).

The requirement for the inclusion of backscatter effects here is the consideration of locally negative values of ℓ_*. This has significant consequences: it corresponds to the consideration of locally negative time scales $\tau_L = \ell_* \, \Delta \, / \, k_r^{1/2}$. It is worth noting that such an approach can be justified. The appearance of linear velocity terms with negative frequencies can be interpreted as stochastic forcing in addition to the last term in (6.5b). Obviously, the condition for the consideration of such terms is to assure that the mean of τ_L is always positive. Nevertheless, it is obvious that the need for the consideration of negative time scales supports the criticism of the concept of the dynamic model, see the discussion by Speziale (1998). First, one has to appreciate that the success of the dynamic calculation of c_S arises from the compensation of deficiencies of (6.26). Second, a relevant argument against this concept is that it exacerbates the problem of constructing unified models (a dynamic model cannot recover a RANS model in the large-Δ limit), see the discussion of this question in chapter 7.

In the next order of approximation, shear contributions up to second-order are considered in (6.19) so that $B^*_{(2)} = - S^* - (S^* \, \Sigma^* - \Sigma^* \, S^*) + 2 \, (S^{*2} - \{S^{*2}\} \, I \, / \, 3)$, or,

$$\tau_{ij}^{(2)} = -2\nu_r \overline{S}_{ij} - \nu_r \tau_L \left(\overline{S}_{ik} \overline{\Sigma}_{kj} - \overline{\Sigma}_{ik} \overline{S}_{kj} \right) + 2\nu_r \tau_L \left(\overline{S}_{ik} \overline{S}_{kj} - \frac{1}{3} \overline{S}_{nk} \overline{S}_{kn} \delta_{ij} \right). \tag{6.28}$$

This expression follows from equation (6.17a) if B^* is replaced in the production terms by $- S^*$ according to the first approximation. Equation (6.22) (or the equality of ε_r with the production P_r that follows from the use of (6.28)) results now in the following expression for k_r,

$$k_r^{(2)} = \frac{1 + 1.5 C_0}{6} \kappa^2 \ell_*^{\,2} \Delta^2 | \, \overline{S} \, |_r^{\,2} \, . \tag{6.29}$$

Here we introduced the positive variable κ that is given as the solution of a third-order equation,

$$0 = \kappa^3 - \kappa + s_* . \tag{6.30}$$

The last term in (6.30) is given by $s_* = \lambda \, s$, where we introduced

$$\lambda = \sqrt{\frac{27}{8 + 12 C_0}}, \qquad s = \frac{\ell_*}{|\, \ell_* \,|} \frac{III_S}{\left(- II_S \right)^{3/2}} . \tag{6.31}$$

Here, s is similar to the generalized skewness function used by Kosović (1997) and defined in terms of the invariants (Lumley 1978)

$$II_S = - | \, \overline{S} \, |_r^{\,2} \, / 4, \qquad III_S = \left\{ \overline{S}^3 \right\} / 3. \tag{6.32}$$

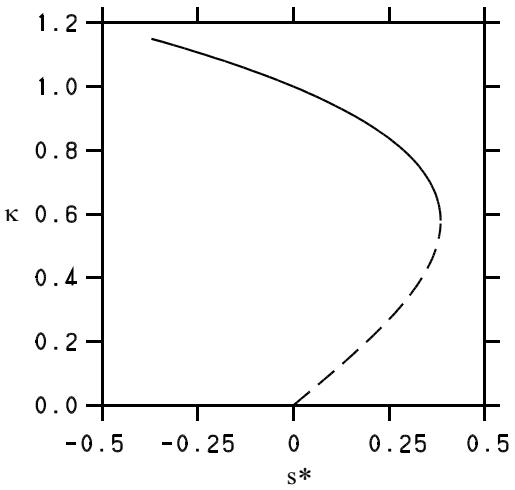

Fig. 6.2. κ as a function of s_* as given by equation (6.30).

The variation of κ is illustrated in Fig. 6.2, which shows all positive solutions of equation (6.30). Their existence requires that $s_* \le 2 / 27^{1/2}$. The dashed curve for the case $\kappa \le 1 / 3^{1/2}$ is unphysical because it is inconsistent with $\kappa = 1$ at $s_* = 0$. The solid curve is given by the relation $\kappa = 2 \cos(\varphi / 3) / 3^{1/2}$, where φ is defined by $\cos(\varphi) = - 3^{3/2} s_* / 2$.

To compare (6.28) with other findings we insert the definitions of $\overline{S}_{ik}$ and $\overline{\Sigma}_{ik}$,

$$\tau_{ij}^{(2)} = -2\kappa c_S \Delta^2 \, | \overline{S} |_r \, \overline{S}_{ij} + \frac{\ell_*^2 \Delta^2}{3} \left[\frac{\partial \overline{U}_i}{\partial x_k} \frac{\partial \overline{U}_j}{\partial x_k} - \frac{\delta_{ij}}{3} \frac{\partial \overline{U}_l}{\partial x_k} \frac{\partial \overline{U}_l}{\partial x_k} + \right.$$

$$\left. + \frac{1}{2} \left(\frac{\partial \overline{U}_i}{\partial x_k} \frac{\partial \overline{U}_k}{\partial x_j} + \frac{\partial \overline{U}_j}{\partial x_k} \frac{\partial \overline{U}_k}{\partial x_i} \right) - \frac{\delta_{ij}}{3} \frac{\partial \overline{U}_l}{\partial x_k} \frac{\partial \overline{U}_k}{\partial x_l} \right]. \qquad (6.33)$$

It is worth emphasizing that the justification for the expression (6.33) obtained for the anisotropic part of the SGS stress tensor arises from the fact that it is implied by the stochastic model (6.5a-c). The available support for (6.5a-c) was described in section 6.1.2. It was pointed out that the consideration of (6.5a-c) corresponds to the analysis of the simplest possible model for the physics of SGS fluctuations. Consequently, (6.33) represents the simplest model for the SGS stress tensor if one includes shear up to second order.

Compared to existing models of this type, the advantage of (6.33) is given by its consistency. First, this concerns the consistent consideration of quadratic shear terms. The model of Clark et al. (1979), for instance, is generalized by the second line of (6.33) (and the bracket factor, which is calculated here in dependence on ℓ_* whereas Clark's model assumes a fixed value $\ell_* = 0.5$). Second, this concerns the consistent calculation of coefficients of linear and quadratic terms. It is of interest to note that the model (6.33) has the same structure as the model applied by

Kosović (1997). However, the latter model applies coefficients of quadratic contributions which are estimated by heuristic arguments and vanish under conditions where backscatter is negligible. In contrast to this, the coefficients of (6.33) are explained (for both the case that backscatter is relevant or not) as functions of the parameters C_0 and ℓ_* of the velocity model (6.5b). For C_0, a theoretical value will be derived in section 6.2.5. The remaining parameter ℓ_* can be estimated by means of the dynamic procedure (6A.1) given in Appendix 6A. This results in the possibility of performing self-consistent flow simulations.

6.2.4. Scaling analysis

An important question concerns the relevance of quadratic shear contributions in relation (6.28) for the anisotropic part of the SGS stress tensor. To address this, we apply (in analogy to the assessment of the relevance of nonlinear shear contributions to the stress tensor in basic equations) a scaling analysis. We scale τ_{ij} in terms of a characteristic velocity scale U_0 and L_0 that characterizes the spatial scale of the flow considered. The rescaled expression (6.28) then reads

$$\tau_{ij}^{+} = -i_r Kn_r \overline{S}_{ij}^{+} + Kn_r^2 \left\{ \overline{S}_{ik}^{+} \overline{S}_{kj}^{+} - \frac{\delta_{ij}}{3} \left\{ \overline{S}^{+} \overline{S}^{+} \right\} - \frac{1}{2} \left(\overline{S}_{ik}^{+} \overline{\Sigma}_{kj}^{+} - \overline{\Sigma}_{ik}^{+} \overline{S}_{kj}^{+} \right) \right\}. \quad (6.34)$$

The plus refers to scaled quantities of order unity. In particular, we introduced

$$\tau_{ij}^{+} = \frac{\tau_{ij}^{(2)}}{U_0^2}, \qquad \overline{S}_{ik}^{+} = \frac{\overline{S}_{ik} L_0}{U_0}, \qquad \overline{\Sigma}_{ik}^{+} = \frac{\overline{\Sigma}_{ik} L_0}{U_0}. \quad (6.35)$$

Further, two dimensionless numbers are used in (6.34), the SGS Knudsen number Kn_r and turbulence intensity i_r. These parameters are given by the expressions

$$Kn_r = \sqrt{\frac{2}{3}} \frac{\ell}{L_0}, \qquad i_r = \frac{1}{U_0} \sqrt{\frac{2k_r}{3}} = \sqrt{\frac{1+1.5C_0}{6}} \kappa |\overline{S}|_r^{+} \left| Kn_r \right|. \quad (6.36)$$

The consideration of the factor $(2 / 3)^{1/2}$ in Kn_r simplifies the writing of (6.34) and the following discussion. The last term for i_r follows from the use of (6.29) for $k_r^{(2)}$.

Expression (6.34) confirms previous conclusions about the significance of quadratic shear contributions (Kosović 1997; Leonard 1997; Winckelmans et al. 1998). According to the last expression of (6.36), i_r and Kn_r are of the same order of magnitude in general so that the quadratic terms in (6.34) cannot be neglected in comparison to the linear term. Apparently, this finding is significantly different to the corresponding result that follows from the consideration of the same problem on the molecular level. It was shown in section 4.3.4 that quadratic contributions to the deviatoric part π_{ij} of the stress tensor p_{ij} are often of negligible relevance.

Nevertheless, it is essential to appreciate that the relevance of quadratic shear contributions to flow simulations depends significantly on the value of Kn_r. One may differentiate three cases in dependence on the setting of Kn_r, which can be chosen by the numerical resolution of the flow. The first case is given for very small values of Kn_r (less than about 0.004 for the conditions considered by Gicquel et al. (2002)): the contribution of the SGS stress tensor model is about $2\ 10^{-5}$ times smaller than other contributions in (6.3b), i.e., it is irrelevant. The second case is given for small values of Kn_r (near 0.03 regarding the studies of Gicquel et al. (2002)): the details of the SGS stress tensor model are of minor relevance to flow simulations in this case such that the neglect of quadratic shear contributions can be compensated by dynamic adjustments of ℓ_*. The third case is given if Kn_r becomes significantly larger than 0.03. The details of the SGS stress tensor model then become essential, this means quadratic shear contributions have to be involved, in particular, with regard to simulations of anisotropic flows.

6.2.5. The theoretical calculation of parameters

Another question related to the analysis of (6.28) concerns the calculation of the model parameters C_0 and ℓ_*. This will be addressed first with regard to C_0. For that, let us have a closer look at the calculation of the standardized SGS kinetic energy κ via (6.30). The variation of $s_* = \lambda\ s$ shown in Fig. 6.2 has to be explained by its dependence on s because λ is considered as a constant. In particular, we have the constraint $2 / 27^{1/2} = s_*^{max} = \lambda\ s^{max}$, where s_*^{max} and s^{max} denote the maximal values of s_* and s, respectively. For the calculation of s^{max}, we may assume that ℓ_* is positive. The invariants III_S and II_S are the same in every coordinate system, this means we may consider $\overline{S}_{ik}$ in principal axes where the off-diagonal elements are zero. Due to the assumed $\overline{S}_{nn} = 0$, $\overline{S}_{ik}$ is then a function of two independent components. A simple analysis of $III_S / (-II_S)^{3/2}$ as function of these two variables shows that (Lumley 1978)

$$-\frac{2}{\sqrt{27}} \le s \le \frac{2}{\sqrt{27}}. \tag{6.37}$$

By adopting (6.37) in $2 / 27^{1/2} = \lambda\ s^{max}$, we find $\lambda = (27 / (8 + 12\ C_0))^{1/2} = 1$, which corresponds to the value

$$C_0 = \frac{19}{12}. \tag{6.38}$$

This value represents within the frame of FDF methods the asymptotic value of C_0 for high-Reynolds number turbulence. We observe that the result $C_0 \approx 1.58$ obtained here agrees well with corresponding values used for C_0 within the frame of PDF methods, see the explanations given in section 5.4.

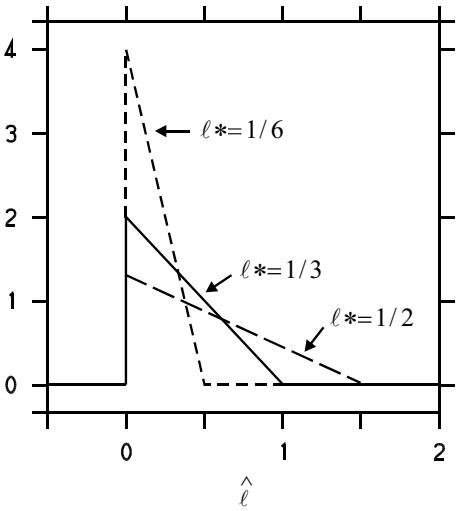

Fig. 6.3. A range of highly idealized eddy length PDFs in sample space $\hat{\ell}$. The mean values ℓ_* are shown with regard to their PDF.

As pointed out with regard to the consideration of backscatter effects in section 6.2.3, there are two ways for the calculation of ℓ_*: the dynamic procedure (6A.1) given in Appendix 6A, or the use of a constant ℓ_* (Gicquel et al. 2002), which corresponds to the application of a constant c_S in LES. The estimation of an optimal ℓ_* requires an assessment of possible variations of ℓ_*. This question will be considered now. ℓ_* may be seen as the mean of the PDF of standardized eddy lengths. According to Kolmogorov's theory, one should expect a distribution of eddy lengths which shows a higher probability for the appearance of small eddies. In particular, the eddy length PDF should approach to zero for values of ℓ_* that are of the order of unity. This assumption can be illustrated by means of the PDF with $\ell_* = 1 / 3$ in Fig. 6.3 (the means ℓ_* of the PDFs shown in Fig. 6.3 are given by a third of the interval length in which the eddy length PDF is nonzero). This figure also presents two further PDFs in order to illustrate the range of variations of the eddy length PDF. The PDF with $\ell_* = 1 / 6$ describes an (extreme) case where all the values of ℓ_* are found below 0.5, and the PDF with $\ell_* = 1 / 2$ describes a case where $\ell_* = 1 / 3 + 1 / 6$ (in contrast to the other PDF with $\ell_* = 1 / 3 - 1 / 6$). As the result of this discussion, one may conclude that Fig. 6.3 suggests the following range of ℓ_* variations that may be expected,

$$\ell_* = \frac{1}{3}\left(1 \pm \frac{1}{2}\right). \tag{6.39}$$

Obviously, the arguments used for the derivation of (6.39) are of heuristic nature, but they provide a rough impression about possible variations of ℓ_*. A discussion of consequences of (6.39) and a direct comparison with ℓ_* estimates obtained by DNS data will be provided below.

One way to prove the estimates obtained for C_0 and ℓ_* is to have a look at their implications for the Smagorinsky constant c_S. The use of (6.38) and (6.39) for C_0 and ℓ_* in (6.27) implies $c_S^{1/2} = 0.17 \pm 0.08$, which agrees well with values usually applied (Pope 2000). Another way to prove the suitability of the C_0 and ℓ_* values obtained here is to use them for the calculation of the Kolmogorov constant C_K that determines the energy spectrum, see (4.86). To do this, we replace c_S on the left-hand side of (6.27) by Lilly's classical result (Lilly 1967), which results in

$$\frac{1}{\pi^2}\left(\frac{2}{3C_K}\right)^{3/2} = c_S = \sqrt{\frac{1+1.5C_0}{54}\ell_*^{\,2}}\,\ell_*. \tag{6.40}$$

The use of $C_0 = 19 / 12$ and $\ell_* = 2\,(8 / 19)^{3/4} / \pi$ which agrees to (6.39) implies then

$$C_K = \frac{19}{12}. \tag{6.41}$$

Therefore, we find that $C_K = C_0 = 19 / 12 \approx 1.58$. This finding (6.41) for C_K agrees well with the results of measurements, which provide $C_K = 55 / 18\,(0.53 \pm 0.055) = 1.62 \pm 0.17$ (Sreenivasan 1995).

6.2.6. Comparison with DNS data

Next, we compare the findings obtained for C_0 and ℓ_* with available DNS data. This can be done by means of the results of Gicquel et al. (2002). In terms of their notation, C_0 and ℓ_* are given by $C_0 = 2\,(\widetilde{C}_1 - 1) / 3$ and $\ell_* = 2 / (\widetilde{C}_1\ \widetilde{C}_\varepsilon)$. The values obtained for these parameters are presented in Fig. 6.4.

The C_0 curve reveals two stages. For $t < 50$, the flow evolves from an initially smooth laminar state to a strong three-dimensional state before the action of the small scales becomes significant (Gicquel et al. 2002). Values of $C_0 \approx 6$ at $t \approx 50$ are consistent with experience obtained within the frame of PDF methods for flows of low complexity as HIST, see the discussion related to the variations of the Kolmogorov constant in section 5.4. For $t > 50$, the typical flow structures of the mixing layer develop (Gicquel et al. 2002). C_0 approaches to $C_0 = 19 / 12$, this means the theoretical finding (6.38) is well supported by these DNS results. The ℓ_* curve is approximately constant for $t > 50$ and found in a very good agreement with the theoretical estimate $\ell_* = 1 / 3$.

It is worth noting that the DNS calculations of C_0 and ℓ_* are well supported by assessments of effects of C_0 and ℓ_* variations on flow simulations. These findings reveal that the use of values near $C_0 = 2.1$ and $\ell_* = 0.5$ results in satisfactory predictions (Gicquel et al. 2002). In particular, it was found that ℓ_* should not be taken larger than $\ell_* = 0.5$, which agrees well with the implications of (6.39).

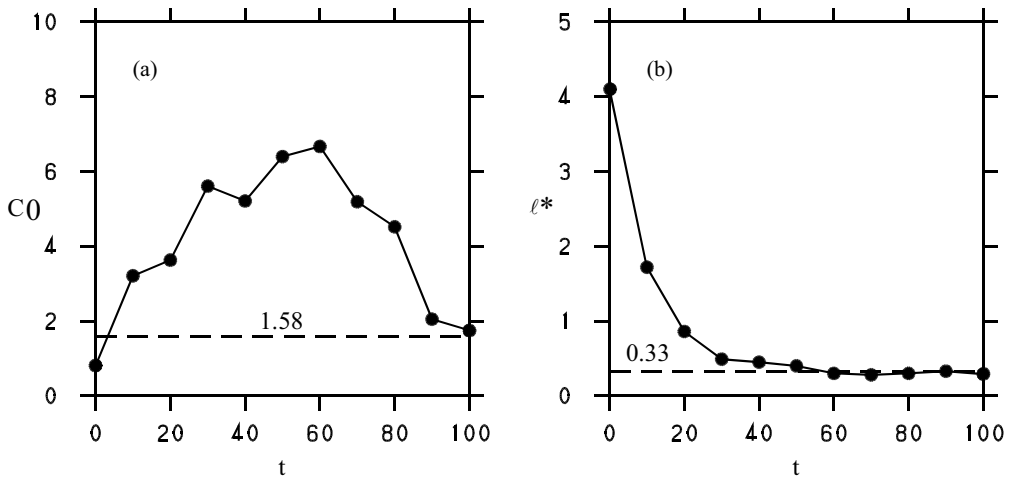

Fig 6.4. The calculation of C_0 and ℓ_* on the basis of the DNS data of Gicquel et al. (2002). t refers to the normalized time. The values $C_0 = 19 / 12$ and $\ell_* = 0.33$, which were obtained in section 6.2.5 by means of theoretical arguments, are shown for a comparison.

6.3. The closure of the scalar FDF transport equation

The next step is the realization of the concept pointed out in section 6.1.4, this means we will derive a closed transport equation for the scalar FDF F_φ.

6.3.1. The scalar-conditioned convective flux

Equation (6.13) for the scalar FDF is unclosed due to the appearance of the scalar-conditioned convective flux $\overline{u_i | \boldsymbol{\theta}}$. The latter quantity is calculated in Appendix 6B on the basis of the velocity-scalar FDF transport equation (6.9). This results in the expression

$$\overline{u_i | \boldsymbol{\theta}}\, F_\varphi = -K_{ik} \frac{\partial F_\varphi}{\partial x_k} \tag{6.42}$$

if counter-gradient terms are neglected, see the explanations given in Appendix 6B. The diffusion coefficient K_{ij} in (6.42) is given by

$$K_{ij} = \tau_L \gamma^{-1}{}_{in} \overline{u_n u_j}, \tag{6.43}$$

where γ^{-1} denotes the inverse matrix of γ which has elements $\gamma_{ij} = \delta_{ij} + \tau_L \, \partial \overline{U}_i / \partial x_j$. A detailed consideration of the calculation of the diffusion coefficient in this way will be presented in section 6.3.2.

The application of (6.42) in (6.13) results in the following scalar FDF equation

$$\frac{\partial}{\partial t}\langle\rho\rangle F_\varphi = -\frac{\partial}{\partial x_i}\langle\rho\rangle\left\{\overline{U}_i F_\varphi - K_{im}\frac{\partial F_\varphi}{\partial x_m}\right\}$$
$$-\frac{\partial}{\partial\theta_\alpha}\langle\rho\rangle\left\{\left[\overline{\Omega}_\alpha - \frac{1}{\tau_\varphi}\left(\theta_\alpha - \overline{\Phi}_\alpha\right) + S_\alpha\right]F_\varphi - G_{\alpha n}K_{nm}\frac{\partial F_\varphi}{\partial x_m}\right\}. \qquad (6.44)$$

$G_{\alpha m}$ is given by (6.7), and the parametrization of the mixing frequency τ_φ^{-1} will be addressed in section 6.3.3. The solution of (6.44) permits the calculation of scalar transport in consistency with the transport equations for filtered scalars,

$$\frac{\partial\overline{\Phi}_\alpha}{\partial t} + \overline{U}_k\frac{\partial\overline{\Phi}_\alpha}{\partial x_k} = \langle\rho\rangle^{-1}\frac{\partial}{\partial x_k}\langle\rho\rangle\left(\nu_{(\alpha)}\delta_{km} + K_{km}\right)\frac{\partial\overline{\Phi}_\alpha}{\partial x_m} + \overline{S}_\alpha, \qquad (6.45)$$

which follow from (6.44) by multiplication with θ_α and integration (relation (6.6) for $\overline{\Omega}_\alpha$ has to be applied). The extension of (6.45) by (6.44) is a requirement to involve the effects of source rates S_α on $\overline{\Phi}_\alpha$ without additional approximations.

A simpler approach than the use of (6.44) to obtain the scalar FDF F_φ is the assumed-shape FDF approach where an analytical form for F_φ is provided to calculate $\overline{S}_\alpha$ in (6.45) via (6.12). Usually, one assumes that F_φ only depends on filtered values $\overline{\Phi}_\alpha$ and scalar variances $V_{\alpha\beta} = \overline{\phi_\alpha\phi_\beta}$. The $\overline{\Phi}_\alpha$ are then calculated according to (6.45), and the $V_{\alpha\beta}$ are parametrized (Wall et al. 2000) or calculated by their transport equation. This approach is simple and relatively effective, but its range of applicability is limited. This is shown in Appendix 6C. It is pointed out there that the assumption of an assumed shape for F_φ is justified if velocity-scalar correlations disappear, i.e., if there is no production mechanism for scalar fluctuations. This assumption cannot be considered to be justified in general. Further, it is worth noting that the application of this approach requires the specification of the shape of F_φ. This poses a non-trivial problem: one has to provide a FDF shape that covers both the initial and final stage of the FDF evolution. For these reasons, the solution of (6.44) represents a much more flexible method compared to the assumed-shape FDF approach.

6.3.2. The diffusion coefficient

Next, we will consider the properties of K_{ij} in more detail. By adopting (6.43) for K_{ij} combined with the Smagorinsky model (6.24) for the SGS stress tensor, the diffusion coefficient K_{ij} is found to satisfy

$$\left(\delta_{in} + \tau_L\overline{S}_{in} + \tau_L\overline{\Sigma}_{in}\right)K_{nj} = 2\nu_r\left(\delta_{ij} - \tau_L\overline{S}_{ij}\right). \qquad (6.46)$$

Here, $\tau_L = \ell_* \Delta / k_r^{1/2}$, and the eddy viscosity is given by $\nu_r = k_r \tau_L / 3$. By adopting the first-order approximation (6.25) for k_r, the latter expression may be rewritten into $\nu_r = c_S \Delta^2 |\overline{S}|_r$. A simplification of (6.46) is given by taking the effects of shear successively into account. In zeroth, first and second order, one finds

$$K^{(0)}_{ij} = \frac{\nu_r}{Sc_t}\delta_{ij}, \tag{6.47a}$$

$$K^{(1)}_{ij} = \frac{\nu_r}{Sc_t}\left(\delta_{ij} - \tau_L \overline{S}_{ij}\right), \tag{6.47b}$$

$$K^{(2)}_{ij} = \frac{\nu_r}{Sc_t}\left(\delta_{in} - \tau_L \overline{S}_{in} - \tau_L \overline{\Sigma}_{in}\right)\left(\delta_{nj} - \tau_L \overline{S}_{nj}\right). \tag{6.47c}$$

The turbulence Schmidt number Sc_t is given here by

$$Sc_t = \frac{1}{2}, \tag{6.48}$$

which follows as a consequence of (6.46). The comparison of these findings for the diffusion coefficient with methods applied previously shows that the theoretical value $Sc_t = 0.5$ obtained here agrees well with values $Sc_t = 0.55 \pm 0.15$ applied in scalar FDF methods (Jaberi et al. 1999). However, in contrast to the usual assumption of the isotropic expression (6.47a) for K_{ij} (Colucci et al. 1998; Jaberi et al. 1999; Zhou & Pereira 2000) one finds an anisotropic relation for it even when the simplest model for the SGS stress tensor is applied.

We turn to the question of the relevance of shear contributions to the diffusion coefficient K_{ij}. For that, we apply the same scaling analysis as in section 6.2.4. By adopting again U_0 and L_0 as characteristic velocity and length scales, we obtain from (6.46) the relation

$$\left(i_r\delta_{in} + Kn_r \overline{S}_{in}^{+} + Kn_r \overline{\Sigma}_{in}^{+}\right)K_{nj}^{+} = i_r Kn_r\left(i_r\delta_{ij} - Kn_r \overline{S}_{ij}^{+}\right), \tag{6.49}$$

where the plus refers to scaled quantities ($K_{nj}^{+} = K_{nj} / U_0 L_0$). The conclusion that can be drawn from (6.49) regarding the relevance of shear contributions is the same as pointed out with reference to τ_{ij}: such contributions are important in general. This is confirmed by studies of the anisotropy of K_{ij} performed by Rogers et al. (1989) and Kaltenbach et al. (1994). These investigations show that K_{ij} is strongly anisotropic and asymmetric even for homogeneous turbulence. For unstratified shear flow one finds for instance for the diagonal elements of the diffusion coefficient $K_{11} / K_{22} = 2.9$ and $K_{33} / K_{22} = 0.53$, and the nonzero off-diagonal elements are characterized by $K_{13} / K_{22} = -1.2$ and $K_{31} / K_{22} = -0.65$ (Kaltenbach et al. 1994).

6.3.3. The scalar mixing frequency

The scalar FDF transport equation (6.44) is still unclosed due to the unknown mixing frequency τ_φ^{-1}. The most convenient way to parametrize this frequency is to relate τ_φ to the relaxation time scale of velocity fluctuations τ_L. This leads to the question of the optimal value and possible variations of the time scale ratio τ_φ / τ_L.

To prepare the discussion of this problem, let us consider the scalar variance transport equation for a non-reacting scalar (referred to without subscript) in analogy to the treatment of the k_r equation in section 6.2. According to the scalar FDF equation (6.44), this scalar variance equation reads

$$\frac{\partial \overline{\phi\phi}}{\partial t} + \overline{U}_k \frac{\partial \overline{\phi\phi}}{\partial x_k} + \langle\rho\rangle^{-1} \frac{\partial \overline{\langle\rho\rangle u_k \phi\phi}}{\partial x_k} = -2\frac{1-R}{\tau_\varphi}\overline{\phi\phi} - 2\overline{u_k\phi}\frac{\partial \overline{\Phi}}{\partial x_k}. \tag{6.50}$$

We used here the abbreviation $R = r_k\, r_k$, where r_k is the correlation coefficient of standardized velocity and scalar fluctuations, $r_k = V^{-1/2}{}_{km}\ \overline{u_m\phi}\ /\ \overline{\phi\phi}^{\,1/2}$. A simple analysis reveals the range $0 \le R < 1$ of R variations. The case $R = 1$ would correspond to a perfect correlation of the scalar considered with the velocity field. This case cannot be realized provided the intensity of the stochastic source term in the velocity equation is positive definite (which is the case if $C_0 \ge 0$). The closure of (6.50) requires the calculation of velocity-scalar correlations. This can be performed by means of (6.42) for the scalar-conditioned convective flux combined with (6.47a) for K_{ij} and $\nu_r = k_r\, \tau_L / 3 = \ell_*^2\, \Delta^2 / (3\, \tau_L)$. One obtains in this way

$$\overline{u_k\phi} = -2\frac{\ell_*{}^2\Delta^2}{3\tau_L}\frac{\partial \overline{\Phi}}{\partial x_k}, \qquad \overline{u_k\phi\phi} = -2\frac{\ell_*{}^2\Delta^2}{3\tau_L}\frac{\partial \overline{\phi\phi}}{\partial x_k}. \tag{6.51}$$

As done with regard to k_r in section 6.2, we neglect all the gradients of $\overline{\phi\phi}$ on the left-hand side of (6.50), which was found to be appropriate for the modeling of small-scale mixing processes, e.g., by Heinz & Roekaerts (2001). We obtain

$$\overline{\phi\phi} = \frac{2}{3}\frac{\ell_*{}^2\Delta^2\tau_\varphi}{(1-R)\tau_L}\frac{\partial \overline{\Phi}}{\partial x_m}\frac{\partial \overline{\Phi}}{\partial x_m} = \frac{2}{3}\left(1+\frac{\tau_\varphi}{\tau_L}\right)\ell_*{}^2\Delta^2\frac{\partial \overline{\Phi}}{\partial x_m}\frac{\partial \overline{\Phi}}{\partial x_m} = \frac{2}{3}\ell_{\varphi*}{}^2\Delta^2\frac{\partial \overline{\Phi}}{\partial x_m}\frac{\partial \overline{\Phi}}{\partial x_m}. \tag{6.52}$$

The first expression for $\overline{\phi\phi}$ follows from (6.50) combined with (6.51). The second expression is obtained by replacing $R = (1 + \tau_\varphi / \tau_L)^{-1}$ according to its definition, where V_{ij} is considered to be isotropic. The last expression introduces the parameter $\ell_{\varphi*}$ by means of the relation $\ell_{\varphi*}{}^2 = \ell_*{}^2\,(1 + \tau_\varphi / \tau_L)$, which assures that the scalar variance is calculated as a positive quantity. Relation (6.52) is often used to

provide the scalar variance within the context of assumed-shape methods (Pierce & Moin 1998; Forkel & Janicka 2000; Wall et al. 2001). $\ell_{\varphi*}$ is then calculated dynamically (Wall et al. 2000) or taken as $\ell_{\varphi*} = 0.5$ (Forkel & Janicka 2000).

The point is that the derivation of (6.52) solves the problem to parametrize τ_φ. The definition of $\ell_{\varphi*}^2$ provides for the mixing scalar frequency τ_φ^{-1}

$$\frac{1}{\tau_\varphi} = \frac{\ell_*^2}{\ell_{\varphi*}^2 - \ell_*^2} \frac{1}{\tau_L}. \tag{6.53}$$

The dependence of τ_φ^{-1} on ℓ_* corresponds to the expectation: the intensity of scalar mixing grows with the characteristic eddy length ℓ_*. The other length scale $\ell_{\varphi*}$ in (6.53) represents a characteristic "scalar eddy" length scale (the linear extension of a cloud of any substance released into a flow). Relation (6.53) provides for it the constraint $\ell_{\varphi*} > \ell_*$ (which is a consequence of $G_{\alpha m}$ in (6.5c)). This means that the characteristic length scale of the scalar field has to be larger than the characteristic eddy length, which is required for the onset of scalar mixing (scalar fields that are smaller than eddies move with them but are not dispersed). Relation (6.53) shows that the mixing frequency τ_φ^{-1} becomes smaller with growing $\ell_{\varphi*}$. This is the expected trend because τ_φ^{-1} has to vanish for $\ell_{\varphi*} >> \ell_*$. These explanations indicate that the variability of $\ell_{\varphi*}$ is at least as high as that of ℓ_*. This is confirmed by the findings of Colucci et al. (1998) and Jaberi et al. (1999), which reveal the need to apply different values for the constants used to parametrize τ_φ^{-1} for various flows. In addition to this, relation (6.53) shows that the consideration of backscatter with regard to τ_L also requires its consideration regarding to τ_φ.

By adopting the relation between τ_L and the dissipation time scale $\tau_r = k_r / \varepsilon_r$ of turbulence,

$$\frac{1}{\tau_L} = \frac{1 + 1.5 C_0}{2\tau_r}, \tag{6.54}$$

which follows from the definition of $\varepsilon_r = 2\, k_r / [(1 + 1.5\, C_0)\, \tau_L]$, we may rewrite (6.53) into the form of the standard model for parametrizations of the scalar mixing frequency τ_φ^{-1},

$$\frac{1}{\tau_\varphi} = \frac{C_\varphi}{2\tau_r}. \tag{6.55}$$

C_φ is a constant that is given according to (6.53) by

$$C_\varphi = (1 + 1.5 C_0) \frac{\ell_*^2}{\ell_{\varphi*}^2 - \ell_*^2}. \tag{6.56}$$

This result shows that C_φ cannot be considered as flow-independent because $\ell_{\varphi *}$ has to be expected to vary with the scalar field considered. Thus, the consideration of scalar fields with significantly different characteristic length scales results in the need to apply different values for C_φ. The use of $C_\varphi(\infty) = 2.5$, see relation (5.92), combined with $C_0 = 19 / 12$ and $\ell_* = 1 / 3$ in (6.56) implies then $\ell_{\varphi *} = 0.5$, which agrees with the assumption of Forkel & Janicka (2000).

6.4. The closure of LES and FDF equations

The model (6.5a-c) for the stochastic dynamics of velocities and scalars was used to improve existing LES equations for velocities and stochastic equations for the transport of scalars. On the other hand, these studies enable conclusions regarding the modeling of the stochastics of SGS variables. The findings obtained with regard to these two questions will be summarized and further discussed here.

6.4.1. The closure of LES equations

The stochastic model (6.5a-c) was reduced to a closed LES equation for the velocity field and a scalar FDF equation. A further reduction of this FDF equation to a closed scalar LES equation requires serious assumptions that are often not satisfied, see the detailed explanations given in Appendix 6C. One obtains in this way generalizations of presently applied models for the anisotropic residual stress tensor τ_{ij} and diffusion coefficient K_{ij}. Evidence for these new models is provided by the fact that they are implied by the underlying model (6.5a-c), which is supported by the results of Colucci et al. (1998), Jaberi et al. (1999), Zhou & Pereira (2000) and Gicquel et al. (2002). In addition to this, the consideration of (6.5a-c) may be seen as the analysis of a limiting case: the implications of the most simple model for the dynamics of SGS fluctuations are investigated in this way.

One advantage of the new models for τ_{ij} and K_{ij} is given by their consistency. This means that different contributions in the algebraic expression (6.28) for τ_{ij} are calculated from the same model for the dynamics of instantaneous velocities, which is not the case in other methods (see section 6.2.3). Further, this means that the same model for the instantaneous velocity field is used to calculate within the frame of a hybrid method the filtered velocity field and transport of scalars in physical space. This leads, for instance, to the theoretical estimate $Sc_t = 0.5$ for the ratio of SGS eddy viscosities for the transport of momentum and scalars, and it enables the use of the same model for the SGS stress tensor in equations for velocities and scalars (see section 6.3.2). The application of such consistent methods is known to be of significant relevance with regard to the use of PDF methods (Wouters et al. 1996; Nooren et al. 1997; Muradoglu et al. 1999). Another advantage compared to existing methods is the possibility to assess the

significance of quadratic shear contributions to τ_{ij} and linear (and higher-order) shear contributions to K_{ij}. This was pointed out in sections 6.2.4 and 6.3.2 by means of scaling analyses. It was shown that the relevance of such contributions depends essentially on the SGS Knudsen number Kn_r, which is controlled by the numerical resolution of the flow.

6.4.2. The modeling of the dynamics of SGS fluctuations

The parameters C_0, ℓ_* and $\ell_{\varphi*}$ are essential ingredients of the stochastic model (6.5a-c) for the dynamics of SGS fluctuations. Previously, they were estimated by simulations of one type of a three-dimensional flow: a temporally developing mixing layer with a Reynolds number Re = 50 - 400 (Colucci et al. 1998; Jaberi et al. 1999; Gicquel et al. 2002). Here, the variations of the parameters C_0, ℓ_* and $\ell_{\varphi*}$ were investigated analytically. The theoretical value $C_0 = 19 / 12 \approx 1.58$ was derived for C_0. This value agrees very well with C_0 calculations on the basis of DNS data. It implies a value $C_K = C_0 = 19 / 12$ for the universal Kolmogorov constant that determines the energy spectrum (4.86). The latter result is in accord with $C_K = 1.62 \pm 0.17$ derived by measurements (Sreenivasan 1995). It is worth emphasizing that the derivation of this theoretical value for C_0 simplifies the task to adjust the model parameters to a flow considered. It enables self-consistent flow simulations by adopting the dynamic procedure (6A.1) for the estimation of ℓ_* and a corresponding calculation of $\ell_{\varphi*}$. An alternative to this approach is the use of a constant value for ℓ_* (Gicquel et al. 2002), which corresponds to the application of a constant c_S in LES. The estimation of such an optimal value resulted in $\ell_* = 1 / 3 \pm 50\%$. It was shown that the choice $\ell_* = 1 / 3$ agrees very well with the results of DNS. The analogous calculation of $\ell_{\varphi*}$ led to the estimate $\ell_{\varphi*} = 1 / 2$. Nevertheless, significant variations of this value (by more than 50%) have to be expected in dependence on the scalar field considered, see the explanations in section 6.3.3.

As pointed out in the beginning of this chapter, the idea of the analysis presented here was to investigate the implications of the most simple model for the dynamics of SGS fluctuations. A valid question is then whether the model structure considered is already sufficient to perform accurate simulations of the stochastics of SGS processes. With regard to this question, it is worth emphasizing that the results reported here do not give any hint for the need to extend (6.5a-c) by involving for instance interactions between the dynamics of different instantaneous velocity components. As shown above, the stochastic model (6.5a-c) implies models for the SGS stress tensor and diffusion coefficient that are more complex than presently applied standard models. In addition to this, the consideration of an anisotropic expression for the frequency of the velocity relaxation instead of τ_L^{-1} implies the need to introduce additional model parameters, which makes the task of finding optimal parameter values more complicated.

Appendix 6A: The dynamic eddy length scale calculation

The formula for the calculation of ℓ_* via a dynamic procedure can be obtained by extending the corresponding calculation of c_S for the Smagorinsky model (Pope 2000) to the case that τ_{ij} is given by (6.28). One obtains in this way

$$\sqrt{\ell_*^{\,2}}\,\ell_* = \begin{cases} (c_3 + c_4)\left[c_1 - c_2\right]^{-1} \le 0 & \text{if} \quad c_3 \le -c_4 \\ (c_3 - c_4)\left[c_1 + c_2\right]^{-1} \ge 0 & \text{if} \quad c_4 \le c_3 \end{cases}, \tag{6A.1}$$

where the following parameters are introduced,

$$c_1 = \frac{\kappa^2}{16\lambda^2} A_{ij}A_{ji} + B_{ij}B_{ji}, \quad c_2 = \frac{\kappa}{2\lambda} A_{ij}B_{ji}, \quad c_3 = \frac{\kappa}{4\lambda} L_{ij}A_{ji}, \quad c_4 = L_{ij}B_{ji}. \tag{6A.2}$$

The matrices in these expressions are defined by

$$L_{ij} = \widetilde{\overline{U}_i \overline{U}_j} - \widetilde{\overline{U}}_i \widetilde{\overline{U}}_j - \frac{1}{3}\left(\widetilde{\overline{U}_n \overline{U}_n} - \widetilde{\overline{U}}_n \widetilde{\overline{U}}_n\right)\delta_{ij},$$

$$A_{ij} = 2\overline{\Delta}^2 \widetilde{|\overline{S}|_r \overline{S}_{ij}} - 2\widetilde{\overline{\Delta}}^2 |\widetilde{\overline{S}}|_r \widetilde{\overline{S}}_{ij},$$

$$B_{ij} = \frac{\overline{\Delta}^2}{3}\left\{2\widetilde{\overline{S}_{ik}\overline{S}_{kj}} - \frac{2}{3}\widetilde{\overline{S}_{nk}\overline{S}_{kn}}\,\delta_{ij} - \widetilde{\overline{S}_{ik}\overline{\Sigma}_{kj}} + \widetilde{\overline{\Sigma}_{ik}\overline{S}_{kj}}\right\} -$$

$$- \frac{\widetilde{\overline{\Delta}}^2}{3}\left\{2\widetilde{\overline{S}}_{ik}\widetilde{\overline{S}}_{kj} - \frac{2}{3}\widetilde{\overline{S}}_{nk}\widetilde{\overline{S}}_{kn}\delta_{ij} - \widetilde{\overline{S}}_{ik}\widetilde{\overline{\Sigma}}_{kj} + \widetilde{\overline{\Sigma}}_{ik}\widetilde{\overline{S}}_{kj}\right\}. \tag{6A.3}$$

The tilde denotes the double-filtering operation, and $\overline{\Delta}$ and $\widetilde{\overline{\Delta}}$ are the grid and test filter width, respectively (Pope 2000, p. 619) ($\overline{\Delta}$ is used here instead of Δ in sections 6.2 and 6.3). κ and λ are defined by (6.30) and (6.31). One may prove that (6A.1) provides a unique determination of ℓ_* for all realizable cases. c_4 has to be positive and the case $-c_4 \le c_3 \le c_4$ is unrealizable.

The neglect of shear contributions of second-order in (6.28) for τ_{ij} corresponds with the assumption that τ_{ij} is given by the Smagorinsky model (6.24). In this case, expression (6A.1) reduces to the well-known formula for the dynamic calculation of the Smagorinsky constant c_S,

$$\sqrt{\frac{1+1.5C_0}{54}}\sqrt{\ell_*^{\,2}}\,\ell_* = c_S = \frac{L_{ij}A_{ji}}{A_{mn}A_{nm}}. \tag{6A.4}$$

Appendix 6B: The scalar-conditioned convective flux

The velocity-scalar FDF equation (6.9) can be used to calculate the scalar-conditioned convective flux. Without adopting further assumptions one obtains

$$\overline{u_i|\,\boldsymbol{\theta}} = D_{i,(1)}'' + D_{i,(2)}'' - \frac{K_{ik}}{F_\varphi}\frac{\partial F_\varphi}{\partial x_k}. \tag{6B.1}$$

Here, $K_{ik} = \tau_L\ \gamma^{-1}{}_{in}\ \overline{u_n u_k}$ represents a diffusion coefficient, where γ^{-1} refers to the inverse matrix of γ which has elements $\gamma_{ij} = \delta_{ij} + \tau_L\,\partial\,\overline{U}_i / \partial x_j$. The first two terms on the right-hand side represent fluctuating drift terms that vanish in the mean. They are given by

$$D_{i,(1)}'' = -\gamma^{-1}{}_{im}\frac{\tau_L}{F_\varphi}\left[\frac{\partial}{\partial t}\overline{u_m|\,\boldsymbol{\theta}}\,F_\varphi + \overline{U}_k\frac{\partial}{\partial x_k}\overline{u_m|\,\boldsymbol{\theta}}\,F_\varphi\right], \tag{6B.2a}$$

$$D_{i,(2)}'' = -\frac{\tau_L\gamma^{-1}{}_{im}}{F_\varphi}\left(\frac{\partial}{\partial\theta_\alpha}\left[\overline{\Omega}_\alpha - \frac{\theta_\alpha - \overline{\Phi}_\alpha}{\tau_\varphi} + S_\alpha\right]\overline{u_m|\,\boldsymbol{\theta}}\,F_\varphi + \frac{\partial G_{\alpha k}\,\overline{u_m u_k|\,\boldsymbol{\theta}}\,F_\varphi}{\partial\theta_\alpha} - \right.$$

$$\left. - \frac{1}{\langle\rho\rangle}\frac{\partial}{\partial x_j}\langle\rho\rangle\left(\overline{u_m u_j} - \overline{u_m u_j|\,\boldsymbol{\theta}}\right)F_\varphi\right). \tag{6B.2b}$$

Contributions due to $D_{i,(1)}''$ can be neglected in accord with the neglect of such terms in the transport equation for the SGS stress tensor, see section 6.2.2. To see the effects of $D_{i,(2)}''$, we consider it (in consistency with the scalar equation (6.5c)) as a linear function of scalar fluctuations,

$$D_{i,(2)}'' = \tau_L\gamma^{-1}{}_{im}\left[\overline{S_\nu''u_m} - \langle\rho\rangle^{-1}\frac{\partial\langle\rho\rangle\overline{u_m u_k\phi_\nu}}{\partial x_k}\right]V^{-1}{}_{\nu\mu}\left(\theta_\mu - \overline{\Phi}_\mu\right). \tag{6B.3}$$

$V^{-1}{}_{\nu\mu}$ refers to the inverse scalar variance matrix V with elements $V_{\alpha\beta} = \overline{\phi_\alpha\phi_\beta}$. Expression (6B.3) assures that the effect of $D_{i,(2)}''$ on the SGS scalar flux, which is given according to (6B.1) by

$$\overline{u_i\phi_\alpha} = \overline{D_{i,(1)}''\phi_\alpha} + \overline{D_{i,(2)}''\phi_\alpha} - K_{ik}\frac{\partial\overline{\Phi}_\alpha}{\partial x_k}, \tag{6B.4}$$

is the same as that obtained by applying (6B.2b) in (6B.4). The first term inside the bracket of (6B.3) may arise from chemical reactions. According to (6B.4), its contribution to the SGS scalar flux is given by $\tau_L\ \gamma^{-1}{}_{im}\ \overline{S_\alpha''u_m}$. The consideration

of the usual structure of S_α reveals that this term involves the dependence of $\overline{u_i\phi_\alpha}$ on the scalar fluxes of all the other species. Such cross-diffusion contributions are neglected in PDF methods so that their neglect in FDF methods appears to be well justified, too. The second term inside the bracket of (6B.3) is related to turbulent diffusion. Such contributions are usually also neglected. Thus, $D_{i,(2)}$" appears to be of the same minor relevance as $D_{i,(1)}$" under many conditions.

Appendix 6C: An assumed-shape FDF method

To show the conditions for the applicability of the assumed-shape FDF approach, we reduce equation (6.44) to a scalar FDF with analytical shape. For this, it is convenient to consider (6.44) in terms of its equations for realizations,

$$\frac{d}{dt}x_i^* = \overline{U}_i + \frac{1}{\langle\rho\rangle}\frac{\partial\langle\rho\rangle K_{ij}}{\partial x_j} + \sqrt{2K}_{ij}\frac{dW_j}{dt}, \tag{6C.1a}$$

$$\frac{d}{dt}\Phi_\alpha^* = \overline{\Omega}_\alpha - \frac{1}{\tau_\varphi}\left(\Phi_\alpha^* - \overline{\Phi}_\alpha\right) + \frac{1}{\langle\rho\rangle}\frac{\partial\langle\rho\rangle G_{\alpha m}K_{mj}}{\partial x_j} + S_\alpha + G_{\alpha m}\sqrt{2K}_{mj}\frac{dW_j}{dt}, \tag{6C.1b}$$

where one has to apply the elements ij of the matrix $(2\,K)^{1/2}$ (this means not the square root of matrix elements). Next, we split the problem to calculate the statistics of Φ^*_α into the problem to calculate filtered scalars $\overline{\Phi}_\alpha$ and variances $V_{\alpha\beta} = \overline{\phi_\alpha\phi_\beta}$, and the problem to calculate the statistics of standardized variables

$$\hat{\Phi}_\alpha^* = V^{-1/2}{}_{\alpha\mu}\left(\Phi_\mu^* - \overline{\Phi}_\mu\right). \tag{6C.2}$$

According to (6C.1b), the dynamics of the latter quantities read

$$\frac{d}{dt}\hat{\Phi}_\alpha^* = -\frac{1}{2}V^{-1/2}{}_{\alpha\mu}\left(\frac{dV_{\mu\nu}}{dt} + \frac{2V_{\mu\nu}}{\tau_\varphi}\right)V^{-1/2}{}_{\nu\beta}\hat{\Phi}_\beta^* + \hat{S}_\alpha" + V^{-1/2}{}_{\alpha\mu}G_{\mu n}\sqrt{2K}_{nm}\frac{dW_m}{dt}, \tag{6C.3}$$

where $\hat{S}_\alpha" = V^{-1/2}{}_{\alpha\mu}\,S_\mu"$ refers to the rescaled fluctuation of S_α. For it we assume

$$\hat{S}_\alpha" = -\tau_\varphi{}^{-1}D^s{}_{\alpha\beta}\hat{\Phi}_\beta^*. \tag{6C.4}$$

Here, $D^s{}_{\alpha\beta} = (D_{\alpha\beta} + D_{\beta\alpha})/2$ represents the symmetric component of generalized Damköhler numbers that are defined by

$$D_{\alpha\beta} = -\tau_\varphi\,\overline{\hat{S}_\alpha"\hat{\phi}_\beta}. \tag{6C.5}$$

Assumption (6C.4) is fully consistent with the effect of S_α" on scalar variances $V_{\alpha\beta}$. This may be seen by considering the variance transport equations

$$\frac{\partial V_{\alpha\beta}}{\partial t} + \overline{U}_k \frac{\partial V_{\alpha\beta}}{\partial x_k} + \langle\rho\rangle^{-1} \frac{\partial \langle\rho\rangle \overline{u_k \phi_\alpha \phi_\beta}}{\partial x_k} + \overline{u_k \phi_\beta} \frac{\partial \overline{\Phi}_\alpha}{\partial x_k} + \overline{u_k \phi_\alpha} \frac{\partial \overline{\Phi}_\beta}{\partial x_k} =$$

$$= -\frac{2}{\tau_\varphi} V_{\alpha\beta} + G_{\alpha m} \overline{u_m \phi_\beta} + G_{\beta m} \overline{u_m \phi_\alpha} + \overline{S_\alpha" \phi_\beta} + \overline{S_\beta" \phi_\alpha}, \qquad (6C.6)$$

which follow from (6.44). The use of (6C.4) and (6C.6) in (6C.3) then results in

$$\frac{d}{dt} \hat{\Phi}_\alpha^* = \frac{1}{2} V^{-1/2}{}_{\alpha\mu} \left(\frac{1}{\langle\rho\rangle} \frac{\partial \langle\rho\rangle \overline{u_k \phi_\mu \phi_\beta}}{\partial x_k} + \overline{u_k \phi_\beta} \frac{\partial \overline{\Phi}_\mu}{\partial x_k} + \overline{u_k \phi_\mu} \frac{\partial \overline{\Phi}_\beta}{\partial x_k} - G_{\mu m} \overline{u_m \phi_\beta} - \right.$$

$$\left. - G_{\beta m} \overline{u_m \phi_\mu} \right) V^{-1/2}{}_{\beta\nu} \hat{\Phi}_\nu^* + V^{-1/2}{}_{\alpha\mu} G_{\mu n} \sqrt{2K}_{nm} \frac{dW_m}{dt}, \quad (6C.7)$$

where $d\overline{\Phi}_\alpha / dt = \overline{d\Phi_\alpha / dt}$ is used. Equation (6C.7) reveals that the standardized variables are unchanged ($d\hat{\Phi}_\alpha^* / dt = 0$) if there are no velocity-scalar correlations. The FDF of standardized variables is known then: it is the initial FDF. It is worth noting that the joint initial FDF has to be provided as the product of marginal FDFs because there is no correlation between different standardized variables,

$$\overline{\hat{\phi}_\alpha \hat{\phi}_\beta} = \delta_{\alpha\beta}. \qquad (6C.8)$$

The calculation of the scalar FDF via its transport equation is reduced in this case of vanishing velocity-scalar correlations to the calculation of filtered scalars and variances. We may write equation (6.45) as

$$\frac{\partial \overline{\Phi}_\alpha}{\partial t} + \overline{U}_k \frac{\partial \overline{\Phi}_\alpha}{\partial x_k} = \langle\rho\rangle^{-1} \frac{\partial}{\partial x_k} \langle\rho\rangle \left(\nu_{(\alpha)} \delta_{km} + K_{km} \right) \frac{\partial \overline{\Phi}_\alpha}{\partial x_m} + V^{1/2}{}_{\alpha\mu} \overline{\hat{S}}_\mu, \qquad (6C.9)$$

where the $V^{1/2}{}_{\alpha\beta}$ satisfy according to (6C.6)

$$\frac{\partial V^{1/2}{}_{\alpha\beta}}{\partial t} + \overline{U}_k \frac{\partial V^{1/2}{}_{\alpha\beta}}{\partial x_k} = -\frac{1}{\tau_\varphi} \left\{ \delta_{\alpha\mu} + D^s{}_{\alpha\mu} \right\} V^{1/2}{}_{\mu\beta}. \qquad (6C.10)$$

The equations (6C.9) and (6C.10) are closed because $\overline{\hat{S}}_\alpha$ and $D^s{}_{\alpha\beta}$ can be obtained easily if the FDF of the standardized variables is specified. Equation (6C.10) reveals that only scalar fluctuations that arise from initial conditions enter equation (6C.9): there is no production mechanism for scalar fluctuations if velocity-scalar correlations vanish. The scalar variances decay then according to (6C.10).

7. The unification of turbulence models

The separate consideration of stochastic models for large-scale and small-scale turbulence in chapters 5 and 6, respectively, leads to the question of how these approaches can be merged into one modeling approach. This is of fundamental importance from a theoretical point of view, but industrial applications of turbulence models and basic studies by DNS also require the development of unified turbulence models, as pointed out in section 7.1. The question of how such turbulence models can be constructed will be addressed in section 7.2 on the basis of the discussions presented in the previous chapters. Finally, some unsolved questions related to these developments will be discussed in section 7.3.

7.1. The need for the unification of turbulence models

The development of computational methods for turbulent reacting flows is essentially driven by industrial interests and requirements. To understand needs for further methodological developments, let us have a closer look at current and future applications of turbulence models for solving industrial (technological and environmental) problems.

7.1.1. Industrial applications of turbulence models

The current use of computational methods is illustrated in Fig. 7.1, which closely follows an analysis of Pope (1999). Obviously, most applications are performed on the basis of the simplest (RANS) models. In particular, the k-ε model and (less often) Reynolds-stress models (RSM), which make use of transport equations to obtain the Reynolds stresses, are the models which are usually employed. As pointed out in section 4.6, the use of RANS equations for reacting flow calculations is faced with serious problems regarding the closure of mean reaction rate terms. This problem can be solved by extending RANS to PDF methods. Nevertheless, there are relatively few applications of PDF methods to the solution of industrial problems at present. The main reason for this is the lack of availability of suitable PDF codes. Promising developments to solve this problem were presented recently by FLUENT (2003).

S. Heinz, *Statistical Mechanics of Turbulent Flows*

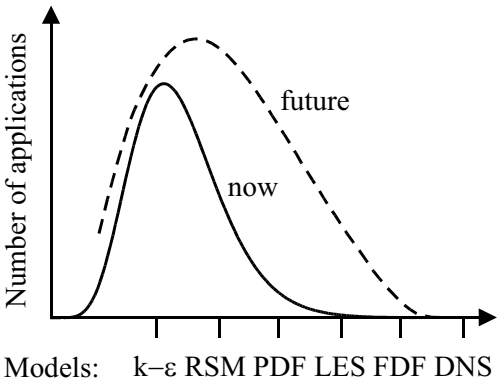

Fig. 7.1. A slightly extended prognosis of Pope (1999), who considered the current and future (next 10 - 20 years) use of turbulence models for industrial applications. RANS models are split into algebraic (k-ε) and Reynolds stress models (RSM). The latter apply transport equations to calculate the Reynolds stresses.

Regarding the future use of computational methods for industrial applications, an important conclusion from previous developments is that a simple displacement of the distribution in Fig. 7.1 towards more advanced methods (an abandonment of RANS in favor of LES) will probably not take place. The general trend is to use the simplest models as much as possible. Thus, it is likely that the contributions of PDF, LES and possibly FDF methods grow, but most of the applications will be still performed on the basis of RANS methods.

A significant problem related to the use of RANS models for industrial applications is the assessment and optimization of the model performance. In general, the use of DNS is too expensive for that purpose. Measurements are also very expensive and provide only partial (and often relatively inaccurate) information. As pointed out in chapter 1, possible deficiencies of RANS models are closely related to the underlying relative coarse filtering. The most natural way to assess the suitability of RANS models, therefore, is to investigate the consequences of applying (by the use of a RANS method) a large filter width Δ. This can be done by adopting LES predictions for comparisons, provided the LES equations recover the RANS model considered in the large-Δ limit. The latter is not guaranteed, however, in the majority of existing LES models. This leads to the need for the construction of unified models that can be used, depending on the resolution, as either LES or RANS methods (Speziale 1998); see Fig. 7.2 for an illustration.

7.1.2. Basic studies by DNS

It is essential to note that the requirement of developing unified turbulence models is not restricted to the need to represent RANS and PDF equations as large-Δ limits of LES and FDF equations, respectively, but a corresponding deepening of the relations between DNS and LES / FDF equations will also be very helpful. The reason for this is given by the fact that basic research performed on the basis of DNS studies is faced with some significant problems, as pointed out next.

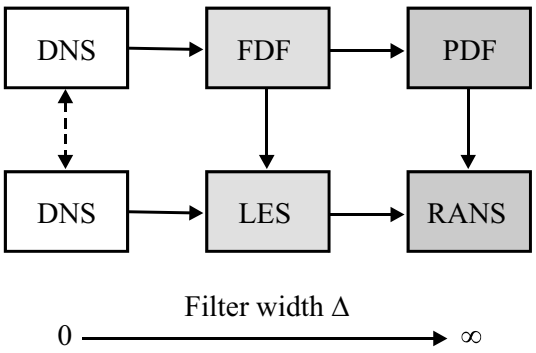

Fig. 7.2. An illustration of unified turbulence models. Equations for filtered variables are given below. They can be applied as DNS, LES or RANS models, depending on the choice of Δ. The upper line shows corresponding stochastic models (SGS fluctuations vanish for $\Delta \to 0$ such that FDF methods reduce to DNS).

The first problem related to the use of DNS is the tremendous computational effort of DNS, which hampers the efficient progress of basic research significantly: one has to limit investigations to a few cases, and such investigations may require years. Second, significant fluctuations of DNS data even at moderate Reynolds numbers may lead to non-trivial problems regarding the physical interpretation of DNS results, as given, for example, with regard to investigations of structural compressibility effects (Sarkar 1995). Third, the Reynolds number restrictions of DNS make it impossible (for the foreseeable future) to calculate many relevant flows. With regard to this problem, it is often argued that the Reynolds number has a limited effect on the flow physics, such that one can use DNS to calculate flows that are very similar to high-Reynolds number flows. This may be true for some non-reacting flows, but it is not true in general with regard to reacting flows where Reynolds number effects may cause significant variations of the competition between mixing and reaction (Baldyga & Bourne 1999; Heinz & Roekaerts 2001).

For these reasons, there is a need for the construction of computational methods that have a predictive power similar to DNS, but are more efficient and applicable to high-Reynolds number and reacting flows. One may expect that the FDF approach is capable of providing such an alternative to DNS, at least when it is used in conjunction with a sufficiently small spatial resolution: see the discussion in section 6.2.4. Compared to LES, this approach has, for instance, the advantage that dynamic effects and quadratic (and higher-order) shear contributions to the SGS stress tensor are involved. With regard to reacting flow calculations, it is relevant that chemical reactions can be taken into account as done in DNS.

7.2. Unified turbulence models

There are several ways to tackle a unification of turbulence models (see, for instance, Speziale (1998), Germano (1999), Peltier et al. (2000), Sagaut (2002) and the references therein). The following discussion is based on the developments

made in chapters 5 and 6. The goal is to demonstrate how a basic solution for the unification of turbulence models can be found. For simplicity, attention will be restricted to the consideration of an incompressible flow. The inclusion of compressibility effects can be performed straightforwardly on this basis.

7.2.1. A unified stochastic model

First, we consider the question of the unification of turbulence models at the level of stochastic equations. The most flexible approach for modeling the dynamics of turbulent fluctuations was discussed in chapter 6. By restricting the attention to velocities, such a stochastic FDF model reads, according to (6.5b),

$$\frac{d}{dt} x_i^* = U_i^*, \tag{7.1a}$$

$$\frac{d}{dt} U_i^* = \overline{\Gamma}_i - \frac{1+1.5C_0}{2\tau_r}\left(U_i^* - \overline{U}_i\right) + \overline{F}_i + \sqrt{C_0 \frac{k_r}{\tau_r}} \frac{dW_i}{dt}, \tag{7.1b}$$

where relation (6.54) and $\varepsilon_r = k_r / \tau_r$ were applied to rewrite τ_L and ε_r. To close the equations (7.1a-b), one has to provide a model for τ_r. This can be done by involving an equation for ε_r in correspondence to (5.84).

The properties of the model (7.1a-b) depend essentially on the choice of the filter function G that is used for the definition of filtered velocities,

$$\overline{U}_i = \int d\mathbf{r}\; U_i(\mathbf{x}+\mathbf{r},t)\, G(\mathbf{r}). \tag{7.2}$$

First of all, G is determined by the filter width Δ. By choosing $\Delta << \eta$, where η is the Kolmogorov length scale, G becomes equivalent to a delta function, $G = \delta(\mathbf{r})$. In this case, SGS velocity fluctuations disappear because $\overline{U}_i = U_i$. This consequence agrees with the implications of the equations (7.1a-b): SGS velocity fluctuations have to relax to zero in the case that $\Delta << \eta$ since there is no generation mechanism for them (k_r in the noise term vanishes according to (6.25)). The use of the transport equation for $\overline{U}_i$ that is implied by (7.1a-b) then corresponds to the solution of the Navier-Stokes equations; this means one applies DNS. The other limit case is given by choosing Δ very large, i.e., $\Delta >> \mu$, where μ is a characteristic eddy length scale. The filter operation (7.2) then corresponds to the ensemble average (see the explanations given in chapter 1), so that the equations (7.1a-b) represent a PDF model (the SLM described in section 5.2). To specify μ, we will adopt below $\mu = L = k^{3/2} / \varepsilon$, which was used by Peltier et al. (2000) for their fully-developed channel flow simulations. It is worth noting, however, that other choices of μ may be more appropriate to simulate other anisotropic and inhomogeneous flows.

Therefore, the equations (7.1a-b) represent a universal model in the sense that they can be applied at any level of resolution. Nevertheless, this does not mean that the accuracy of these equations is the same at each of these levels, see section 7.3.

7.2.2. A unified model for filtered variables

Next, we consider the same question as in section 7.2.1, but now at the level of transport equations for filtered velocities. As shown in chapter 6, the model (7.1a-b) implies the following equation for filtered velocities $\overline{U}_i$ (see equation (6.3b)),

$$\frac{\partial \overline{U}_i}{\partial t} + \overline{U}_k \frac{\partial \overline{U}_i}{\partial x_k} = 2\nu \frac{\partial \overline{S}_{ik}}{\partial x_k} - \frac{1}{\langle \rho \rangle} \frac{\partial \left(\langle p \rangle + 2 \langle \rho \rangle k_r / 3 \right)}{\partial x_i} - \frac{\partial \tau_{ik}}{\partial x_k} + \overline{F}_i, \tag{7.3}$$

where (6.15) is used to rewrite $\overline{u_k u_i}$. To close (7.3), one needs a model for τ_{ik} ($\langle \rho \rangle k_r$ can be combined with $\langle p \rangle$ to produce a modified pressure, which satisfies the Poisson equation that is implied by (7.3) and the continuity condition). In agreement with the discussions in chapters 5 and 6, we adopt the parametrization

$$\tau_{ik} = -2\nu_u \overline{S}_{ik}, \tag{7.4}$$

where ν_u is introduced as a turbulent viscosity that unifies (for the incompressible flow considered) the corresponding expressions for the deviatoric parts of the SGS and Reynolds stress tensor. In particular, according to the relations (6.24) and (5.78) we know the following expressions for ν_u in the limits of very small and large Δ:

$$\nu_u = \begin{cases} \nu_r & (\Delta << L) \\ \nu_T & (\Delta >> L) \end{cases}. \tag{7.5}$$

As described in chapters 5 and 6, the SGS viscosity ν_r is given by

$$\nu_r = c_S \Delta^2 \, | \overline{S} |_r, \tag{7.6}$$

and the turbulent viscosity ν_T by

$$\nu_T = \frac{C_\mu}{\tau \, | \overline{S} |} L^2 \, | \overline{S} | = C_{\mu^*}{}^{3/2} L^2 \, | \overline{S} |. \tag{7.7}$$

The first expression for ν_T follows from relation (5.79) by adopting the definition $L = k^{3/2} / \varepsilon$. The second expression makes use of the abbreviation

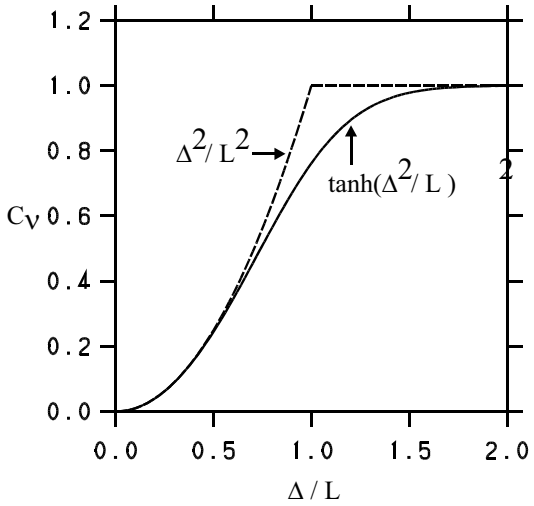

Fig. 7.3. The dependence of the transfer function C_ν on Δ / L. The dashed lines show its behaviour for small and large Δ, respectively. The solid line describes a transition between these two limit cases.

$$C_{\mu^*}^{3/2} = \frac{C_\mu}{\tau\,|\,\overline{S}\,|}. \tag{7.8}$$

The relations (5.88a-b) taken for a zero gradient Richardson number Ri reveal that an algebraic approximation to $\tau\,|\,\overline{S}\,|$ is given by $\tau\,|\,\overline{S}\,| = (P / C_\mu\,\varepsilon)^{1/2}$. Hence, we find that $C_{\mu^*} = C_\mu$ for a flow where the dissipation ε balances the production P locally.

To generalize the representation of ν_u, we parametrize it in terms of the turbulent viscosity ν_T,

$$\frac{\nu_u}{|\,\overline{S}\,|_r} = C_\nu \frac{\nu_T}{|\,\overline{S}\,|}, \tag{7.9}$$

where ν_r and ν_T are standardized to the fluctuating and non-fluctuating shear rates $|\,\overline{S}\,|_r$ and $|\,\overline{S}\,|$, respectively. C_ν is introduced via relation (7.9) as a proportionality parameter. According to (7.5), we know C_ν in the limits of very small and large Δ,

$$C_\nu = \begin{cases} \dfrac{c_S}{C_{\mu^*}^{3/2}} \dfrac{\Delta^2}{L^2} = \alpha \dfrac{\Delta^2}{L^2} & (\Delta << L) \\ 1 & (\Delta >> L) \end{cases}. \tag{7.10}$$

Here, we introduced $\alpha = c_S / C_{\mu^*}^{3/2}$. The use of $C_{\mu^*} = 0.09$ and $c_S^{1/2} = 0.17$ (see the discussion in chapters 5 and 6) implies then that $\alpha = 1.07 \approx 1$. These two limit cases of C_ν for small and large Δ are shown in Fig. 7.3, where the corresponding trends are extended to Δ = L. Nevertheless, it is plausible to expect C_ν as a function which provides a smooth transition between the limits of small and large Δ. An

example for such a function is also presented in Fig. 7.3, which is given by

$$C_v = \tanh\left(\Delta^2 / L^2\right). \tag{7.11}$$

The fact that this function reaches the asymptotic limit $C_v = 1$ by $\Delta = 2\,L$ can be made plausible by examining Fig. 4.3: the filter width Δ becomes of the order of the size of the domain considered in this case. The combination of relation (7.4) with (7.9) results then in a unified expression for τ_{ik}. First steps to realize similar unified DNS-LES-RANS methods computationally are currently under investigation; see, for instance, Peltier et al. (2000).

7.3. Some unsolved questions

A basic solution for the unification of turbulence models was presented in section 7.2. However, the development of a more complete stochastic theory for turbulent flows still requires answers to some relevant questions. This will be pointed out next on the basis of a discussion of the structure and parameters of unified turbulence models.

7.3.1. The structure of unified turbulence models

The performance of the equations (7.1a-b) as a PDF method was discussed in detail in chapter 5. It was shown there that this SLM may be seen as a reasonable model for a wide range of flows. However, the SLM does not represent a very accurate model in every case: the neglect of the anisotropy of the turbulent mixing frequency – G_{ik} may result in errors of about 20%, see section 5.3.3. To overcome these deficiencies one has to extend (7.1a-b) to a more complex model, for instance to the LM. Further, it was shown that Kolmogorov-scale processes are not involved by adopting any specification of the GLM for simulations of turbulent flows with finite Reynolds numbers. To take them into account, one has to extend these models to acceleration models (Pope 2002).

In contrast to the use of (7.1a-b) as a PDF method, these equations appear to be sufficiently accurate if they are used as an FDF method; this means with relatively small Δ. In addition to this, one finds that the suitability of simpler methods (as given by algebraic SGS stress tensor models discussed in chapter 6) increases with decreasing filter width Δ (see the discussion at the end of section 6.2.4). Further evidence for this may be obtained by calculating the SGS stress tensor directly through developing $U_iU_j(\mathbf{x} + \mathbf{r}, t)$ and $U_i(\mathbf{x} + \mathbf{r}, t)$ into Taylor series at $\mathbf{r} = 0$ and studying, after integration over $\mathbf{r}$, the effect of moments of the filter function G.

The conclusion that can be drawn from these facts is that the filter width Δ has an influence on the accuracy of the stochastic model (7.1a-b) and LES equation

(7.3) combined with (7.4) for τ_{ik}: these models are applicable at all scales, but their accuracy varies in dependence on the scale considered. The details of this dependence are, however, unknown at present. Obviously, the clarification of this question would be very helpful for a better understanding of the suitability of different equation structures for various scales (filter widths Δ).

7.3.2. The parameters of unified turbulence models

An important question that is related to the performance of turbulence models concerns the calculation of model parameters. This is known to be relevant because model deficiencies often can be minimized by optimizing the choice of model parameters. The discussion of this question will be restricted to the consideration of C_0 and ℓ_*, which are required to close the models described in section 7.2 (see chapter 6). It is worth noting that corresponding explanations also apply to other parameters (the discussion with regard to ℓ_* also applies to $\ell_{\varphi*}$).

With regard to the choice of C_0, one needs knowledge about the relevance of Reynolds number effects and the universality of the Kolmogorov constant $C_0(\infty)$ (which is the limit of C_0 at high Reynolds numbers). Within the framework of PDF methods, one finds $C_0 \approx 2$ (independent of Re) with regard to flows that are similar to those found in reality (see section 5.4). Within the framework of FDF methods, one finds $C_0 \approx 1.6$ independent of Re, which agrees very well with the universal Kolmogorov constant C_K that determines the energy spectrum (see section 6.2.5). These observations are made for flows where, however, the Reynolds number was far from being very high, and the influence of the spatial resolution was not investigated until now. Therefore, further investigations are needed to obtain a more complete understanding of the dependence of C_0 on the Reynolds number. This is of crucial importance to theoretical analyses (it has the same relevance as corresponding investigations of the universality of the Kolmogorov constant C_K, see Sreenivasan (1995)), and it is important with regard to the optimization of the performance of turbulence models: it offers the possibility to focus the variation of model parameters on the consideration of ℓ_* variations.

With regard to the calculation of ℓ_*, one has the choice of applying either constant values $\ell_* = (1 \pm 0.5) / 3$ or dynamic concepts to provide ℓ_*. The latter appears to be very attractive because it corresponds (in combination with the choice $C_0 = 1.6$) with the use of a computational method without adjustable parameters, which can be applied for objective assessments of relevant flows which cannot be calculated by DNS. The disadvantage of such a dynamic model, however, is that it cannot recover a RANS model in the large-Δ limit, so that it does not represent a universal model. Thus, there are certainly some questions concerning the most appropriate way to specify ℓ_* and corresponding parameters in unified turbulence models.

8. References

Abramowitz, M. & Stegun, I. A. 1984 Pocketbook of Mathematical Functions. Verlag Harri Deutsch, Thun, Frankfurt/Main.

Adumitroaie, V., Ristorcelli, J. R. & Taulbee, D. B. 1999 Progress in Favré-Reynolds Stress Closures for Compressible Flows. Phys. Fluids 11, 2696-2719.

Alexeev, B. V. 1994 The Generalized Boltzmann Equation, Generalized Hydrodynamic Equations and their Application. Phil. Trans. R. Soc. London A 449, 417-443.

Antonia, R. A., Teitel, M., Kim, J. & Browne, L. W. B. 1992 Low-Reynolds Number Effects in a Fully Developed Channel Flow. J. Fluid Mech. 236, 579-605.

Baldyga, J. & Bourne, J. R. 1999 Turbulent Mixing and Chemical Reactions. John Wiley & Sons, Chichester, New York, Weinheim, Brisbane, Singapore, Toronto.

Baurle, R. A. & Girimaji, S. S. 1999 An Assumed PDF Turbulence-Chemistry Closure with Temperature-Composition Correlations. In: 37th AIAA Aerospace Sciences Meeting and Exhibit, AIAA 99-0928, Reno, NV.

Bird, G. A. 1994 Molecular Gas Dynamics and the Direct Simulation of Gas Flows. Clarendon Press, Oxford.

Blaisdell, G. A., Mansour, N. N. & Reynolds, W. C. 1993 Compressibility Effects on the Growth and Structure of Homogeneous Turbulent Shear Flow. J. Fluid Mech. 256, 443-485.

Canuto, V. M. 1992 Turbulent Convection with Overshooting: Reynolds Stress Approach. Astrophys. J. 392, 218-232.

Canuto, V. M., Minotti, F., Ronchi, C., Ypma, R. M. & Zeman, O. 1994 Second-Order Closure PBL Model with New Third-Order Moments: Comparison with LES Data. J. Atmos. Sci. 51, 1605-1618.

Cercignani, C. 1988 The Boltzmann Equation and its Application. Springer-Verlag, New York, Berlin, Heidelberg, London, Paris, Tokyo.

Chassaing, P., Antonia, R. A., Anselmet, F., Joly, L. & Sarkar, S. 2002 Variable Density Fluid Turbulence. Fluid Mechanics and its Applications 69, Kluwer Academic Publishers, Dordrecht, Boston, London.

Clark, R. A., Ferziger, J. H. & Reynolds, W. C. 1979 Evaluation of Subgrid-Scale Models using an Accurately Simulated Turbulent Flow. J. Fluid Mech. 91, 1-16.

S. Heinz, *Statistical Mechanics of Turbulent Flows*

Colucci, P. J., Jaberi, F. A., Givi, P. & Pope, S. B. 1998 Filtered Density Function for Large Eddy Simulations of Turbulent Reactive Flows. Phys. Fluids 10, 499-515.

Craft, T. J., Kidger, J. W. & Launder, B. E. 1997 Importance of Third-Moment Modeling in Horizontal, Stably-Stratified Flows. Proceedings of the 11th Symposium on Turbulent Shear Flows, Grenoble, France, 2013-2018.

Craft, T. J. 1998 Developments in a Low-Reynolds Number Second-Moment Closure and its Application to Separating and Reattaching Flows. Int. J. Heat and Fluid Flow 19, 541-548.

Delarue, B. J. & Pope, S. B. 1997 Application of PDF Methods to Compressible Turbulent Flows. Phys. Fluids 9, 2704-2715.

Delarue, B. J. & Pope, S. B. 1998 Calculation of Subsonic and Supersonic Turbulent Reacting Mixing Layers Using Probability Density Function Methods. Phys. Fluids 10, 487-498.

Dreeben, T. D. & Pope, S. B. 1997 Wall-Function Treatment in PDF Methods for Turbulent Flows. Phys. Fluids 9, 2692-2703.

Du, S., Wilson, J. D. & Yee, E. 1994a Probability Density Functions for Velocity in the Convective Boundary Layer, and Implied Trajectory Models. Atmos. Environ. 28, 1211-17.

Du, S., Wilson, J. D. & Yee, E. 1994b On the Moments Approximation Method for Constructing a Lagrangian Stochastic Model. Bound.-Layer Meteorol. 40, 273-292.

Du, S., Sawford, B. L., Wilson, J. D. & Wilson, D. J. 1995 Estimation of the Kolmogorov Constant (C_0) for the Lagrangian Structure Function, using a Second-Order Lagrangian Model of Grid Turbulence. Phys. Fluids 7, 3083-3090.

Durbin, P. A. & Speziale, C. G. 1994 Realizability of Second-Moment Closure via Stochastic Analysis. J. Fluid Mech. 280, 395-407.

Durbin, P. A. & Petterson, B. A. 2001 Statistical Theory and Modeling for Turbulent Flows. John Wiley & Sons, Chichester, New York, Weinheim, Brisbane, Singapore, Toronto.

Eifler, P. & Kollmann, W. 1993 PDF Prediction of Supersonic Hydrogen Flames. In: 31th AIAA Aerospace Sciences Meeting and Exhibit, AIAA 93-0448, Reno, NV.

Einstein, A. 1905 Über die von der molekular-kinetischen Theorie der Wärme geforderte Bewegung von in ruhenden Flüssigkeiten suspendierten Teilchen. Ann. Phys. (Leipzig) 17, 549-560.

Esposito, R. Lebowitz, J. L. & Marra, R. 1999 On the Derivation of Hydrodynamics from the Boltzmann Equation. Phys. Fluids 11, 2354-2366.

Eswaran, V. & Pope, S. B. 1988 Direct Numerical Simulations of the Turbulent Mixing of a Passive Scalar. Phys. Fluids 31, 506-520.

FLUENT Inc. 2003 FLUENT 6.1 User's Guide. Lebanon, New Hampshire, USA.

Fokker, A. D. 1914 Die mittlere Energie rotierender elektrischer Dipole im Strahlungsfeld. Ann. Physik 43, 810-820.

Forkel, H. & Janicka, J. 2000 Large-Eddy Simulation of a Turbulent Hydrogen Diffusion Flame. Flow, Turb. and Combust. 65, 163-175.

Fox, R. O. 1992 The Fokker-Planck Closure for Turbulent Molecular Mixing: Passive Scalars. Phys. Fluids A 4, 1230-1244.

Fox, R. O. 1994 Improved Fokker-Planck Model for the Joint Scalar, Scalar Gradient PDF. Phys. Fluids 6, 334-348.

Fox, R. O. 1996 On Velocity-Conditioned Scalar Mixing in Homogeneous Turbulence. Phys. Fluids 8, 2678-2691.

Freund, J. B. 1997 Compressibility Effects in a Turbulent Annular Mixing Layer. PhD thesis, Mechanical Engineering Department, Stanford University.

Freund, J. B., Lele, S. K. & Moin, P. 2000a Compressibility Effects in a Turbulent Annular Mixing Layer. Part 1. Turbulence and Growth Rate. J. Fluid Mech. 421, 229-267.

Freund, J. B., Moin, P. & Lele, S. K., 2000b Compressibility Effects in a Turbulent Annular Mixing Layer. Part 2. Mixing of a Passive Scalar. J. Fluid Mech. 421, 269-292.

Friedrich, R. & Bertolotti, F. P. 1997 Compressibility Effects due to Turbulent Fluctuations. Appl. Sci. Res. 57, 165-194.

Friedrich, R. 1999 Modeling of Turbulence in Compressible Flows. In: Transition, Turbulence and Combustion Modeling, edited by Hanifi, A., Alfredsson, P. H., Johansson, A. V. & Henningson, D. S., Kluwer Academic Publishers (ERCOFTAC Series), Dordrecht, Boston, London, 243-348.

Frisch, U. 1995 Turbulence: The Legacy of A. N. Kolmogorov. Cambridge University Press, Cambridge.

Gao, F. & O'Brien, E. E. 1993 A Large-Eddy Simulation Scheme for Turbulent Reacting Flows. Phys. Fluids A5, 1282-1284.

Gardiner, C. W. 1983 Handbook of Statistical Methods. Springer-Verlag, Berlin, Heidelberg, New York, Tokyo.

Gatski, T. B. & Speziale, C. G. 1993 On Explicit Algebraic Stress Models for Complex Turbulent Flows. J. Fluid Mech. 254, 59-78.

Gerlinger, P., Möbus, H. & Brüggemann, D. 2001 An Implicit Multigrid Method for Turbulent Combustion. J. Comp. Phys. 167, 247-276.

Germano, M., Piomelli, U., Moin, P. & Cabot, W. H. 1991 A Dynamic Subgrid-scale Eddy Viscosity Model. Phys. Fluids A3, 1760-1765.

Germano, M. 1999 From RANS to DNS: Towards a Bridging Model. In: Direct and Large Eddy Simulation III, edited by Voke, P. R., Sandham, N. D. & Kleiser, L., Kluwer Academic Publishers, Dordrecht, 225-236.

Gerz, T., Schumann, U. & Elghobashi, S. E. 1989 Direct Numerical Simulation of Stratified Homogeneous Turbulent Shear Flows. J. Fluid Mech. 200, 563-594.

Gicquel, L. Y. M., Givi, P., Jaberi, F. A. & Pope, S. B. 2002 Velocity Filtered Density Function for Large Eddy Simulation of Turbulent Flows. Phys. Fluids 14, 1196-1213.

Givi, P. 1989 Model-free Simulations of Turbulent Reactive Flows. Prog. Energy Combust. Sci. 15, 1-107.

Grabert, H. 1982 Projection Operator Technique in Nonequilibrium Statistical Mechanics. Springer-Verlag, Berlin, Heidelberg, New York, Tokyo.

Heinz, S. & Schaller, E. 1996 On the Influence of Non-Gaussianity on Turbulent Transport. Bound.-Layer Meteorol. 81, 147-166.

Heinz, S. 1997 Nonlinear Lagrangian Equations for Turbulent Motion and Buoyancy in Inhomogeneous Flows. Phys. Fluids 9, 703-716.

Heinz, S. 1998a Time Scales of Stratified Turbulent Flows and Relations between Second-Order Closure Parameters and Flow Numbers. Phys. Fluids 10, 958-973.

Heinz, S. 1998b Connections between Lagrangian Stochastic Models and the Closure Theory of Turbulence for Stratified Flows. Int. J. Heat and Fluid Flow 19, 193-200.

Heinz, S. & van Dop, H. 1999 Buoyant Plume Rise described by a Lagrangian Turbulence Model. Atmos. Environ. 33, 2031-2043.

Heinz, S. & Roekaerts, D. 2001 Reynolds Number Effects on Mixing and Reaction in a Turbulent Pipe Flow. Chem. Eng. Sci. 56, 3197-3210.

Heinz, S. 2002 On the Kolmogorov Constant in Stochastic Turbulence Models. Phys. Fluids 14, 4095-4098.

Heinz, S. 2003a On Fokker-Planck Equations for Turbulent Reacting Flows. Part 1. Probability Density Function for Reynolds-averaged Navier-Stokes Equations. Flow, Turb. and Combust. (in press).

Heinz, S. 2003b On Fokker-Planck Equations for Turbulent Reacting Flows. Part 2. Filter Density Function for Large Eddy Simulation. Flow, Turb. and Combust. (in press).

Hinz, A., Hassel, E. P. & Janicka, J. 1999 Numerical Simulation of Turbulent Non-Equilibrium Methane-Air Jet Flames using Monte Carlo PDF Method. In: Turbulence and Shear Flow-1, edited by S. Banarjee & J. K. Eaton, Begell House Inc., New York, Wallingford, 333-338.

Holtslag, A. A. M. & Moeng, C-H. 1991 Eddy Diffusivity and Countergradient Transport in the Convective Atmospheric Boundary-Layer. J. Atm. Sci. 48, 1690-1698.

Hsu, A. T., Tsai, Y-L. P. & Raju, M. S. 1994 Probability Density Function Approach for Compressible Turbulent Reacting Flows. AIAA J. 32, 1407-1415.

Ilyushin, B. B. & Kurbatski, A. F. 1997 Modeling of Turbulent Transport in PBL with Third-Order Moments. Proceedings of the 11th Symposium on Turbulent Shear Flows, Grenoble, France, 2019-2024.

Jaberi, F. A., Colucci, P. J., James, S., Givi, P. & Pope, S. B. 1999 Filtered Mass Density Function for Large-Eddy Simulation of Turbulent Reacting Flows. J. Fluid Mech. 401, 85-121.

Jaynes, E. T. 1957 Information Theory and Statistical Mechanics. Phys. Rev. 106, 620-630.

Jenny, P., Pope, S. B., Muradoglu, M. & Caughey, D. A. 2001a A Hybrid Algorithm for the Joint PDF Equation of Turbulent Reactive Flows. J. Comput. Phys. 166, 218-252.

Jenny, P., Muradoglu, M., Liu, K., Pope, S. B. & Caughey, D. A. 2001b PDF Simulations of a Bluff-Body Stabilized Flow. J. Comput. Phys. 169, 1-23.

Juneja, A. & Pope, S. B. 1996 A DNS Study of Turbulent Mixing of two Passive Scalars. Phys. Fluids 8, 2161-2184.

Kaltenbach, H.-J., Gerz, T. & Schumann, U. 1994 Large-Eddy Simulation of Homogeneous Turbulence and Diffusion in Stably Stratified Flows. J. Fluid Mech. 280, 1-40.

Kassinos, S., Reynolds, W. C. & Rogers, M. M. 2001 One-Point Turbulence Structure Tensors. J. Fluid Mech. 428, 213-248.

Kawamura, H., Sasaki, J. & Kobayashi, K. 1995 Budget and Modeling of Triple Moment Velocity Correlations in a Turbulent Channel Flow Based on DNS. Proceedings of the 10th Symposium on Turbulent Shear Flows, Pennsylvania State University, 2613-2618.

Kerstein, A. R. 1999 One-Dimensional Turbulence: Model Formulation and Application to Homogeneous Turbulence, Shear Flows, and Buoyant Stratified Flows. J. Fluid Mech. 392, 277-334.

Kloeden, P. E. & Platen, E. 1992 Numerical Solution of Stochastic Differential Equations. Applications of Mathematics 23 (Stochastic Modeling and Applied Probability), Springer-Verlag, Berlin.

Kollmann, W. 1990 The PDF Approach to Turbulent Flow. Theoretical and Computational Fluid Dynamics 1, 249-285.

Kolmogorov, A. N. 1941 The local Structure of Turbulence in Incompressible Viscous Fluid for Very Large Reynolds Numbers. Dokl. Akad. Nauk SSSR 30, 299-303 (in Russian).

Kosović B. 1997 Subgrid-scale Modeling for the Large-Eddy Simulation of High-Reynolds Number Boundary Layers. J. Fluid Mech. 336, 151-182.

Kramers, H. A. 1940 Brownian Motion in a Field of Force and the Diffusion Model of Chemical Reactions. Physica 7, 284-304.

Krieger, G., Hassel, E. P., Janicka, J. & Chen, J.-Y. 1997 Monte Carlo and Presumed PDF Modeling of Turbulent Hydrogen-Nitrogen Diffusion Flames. In: Turbulence, Heat and Mass Transfer 2, edited by K. Hanjalic & T. W. J. Peeters, Delft University Press, 695-702.

Kuo, K. K. 1986 Principles of Combustion. Wiley Interscience, New York, Chichester, Brisbane, Toronto, Singapore.

Landau, L. D. & Lifshitz, E. M. 1963 Fluid Mechanics. Second Edition, Pergamon Press, Oxford, London, Paris, Frankfurt.

Langevin, P. 1908 Sur la théorie du mouvement Brownien. Comptes Rendus Acad. Sci., Paris 146, 530-533.

Launder, B. E. 1990 Phenomenological Modeling: Present and Future. In: Wither Turbulence? Turbulence at the Crossroads, edited by Lumley, J. L., Springer-Verlag, Berlin, 439-485.

Lebowitz, J. L. & Bergmann, P. G. 1957 Irreversible Gibbsian Ensembles. Ann. Phys. (New York) 1, 1-23.

Lele, S. K. 1994 Compressibility Effects on Turbulence. Ann. Rev. Fluid Mech. 26, 211-154.

Leonard, A. 1997 Large-Eddy Simulation of Chaotic Convection and Beyond. In: 35th AIAA Aerospace Sciences Meeting and Exhibit, AIAA 97-0204, Reno, NV, 1-8.

Levermore, C. D., Morokoff, W. J. & Nadiga, B. T. 1998 Moment Realizability and the Validity of the Navier-Stokes Equations for Rarefied Gas Dynamics. Phys. Fluids 12, 3214-3226.

Lilly, D. K. 1967 The Representation of Small-scale Turbulence in Numerical Simulation of Experiments. In: Proc. IBM Scientific Computing Symp. on Environmental Sciences, edited by Goldstine, H. H., Yorktown Heights, NY, 195-210.

Lilly, D. K. 1992 A Proposed Modification of the Germano Subgrid-scale Closure Method. Phys. Fluids A4, 633-635.

Lindenberg, K. & West, J. W. 1990 The Nonequilibrium Statistical Mechanics of Open and Closed System. VHC Publishers, Inc., New York, Weinheim, Cambridge.

Liu, S., Menevau, C. & Katz, J. 1994 On the Properties of Similarity Subgrid-scale Models as Deduced from Measurements in a Turbulent Jet. J. Fluid Mech. 275, 83-119.

Luhar, A. K., Hibberd, M. F. & Hurley, P. J. 1996 Comparison of Closure Schemes used to specify the Velocity PDF in Lagrangian Stochastic Dispersion Models for Convective Conditions. Atmos. Environ. 30, 1407-1418.

Lumley, J. L. 1978 Computational Modeling of Turbulent Flows. Adv. in Applied Mech. 18, 123-175.

Madnia, C. K. & Givi, P. 1993 Direct Numerical Simulation and Large Eddy Simulation of Reacting Homogeneous Turbulence. In: Large Eddy Simulations of Complex Engineering and Geophysical Flows, edited by Galperin, B. & Orszag, S. A., Cambridge University Press, Cambridge, 315-346.

Marcienkiewicz, J. 1939 Sur une propriété de la loi de Gauss. Math. Z. 44, 612-618.

Menevau, C. & Katz, J. 2000 Scale-Invariance and Turbulence Models for Large-Eddy Simulation. Annu. Rev. Fluid Mech. 32, 1-32.

Minier, J.-P. & Peirano, E. 2001 The PDF Approach to Turbulent Polydispersed Two-phase Flows. Physics Reports 352, 1-214.

Möbus, H., Gerlinger, P. & Brüggemann, D. 1998 Efficient Methods for Particle Temperature Calculations in Monte Carlo PDF Methods. ECCOMAS 98, John Wiley & Sons Ltd., 162-168.

Möbus, H., Gerlinger, P. & Brüggemann, D. 1999 Monte Carlo PDF Simulation of Compressible Turbulent Diffusion Flames Using Detailed Chemical Kinetics. In: 37th AIAA Aerospace Sciences Meeting and Exhibit, AIAA 99-0198, Reno, NV.

Moin, P. & Mahesh, K. 1998 Direct Numerical Simulation: A Tool for Turbulence Research. Annu. Rev. Fluid Mech. 30, 539-578.

Monin, A. S. & Yaglom, A. M. 1971 Statistical Fluid Mechanics: Mechanics of Turbulence, Volume 1, Cambridge, MA: MIT Press.

Monin, A. S. & Yaglom, A. M. 1975 Statistical Fluid Mechanics: Mechanics of Turbulence, Volume 2, Cambridge, MA: MIT Press.

Moser, R. D., Kim, J. & Mansour, N. N. 1999 Direct Numerical Simulation of Turbulent Channel Flow up to $Re_\tau = 590$. Phys. Fluids 11, 943-945.

Moyal, J. E. 1949 Stochastic Processes and Statistical Physics. J. Roy. Stat. Soc. (London) B 11, 150-210.

Muradoglu, M., Jenny, P., Pope, S. B. & Caughey, D. A. 1999 A Consistent Hybrid Finite-Volume/Particle Method for the PDF Equations of Turbulent Reactive Flows. J. Comput. Phys. 154, 342-371.

Muradoglu, M., Pope, S. B. & Caughey, D. A. 2001 The Hybrid Method for the PDF Equations of Turbulent Reactive Flows: Consistency Conditions and Correction Algorithms. J. Comput. Phys. 172, 841-878.

Nooren, P. A., Wouters, H. A., Peeters, T. W. J. & Roekaerts, D. 1997 Monte Carlo PDF Modeling of a Turbulent Natural-Gas Diffusion Flame. Combustion Theory and Modeling 1, 79-96.

Nooren, P. A. 1998 Stochastic Modeling of Turbulent Natural-Gas Flames. PhD thesis, TU Delft.

Overholt, M. R. & Pope, S. B. 1996 Direct Numerical Simulation of a Passive Scalar with Imposed Mean Gradient in Isotropic Turbulence. Phys. Fluids 8, 3128-3148.

Pantano, C. & Sarkar, S. 2002 A Study of Compressibility Effects in the High-Speed Turbulent Shear Layer using Direct Simulation. J. Fluid Mech. 451, 329-371.

Pawula, R. F. 1967 Approximation of Linear Boltzmann Equation by Fokker-Planck Equation. Phys. Rev. 162, 186-188.

Peltier, L.J., Zajaczkowski, F. J. & Wyngaard, J. C. 2000 A Hybrid RANS/LES Approach to Large-Eddy Simulation of High-Reynolds-Number Wall-Bounded Turbulence. Proceedings of the ASME FEDSM'00: ASME 2000 Fluids Engineering Division Summer Meeting, Boston, Massachusetts, FEDSM2000-11177.

Peters, N. 2001 Turbulent Combustion. Cambridge University Press, Cambridge.

Pierce, C. & Moin, P. 1998 A Dynamic Model for Subgrid-Scale Variance and Dissipation Rate of a Conserved Scalar. Phys. Fluids 10, 3041-3044.

Piomelli, U., Cabot, W. H., Moin, P. & Lee, S. 1991 Subgrid-scale Backscatter in Turbulent and Transitional Flows. Phys. Fluids A3, 1766-1771.

Piomelli, U. 1999 Large-Eddy Simulation: Achievements and Challenges. Prog. Aerosp. Sci. 35, 335-362.

Piquet, J. 1999 Turbulent Flows. Models and Physics. Springer-Verlag, Berlin, Heidelberg, New York.

Planck, M. 1917 Uber einen Satz der statistischen Dynamik and seine Erweiterung in der Quantentheorie. Sitzber. Preuß. Akad. Wiss., 324-341.

Pope, S. B. 1975 A More General Effective Viscosity Hypothesis. J. Fluid Mech. 72, 331-340.

Pope, S. B. 1985 PDF Methods for Turbulent Reactive Flows. Prog. Energy Combust. Sci. 11, 119-192.

Pope, S. B. 1990 Computations of Turbulent Combustions: Progress and Challenges. 23rd Symposium (International) on Combustion, The Combustion Institute, 591-612.

Pope, S. B. 1994a On the Relationship between Stochastic Lagrangian Models of Turbulence and Second-Moment Closures. Phys. Fluids 6, 973-985.

Pope, S. B. 1994b A Fortran Code to solve the Modeled Joint PDF Equations for Two-dimensional Recirculating Flows. Cornell University, unpublished.

Pope, S. B. 1998 The Vanishing Effect of Molecular Diffusivity on Turbulent Dispersion: Implications for Turbulent Mixing and the Scalar Flux. J. Fluid Mech. 359, 299-312.

Pope, S. B. 1999 A Perspective on Turbulence Modeling. In: Modeling Complex Turbulent Flows, edited by Salas, M. D., Hefner, J. N. & Sakell, L., Kluwer, 53-67.

Pope, S. B. 2000 Turbulent Flows. Cambridge University Press, Cambridge.

Pope, S. B. 2002 A Stochastic Lagrangian Model for Acceleration in Turbulent Flows. Phys. Fluids 14, 2360-2375.

Repp, S., Sadiki, A., Schneider, C., Hinz, A., Landenfeld, T. & Janicka, J. 2002 Prediction of Swirling Confined Diffusion Flame with a Monte Carlo and a Presumed-PDF-Model. Int. J. Heat Mass Trans. 45, 1271-1285.

Réveillon, J. & Vervisch, L. 1998 Subgrid Scale Turbulent Micromixing: Dynamic Approach. AIAA J. 36, 336-341.

Richardson, L. F. 1922 Weather Prediction by Numerical Process. Cambridge University Press. Cambridge.

Risken, H. 1984 The Fokker-Planck Equation. Springer-Verlag, Berlin, Heidelberg, New York.

Roekaerts, D. 1991 Use of a Monte Carlo PDF Method in a Study of the Influence of Turbulent Fluctuations on Selectivity in a Jet-stirred Reactor. Appl. Sci. Res. 48, 271-300.

Rogers, M. M., Mansour, N. N. & Reynolds, W. C. 1989 An Algebraic Model for the Turbulent Flux of a Passive Scalar. J. Fluid Mech. 203, 77-101.

Sagaut, P. 2002 Large Eddy Simulation for Incompressible Flows. Second Edition, Springer-Verlag, Berlin, Heidelberg, New York.

Sarkar, S. 1995 The Stabilizing Effect of Compressibility in Turbulent Shear Flow. J. Fluid Mech. 282, 163-186.

Sawford, B. L. 1991 Reynolds Number Effects in Lagrangian Stochastic Models of Turbulent Dispersion. Phys. Fluids A3, 1577-1586.

Sawford, B. L. 1993 Recent Developments in the Lagrangian Stochastic Theory of Turbulent Dispersion. Bound.-Layer Meteorol. 62, 197-215.

Sawford, B. L. 1999 Rotation of Lagrangian Stochastic Models of Turbulent Dispersion. Bound.-Layer Meteorol. 93, 411-424.

Sawford, B. L. & Yeung, P. K. 2001 Lagrangian Statistics in Uniform Shear Flow: Direct Numerical Simulation and Lagrangian Stochastic Models. Phys. Fluids 13, 2627-2634.

Shannon, C. H. 1948 A Mathematical Theory of Communication. Bell. System Tech. J. 27, 379-423.

Schumann, U. 1987 The Countergradient Heat Flux in Turbulent Stratified Flows. Nucl. Eng. Design 100, 255-262.

Speziale, C. G. & Xu, X. 1996 Towards the Development of Second-Order Closure Models for Nonequilibrium Turbulent Flows. Int. J. Heat and Fluid Flow 17, 238-244.

Speziale, C. G. 1998 Turbulence Modeling for Time-Dependent RANS and VLES: A Review. AIAA J. 36, 173-184.

Sreenivasan, K. R. 1995 On the Universality of the Kolmogorov Constant. Phys. Fluids 7, 2778-2784.

Subramaniam, S. & Pope, S. B. 1998 A Mixing Model for Turbulent Reactive Flows based on Euclidean Minimum Spanning Trees. Combust. Flame 115, 487-514.

Taylor, G. I. 1921 Diffusion by Continuous Movements. Proc. Lond. Math. Soc. 20, 196-212.

Tennekes, H. & Lumley, J. L. 1972 A First Course in Turbulence. MIT Press.

Thomson, D. J. 1987 Criteria for the Selection of Stochastic Models of Particle Trajectories in Turbulent Flows. J. Fluid Mech. 180, 529-556.

Thomson, D. J. & Montgomery, M. R. 1994 Reflection Boundary Conditions for Random Walk Models of Dispersion in Non-Gaussian Turbulence. Atmos. Environ. 28, 1981-1987.

Vreman, B., Geurts, B. & Kuerten, H. 1994 Realizability conditions for the Turbulent Stress Tensor in Large-Eddy Simulation. J. Fluid Mech. 278, 351-362.

Wall, C., Boersma, B. J. & Moin, P. 2000 An Evaluation of the Assumed Beta Probability Density Function Subgrid-Scale Model for Large Eddy Simulation of Nonpremixed, Turbulent Combustion with Heat Realize. Phys. Fluids 12, 2522-2529.

Wei T. & Willmarth, W. W. 1989 Reynolds Number Effects on the Structure of a Turbulent Channel Flow. J. Fluid Mech. 204, 57-95.

Weinman, K. A. & Klimenko, A. Y. 2000 Estimation of the Kolmogorov Constant C_0 by Direct Numerical Simulation of a Continuous Scalar. Phys. Fluids 12, 3205-3220.

Wilcox, D. C. 1998 Turbulence Modeling for CFD. Second edition, DCW Industries, Inc.

Wilson, J. D. & Sawford, B. L. 1996 Review of Lagrangian Stochastic Models for Trajectories in the Turbulent Atmosphere. Bound.-Layer Meteorol. 78, 191-210.

Winckelmans, G. S., Wray, A. A. & Vasilyev, O. V. 1998 Testing of a New Mixed Model for LES: The Leonard Model Supplemented by a Dynamic Smagorinsky Term. Proc. Summer Program, Center for Turbulence Research (Stanford University and NASA Ames), 367-388.

Wouters, H. A., Nooren, P. A., Peeters, T. W. J. & Roekaerts, D. 1996 Simulation of a Bluff-Body Stabilized Diffusion Flame Using Second-Moment Closure and

Monte Carlo Methods. In: Twenty-Sixth Symp. (International) on Combust., The Combustion Institute, Pittsburgh, 177-185.

Wouters, H. A. 1998 Lagrangian models for turbulent reacting flow. PhD thesis, TU Delft.

Yeung, P. K. & Pope, S. B. 1989 Lagrangian Statistics from Direct Numerical Simulations of Isotropic Turbulence. J. Fluid Mech. 207, 531-586.

Zhou, X. Y. & Pereira, J. C. F. 2000 Large Eddy Simulation (2D) of a Reacting Plane Mixing Layer Using Filtered Density Function Closure. Flow, Turb. and Combust. 64, 279-300.

Zubarev, D., Morozov, V. & Röpke, G. 1996 Statistical Mechanics of Nonequilibrium Processes. Vol. 1: Basic Concepts, Kinetic Theory. Akademie Verlag (VCH Publishers), Berlin.

Zubarev, D., Morozov, V. & Röpke, G. 1997 Statistical Mechanics of Nonequilibrium Processes. Vol. 2: Relaxation and Hydrodynamic Processes. Akademie Verlag (VCH Publishers), Berlin.

9. Author index

10. Subject index

Boldface page numbers indicate principal references.